Expression and Function of APRIL and GDF-5 in the developing hippocampus

A thesis submitted to Cardiff University
for the degree of PhD in Neurosciences
2013

Catarina Raquel de Sousa Osório

Cardiff School of Biosciences
Cardiff University

Aos meus melhores amigos
Maria Fernanda
e António José Osório

DECLARATION

This work has not been submitted in substance for any other degree or award at this or any other university or place of learning, nor is being submitted concurrently in candidature for any degree or other award.

Signed Catarina Osório (candidate) Date 25.11.13

STATEMENT 1

This thesis is being submitted in partial fulfillment of the requirements for the degree of PhD (insert MCh, MD, MPhil, PhD etc, as appropriate)

Signed Catarina Osório (candidate) Date 25.11.13

STATEMENT 2

This thesis is the result of my own independent work/investigation, except where otherwise stated.
Other sources are acknowledged by explicit references. The views expressed are my own.

Signed Catarina Osório (candidate) Date 25.11.13

STATEMENT 3

I hereby give consent for my thesis, if accepted, to be available for photocopying and for inter-library loan, and for the title and summary to be made available to outside organisations.

Signed ..... (candidate) Date .....

STATEMENT 4: PREVIOUSLY APPROVED BAR ON ACCESS

I hereby give consent for my thesis, if accepted, to be available for photocopying and for inter-library loans **after expiry of a bar on access previously approved by the Academic Standards & Quality Committee.**

Signed Catarina Osório (candidate) Date 25.11.13

Acknowledgments

Many thanks to Professor Alun Davies for his supervision and support over the last few years. Thank you for giving me the opportunity to work in your lab where I gained some valuable experiences, your advice and permanent good nature.

A special thanks to Dr. Sean Wyatt who was always available to discuss science in an enthusiastic manner, all the support and patience to listen all the students, all the technical teaching, support and experimental discuss.

I also thank Dr. Alfredo Rodriguez-Tébar for letting me work in his lab, for making me feel at home, his precious advice for the projects, enthusiasm in science and good nature.

A special thanks to Dr. Pedro Chacón for all his support in the lab, exciting ideas, all the teaching, research expertise and input he gave to the projects, and above all for being a good friend: Muchas gracias amigo Pedro! Likewise, I want to thank colleagues and also friends Dr. Lilian Kisiswa, Dr to be Matthew White and Dr. Thomas Vizard for all the help in the lab, and for being good friends all this time. I thank all members of the Davies´s lab past and present for a warm welcome, creating a good working environment and be always supportive.

To old friends: Cátia, Ana Raquel, Vânia, Ana Costa, Débora, João e Ana Pereira, Tiago, and new friends: Ana Garcia and Welsh friends with whom I can count on every occasion.

Finalmente, quero agradecer à minha família, a quem dedico este trabalho, nomeadamente aos meus pais e amigos Maria Fernanda e António José Osório. Não esquecer as minhas avós Arminda e Alzira, tia Margarida e prima Paula, tio Avelino, tia Mariazinha e prima Xani, com os quais posso sempre contar, obrigada pelo vosso apoio e amizade. Dedico ainda este trabalho à memória do meu avô Belmiro, exemplo que quem não precisou de graus académicos para ser curioso, autodidacta, corajoso, amigo e um excelente avô.

Abstract

Neurite size and morphology are key determinants of the functional properties of neurons. In this thesis, it is described for the first time the expression of APRIL (A Proliferation-Inducing Ligand, TNFSF13) in the nervous system. APRIL is a member of the tumour necrosis factor superfamily and one of its receptors BCMA (B-Cell Maturation Antigen, TNFRSF17) are co-expressed in pyramidal neurons throughout the fetal and postnatal mouse hippocampus. The effect of APRIL on axon elongation is inhibited by the expression of a truncated BCMA receptor in the neurons, suggesting that BCMA mediates this effect. APRIL promotes rapid phosphorylation of ERK1/2, Akt and GSK-3β in cultured pyramidal neurons, and pharmacological inhibition of either MEK1/2 or PI3K, upstream activators of ERK1/2 and Akt/GSK-3β signalling, respectively, completely inhibits the axon growth-promoting action of APRIL. These findings reveal that APRIL selectively enhances axon growth from developing hippocampal pyramidal neurons by a mechanism that depends on BCMA and activation of ERK1/2 and Akt/GSK-3β signalling.

In this thesis, it is also shown that GDF-5 (growth-differentiation factor 5), a member of the transforming growth factor-β superfamily with a well-characterized role in limb morphogenesis, is a key regulator of the growth and elaboration of pyramidal neuron dendrites in the developing hippocampus. Pyramidal neurons co-express GDF-5 and its preferred receptors bone morphogenetic protein receptor-IB and bone morphogenetic protein receptor-II during development. In culture, GDF-5 substantially increased dendrite, but not axon, elongation from these neurons by a mechanism that depends activation of Smads1/5/8 and upregulation of the Hes5 transcription factor. *In vivo*, the apical and basal dendritic arbors of pyramidal neurons throughout the hippocampus were very markedly stunted in both homozygous and heterozygous *Gdf-5* null mutants, indicating that dendrite size and complexity are exquisitely sensitive to the level of endogenous GDF-5 synthesis.

Abbreviations

Aβ - amyloid-β
ActR - activin receptor
ADAM - a disintegrin and metalloproteinase domain
Akt - Ak transforming/protein kinase B
ALK - activin receptor-like kinase
ALS - amyotrophic lateral sclerosis
AMPA - α-amino-3-hydroxy-5-methyl-4-isoxazolepropionic acid
AOB - accessory olfactory bulbs
APC - adenomatous polyposis coli
aPKC - atypical protein kinase C
APP - amyloid precursor protein
APRIL - a proliferation-inducing ligand
Arg - arginine
AT base paring - adenosine-thymidine base pairing
ATP - adenosine triphosphate
BAFF - B-cell-activator factor
BAFFR - BAFF receptor
Bcl-2 - B-cell lymphoma 2
B-CLL - B-cell chronic lymphocytic leukemia
BCMA - B-cell maturation antigen
BDNF - brain-derived neurotrophic factor
BFCN - basal forebrain cholinergic neurons
BHK - baby hamster kidney
bHLH - basic helix-loop-helix
BMP - bone morphogenetic protein
BMPR - bone morphogenetic protein receptor
BNST - bed nucleus of stria terminalis
bp - base pairs
BrdU - 5-bromo-2'-deoxyuridine
BRE - BMP responsive element
BSA - bovine serum albumin

°C - degree Celsius

Ca^{2+} - calcium (2+)

CA - constitutively active

CA - Cornu Ammonis

CaMKII - Ca^{2+}/calmodulin-dependent protein kinase II

cAMP - cyclic adenosine monophosphate

CD - cluster of differentiation

CD95L - cluster of differentiation 95 ligand

Cdc - cell division cycle

CDFC - context dependent fear conditioning

CDK - cyclin-dependent kinase

CDMP - cartilage-derived morphogenetic protein

cDNA - complementary DNA

CGT - chondrodysplasias Grebe type I

CHTT - chondrodysplasias Hunter-Thompson type

CK - casein kinase

CLASP - CLIP-associated proteins

CLIP - class II associated invariant chain peptide

cm - centimeter

CMV - cytomegalovirus

CNS - central nervous system

CNTF - ciliary neurotrophic factor

copGFP - copepod *Pontellina plumata* GFP

COX2 - cyclo-oxygenase 2

CRD - cysteine-rich domain

CREB - cAMP response element-binding protein

CRMP-2 - collapsin response mediator protein-2

CSL - CBF1, RBP-Jk, J kappa-recombination signal-binding protein, suppressor of hairless, Lag-1)

CT-1 - cardiotrophin-1

Ct value - cycle threshold value

DAPI - 4',6-diamidino-2-phenylindole

DcR3 - decoy receptor 3

DG - dentate gyrus

DISC - dead-inducing signalling complex

DIV - day *in vitro*

DMEM - Dulbecco's modified Eagle's medium

DMSO - dimethyl sulfoxide

DN - dominant negative

DNA - deoxyribonucleic acid

dNTPs - deoxynucleotide triphosphates

Dpp - decapentaplegic

DPX - distyrene, plasticizer, xylene

DR3 - death receptor 3

DRG - dorsal root ganglion

DTT - dithiothreitol

DVR - decapentaplegic (Dpp) and vegetal-1 (Vg1)-related

E - embryonic day

EC - entorhinal cortex

EDA - ectodyplasin-A

EDTA - ethylenediaminetetraacetic acid

EF1 - elongation factor 1

ELISA - Enzyme-Linked Immunosorbent Assay

E-LTP - early-phase of LTP

ERK - extracellular signal regulated kinase

FADD - Fas associated death domain

FasL - Fas ligand

FBS - foetal bovine serum

Fn14 - fibroblast growth factor-inducible 14

FRET - fluorescence resonance energy transfer

Fwd - Forward

g - G force

g - gram

GABA - gamma-aminobutyric acid

GAPDH - glyceraldehyde 3-phosphate dehydrogenase

GC base paring - Guanine and Cytosine base paring

GDF - growth differentiation factor

$Gdf5^{bp\text{-}J}$ - growth differentiation factor 5, brachypodism-Jackson

GDNF - glial cell-derived neurotrophic factor

GFP - green fluorescent protein

GITR - glucocorticoid-induced TNF receptor-related receptor

Grb2 - growth factor receptor-bound protein 2

GSK-3β - glycogen synthase kinase 3 beta

GTP - guanosine-5'-triphosphate

^{3}H - tritium

HBSS - Hank´s balanced salt solution

HCl - hydrochloric acid

HEK - human embryonic kidney

Hes - hairy and enhancer of split

HET - heterozygous

HGF - hepatocyte growth factor

HRP - horseradish peroxidase

HSPG - heparan sulphate proteoglycans

HVEM - herpes virus entry mediator

IFN-γ - interferon -γ

IgM - immunoglobulin M

IL-6 - interleukin-6

JNK - Jun N-terminal kinase

JPS - Juvenile Polyposis syndrome

KDa - kilodalton

KO - knockout

LAP - latency associated peptide

LB - Luria Bertani

LEF1/TCF - lymphoid enhancer binding factor 1/T cell-specific factor

LIF - leukaemia inhibitory factor

LIGHT - ligand for herpes virus entry mediator and lymphotoxin receptor

LIMK1 - LIM domain kinase 1

LLC - large latent complex

L-LTP - late-phase of LTP

LPA - Oleoyl-L-α-lysophosphatidic acid sodium salt

LPS - lipopolysaccharide

LTD - long-term depression

LTM - long-term memory

LTP - long-term potentiation

LTβR - lymphotoxin-β receptor

M - molar

MAM - methylazoxymethanol

MAP-2 - microtubule-associated protein 2

MAPK - mitogen-activated protein kinase

MAPKKK - MAPK kinase kinase

MCAO - middle cerebral artery occlusion

MCS - multiple cloning site

MDD - major depressive disorder

MEK - mitogen-activated protein kinase/extracellular signal-regulated kinase kinase

mg - milligram

Mg^{2+} - magnesium (2+)

MH1 - Mad homology 1

min - minute

MIS - Mullerian inhibiting substance

ml - milliliter

mm -millimeter

mM - millimolar

MMP-9 - metalloproteinase 9

MOB - main olfactory bulbs

MRI - Magnetic resonance imaging

mRNA - messenger ribonucleic acid

MSP - macropage stimulatory protein

MWM - Morris water maze

NaOH - sodium hydroxide

NF-AT - nuclear factor of activated T cells transcription factor

NF-κB - nuclear factor-κB

ng - nanogram

NGF - nerve growth factor

NICD - notch intracellular domain

NIK - NF-κB inducing kinase

NK - natural killer cells

nm - nanometer

NMDA - N-methyl-D-aspartate

NRIF - Neurotrophin receptor interacting factor

n.s. - non-significant

NT-3 - neurotrophin-3

NuAc - nucleus accumbens

6-OHDA – 6-Hydroxydopamine

OPG - osteoprotegerin

OSM - oncostatin-M

P - postnatal age

p - p-value

p75NTR - p75 neurotrophin receptor

PAG - periaqueductal gray

PAGE - polyacrylamide gel electrophoresis

Par - partitioning defective

PBS - phosphate buffered saline

PBS-T - PBS tween

PCR - polymerase chain reaction

PDGF - platelet-derived growth factor

PFA - paraformaldehyde

PI3K - phosphatidyl inositol 3 kinase

PKC - protein kinase C

PLAD - pre-ligand assembly domain

PLCγ1 - phospholipase C gamma 1

PNS - peripheral nervous system

PP2A - protein phosphatase-2A

PS1- presenilin-1

PTEN - phosphatase and tensin homolog deleted on chromosome 10 phosphatase

PTP1B - Tyrosine-protein phosphatase non-receptor type 1

PVDF - polyvinylidene fluoride

Q-PCR - quantitative-PCR

Rac1 - Ras-related C3 botulinum toxin substrate 1

RANKL - receptor activator of nuclear factor-κB ligand

Ras - Rat sarcoma

Rev - Reverse

RhoA - Ras homolog gene family, member A

RIP - receptor-interacting protein

RIPA - radioimmunoprecipitation

RNA - ribonucleic acid

Ror2 - receptor tyrosine kinase-like orphan receptor 2

rpm - rotations per minute

RPMI - Roswell Park Memorial Institute

RT - reverse transcriptase

RT - room temperature

SBS - Smad-binding site

SCG - superior cervical ganglia

SDHA - succinate dehydrogenase complex, subunit A, flavoprotein variant

SDS - sodium dodecyl sulfate

sec - second

SEM - standard error of the mean

Sema3A - Semaphorin-3A

ser - serine

SGZ - subgranular zone

shRNA - short hairpin RNA

siRNAs - small interference RNAs

SLE - systemic lupus erythematosus

Smad - SMA (small body size) and mothers against decapentaplegic (MAD)

SPC - subtilisin-like proprotein convertase

Sub - subiculum

Ta - annealing temperature

TACI - transmembrane activator and cyclophilin ligand interactor

TAK1 - TGF-β activated kinase 1

T-CAT - T-maze spontaneous alternation task

TCF - T cell-specific factor

TGF-β - transforming growth factor-β

THD - TNF homology domain

Thr - threonine

TIM - TNF-receptor associated factor (TRAF)-interacting motif

TL1A - TNF-like factor 1A

Tm - melting temperature

TMB - 3,3’5’5’-tetramethylbenzidine base

TNF - tumour necrosis factor

TNFRSF - tumour necrosis factor receptor superfamily

TNFSF - tumour necrosis factor superfamily

tPA - tissue plasminogen activator

TRADD - TNFR associated death domain

TRAF - TNF-receptor associated factor

TRAIL - TNF-related apoptosis-inducing ligand

Trk - tropomyosin-related kinase

TUNEL - terminal deoxynucleotidyl transferase dUTP nick and labeling

TWEAK - TNF-like weak inducer of apoptosis

Tyr - tyrosine

UV - ultraviolet

V - volt

VEGF - vascular endothelial growth factor

VEGI - vascular endothelial cell growth inhibitor

Vg1 - vegetal-1

VTA - ventral tegmental area

Wit - wishful thinking

WT - wild type

XEDAR - X-linked EDA receptor

XLHED - X-linked hypohidrotic ectodermal dysplasia

μg - microgram

μl - microliter

μm - micrometer

μM - micromolar

Δ-G - change in Gibbs free energy

Table of Contents

Acknowledgments i
Abstract ii
Abbreviations iii
Table of contents xi
Table of figures xv
Tables xviii

Chapter 1: General Introduction 1
1.1. Hippocampus 2
1.1.1. Early development and anatomical structure 2
1.1.2. Hippocampal connections 3
1.1.3. Hippocampal neurons 5
1.1.4. Hippocampal functions and associated neuropathologies 12
1.2. Regulation of neuron survival and outgrowth 16
1.2.1. The “neurothrophic hypothesis” 16
1.2.2. The Neurotrophin family of neurotrophic factors 17
1.2.3. The roles of Neurotrophins in the Hippocampus 20
1.2.4. Non-Neurotrophin regulators of hippocampal survival, process outgrowth and function 26
1.3. The Tumor Necrosis Factor superfamily 29
1.3.1. TNF ligands 29
1.3.2. TNF receptors 32
1.3.3. Intracellular signalling pathways downstream of TNFRSF activation 34
1.3.4. Physiological roles of the TNFSF 37
1.3.5. TNFSF in the nervous system 41
1.4. TGF-β superfamily 44
1.4.1. TGF-β superfamily Ligands 44
1.4.2. TGF-β superfamily Receptors 47
1.4.3. Cell Signalling 49
1.4.3.1. The Smad pathway 49
1.4.3.1.1. Cross-talk between R-Smads other signalling pathways 51
1.4.3.2. Non-Smad pathways 52
1.4.4. Physiological roles of the TGF-β superfamily 53
1.4.5. TGF-β superfamily in the nervous system 56
1.5. Aims 60
1.5.1. Hypothesis 60
1.5.2. Specific aims 60

Chapter 2: Material and Methods 61
2.1. Animal husbandry 62
2.2. Cell culture 62

2.2.1. Preparation of Tungsten needles 62
2.2.2. Preparation of culture dishes 63
2.2.3. Preparation of culture media 63
2.2.4. Hippocampal dissection 63
2.2.4.1. Hippocampal primary cultures 64
2.2.4.2. Explants in 3D Matrigel cultures 65
2.2.5. Cell lines cultures 66
2.3. Transfection 67
2.3.1. Transfection vectors 67
2.3.2. Plasmid preparation 72
2.3.2.1. Transformation 72
2.3.2.2. Mini and Midi plasmid preps 72
2.3.3. Liposome-mediated transfection 73
2.3.4. Non-liposomal-mediated transfection 74
2.3.5. Imaging 74
2.4. Luciferase assays 74
2.5. Quantification of neurite outgrowth 75
2.6. Quantification of hippocampal area and neuron survival 75
2.7. Reverse transcription 76
2.7.1. Principle 76
2.7.2. Total RNA extraction 77
2.7.3. RNA quantification 77
2.7.4. cDNA synthesis 77
2.8. Real-time PCR 78
2.8.1. Principle 78
2.8.2. Design of primers and probes 83
2.8.3. Real-time PCR procedure 85
2.8.4. Data analysis 85
2.9. Immunohistochemistry 86
2.9.1. Principle 86
2.9.2. Immunocytofluorescence of dissociated cultures 86
2.9.3. Preparation of brain frozen sections 87
2.9.3.1. Immunohistofluoroscence staining of frozen sections 87
2.9.4. Golgi staining 88
2.9.5. Imaging 88
2.10. Western blotting 89
2.10.1. Principle 89
2.10.2. Protein extraction 90
2.10.3. Protein quantification 90
2.10.4. Western blotting procedure 91
2.10.5. Protein densitometry 92
2.11. Elisa 94
2.11.1. Principle 94
2.11.2. Sample collection 94

2.11.3. Procedure 94
2.12. Statistical analysis 95

Chapter 3: Expression pattern of APRIL and its receptors in the developing hippocampus 96
3.1. Introduction 97
3.2. Aims 100
3.3. Results 100
3.3.1. Stage specific development of cultured hippocampal neurons 100
3.3.2. The expression of APRIL, BCMA and TACI mRNAs in the developing hippocampus and in hippocampal cultures 102
3.3.3. Expression of APRIL, BCMA and TACI proteins in 7DIVs hippocampal cultures 106
3.3.4. Cellular localisation of APRIL, BCMA and TACI proteins in hippocampal neurons 108
3.3.5. Localisation of APRIL, BCMA and TACI proteins in the hippocampus 111
3.3.6. APRIL is secreted by cultured hippocampal neurons 112
3.4. Discussion 113

Chapter 4: APRIL promotes the growth of hippocampal axons through MAPK and PI3K/Akt/GSK-3β signalling pathways 117
4.1. Introduction 118
4.2. Aims 119
4.3. Results 119
4.3.1. APRIL increases hippocampal neuron axon length 119
4.3.2. APRIL does not increase hippocampal dendritic outgrowth 122
4.3.3. BCMA mediates APRIL-promoted axonal elongation from cultured hippocampal neurons 124
4.3.4. Heparan sulphate proteoglycans are not essential for APRIL -promoted axon growth from cultured hippocampal neurons 126
4.3.5. Signalling transduction induced by APRIL in hippocampal neurons activation of MAPK and PI3K/Akt-PKB/GSK-3β pathways 129
4.4. Discussion 140

Chapter 5: GDF-5, BMPR-Ib and BMPR-II expression in the developing hippocampus 151
5.1. Introduction 152
5.2. Aims 155
5.3. Results 155
5.3.1. The expression of GDF-5, BMPR-Ib and BMPR-II mRNAs in the developing mouse hippocampus and cultured E18 hippocampal neurons 155

5.3.2. The expression of GDF-5, BMPR-Ib and BMPR-II proteins in the developing mouse hippocampus 159
5.3.3. Cellular localisation of GDF-5, BMPR-Ib and BMPR-II proteins in cultured pyramidal neurons 161
5.3.4. Localisation of GDF-5, BMPR-Ib and BMPR-II proteins in the developing hippocampus 163
5.4. Discussion 170

Chapter 6: GDF-5 promotes hippocampal dendritic growth by regulating Smad1/5/8 signalling and induction of hairy of split-1 and -5 expression 173
6.1. Introduction 174
6.2. Aims 175
6.3. Results 176
6.3.1. GDF-5 increase dendritic but not axonal outgrowth from cultured hippocampal neurons 176
6.3.2. BMPR-Ib and BMPR-II receptors mediate GDF-5 promoted dendrite growth 180
6.3.3. Signalling pathways induced by GDF-5 in hippocampal neurons: activation of Smad1/5/8 transcription factors 186
6.3.4. Signal transduction induced by GDF-5 in hippocampal neurons: induction of hairy and enhancer-of-split-1 (Hes1) and -5 (Hes5) expression 192
6.3.5. Hippocampal pyramidal dendrites are greatly reduced in size in brachypod mice 199
6.4. Discussion 201

Chapter 7: General Discussion, Conclusions and Future Work 216
7. General Discussion, Conclusions and Future Work 217

References 229
Appendices 264

Table of Figures

Figure 1: Hippocampus location in the human and rodent brain. 3
Figure 2: Input and output pathways in the mouse hippocampus. 4
Figure 3: Hippocampal formation. 5
Figure 4: The 5 stages of development of hippocampal neurons *in vitro*. 7
Figure 5: Stages of Axon outgrowth. 9
Figure 6: The Neurotrophin family of neurotrophic factors and their receptors. 18
Figure 7: Neurotrophin receptor signalling. 19
Figure 8: The TNF superfamily. 31
Figure 9: The pre-ligand assembly domain model. 33
Figure 10: TNFRSF signalling pathways. 36
Figure 11: The TGF-β superfamily. 45
Figure 12: The cysteine knot motif is conserved among members of the TGF-β superfamily. 46
Figure 13: Interactions of type II and type I receptors define downstream signalling mechanisms. 49
Figure 14: TGF-β superfamily receptor signalling through Smad and non-Smad dependent pathways. 53
Figure 15: Hippocampus dissection at E16.5. 64
Figure 16: Schematic representation of pCDH-CMV-MCS-EF1-copGFP dual-expression vector. 70
Figure 17: Reverse Transcription. 76
Figure 18: Polymerase Chain Reaction. 78
Figure 19: Real-time PCR Amplification Plot on a Stratagene Mx3000P Thermocycler. 80
Figure 20: Graph showing the melting temperature of GAPDH real-time PCR products on a Stratagene Mx3000P Thermocycler. 81
Figure 21: Taqman probe mechanism. 82
Figure 22: Standard curve. 86
Figure 23: The stages of hippocampal neuron development *in vitro*. 101
Figure 24: The relative expression levels of APRIL and BCMA mRNAs in the developing and adult mouse hippocampus and adult mouse thymus and spleen. 103
Figure 25: The relative expression levels of APRIL, BCMA and TACI mRNAs at different time points in E18 hippocampal cultures. 105
Figure 26: Western blots showing APRIL, BCMA and TACI protein Expression in 7DIVs hippocampal neurons. 107
Figure 27: The cellular localisation of APRIL, BCMA and TACI proteins in 7DIVs hippocampal neurons. 109
Figure 28: APRIL expression in macrophages. 110

Figure 29: APRIL, BCMA and TACI expression in lymphocytes. 110
Figure 30: Localisation of APRIL, BCMA and TACI proteins in the developing mouse hippocampus. 111
Figure 31: Hippocampal neurons secrete APRIL. 112
Figure 32: APRIL promotes axonal outgrowth from cultured hippocampal neurons. 120
Figure 33: APRIL promotes axonal outgrowth from cultured hippocampal neurons. 121
Figure 34: APRIL does not promote dendritic outgrowth from cultured hippocampal neurons. 123
Figure 35: BCMA mediates APRIL promoted-axonal outgrowth from cultured hippocampal neurons. 125
Figure 36: APRIL does not require HSPGs to promote axonal outgrowth from cultured hippocampal neurons. 127
Figure 37: APRIL does not require HSPGs to promote axonal outgrowth from cultured hippocampal neurons. 128
Figure 38: ERK activation is required for APRIL-promoted axonal growth. 130
Figure 39: APRIL increases ERK phosphorylation. 131
Figure 40: PI3K activity is required for APRIL-promoted axonal growth. 133
Figure 41: Akt activity is required for APRIL-promoted axonal growth. 135
Figure 42: APRIL enhances the phosphorylation of Akt. 136
Figure 43: Enhancing GSK-3β kinase activity prevents APRIL-promoted axonal growth. 138
Figure 44: APRIL enhances the phosphorylation of GSK-3β. 139
Figure 46: Relative expression of GDF-5, BMPR-Ib and BMPR-II mRNAs in the developing and adult mouse hippocampus. 157
Figure 47: Relative levels of GDF-5, BMPR-Ib and BMPR-II mRNAs expressed by cultured hippocampal neurons. 158
Figure 48: GDF-5, BMPR-Ib and BMPR-II protein expression in the developing hippocampus. 160
Figure 49: The cellular location of GDF-5, BMPR-Ib and BMPR-II proteins in 7DIVs hippocampal neurons. 162
Figure 50: GDF-5 distribution in the developing hippocampus. 164
Figure 51: BMPR-Ib distribution in the developing hippocampus. 166
Figure 52: BMPR-II distribution in the developing hippocampus. 168
Figure 53: GDF-5 does not promote axonal outgrowth from cultured hippocampal neurons. 176
Figure 54: GDF-5 does not promote axonal outgrowth from cultured E18 hippocampal neurons. 177
Figure 55: GDF-5 promotes dendritic outgrowth from cultured E18 hippocampal neurons. 178
Figure 56: GDF-5 promotes dendritic outgrowth from cultured E18 hippocampal neurons. 179
Figure 57: BMPR-Ib mediates GDF-5-promoted dendrite growth. 182

Figure 58: BMPR-Ib is required for GDF-5-promoted dendrite growth. 183
Figure 59: BMPR-II mediates GDF-5-promoted dendrite growth. 185
Figure 60: GDF-5 promotes the phosphorylation and activation of Smads1/5/8. 187
Figure 61: Dominant-negative Smad4 inhibits GDF-5 promoted dendritic growth. 189
Figure 62: Smad6 and Smad7 inhibit GDF-5 promoted dendritic growth. 190
Figure 63: GDF-5 enhances Smad transcriptional activation. 191
Figure 64: GDF-5 increases the expression of Hes1 and Hes5 mRNAs. 192
Figure 65: Activation of Hes5 promoter activity by Smads. 193
Figure 66: Hes6 overexpression prevents GDF-5 promoted dendritic growth. 196
Figure 67: Hes5-shRNA prevents GDF-5 promoted dendrite growth. 197
Figure 68: Hes5 regulates the growth of hippocampal neuron dendrites. 198
Figure 69: Reduced size and complexity of pyramidal dendrites in *Gdf-5*^{bp} mice 199 200
Figure 74: APRIL promotes hippocampal axonal growth by binding to BCMA and inducing the activation of ERK1/2 and PI3K/Akt signalling. 219
Figure 75: GDF-5 promotes hippocampal dendrite elongation by binding to a receptor complex consisting of BMPR-Ib and BMPR-II. 225

Tables

Table 1: Cellular location and expression of the TNFSF and TNFRSF members. 34
Table 2: Recombinant ligands and compounds. 67
Table 3: Plasmid description. 71
Table 4: SYBR Green real-time PCR amplification. 84
Table 5: Taqman probe real-time PCR amplification. 84
Table 6: Incubation time in 4% PFA for mouse brains. 87
Table 7: Primary antibodies used in the study. 89
Table 8: Secondary antibodies used in the study. 89
Table 9: Standard curve dilutions for Bradford assay. 91
Table 10: Primary antibodies used in the study. 93
Table 11: Secondary antibodies used in the study. 93

Chapter 1

General Introduction

1.1. Hippocampus

1.1.1. Early development and anatomical structure

The central nervous system (CNS) develops from the neural tube. Shortly after closure, the neural tube becomes subdivided into the prosencephalon (forebrain), mesencephalon (midbrain), rhombencephalon (hindbrain) and spinal cord. As development proceeds, the prosenchephalon develops into the telencephalon and diencephalon[1-4]. By embryonic day (E) E10.5-E12.5, in the mouse, the neuroepithelium of the dorso-medial telencephalon invaginates to form two medial structures, the hippocampal primordia, that are mainly comprised of proliferating progenitor cells that will differentiate into the different cell types present in the mature hippocampal formation as development proceeds[5-7]. In 1990, Altman and Bayer injected ^{3}H-thymidine into the developing rat hippocampus at sequential, closely spaced time points to determine the origins of the different cell populations that make up the hippocampus, their routes of migration and their subsequent order of settling. They identified three components of the hippocampal primordial neuroepithelium: the ammonic neuroepithelium that will generate pyramidal cells, the primary dentate neuroepithelium that gives rise to granule cells and the fimbrial glioepithelium that will produce the glial cells of the fimbria[4,8,9].

In humans, the hippocampal formation is located in the medial portion of each temporal lobe of the cortex, whereas in rodents the hippocampus is an elongated, C-shaped structure, with hippocampi from each hemisphere leaning together at the top and spread apart at the base, with a septotemporal axis running from the septal nuclei rostrally ("septal pole") to the temporal cortex ventrocaudally ("temporal pole")[10] (Fig.1). In both humans and rodents, the hippocampal formation consists of the following regions: dentate gyrus (DG), hippocampus, subiculum, presubiculum, parasubiculum and the entorhinal cortex (EC). The hippocampus itself is divided into three subdivisions: CA1, CA2 and CA3, which contain densely, packed pyramidal neurons and more loosely arranged interneurons. CA is an abbreviation of "Cornu Ammonis", a Latin designation for the shape of the hippocampus that resembles the ram's horn of the Egyptian god, Amun. CA2 is a marginal region and is mainly a

transition between the CA1 and CA3 fields[11]. Pyramidal neurons in these latter two fields are morphologically and neurochemically distinct, although they are generated from the same precursor cells.

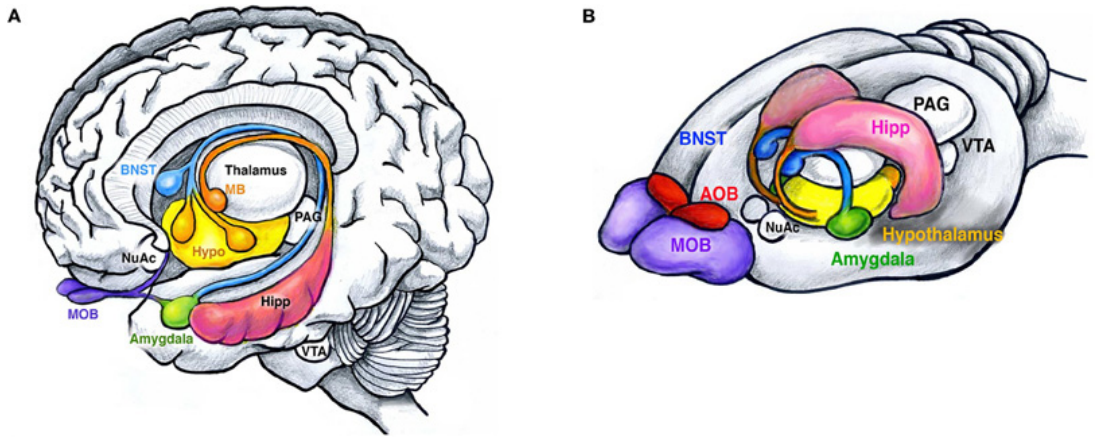

Figure 1: **Hippocampus location in the human and rodent brain.**
(A) Human brain showing the hippocampus (pink) attaching with the mamillary bodies (orange) through the fimbria-fornix. (B) Hippocampus (pink) location in the rodent brain. The images in A and B also show: the amygdala (green), bed nucleus of stria terminalis (BNST, blue), hypothalamus (yellow), main olfactory bulbs (MOB, purple), the nucleus accumbens (NuAc), ventral tegmental area (VTA), and the periaqueductal gray (PAG). In rodents (B), the olfactory bulbs are enlarged when compared to humans. Image B also shows the accessory olfactory bulbs (AOB, red)[12].

1.1.2. Hippocampal connections

The basic circuit of the hippocampus involves the DG, CA3 and CA1 areas establishing a tri-synaptic loop[13]. A major external input into the hippocampus is from the perforant pathway that comprises axons from layer II of the EC projecting to the DG granule cells. Perforant path axons innervate the outer and the middle third of granule cell dendritic trees. Granule cells of the DG project axons (mossy fibers) to pyramidal neurons within the CA3 area and these, in turn, project axons (Schaffer collaterals) to ipsilateral CA1 pyramidal neurons and contralateral CA3 and CA1 pyramidal cells through commissural connections. CA1 pyramidal neurons extend axons out of the hippocampus, which synapse in the subiculum and deep layers of the EC. This is the simplest synaptic circuit in the hippocampus, but there are several other pathways. For

instance, the CA1 area receives direct inputs from the CA3 subfield, EC layer III and the thalamus (the latter of which projects only to the terminal apical dendritic trees of CA1 pyramidal neurons). The hippocampal area is also innervated by commissural fibers from the contralateral hippocampus as well as receiving sub-cortical inputs from several different regions of the brain[11,13] (Fig.2).

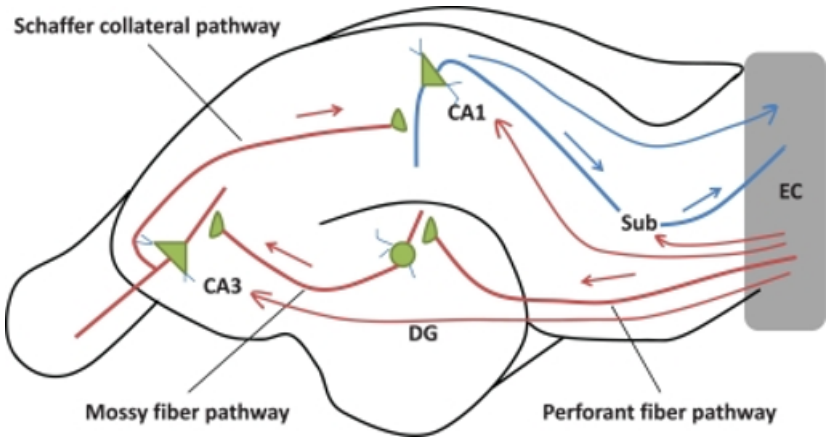

Figure 2: **Input and output pathways in the mouse hippocampus.**
The entorhinal cortex (EC) projects to the dentate gyrus (DG) *via* the Perforant fiber pathway. Granule cells of the DG project axons to CA3 neurons *via* the Mossy fiber pathway. In turn, CA3 neurons provide input to CA1 neurons through the Schaffer collateral pathway. CA1 neurons project fibres out of the hippocampus to synapse in the subiculum (Sub) and EC. Additionally, the EC can also project directly to CA3, CA1 and Sub. The EC is the major output of the hippocampus. The diagram represents a coronal section of the adult mouse hippocampal formation[14].

The CA regions of the hippocampus are stratified into the following different layers: the alveus (mainly composed of myelinated hippocampal, subiculum and fimbria efferents); stratum oriens (the innermost layer contains the basal dendrites of pyramidal neurons); stratum pyramidale (contains the cell bodies of pyramidal neurons); stratum lucidum (only present in CA3 where mossy fibers terminate); stratum radiatum (contains the proximal apical dendrites of pyramidal neurons and receives commissural fibers input from the contralateral hippocampus); stratum lacunosum (area in CA1 and CA2 that receives myelinated Schaffer collateral input from CA3); stratum moleculare

(the most superficial layer in the hippocampus associated with distal apical dendrite terminal arborization and input of perforant pathway fibers from the EC). With the exception of the alveus, all CA field strata also contain the soma of interneurons[4,11,15] (Fig.3).

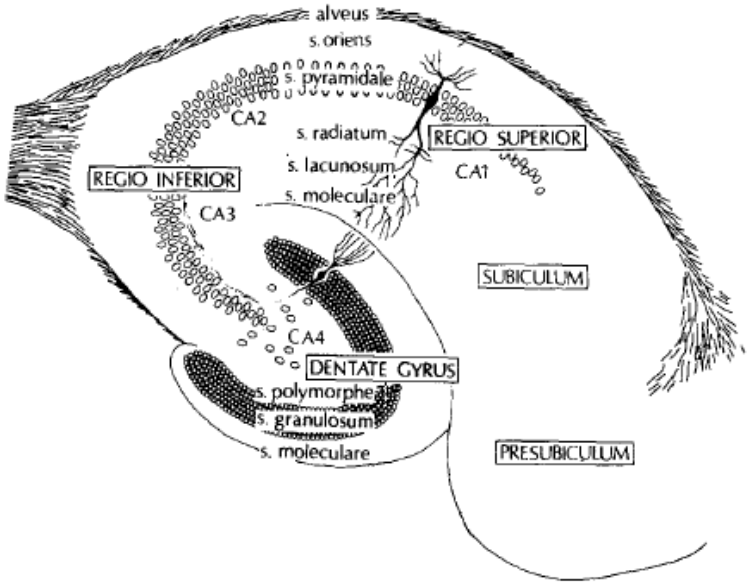

Figure 3: Hippocampal formation.

In this image the dentate gyrus (DG), CA3, CA2 and CA1 fields, the subiculum and presubiculum of the hippocampal formation are represented. Also represented, the different layers in the CA area and in the DG. The diagram represents a coronal section of the adult mouse hippocampal formation[15].

1.1.3. Hippocampal neurons

The mature hippocampus contains glial cells, pyramidal neurons, DG granule cells and interneurons, the latter of which represent less than 10% of the total number of hippocampal cells[5,7]. Whilst neurogenesis begins in the mouse hippocampal primordium at E10.5, the majority of cells present in this structure at E14.5 are still proliferating. In mice, CA3 pyramidal neurons are predominantly generated between E14 and E15 and CA1 pyramidal neurons between E15 and E16[5,6]. The hippocampal regions are intrinsically determined early in neurogenesis and the initial specification of CA1 and CA3 neurons might begin as early as E10.5-E12.5. When isolated at this stage, telencephalic tissue can independently generate features of the patterned fields[5]. From E14.5 to E18.5, pyramidal cells undergo radial migration from the ventricular zone to the hippocampal plate, the future pyramidal layer, via the intermediate zone[9].

During this period, hippocampal neurons also start to undergo neurochemical and functional maturation, a process that extends into the postnatal period[3,9]. At the same time, afferents also extend into the hippocampus[16,17]. Entorhinal axons first enter the mouse hippocampus at E15. At E17, entorhinal fibers appear within the stratum lacunosum-moleculare and the first axons invading the outer molecular layer of DG are evident at E19. Commissural fibers begin to innervate the contralateral hippocampus at E18, targeting the stratum oriens and radiatum. From P2 onwards, commissural fibers are seen terminating in the inner zone of the molecular layer of the DG[16,17].

GABAergic interneurons in the hippocampus provide inhibitory input to control the activity of glutamatergic, excitatory pyramidal neurons and DG granule cells. GABAergic interneurons exert their inhibitory control on the activity of glutamatergic neurons through the activation of postsynaptic GABA receptors. Some interneurons also establish inhibitory synapses with other interneurons. Interneurons are generated in the developing hippocampus before pyramidal neurons and DG granule cells[3,18,19]. Most CA1 and CA3 GABAergic interneurons are generated between E12 and E13, whereas the majority of DG interneurons are born between E13 and E14. Whilst glutamatergic pyramidal neurons originate from the neuroepithelium in the ventricular zone of the dorsal telencephalon and migrate radially across the intermediate zone towards the hippocampal plate[3], the origin and migration path of hippocampal GABAergic interneurons is still not certain. To date, the available evidence has suggested that a large number of GABAergic interneurons originate in the subpallium telencephalon, migrate tangentially, and populate several areas of the cortex, including the hippocampus[18,19].

In contrast to pyramidal neurons and interneurons, 85% of DG granule cells are born postnatally[2,3,7,9]. Most hippocampal glial cells are also generated postnatally from the same multipotent neuroepithelial progenitors that produce hippocampal neurons earlier in development. Astrocytes are generated first followed by oligodendrocytes[20,21].

Pyramidal neurons have a triangular soma and are polarized, with a single axon and multiple dendrites. The dendrites of mature hippocampal pyramidal neurons display numerous spines, small protrusions from the dendritic shaft, which increase the area available for synaptic contacts. The morphology and development of rat hippocampal pyramidal neurons has been well studied in several *in vitro* models. According to Dotti et al.[22], the polarization of late embryonic rat hippocampal neurons in culture follows 5 well-characterised stages (Fig.4). Shortly after the neurons are plated, it is possible to recognize lamelipodia around the cell bodies (Stage 1). Within 12 hours of culture, these lamelipodia give rise to minor processes or neurites (Stage 2). Over the following 12-24 hours, neurons undergo initial polarization, so that by 1.5 days *in vitro* (DIVs) it is possible to distinguish the axon that has started to grow from one of the minor processes (Stage 3). By 4DIVs the remaining neurites start to develop into dendrites (Stage 4). The rate of axonal growth is 5 to 10 times greater than the rate of dendritic growth. Subsequently, by 7DIVs, the neurons are mature and start to establish synaptic connections with their neighbouring neurons (Stage 5)[22-25].

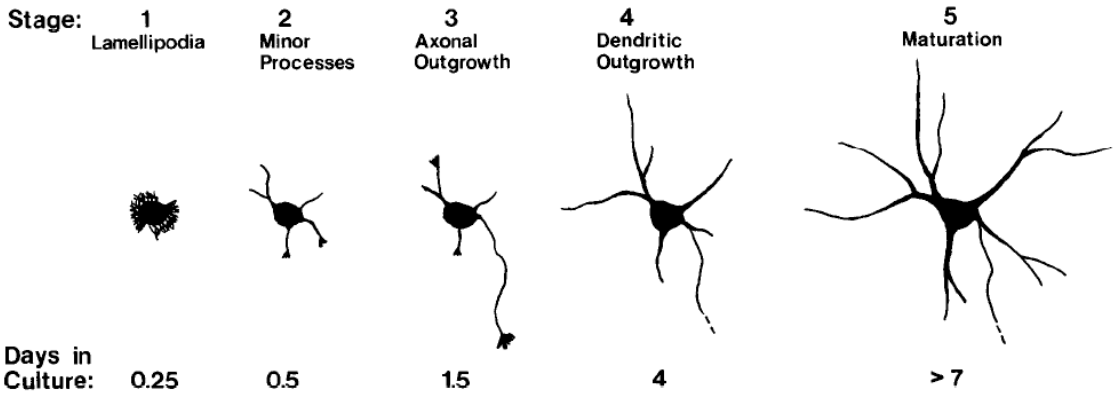

Figure 4: **The 5 stages of development of hippocampal neurons *in vitro*.**
Each stage corresponds to a number of days in culture[22].

Axons differ from dendrites morphologically and functionally, but they also diverge in their distribution of molecules and organelles. For example, polyribosomes and messenger RNA (mRNA) are largely excluded from the axon but are highly abundant within the somatodendritic compartment[26].

Furthermore, axons and dendrites contrast in their distribution of the microtubule-associated proteins (MAP), tau (axonal) and MAP-2 (somatodendritic). Microtubule orientation also differs between axons and dendrites. In axons, microtubules are uniformly oriented with their plus ends distal to the cell body, whereas microtubules are present in both polarity orientations in dendrites[27,28].

Actin filaments and microtubules are necessary to establish and maintain polarity in neurons by converting molecular signals into structural changes[29]. Axonal growth and, consequently the establishment of neuronal polarity, take place at the tip of the growing axon in a highly motile and specialized cellular compartment, the growth cone[30]. The axonal growth cone is composed of a central domain (C-domain), in which microtubules enter to polymerize and transport organelles and vesicles to the area, and a peripheral domain (P-domain) that is highly dynamic and comprises actin filament-rich lamellipodia and filipodia. The C- and P-domains are separated by a transitional zone (T-zone), where microtubules and the minus-ends of actin filaments interact, and it is the dynamic interplay among these structures that leads to neurite extention[30,31].

Traditionally, axons extend continuously following three stages that are influenced by environmental cues: protrusion, engorgement and consolidation (Fig.5). Barbed, fast growing plus-ends of actin filaments (F-actin), which are orientated towards the plasma membrane, continuously incorporate ATP-bound G-actin monomers. Newly incorporated actin monomers are effectively retrogradely transported along the actin filament, as further new monomers are added to the plus end, until they reach the minus-end of the actin filament where bound ATP is hydrolysed to ADP and they are released as monomers. ADP-bound G-actin monomers exchange ADP for ATP and are transported back to the plus end of the actin filament for further incorporation into F-actin. The result of this treadmilling is that actin filaments do not increase in net length, in a static growth cone[32]. During the protrusion phase, the P-domain of the growth cone contacts with a substrate leading to an increase in actin polymerization in the P-domain resulting in filipodial elongatation and foward movement of lamellipodia. At the same time there is a retrograde flow by which

the actin network and the adjacent membrane is pulled back. F-actin retrograde flow is driven both by contractility of the motor protein myosin II, and the 'push' from F-actin polymerization in the P domain. The myosin-dependent contraction together with the retrograde flow leads to a condensation of actin arcs and microtubules, in the C-domain, that suppresses actin polymerization and protrusion.

This phenomenon leads to the second step of axon extention: engorgement. As a result of the retrograde flow, actin filaments disassemble in the T-zone and actin arcs reorient towards the growth direction originating a neurite shaft that is occupied by microtubules (which are guided by the T-zone actin arcs and C-domain actin bundles) and, subsequently, by vesicles and organelles forming the new axonal area[33,34]. Finally, consolidation occurs when the F-actin at the neck of the growth cone depolymerizes and the filopodia retract away from the area of new growth, promoting axon shaft consolidation[30,32] (Fig.5).

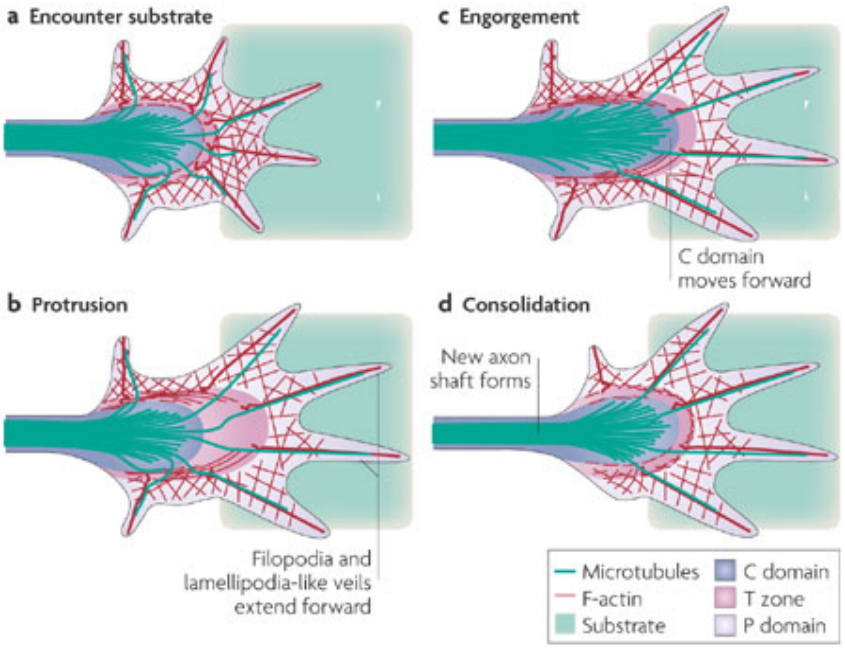

Figure 5: Stages of Axon outgrowth.

The axon outgrowth process occurs at the tip of the growth cone. After (a) encountering an attractive and adhesive substrate the growth cone progress by a sequence of three define stages (b) protrusion, (c) engorgement and (d) consolidation[30].

Conversely, the future dendrites have static growth cones with a rigid actin cytoskeleton and less dynamic properties. As mention before, microtubules are present in both polarity orientations in dendrites. However, during stage 4 of development, in hippocampal neurons, minus-end distal microtubules in dendrites emerge first, and by stage 5 both microtubule orientations are equally abundant in proximal dendrites. In more distal dendrites, however, plus-end out microtubules dominate[27]. Studies suggest that motor proteins differentially organize the orientation of axonal and dendritic microtubules. For instance, the mitotic microtubule-based motor CHO1[35] and structural MAPs, such as MAP2[36] and MAP1A[37] are enriched in dendrites and are implicated in dendritic differentiation and maintenance. Suppression of one of these genes leads to inhibition of dendritic differentiation and branching. The axonal exclusion or reduced levels of these proteins may also explain the reason why microtubules are only oriented in dendrites with a mixed polarity[38].

Specific microtubule associated proteins have been identified that influence axon specification and elongation. For example, collapsin response mediator protein-2 (CRMP-2) is preferentially associated with microtubules within axons, although it also binds tubulin dimers. The association of CRMP-2 with both tubulin dimers and polymers promotes rapid microtubule assembly and increases axonal length. Overexpression of CRMP-2 enhances axonal elongation from cultured hippocampal neurons, whereas expression of a mutant form of CRMP-2 reduces axonal length[39]. Regulators of actin cytoskeleton dynamics, in particular the Rho family of small GTPases comprising Rho, Rac, and Cdc42, have also been shown to play important roles in establishing neural polarity and neuronal morphology. For example, transgenic mice overexpressing a constitutively active mutant form of Rac1 display a significant reduction in the number of Purkinje cell axon terminals in deep cerebellar nuclei with no changes in dendritic tree complexity[40]. In *C. elegans,* Cdc42 and Rac1 activated forms associate with a complex consisting of the polarity inducing scaffold proteins Par3 and Par6 and the atypical protein kinase C (aPKC). Par3 and Par6 are initially distributed at the tip of all the processes of cultured embryonic rat hippocampal neurons prior to axon specification[41]. As axon

growth is initiated, local phosphatidylinositol 3-kinase (PI3K) activity leads to the redistribution of Par3 and Par6, so that they become selectively localised at the tips of elongating axons and absent from putative dendrites[42]. Interestingly, the overexpression of either Par3 or Par6 prevents the specification of a single axon. In addition to the intrinsic signals described above, extrinsic signals, such as neurotrophic factors, can modulate neuron polarity during morphological development[41].

Although pyramidal neuron apical and basal dendrites develop more side branches after birth, dendritic structure is still very simple until afferent synapses invade the hippocampal region by postnatal days 3-5 (P3-5). At this point, dendrites reach their full potential in terms of elongation, branching, pruning and dendritic spine development, acquiring mature dendritic morphology by P20 in the rat. The pattern of mature dendritic arborisation is determined by a combination of cell intrinsic programs and extrinsic micro-environmental cues[7]. There are five main processes through which mature dendritic arbours are formed. First, dendrites grow and acquire a shape and function that is distinct from axons. This step seems to be modulated, at least to some extent, by neurotrophic factors. Second, dendrites grow towards a defined target so that correct neuronal connections can be established. Semaphorin-3A (Sema3A) is a key molecule that regulates both axon and dendrite guidance in the nervous system. In accordance with this, Sema3A deficient mice show defects in the guidance of cortical pyramidal neuron dendrites[43]. Third, dendritic branches are formed at defined intervals. Fourth, mature dendrites develop dendritic spines. Dendritic spines are micron-sized protrusions of the dendritic membrane that receive over 90% of excitatory input and are highly dynamic[44]. They are found on both excitatory and inhibitory neurons including, glutamatergic pyramidal neurons of the neocortex and hippocampus and GABAergic cerebellar Purkinje neurons. The number and shape of dendritic spines are varied and highly changeable and are regulated by both physiological and pathological events[45]. Actin filaments dynamics are the main driver behind changes in spine number, shape and function[46,47]. Since, as mentioned above, Rho GTPases play an important role in regulating the actin

cytoskeleton, Rho GTPases are major effectors of changes in spine number, shape and size, thereby tuning synaptic strength. Inhibition of Rac1 in hippocampal organotypic cultures induces long and thin spines and reduces spine growth and motility. In contrast, new and protrusive dynamic spines are produced in the absence of Rho kinase activity[48]. In the final stage of dendrite development, dendrites are precisely controlled to stop growing and acquire their mature shape[49,50]. An important consequence of the intricate control of dendrite growth and branching is that mature hippocampal pyramidal neuron dendrites are spatially arranged so that they are non-overlapping, a phenomenon known as tiling[51]. Since, tiling avoids the clumping and overlapping of dendrites, it maximises the available dendrite surface that can receive afferent synaptic input. Tiling is brought about by contact-mediated mutual repulsion of dendrites between similar neurons; a process that is controlled by a number of recently identified cell surface molecules in invertebrates[51]. The molecular mechanisms that regulate tiling in the mammalian nervous system are currently largely unknown.

1.1.4. Hippocampal functions and associated neuropathologies

The hippocampus has been widely studied due to its roles in learning[52], memory[53], navigation and spatial orientation[54-56].

In 1957, Scoville and Milner reported a case study of a patient whose epileptic seizures were ameliorated following the bilateral removal of the medial temporal lobe. Consequently, the patient suffered a severe loss of memory of the events immediately prior to the surgery, as well as a partial retrograde amnesia of events in the three years leading up to his operation. The patients' cognitive, perceptual and motor learning abilities remained unaltered. These observations suggested that the hippocampal area plays a critical role in our declarative memory: the memories that can be consciously recalled, such as facts, knowledge and personal experience[53,57].

Memories are believed to be stored in the brain's synaptic connections, particularly within the hippocampus. Therefore, synaptic plasticity is widely considered to be the cellular mechanism behind learning and memory[58]. One of the most studied forms of synaptic plasticity is long-term potentiation (LTP)

within the hippocampus. LTP is an electrophysiological measure of a sustained increase in synaptic efficacy or strength. LTP can be divided into early-phase (E-LTP) and late-phase (L-LTP) events that are induced by different mechanisms and have different properties[59]. E-LTP last for 1-2 hours following a single high frequency burst of electrical activity and consists of the modification of existing synapses. E-LTP results from the phosphorylation of post-synaptic proteins, induced by rapid calcium (Ca^{2+}) influx through NMDA channels and the activation of Ca^{2+} regulated cytosolic proteins, together with the phosphorylation of pre-synaptic proteins by a process that is facilitated by the neurotrophin brain-derived neurotrophic factor (BDNF)[58,59]. E-LTP is responsible for short-term memory or episodic memory. L-LTP results from repetitive high frequency bursts of electrical activity and lasts from several hours to several days. L-LTP requires new mRNA and protein synthesis to induce structural changes in dendritic spines and synapses and alterations in the repertoire and expression levels of synapse related proteins. L-LTP appears to be facilitated by BDNF that is released from hippocampal neurons in an activity dependent manner[58]. L-LTP plays a role in the formation of long-term memory (LTM) and learning[52,58,59]. The roles of BDNF in E-LTP, L-LTP, LTM and learning will be further discussed below.

Perturbations of normal hippocampal circuitry and function underlie many common neuropathological conditions. For example, the hippocampus is the primary brain structure affected in Alzheimer's disease. Post-mortem analysis of the hippocampi from Alzheimer's sufferers and rodent models of Alzheimer's disease have revealed that the disease is associated with the loss of cholinergic afferents from basal forebrain neurons[60]; the emergence of pyramidal neurons with dystrophic dendrites possessing a reduced number of spines[61] and a reduction in synaptic transmission and reduced synaptic plasticity[62]. Together, these abnormalities lead to the reduction of synaptic connectivity within the hippocampus and, consequently, the well-established symptoms of Alzheimer's disease such as memory decline, disorientation and ultimately amnesia. Epilepsy in humans and animal models is associated with extensive neuronal loss within the hippocampal formation (pyramidal neurons, DG granule cells, EC

neurons, subiculum neurons and interneurons) and aberrant axon collaterals that result in the formation of new circuits and disruption of existing circuits[63,64]. Another important neuropathy associated with hippocampal damage is schizophrenia. A decreased number of hippocampal interneurons and a generalised shrinkage of the hippocampus have been frequently reported[65,66]. Post-mortem and magnetic resonance imaging studies have shown that major depressive disorder (MDD) is also associated with a reduction in volume of the hippocampal formation[67]. Chronically elevated levels of circulating glucocorticoids appear to be the underlying cause of hippocampal formation shrinkage in MDD. The reduction in volume of the hippocampal formation does not appear to be due to significant neuronal death, but may reflect the retraction of pyramidal neuron dendritic arbours, the loss of glial cells or a decrease in adult neurogenesis within the DG[67].

Active adult neurogenesis occurs in the subgranular zone (SGZ) of the DG, where new DG granule cells are generated, and in the subventricular zone of the lateral ventricles, where newly generated neurons migrate through the rostral migratory stream to the olfactory bulb[68]. In the case of the SGZ, newly generated, immature neurons migrate into the inner granule cell layer and differentiate into DG granule cells. Newly born granule cells project their dendrites into the molecular layer and their axons to the CA3 pyramidal cell layer to establish new synaptic connections. From a functional point of view, hippocampal neurogenesis plays an important role in structural plasticity and network maintenance[68]. Newborn neurons are critical for learning and memory and exhibit hyper-excitability and enhanced synaptic plasticity of their glutamatergic inputs during a critical period of maturation in the hippocampus[69]. Interestingly, the induction of LTP at perforant pathway-granule cell synapses stimulates the proliferation of progenitor cells in the DG and promotes the survival of newly differentiated neurons[70].

Behavioural studies have attempted to correlate the number of newborn granule cells with an animal's cognitive ability; however, results have been inconsistent[71]. Nevertheless, some studies have indicated that adult neurogenesis is required for certain hippocampus-dependent tasks, but not

others. For instance the ablation of adult neurogenesis in rats by methylazoxymethanol acetate (MAM) treatment prevents the improvement of long-term recognition memory by environmental enrichment in rats[72,73].

Aberrant adult neurogenesis appears to contribute to neuropathological conditions. For example, the induction of seizures in rats by kainic acid administration induces increased SGZ progenitor proliferation that is associated with long-term cognitive impairment[74]. Key molecules involved in Alzheimer's disease pathogenesis, such as ApoE, presenilin-1 (PS1), and amyloid precursor protein (APP) and its metabolites, have been shown to modulate hippocampal neurogenesis[75]. Alterations in hippocampal neurogenesis have been demonstrated at very early stage of Alzheimer's disease progression, and it is possible that these perturbations in neurogenesis may exacerbate neuronal vulnerability to the causative agents of Alzheimer's disease, enhance disease progression and contribute to memory impairment[75]. Furthermore, although a reduction in neurogenesis by itself is not likely to induce depression, antidepressant treatments increase neurogenesis in the DG[76].

1.2. Regulation of neuron survival and outgrowth

1.2.1. The "neurotrophic hypothesis"

In the developing nervous system, more neurons are generated than the ones required in the adult. Initial observations in the developing peripheral nervous system (PNS) of chick and rodents revealed that many newly generated neurons die shortly after their axons reach their target fields[77-79]. This developmental neuronal death removes superfluous neurons and matches the number of neurons to the density of target field innervation that is required. According to the "Neurotrophic Hypothesis" the target field contains limiting amounts of survival promoting neurotrophic factors and only the neurons that are able to obtain sufficient amounts of neurotrophic factor support will survive[80]. Depending on the peripheral ganglion in question, 20% to 80% of neurons will not obtain sufficient neurotrophic factor support from their target fields and will therefore die by apoptosis. This hypothesis was initially formulated and supported by experiments demonstrating that Nerve Growth Factor (NGF), the first neurotrophic factor to be identified, promotes the *in vitro* survival of developing chick and rodent sympathetic neurons and some kinds of peripheral sensory neurons[77,79,81,82]. More recently, this *in vitro* data has been supported by *in vivo* evidence[80,82,83]. Anti-NGF antibodies administered during the phase of target field innervation eliminate NGF dependent neurons, whereas the addition of exogenous NGF prevents developmental neuronal death in these populations. Moreover, *NGF* knockout (KO) mice and mice with a null mutation in the gene encoding the NGF receptor, tropomyosin-related kinase A (TrkA), display a significant loss of NGF dependent neurons compared to wild type (WT) mice[80,82-85]. Over time, the neurotrophic hypothesis has been modified in the light of new data demonstrating that neurotrophic factors promote differentiation, target field innervation, axon terminal arborisation and regulate the functional properties of neurons, in addition to supporting neuronal survival[80]. Moreover, some developing peripheral neurons require the sequential support of more than one neurotrophic factor as they develop, intermediate target fields can be a source of neurotrophic factor support and some neurotrophic factors can be synthesised by neurons themselves and act in a paracrine and/or autocrine manner within ganglia. In addition, the

neurotrophic hypothesis does not apply to some populations of CNS neurons (see 1.2.3. below). Nonetheless, the neurotrophic hypothesis has largely stood the test of time and remains the best explanation of how peripheral neuron numbers are matched to the functional requirements of target fields[80].

1.2.2. The Neurotrophin family of neurotrophic factors

Since the discovery and characterisation of NGF, three other homologous proteins have been discovered in mammals: BDNF, neurotrophin-3 (NT-3), and neurotrophin-4 (NT-4). Together, NGF, BDNF, NT-3 and NT-4 make up the Neurotrophin family of neurotrophic factors that act directly on neurons to support their survival, target field innervation, functional differentiation and maturation and synaptic activity[83,86]. These four molecules are structurally and functionally related and are synthesised and secreted by innervated target organs, endocrine cells, cells from the immune system, glial cells, and neurons. Neurotrophins are functional as non-covalent homodimers and signal through two types of receptors: the Trk (tropomyosin-related kinase) receptors that belong to the tyrosine kinase family, and p75NTR (p75 neurotrophin receptor), which is a common receptor for all the neurotrophins[87-89]. p75NTR belongs to the tumour necrosis factor (TNF) receptor superfamily (TNFRSF) and has a death domain, a region of approximately 80 amino acid residues, in the intracellular cytoplasmic domain.

The Neurotrophins preferentially bind to one member of the Trk family. NGF preferentially binds to TrkA, BDNF and NT-4 to TrkB and TrkC is the preferred receptor for NT-3, although NT-3 displays promiscuity and can also bind to and activate TrkA and TrkB in the absence of p75NTR expression[88,89] (Fig.6). Upon binding to their cognate Trk receptor, neurotrophins induce receptor dimerization and subsequent phosphorylation of multiple tyrosine residues in the intracellular tyrosine kinase domain. Adaptor proteins, such as Shc and Frs2, bind to phosphorylated tyrosine residue 490 and initiate intracellular signalling cascades, such as the Ras/extracellular signal regulated kinase (ERK) and PI3K/Ak transforming/protein kinase B (Akt/PKB) pathways. Activation of these pathways enhances neuronal survival, differentiation and maturation, promotes target field innervation and regulates the functional

properties of neurons[89]. In addition, phospholipase C gamma (PLCγ) binds directly to phosphorylated tyrosine residue 785, leading to Ca^{2+} and protein kinase C (PKC) mobilization, enhanced process outgrowth and synaptic plasticity[89] (Fig.7).

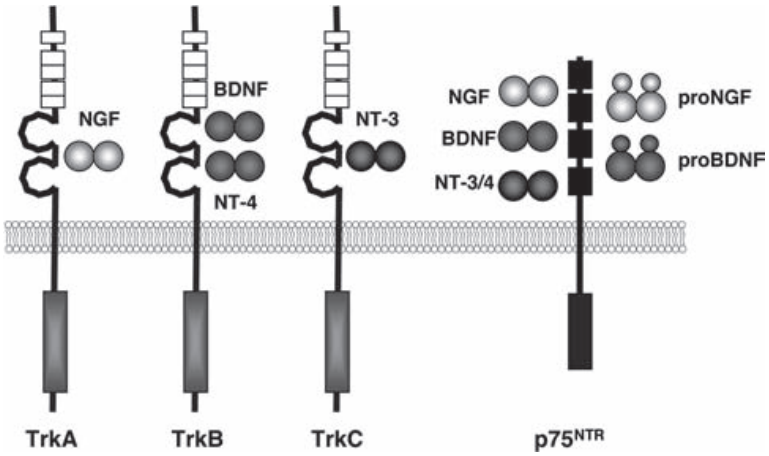

Figure 6: **The Neurotrophin family of neurotrophic factors and their receptors.**
NGF binds to TrkA, BDNF and NT-4 to TrkB and NT-3 to TrkC. All the Neurotrophins can bind to the common p75NTR receptor. Pro-NGF and pro-BDNF can also interact with p75NTR, but not Trk receptors[88].

Neurotrophin signalling from the p75NTR can have different outcomes depending on whether the cognate Trk receptor is expressed and whether other non-Trk receptors are present. For example, p75NTR can potentiate signalling by TrkA to enhance NGF-promoted survival and target field innervation as well as increasing the specificity of Trk receptors for their preferred neurotrophin[89,90]. In the presence of cognate Trk expression, neurotrophins binding to p75NTR can promote process outgrowth by modulating the activity of the small GTPase, RhoA, and promote survival via activation of nuclear factor-κB (NF-κB) signalling. In the absence of cognate Trk expression, neurotrophin binding to p75NTR leads to apoptosis by a number of signalling mechanisms including: TNF-receptor associated factor 6 (TRAF6) mediated activation of Jun N-terminal kinase (JNK), nuclear translocation of the p75NTR intracellular domain bound to the transcription factor neurotrophin receptor interacting factor (NRIF) and/or interference of PI3K/Akt survival signalling by p75NTR induced generation of ceramide by membrane sphingomyelinase[89,90].

Each of the four members of the neurotrophin family is synthesised as a proneurotrophin precursor protein that is proteolytically cleaved to generate the corresponding mature neurotrophin[91]. The pro-domains of neurotrophins have been shown to play a critical role in ensuring correct protein folding of mature neurotrophins and their subsequent targeting to the secretory pathway. Pro-NGF and Pro-BDNF can induce apoptosis, in the absence of mature neurotrophin induced Trk signalling, by binding to p75NTR. Importantly, the receptor sortilin can form a high affinity pro-neurotrophin receptor complex with p75NTR that more efficiently signals cell death than p75NTR alone[91].

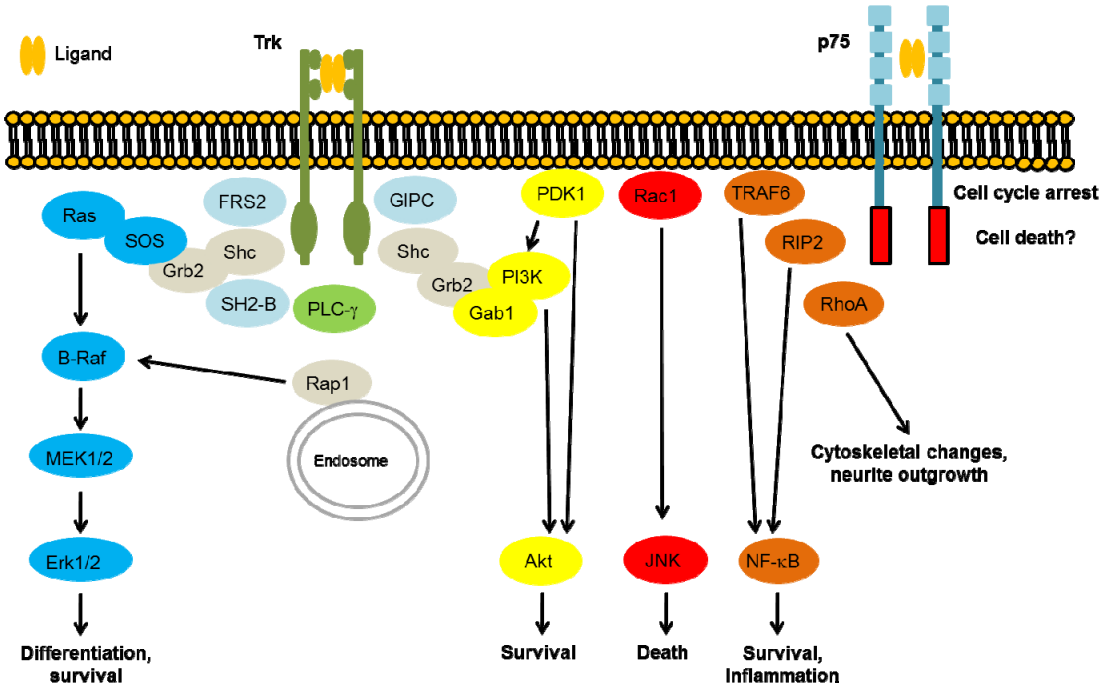

Figure 7: Neurotrophin receptor signalling.

Following ligand binding, Trk receptors recruit and promote the phosphorylation of PLC-γ and adaptor proteins, such as Shc and Frs2. The recruitment and phosphorylation of adaptor proteins leads to the subsequent activation of PI3K and ERK signalling pathways and enhanced neuronal differentiation and survival. p75NTR receptor ligation leads the recruitment of adaptor proteins, like TRAF6, RIP2 and Rac1, and the subsequent activation of NF-κB and/or JNK signalling pathways and/or the modulation of RhoA activity. Depending on the cellular context, p75NTR can promote neuronal survival, apoptosis, neurite elongation or growth arrest (adapted[92]).

In addition to the neurotrophins, a number of other protein families have been identified that regulate the differentiation, survival, growth, maturation and functional properties of certain population of CNS and PNS neurons. These include; the glial cell-derived neurotrophic factor (GDNF) family (GDNF, neurturin, artemin and persephin)[93], the neurotrophic cytokines (ciliary neurotrophic factor (CNTF), leukaemia inhibitory factor (LIF), oncostatin-M (OSM), cardiotrophin-1 (CT-1) and interleukin-6 (IL-6))[83], the hepatocyte growth factor (HGF)[94] and the macrophage-stimulating protein (MSP)[95]. With the exception of a potential role for GDNF in promoting synapse formation in the hippocampus[96], there is little experimental evidence, to date, suggesting that members of these protein families play significant neurotrophic roles in the developing and adult hippocampus. For this reason, the biology of these neurotrophic factors and their receptors will not be discussed further.

1.2.3. The roles of Neurotrophins in the Hippocampus

The highest concentrations of NGF mRNA within the CNS are found in the cortex and hippocampus[97], major targets of the TrkA-positive, NGF-responsive cholinergic neurons of the basal forebrain nuclei[98]. Recent studies examining mice with CNS specific conditional deletions of TrkA and NGF has revealed that, contrary to the neurotrophic hypothesis, NGF/TrkA signalling is not required to support the developmental survival of the vast majority of basal forebrain cholinergic neurons (BFCNs). However, NGF/TrkA signalling is required for the correct development of cholinergic circuitry within the hippocampus and for enhancement of the cholinergic phenotype[99,100]. The levels of NGF within the hippocampus are modulated by BFCN induced depolarization of hippocampal neurons[101,102]. NGF, via its modulation of BFCN function, has been shown to play a role in facilitating hippocampal LTP in the adult rat brain[103,104]. NGF also appears to directly contribute to LTP in the rat DG by direct activation of TrkA on DG neurons[105] and infusion of exogenous NGF into the lateral ventricles of rats improves LTM formation by a mechanism that is associated with the phosphorylation of hippocampal TrkA, an increase in the expression of synaptic proteins and an increase in the number and maturity of dendritic spines on dendrites projecting from CA3 pyramidal neurons[106].

Whilst TrkA expression is low in the adult rodent hippocampus[107], embryonic mouse and rat hippocampal neurons express TrkA in culture and NGF rescues these neurons from glutamate or staurosporine induced apoptosis[108]. The anti-apoptotic effects of NGF require both TrkA and p75NTR signalling. NGF also promotes axon elongation from cultured mouse embryonic hippocampal neurons by a mechanism that is mediated by p75NTR and involves activation of casein kinase 2 (CK2), inhibition of PTEN and subsequent phosphorylation and inhibition of glycogen synthase kinase-3 beta (GSK-3β)[109]. In addition, p75NTR mediated NGF signalling regulates dendrite morphology in cultures of embryonic mouse hippocampal neurons. NGF reduces the number of primary dendrites and promotes the elongation of remaining dendrites by protein tyrosine phosphatase 1B (PTP1B) mediation of NF-κB activation[110,111].

NT-3 and TrkC mRNAs are both expressed at high levels in the developing and adult rodent hippocampus[107,112,113]. Despite this, NT-3 only marginally increases the survival of E17 rat hippocampal neurons cultured for 6 days in defined medium[114] and does not enhance the survival of E18 rat hippocampal neurons after 8 days in culture[115]. However, NT-3 does induce TrkC phosphorylation, c-fos protein expression and the activation of p21Ras and mitogen-activated protein kinase (MAPK) in embryonic rat hippocampal cultures, in addition to promoting the expression of calbindin-D_{28K} in a sub-population of pyramidal neurons[115,116]. NT-3 also promotes the expression of the dendritic marker, MAP-2 and the synaptic marker, synapsin1 in cultures of E16 rat hippocampal neurons[117]. Interestingly, It appears as if spontaneous activity within pyramidal neurons leads to glutamate mediated autocrine release of NT-3, which then promotes the expression of calbindin-D_{28K} [118].

NT-3 promotes the formation of active excitatory synapses in long-term cultures of E16 rat hippocampal neurons by increasing the number and density of membrane docked pre-synaptic vesicles in the absence of significant morphological changes to dendrite architecture[119]. The role of NT-3 in hippocampal synaptogenesis and synapse maturation has been investigated in TrkC null mutant mice[120]. The loss of NT-3/TrkC signalling does not alter the innervation of the hippocampus by the EC and commissural afferents per se,

nor does it alter the topographical pattern of hippocampal connections. However, *TrkC* mutant pups display a reduction in the number of axon collaterals associated with EC and commissural afferents together with a reduction in the expression of pre-synaptic proteins associated with vesicle exocytosis and neurotransmitter release[120].

In addition to regulating synaptogenesis, NT-3 modulates dendrite morphology in short-term (4-6 days) cultures of embryonic rat hippocampal neurons. NT-3 reduces the complexity and length of dendrites in these cultures by a mechanism that involves PLC-γ mediated opening of the non-selective cation channel, TrpC5, subsequent influx of Ca^{2+} and Ca^{2+} dependent activation of Ca^{2+}/calmodulin-dependent protein kinase II (CaMKII)[121]. In contrast, NT-3, promotes axon elongation and branching from E18 rat hippocampal neurons after 48 hours in culture[122].

The neurotrophic properties of BDNF have been extensively investigated within the hippocampus. BDNF expression in the developing hippocampus is relatively low during the embryonic period and increases markedly during the first few postnatal weeks[123]. Whilst exogenous BDNF does not promote the survival of embryonic rat hippocampal neurons cultured at high-density[114], it does enhance their survival in low-density cultures[124]. This, together with the observation that hippocampal neurons from *Bdnf* null mutant mouse embryos show reduced survival compared to wild type neurons in high-density cultures, suggests that autocrine BDNF normally supports hippocampal neuron survival in high-density cultures[124]. Despite this, *Bdnf* null mutant mice do not display an overt loss of neurons in the hippocampus, although these mice die soon after birth before the hippocampus is fully developed[125,126]. Conditional *Bdnf* KO mice, that lack BDNF specifically in the CNS and survive to adulthood, also show no significant hippocampal neuron loss[123]. Similarly, mice with a reduced expression of TrkB do not have a reduced number of pyramidal neurons or interneurons within CA1, although they display a significant loss of cortical pyramidal neurons[127].

BDNF increases dendrite number and dendrite branching in cultures of embryonic rodent pyramidal neurons[128,129]. However, BDNF does not seem to

regulate dendritic complexity in postnatal rodent hippocampal slice cultures[130]. In accordance with this, conditional deletion of *Bdnf* in the mouse CNS does not affect the complexity of CA1 pyramidal neuron dendrites[123].

BDNF has been shown to play an important role in regulating synapse formation and synaptic activity during development, both *in vitro* and *in vivo*. BDNF promotes the formation of excitatory synapses in long-term hippocampal cultures derived from E16 rat embryos[119]. Interestingly, BDNF also increases the number of inhibitory synapses in these cultures, by a mechanism that appears to rely upon BDNF promoted elongation of interneuron axons, thereby suggesting that pyramidal neurons and interneurons within the cultures both express functional TrkB[119]. In accordance with this, late gestation mouse embryos overexpressing BDNF in the CNS display precocious development of GABAergic synapses within the hippocampus and an upregulation of the KCC2 potassium/chloride co-transporter, that turns GABA responses from excitatory to inhibitory, within pyramidal neurons[131]. Whilst BDNF appears to potentiate GABAergic synapse formation and activity in the developing hippocampus, it has been reported to inhibit the GABAergic responses of pyramidal neurons within the adult hippocampus[132]. Acutely applied BDNF enhances excitatory glutamatergic synaptic transmission within 5 minutes in embryonic rat hippocampal cultures[133-135]. It appears as if BDNF mediated enhanced synaptic transmission requires the activation of pre-synaptic TrkB receptors, since viral transfection of a signalling deficient truncated TrkB cDNA into cultured pre-synaptic hippocampal neurons, but not post-synaptic neurons, prevents BDNF induced synaptic potentiation[136].

BDNF can potentially act on pre-synaptic axons and/or post-synaptic dendrites to promote the morphological and molecular changes that lead to synapse formation in the developing hippocampus. The relative importance of these two modes of action has been addressed *in vivo* by using conditional *TrkB* mouse mutants that lack TrkB expression in specific hippocampal neuron populations. Embryonic deletion of TrkB specifically from CA3 neurons results in a significant reduction in the density of CA3 neuron axon varicosities in the basal dendritic field of CA1 neurons and a significant loss of staining for the pre-synaptic marker synaptophysin compared to wild type mice[137]. In contrast, CA1

neuron dendrite complexity and dendritic spine density are not altered and staining for the post-synaptic marker PSD-95 in CA1 is similar to that of wild type mice. Whilst embryonic deletion of TrkB from both CA1 and CA3 neurons does not alter CA1 neuron dendrite size and complexity, it does significantly reduce the number of spines on the dendrites of these neurons and significantly decreases the expression of both synaptophysin and PSD-95. Deletion of TrkB from CA1 and CA3 neurons in the second postnatal month after synapse formation is complete does not alter CA1 dendritic spine number or the expression of pre or postsynaptic markers. Therefore, it suggests that BDNF/TrkB signalling is required both pre- and post-synaptically for correct synapse formation within the developing, but not adult hippocampus[137].

In addition to its role in regulating synaptogenesis and synaptic activity in the developing hippocampus, BDNF is crucial for synaptic plasticity, LTP, long-term depression (LTD) and LTM in the postnatal hippocampus. For example, BDNF increases dendritic spine density on apical dendrites of pyramidal neurons in postnatal rat hippocampal slices[138-140] by a mechanism that is dependent on ERK1/2 activation[130]. Whilst, as mentioned above, exogenous BDNF does not increase the length or complexity of CA1 or CA3 pyramidal neuron dendrites in postnatal slice cultures[130], it does significantly increase the number of basal dendrites and the extent of axonal branching in DG granule cells[141]. In addition to modulating spine density in hippocampal slice cultures, BDNF also increases the number of membrane docked pre-synaptic neurotransmitter vesicles in the synaptic buttons of pyramidal neuron axons and enhances quantal excitatory neurotransmitter release[139].

BDNF can be secreted from pre-synaptic axon terminals and/or post-synaptic spines in an activity dependent manner[58], although the secretion of BDNF from dendrites has recently been questioned[142]. A polymorphism in BDNF, whereby valine (Val) 66 is substituted by methionine (Met), reduces activity dependent BDNF secretion[143]. In addition to enhancing BDNF secretion, neural activity directly promotes the transcription of BDNF[144]. Released BDNF can act either on pre-synaptic terminals or post-synaptic spines at glutamatergic synapses to initiate TrkB dependent signalling pathways and induce LTP. The

role of secreted BDNF in E-LTP has been relatively well characterised. BDNF facilitates the induction of E-LTP by enhancing synaptic responses to tetanus stimulation by a mechanism that is thought to involve the promotion of synaptic vesicle docking and the redistribution and phosphorylation of synaptic proteins[58]. Short-term episodic memory is largely dependent on E-LTP and is impaired in humans carrying the Val66Met BDNF polymorphism demonstrating the important role of activity dependent BDNF secretion in establishing and maintaining E-LTP[143].

As previously mentioned, L-LTP is dependent on new protein synthesis. One of the proteins that is newly synthesised in response to L-LTP inducing stimuli is BDNF itself[58]. The central role of BDNF in establishing L-LTP has been demonstrated by a number of different approaches. For example, there is a significant reduction in theta burst and forskolin induced L-LTP in *Bdnf*$^{+/-}$ mice compared to wild type mice[145,146]. In addition, L-LTP induction is inhibited in hippocampal slices when they are incubated with either an anti-BDNF or TrkB antibody or a TrkB-Fc chimera that sequesters free BDNF[147]. Moreover, L-LTP induction is also impaired in *TrkB* null mutant mice compared to wild type mice[148]. However, L-LTP induced by tetanic stimulation is normal in *Bdnf*$^{+/-}$ mice, suggesting that not all forms of L-LTP require BDNF[149]. Mature BDNF is generated from pro-BDNF by plasmin dependent cleavage, a process that is dependent on the generation of plasmin from plasminogen by tissue plasminogen activator (tPA). Transgenic mice lacking functional tPA and/or plasminogen expression have been used to demonstrate that the conversion of pro-BDNF to mature BDNF by tPA/plasmin is essential for the generation of L-LTP at hippocampal synapses[150]. Interestingly, pro-BDNF appears to regulate NMDA receptor-dependent LTD at hippocampal synapses, an effect that is mediated by p75NTR[151]. By binding to p75NTR, pro-BDNF also induces growth cone collapse, dendritic pruning, a reduction in dendritic spine formation and the removal of synaptic AMPA glutamate receptors from hippocampal neurons[152,153].

There is strong experimental evidence that BDNF plays a role in the acquisition of long-term memory. For example BDNF mRNA levels are increased in the hippocampus of rodents that are given spatial task training such as the Morris water maze (MWM)[154]. Hippocampal BDNF mRNA levels are also increased in aversive and context dependent fear conditioning (CDFC) paradigms[155,156]. In accordance with this, *Bdnf*$^{+/-}$ mice are impaired in MWM acquisition[157] and CDFC[158] compared to wild type mice. Similarly, mice with a conditional postnatal deletion of *TrkB* in the forebrain are impaired in the acquisition of spatial tasks compared to wild type mice[148] whereas mice overexpressing TrkB display enhanced learning capabilities[159]. Moreover, the infusion of an anti-BDNF antibody or antisense BDNF mRNA into the hippocampus of rats before training prevents memory formation and retention in a number of learning paradigms[155,160,161].

1.2.4. Non-Neurotrophin regulators of hippocampal survival, process outgrowth and function

Apart from the Neurotrophins, other examples of secreted proteins that modulate hippocampal neuron survival, process outgrowth and function include the founding members of the TNF and the transforming growth factor β (TGF-β) superfamilies, TNF-α and TGF-β.

In the adult CNS, TNF-α is mainly expressed by microglia and astrocytes, particularly after injury, ischemia or infection, although neurons can also express TNF-α[162,163]. Both TNF-α and TNF receptors have been detected in the developing brain[162,163]. TNF-α can signal through two different receptors, TNFR1, which contains an intracellular death domain, and TNFR2, which lacks a death domain[164]. TNF-α induces apoptosis in 5 days cultures of E15 mouse hippocampal neurons in a dose dependent manner[165]. However, hippocampal neurons in cultures established from *Tnfr1*$^{-/-}$ mice are refractory to TNF-α induced cell death, whereas hippocampal neurons from *Tnfr2*$^{-/-}$ are more susceptible to the apoptotic effects of TNF-α. TNF-α induced activation of TNFR1 promotes apoptosis in hippocampal cultures via NF-κB dependent signalling and activation of TNFR2 by TNF-α promotes hippocampal neuron survival by activating p38 MAPK signalling pathways[165].

In addition to regulating the survival of developing hippocampal neurons, TNF-α also regulates process outgrowth from cultured hippocampal neurons[166]. TNF-α reduces the length and degree of branching of axons and dendrites in glial cell enriched low-density cultures of E16 embryonic mouse hippocampal neurons without affecting neuron survival. Interestingly, culturing hippocampal neurons on activated glial cells that secrete TNF-α can mimic this effect. TNF-α induced reduction in hippocampal neuron process outgrowth and branching is mediated via activation of the GTPase RhoA signalling pathway[166]. TNF-α has been shown to regulate the expression of NGF and BDNF in the developing hippocampus[167]. *Tnf-α*$^{-/-}$ mice contain significantly more NGF protein in the developing hippocampus at P14 and P21, but not in the adult, compared to wild type mice. In contrast, adult *Tnf-α*$^{-/-}$ mice express lower levels of BDNF protein in their hippocampi compared to wild type mice. In addition to altering neurotrophin levels within the hippocampus, the loss of TNF-α also results in a decrease in the complexity of the apical dendrites of neonatal CA1 and CA3 pyramidal neurons when compared to wild type mice and improves the performance of adult mice in spatial learning tasks[167]. Finally, increased levels of TNF-α mRNA and protein have been detected in various brain regions in several neurological disorders including: ischemia[168], traumatic brain injury[169], multiple sclerosis[170], Alzheimer's disease[171] and Parkinson's disease[172].

Like TNF-α, TGF-β expression is upregulated after brain injury. However, in contrast to TNF-α whose upregulation following injury is associated with negative outcomes within the CNS, the injury induced increase in TGF-β expression has been suggested to be part of an endogenous protective mechanism, in particular within the hippocampus[173]. In support of this, TGF-β protects cultured neonatal rat hippocampal neurons from staurosporine-induced apoptosis by inhibiting the conversion of pro-caspase-3 to active caspase-3[174]. More recently, TGF-β was shown to increase dendritic length, as well as GABAergic connectivity, in cultures of embryonic mouse hippocampal neurons[175]. Oligomeric, soluble amyloid-β (Aβ) has a number of deleterious effects on cultured hippocampal neurons including induction of apoptosis, reducing the length and increasing the number of primary dendrites and

reducing GABAergic connectivity. Importantly, TGF-β ameliorates the deleterious effects of Aβ on cultured hippocampal neurons by a signalling pathway that involves activation of NF-κB and induction of the expression of the hairy and enhancer of split 1 (Hes-1) transcription actor[175].

Other members of the TNF-α and TGF-β superfamilies have recently been implicated in the regulation of nervous system development, connectivity and function[176-181]. Proteins that were primarily identified and characterised from studies on the immune system, organogenesis and cellular specification are now emerging as potent regulators of neuronal differentiation, survival, growth, maturation and function. These novel neuroactive factors are now also being explored in the context of neuropathology, either as neuroprotective or neurotoxic proteins. The TNF-α and TGF-β superfamilies contain a large number of members, many of which have yet to be tested for potential regulatory roles in the developing and adult nervous system. The following sections will focus on the structure, expression and function of members of the TNF-α and TGF-β superfamilies.

1.3. The Tumour Necrosis Factor superfamily

The discovery of TNF was closely associated with the pursuit of a treatment for cancer. In 1891, American oncologist W. Colley observed that bacterial extracts could lead to the shrinkage of certain tumours[182]. Later, Shear and colleagues isolated lipopolysaccharide (LPS) from gram-negative bacterial extracts and verified that LPS could induce tumour necrosis[183]. In 1962, O'Malley and co-workers demonstrated that LPS injection into mice induced the release of a factor into their serum that caused tumour regression[184] and, in 1975, this factor was renamed Tumour Necrosis Factor by L. Old and colleagues after the confirmation that it was able to kill cancer cells in mice and in culture[185,186].

Over time, several other proteins structurally related to TNF were discovered and characterised. The TNF superfamily (TNFSF) includes 19 ligands and the TNF receptor superfamily (TNFRSF) contains 29 receptors. Together the TNFSF and TNFRSF superfamilies regulate the survival, death, proliferation and differentiation of numerous cell types. Although TNFSF members were first identified in the immune system, they are also expressed in lymphoid, ectodermal, mammary and neuronal tissues[187]. The main biological activities of TNFSF members are to induce and regulate the protective immune response following infection, to induce inflammation and to regulate the organogenesis and maintenance of secondary lymphoid organs. Members of the TNFSF have been associated with a number of different pathological conditions including: cancer, autoimmune diseases, neuropathologies, cardiovascular diseases and metabolic disorders[188,189].

1.3.1. TNF ligands

Ligands of the TNFSF are predominantly synthesised as type II transmembrane proteins with amino-terminal intracellular domain and carboxy-terminal extracellular domain. Two exceptions to this are TNF-β and the vascular endothelial cell growth inhibitor/TNF-like factor 1A (VEGI/TL1A) that are both secreted[190] (Fig.8).

Some transmembrane TNFSF ligands can also exist and function as soluble forms following release from the cell surface by proteolysis[191,192].

Examples of TNFSF ligands that are cleaved from the plasma membrane include TNF-α and the receptor activator of NF-κB ligand (RANKL), that are both cleaved by the protease ADAM (a disintegrin and metalloprotease domain), and Fas ligand (CD95L/FasL) that is cleaved by matrilysin. In addition, B-cell-activating factor (BAFF), ectodyplasin-A (EDA), TNF-like weak inducer of apoptosis (TWEAK) and a proliferation-inducing ligand (APRIL) are released from the plasma membrane by members of the furin protease family[190]. The solubilisation of some ligands is very important for their physiological function. For instance, a mutation in the furin gene that cleaves EDA from the plasma membrane is sufficient to cause the genetic disorder X-linked hypohidrotic ectodermal dysplasia (XLHED)[191]. Conversely, the robust cytotoxic activity of membrane bound FasL is dramatically reduced upon cleavage from the plasma membrane[192]. The transmembrane location of most TNFSF ligands suggests that they primarily act locally; however, soluble forms may allow these ligands to act on distant cellular targets[187,190,193].

Both soluble and transmembrane TNFSF proteins are active as self-assembled, non-covalent trimers. The C-terminal domain of these proteins contains a “TNF homology domain” (THD) that consists of a 150 amino acid long sequence of aromatic and hydrophobic residues responsible for trimer assembly. Each monomer folds into anti-parallel β-pleated sheets with a “jellyroll” topology, which then interacts with other, folded monomers at hydrophobic interfaces[193,194]. The THD domains are responsible for the binding of trimeric ligands to their respective receptors. Therefore, each ligand complex has three binding sites to activate three receptors[195]. The external receptor binding surfaces of ligand trimers show little sequence similarity amongst TNFSF members, which is crucial for ensuring receptor selectivity. Despite this, some ligands and receptors can bind to more than one partner, which increases system complexity[195] (Fig.8). There is a 25%-30% amino acid similarity of the THD sequence among TNFSF ligands that is confined to internal aromatic residues not involved in receptor binding. The amino acid conservation in the internal region of the THD allowed for the identification of additional ligands of the TNFSF, such as TNF-related apoptosis-inducing ligand (TRAIL), RANKL,

TL1A and BAFF. Among the TNFSF ligands, TRAIL and FasL have the highest homology in this domain[190]. TNFSF ligands also include; lymphotoxin β (LT-β), OX40L, CD40L, CD27L, CD30L, 4-1BBL, a cellular ligand for herpes virus entry mediator and lymphotoxin receptor (LIGHT) and glucocorticoid-induced TNFR family-related receptor ligand (GITRL)[188].

Typically, most TNFSF ligands are predominantly expressed in cells of the immune system, such as macrophages, natural killer (NK) cells, B cells, T cells, dendritic cells, monocytes and lymphoid cells[190]. Exceptions to this include EDA1 and EDA2, which are expressed in skin, and TL1A, which is expressed in endothelial cells. APRIL is also expressed by tumour cells and RANKL by osteoblasts[188,190] (Table 1).

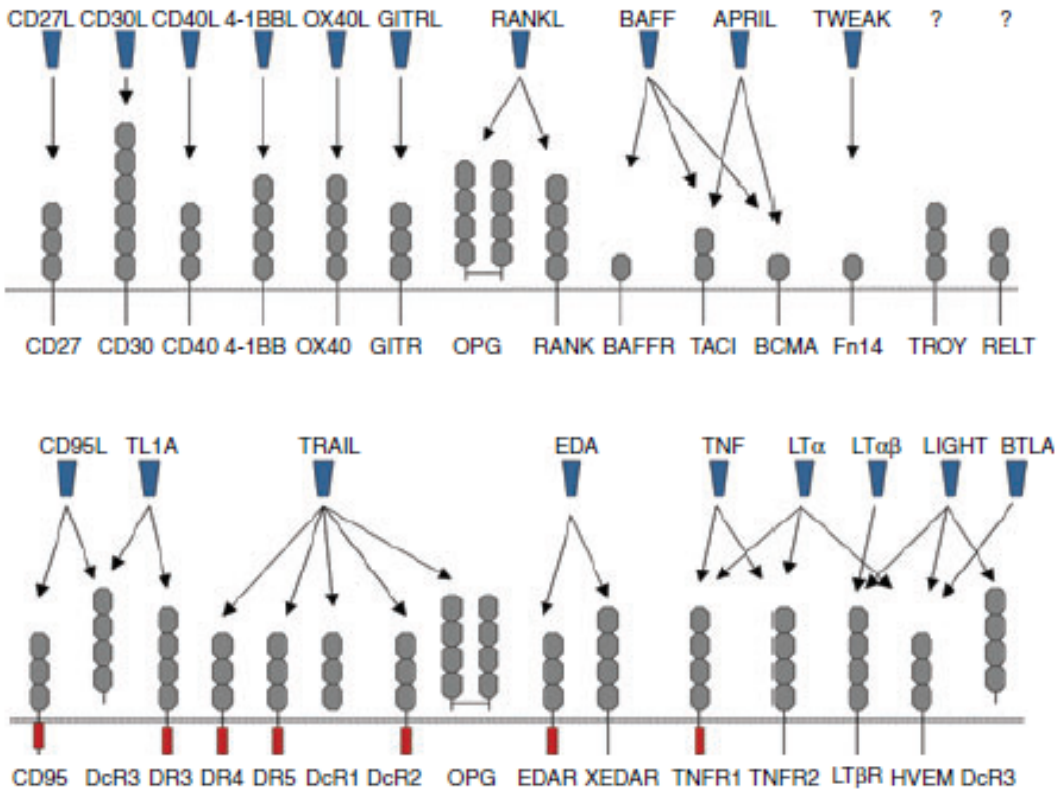

Figure 8: The TNF superfamily.

The 19 ligands are represented in blue and the 29 receptors showing the number of cysteine-rich domains in grey and the death domains in red. The arrows correspond to the interactions between ligands and receptors. The question marks symbolize ligands yet to be discovered[188].

1.3.2. TNF receptors

The 29 TNF receptors so far discovered share highly conserved cysteine-rich domains (CRDs) in their extracellular portion (Fig.8). The canonical motif of these domains comprises three disulfide bonds surrounding a core motif of CXXCXXC, an arrangement that creates an elongated molecule. The number of CRDs amongst TNFRSF members is highly variable. For example, BAFF receptor (BAFFR) has only a single partial CRD whilst CD30 has six CRDs[196].

TNF receptors are predominantly type I transmembrane proteins with a carboxy-terminal intracellular domain and an amino-terminal extracellular domains. Exceptions to this include B-cell maturation antigen (BCMA), transmembrane activator and cyclophilin ligand interactor (TACI), BAFFR and X-linked EDA receptor (XEDAR) which, because they lack a signal peptide sequence are termed type III transmembrane proteins[190]. Soluble TNF receptors have also been identified. These can either be generated by a proteolytic process, as is the case for CD27, CD30, CD40, TNFR1 and TNFR2, or by alternative splicing in the case of CD95 and 4-1BB[190,193]. These soluble receptors can modulate the binding of their ligands to transmembrane receptors, thereby regulating ligand-receptor signalling in specific cell environments[190,193].

TNFRSF members can be sub-divided into three main groups according to the intracellular signalling cascades that they initiate and their modes of action[188,190]. The first group includes members that share a death domain in the cytoplasmic tail. This region has approximately 80 amino acids residues and the lack of this domain prevents TNFSF ligand induced apoptosis. The known death receptors are TNFR1, CD95, death receptor (DR3), DR4/TRAILR1, DR5/TRAILR2, DR6, EDAR and the low affinity p75NTR. The receptors of the second group contain one to five TNF-receptor associated factor (TRAF)-interacting motifs (TIMs) in their cytoplasmic domain. Lastly, the third group is comprised of decoy receptors that do not have functional signalling domains and reduce cell signalling by sequestering TNFSF ligands. Members of this group include decoy receptor 3 (DcR3), DcR1/TRAIL-R3 and osteoprotegerin

(OPG). DcR1/TRAIL-R3 is anchored to the membrane by a covalently liked C-terminal glycolipid and DcR3 and OPG are secreted as soluble proteins[188,190].

The first step for ligand induced TNFRSF signalling was thought to be ligand induced trimerization of receptors. However, it is now known that some members of the TNFRSF exist as pre-assembled oligomers on the cell surface due to actions of the pre-ligand assembly domain (PLAD), which is usually in the first CRD[197,198]. PLAD domains facilitate the binding to and recognition of the trimeric ligands (Fig.9).

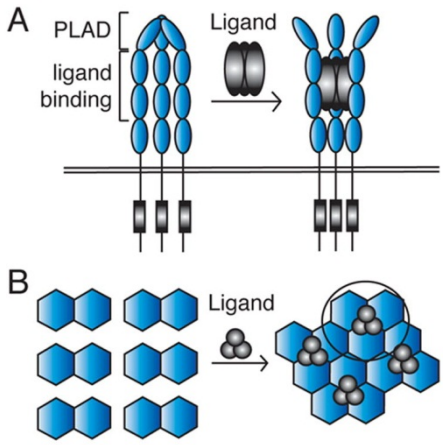

Figure 9: The pre-ligand assembly domain model.
(A) The PLAD facilitates the ligand binding conferring a more stable configuration. (B) View from above: After ligand/receptor binding, ligands and receptors maintain a trimeric symmetry[197].

Although both TNFSF ligands and receptors share common domains between them, there is significant specificity in ligand-receptor interactions. The specificity of ligand-receptor interactions is due to differences in the size and location of the contact area between ligands and receptors, different 3D conformations of both receptors and ligands, alternative modes of interaction between cognate ligands and receptors, the great variety of residues involved in binding recognition sites and different orientations of the CRDs in relation to their ligands[199]. TNFSFRs are expressed in a variety of cell types including immune cells, endothelial cells, lung, colon, spleen, thymus, lymph nodes, osteoblasts, embryonic skin, transformed cells, brain and ganglia of the PNS[177,178,188,190] (Table 1).

Table 1: Cellular location and expression of the TNFSF and TNFRSF members[190].

Cytokine	Cells	Receptor	Cells
LTα	NK, T and B cells	TNFR1 TNFR2	Most normal and transformed cells Endothelial cells and immune cells
TNF	Macrophages, NK, T and B cells	TNFR1, TNFR2	See above
LTβ	DCs, macrophages, T, B and NK cells	LTβR	NK cells, $CD4^+$and $CD8^+$ T cells
CD95L	Activated splenocytes, thymocytes and non-lymphoid tissues, such as the eye and testis	CD95	Most normal and transformed cells
		DCR3	Lung and colon cells
TRAIL	NK cells, T cells and DCs	DR4, DR5 DCR1, DCR2, OPG	Most normal and transformed cells Most normal and transformed cells
TWEAK	Monocytes	FN14	Endothelial cells and fibroblasts
CD27L	NK, T and B cells	CD27	$CD4^+$ and $CD8^+$ T cells
CD30L	T cells and monocytes	CD30	Reed–Sternberg cells
CD40L	T and B cells	CD40	Reed–Sternberg cells
4-IBBL	B cells, DCs and macrophages	4-IBB	Activated T cells, monocytes and NK cells
OX40L	T and B cells	OX40	T cells
APRIL	Macrophages, lymphoid cells and tumour cells	BCMA TACI	B cells, PBLs, spleen, thymus, lymph nodes, liver and adrenals B cells, PBLs, activated T cells, spleen, thymus and small intestine
BAFF	T cells, DCs, monocytes and macrophages	TACI BCMA BAFFR	See above See above B cells, PBLs, resting T cells, spleen and lymph nodes
LIGHT*	T cells, granulocytes, monocytes and DCs	HVEM LTβR	T cells Non-lymphoid haematopoietic cells and stromal cells
VEGI*	Endothelial cells	DR3, DCR3	Activated T cells
GITRL	N. D.	GITR	$CD4^+CD25^+$ T cells
RANKL	Activated T cells and osteoblasts	RANK OPG	Osteoclasts, osteoblasts and activated T cells Osteoclast precursors, endothelial cells and others
EDA1	Skin	EDAR	Ectodermal derivative
EDA2	Skin	XEDAR	Ectodermal derivative
N. D.		DR6	Resting T cells
N. D.		RELT	Lymphoid tissues
N. D.		TROY	Embryo skin, epithelium, hair follicles and brain

1.3.3. Intracellular signalling pathways downstream of TNFRSF activation

When stimulated by their respective ligand, TNFRSF members with a death domain recruit intracellular death domain-containing adaptors such as Fas associated death domain (FADD) and TNFR associated death domain (TRADD)[200]. These adaptors, in turn, trigger the activation of the executioner caspases, caspases 3, 6 and 7, thereby inducing apoptosis. Fas, DR4/TRAILR1 and DR5/TRAILR2 directly interact with FADD while TNFR1 and DR3 directly interact with TRADD. After binding to its receptor, FasL promotes assembly of the death-inducing signalling complex (DISC) that includes FADD, TRADD and pro-caspase 8. DISC formation leads to cleavage of pro-caspase 8 to mature caspase 8, which in turn activates executor caspases, resulting in apoptosis[201]. The association of ligand bound TNFR1 with TRADD can have two outcomes, either apoptosis or the transcription of inflammation related genes. TRADD can associate with FADD and pro-caspase 8 to form the DISC and activate executioner caspases[201]. Alternatively, TRADD can recruit TRAF1, TRAF2 and the receptor-interacting protein (RIP) leading to the activation of JNK and

nuclear NF-κB, thereby preventing apoptosis and initiating inflammatory responses[188] (Fig.10). Similarly, TL1A can both induce apoptosis in tumour cells, via a caspase 3 dependent mechanism, and promote the proliferation of endothelial cells by activating the canonical NF-κB and JNK signalling pathways[202]. The receptor for TL1A has since been identified as DR3, a death domain containing receptor[188]. Therefore, for TNFRSF members containing a death domain, the balance between the initiation of death promoting and non-death promoting signalling pathways is determined by the relative expression levels of TNFSF ligands, receptors and receptor associated adaptor proteins, which are in turn dependent on the cell type and the extracellular environment of the cell[188,203].

The second group of TNFSF receptors contain TIMs in their cytoplasmic domain. After ligand-induced activation, these receptors recruit TRAF family members to the TIMs leading to the activation of several signalling pathways, such as the ERK, PI3K, p38 MAPK, JNK and NF-κB pathways[188]. Once initiated, these signalling pathways regulate a number of processes including cell proliferation, differentiation and apoptosis. The TRAF family comprises six evolutionary conserved proteins that are characterized by a highly conserved TRAF domain. This domain mediates the binding of TRAFs to activated TNF receptors, regulates the formation of homo or heterodimers of TRAFs and modulates the interaction of TRAFs with downstream signalling molecules[203,204]. It is known that TRAF2, 5 and 6 mediate the activation of JNK and NF-κB signalling pathways[188]. For example, the binding of BAFF to BAFFR promotes the survival, differentiation and maturation of B cells via activation of the non-canonical NF-κB pathway. Following ligand binding activated BAFFR binds TRAF3 that, by activating NF-κB inducing kinase (NIK), results in the IKKα dependent phosphorylation of the p100 NF-κB subunit. Phosphorylated p100 is partially degraded giving rise to the p52 NF-κB subunit that subsequently translocates to the nucleus, together with the RelB NF-κB subunit, to regulate the transcription of survival promoting genes[205]. Ligand binding to TIM containing TNFSF receptors can also induce apoptosis. For example, the

TNFSF member LIGHT can induce death in some adenocarcinomas via activation of LTβR[206].

Decoy receptors do not have signalling motifs but instead compete with functional receptors for their cognate ligands, therefore modulating TNFRSF signalling *in vivo*[187,190,203] (Fig.10).

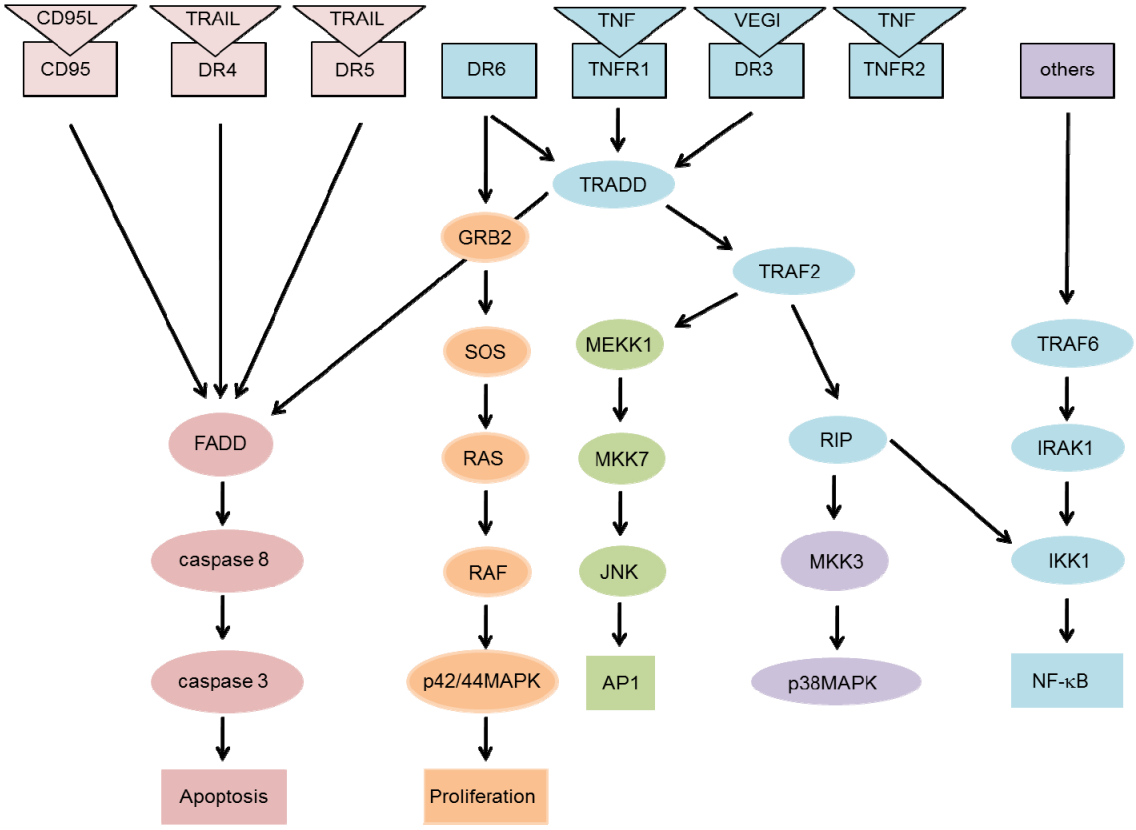

Figure 10: TNFRSF signalling pathways.

Ligand bound CD95, DR4 or DR5 interact with FADD, which in turn activates the caspase cascade leading to apoptosis. The activation of DR6 can lead to either Grb2 mediated MAPK activation, TRADD mediated activation of AP1, p38 and NF-κB signalling pathways or TRADD mediated initiation of apoptosis. TRADD also mediates signalling from activated TNFR1 and DR3 that can lead to survival and/or proliferation and/or the expression of inflammatory cytokines. Alternatively, the engagement of TRADD with ligand bound TNFR1 or DR3 can induce caspase-dependent apoptosis. TNFR2 activates TRAF2 directly. Lastly, other members of the TNFSF can trigger the NF-κB signalling pathway through TRAF 6 (adapted[188]).

Some TNFSF ligands and their cognate receptors are capable of signalling in a bidirectional manner. In addition to ligands initiating signalling from their receptors, the binding of soluble or transmembrane receptors to their membrane bound ligands and can also induce intracellular signalling from these ligands, a process that has been termed reverse signalling. Reverse signalling was initially demonstrated for membrane bound CD40L on T cells[207] and OX40L on B cells[208]. Soon after, CD30L was shown to be capable of reverse signalling[209]. The cross-linking of CD30L by a CD30-Fc fusion protein induced the production of IL-8 by freshly isolated neutrophils. Interestingly CD30L, but not CD30, is expressed on neutrophils ruling out autocrine CD30L/CD30 signalling in neurotrophils[209]. 4-1BBL, also known as CD137L, has recently been shown to be capable of reverse signalling in the kidney[210]. CD137L is expressed on the surface of tubular epithelial cells within the kidney. Following ischemic kidney damage, NK cell expressed CD137 engages tubular cell CD137L resulting in the production of the chemokine receptor 2 ligands, CXCL1 and CXCL2, by these cells. CXCL1 and CXCL2 induce neutrophil recruitment that in turn initiates a cascade of pro-inflammatory events that result in damage to tubular epithelial cells in an ischemia/reperfusion model of kidney damage[210]. The founding member of the TNFSF, TNF-α, can also reverse signal, a discovery that was first made in a mouse macrophage cell line[211]. Reverse signalling through transmembrane TNF-α has also been shown to confer resistance on human monocytes and macrophages to lipopolysaccharide induced apoptosis[212]. In contrast, activation of membrane bound TNF-α by soluble TNFR1 appears to induce the expression and release of TGF-β1 from human monocytes and secreted TGF-β1 then acts, in an autocrine manner, to promote monocyte apoptosis via elevated ERK1/2 and p38 MAPK signalling[213].

1.3.4. Physiological roles of the TNFSF

As mentioned above, TNFSF members and their receptors are mainly involved in regulating the function of the immune system by modulating the survival, differentiation and proliferation of immune cells. Additionally, they are also implicated in the aetiology of a number of pathological conditions.

The secondary lymphoid organs, comprising the spleen, lymph nodes, Peyer's patches, tonsils, appendix and adenoids, are the principal locations for the generation of adaptive immune responses due to the presence of mature, but antigen naive, B and T lymphocytes and antigen-presenting cells. Interestingly, mice with a null mutation for *LTβ* or *LTβR* do not develop lymph nodes and have an abnormal spleen structure and defective humoral immune responses[214]. Furthermore, the deletion of RANKL or its receptor, RANK, also prevents the development of lymph nodes[215,216]. Besides LTβ and RANK, other members of the TNFSF and TNFRSF families, such as TNF-α, CD40 and OX40, are also required for the organogenesis and maintenance of lymphoid organs[188,190]. Additionally, an interaction between CD40 and CD40L has been shown to be required for the induction of B cell-mediated co-stimulatory activity for T cell activation and the development of T cell effector functions[217]. *CD40L* deficient mice are severely impaired in primary T-cell responses and immunoglobulin class switching, and T cells lacking CD40L fail to enter the cell cycle and clonally expand *in vivo*[217]. Similarly, an interaction between B cell expressed OX40L and OX40 on the surface of activated T cells is necessary for the differentiation of activated B cells, into high immunoglobulin-producing B cells, *in vivo*[218].

Many TNFSF and TNFRSF members have been shown to play important roles in regulating haematopoiesis and controlling blood cell number. For example, APRIL, BAFF, BAFFR and TNF-α promote B cell proliferation, CD40 and RANK activate dendritic cells, CD27 and OX40 co-stimulate T cells, OX40, CD27 and HVEM regulate the expression and survival of CD4+ and CD8+ T cells and LIGHT–HVEM signalling seems to play a role in T cell proliferation[188,190]. Once activated by antigen, T cells begin to express FasL which engages with Fas, expressed on the same or neighbouring T cells, to attenuate the immune response by initiating Fas associated death signalling[219]. Moreover, TRAIL can promote T cell apoptosis by inhibiting cell cycle progression[220].

TNFSF and TNFRSF members are also important in regulating the innate immune response following microbial or viral infection, largely by initiating an inflammatory response. For example, mice with a null mutation in *Tnf-α* or *Tnfr1* show a significant reduction in host immune defence after infection with *Listeria monocytogenes, Mycobacterium tuberculosis,* and *Salmonella typhimurium*[221,222]. TNF-α has been recognized as an important defensive molecule against *Mycobacterium tuberculosis* infection due to its ability to increase the phagocytic capacity of macrophages[222]. TNF-α also plays a central role in the recruitment of inflammatory cells and in the initiation of inflammatory processes by stimulating cytokine and cell adhesion molecule production[221,222]. Other members of the TNFSF and TNFRSF families have also been associated with regulating inflammatory responses. For example, TL1A and its receptor, DR3, have been implicated in promoting the production of IFN-γ in ulcerative colitis and Crohn's disease[223]. In a murine collagen arthritis model, BAFF and APRIL play a role in mediating T cell immune responses[224]. RANKL ligand appears to promote inflammation, via the promotion of TNF-α and IL-1 expression, while its decoy receptor, OPG, has the opposite effect, an observation that might be beneficial in developing a treatment to ameliorate rheumatoid inflammation[225].

Although TNF-α was initially characterised as a cytokine with the potential to kill tumours, there is an astonishing amount of evidence that TNF-α mediates the proliferation, invasion and metastasis of tumour cells[226]. For example, *Tnf-α* and *Tnfr1* KO mice are resistant to developing induced skin tumours compared to wild type mice[227,228]. Experimental lung and liver metastases are also attenuated in *Tnfr1*$^{-/-}$ mice compared to wild type mice[226]. It suggests that malignant cells and macrophages synthesise and release TNF-α in some cancers and that released TNF-α can promote tumour development by a number of mechanisms that include the induction of other pro-inflammatory cytokines resulting in a prolonged inflammatory response; direct damage to DNA as a result of increased telomerase expression and inducing the epithelial to mesenchymal transition of malignant cells and promotion of angiogenesis in tumours[226]. TNF-α, and other pro-inflammatory cytokines, initiate NF-κB

signalling from their cognate receptors. Activation of the NF-κB signalling pathway can lead to IKKβ mediated phosphorylation of the tumour suppressor TSC1 that inhibits its tumour suppressing activity[229]. Moreover, upregulation of NF-κB signalling can also lead to increased expression of genes that promote invasion and metastasis, such as matrix metalloproteinase 9 (MMP-9), cyclo-oxygenase 2 (COX2) and vascular endothelial growth factor (VEGF). NF-κB signalling can also suppress apoptosis, which in turn favours tumourigenesis[189,190,226]. In contrast to TNF-α, other members of the family have been explored due to their anti-tumour potential. For example, TRAIL has been shown to induce apoptosis in several transformed cell lines, but not in normal cells[230].

TNFSF and TNFRSF members have been implicated in the development of autoimmune diseases, diseases that are characterised by the immunogenic recognition of self-proteins that results in organ damage due to increased production of pathogenic inflammatory molecules and auto- antibodies[231]. Anti-TNF-α therapy has been successful in reducing disease activity in rheumatoid arthritis[232] and in treating skin lesions in psoriasis[233]. Curiously, elevated levels of BAFF are detected in the serum of patients with systemic lupus erythematosus, suggesting that anti-BAFF antibodies, or inhibitors of BAFF/BAFFR signalling, may present a therapeutic avenue for this condition[234].

TNF-α is produced in the blood and myocardium of patients that are suffering from chronic heart failure, facilitating the progression of disease. Therefore, new therapies have been developed to neutralize the damaging effects of TNF-α in patients with heart failure[235]. RANKL has an important role in modulating bone formation. *RankL* deficient mice display severe osteopetrosis, defects in tooth eruption and a complete lack of osteoclasts as a result of an inability of osteoblasts to support osteoclastogenesis[216]. In accordance with this, mice deficient for the RANKL decoy receptor, OPG, show reduced bone density and increased bone porosity that is reminiscent of osteoporosis[236].

1.3.5. TNFSF in the nervous system

Recently, some TNSF and TNFRSF members have been shown to play important roles in the developing PNS by either regulating neuronal survival or by modulating the extent of axonal growth and arborization, and hence target field innervation. For example, TNF-α and TNFR1 are co-expressed in cultured E16 mouse superior cervical ganglia (SCG) and trigeminal sensory neurons and blocking antibodies against either TNF-α or its receptor enhances the survival of SCG and trigeminal neurons cultured in the absence of NGF at this embryonic age[237]. In accordance with this, TNF-α reduces NGF-promoted survival of cultured E16 SCG and trigeminal neurons and these neurons show significantly greater survival in the absence of NGF in cultures established from *Tnf-α* deficient embryos compared to cultures established from wild type mice. In addition, the SCG and trigeminal ganglia of *Tnf-α* KO embryos contain more healthy neurons and less pyknotic neurons than their wild type counterparts. Together, this data suggests that TNF-α acts by an autocrine loop to modulate the NGF-promoted survival of developing mouse sensory and sympathetic neurons during the period of naturally occurring developmental cell death[237].

LIGHT has been shown to negatively regulate axonal growth and branching from cultured mouse nodose sensory neurons during the perinatal period by a mechanism that involves HVEM mediated inhibition of NF-κB signalling[177]. Similarly, RANKL/RANK signalling has been shown to negatively regulate neurotrophin-promoted neurite outgrowth and branching from cultured postnatal mouse SCG, nodose and trigeminal neurons by a signalling process that involves the phosphorylation of residue serine536 (ser536) of the NF-κB p65 subunit[176]. In contrast, GITRL-GITR signalling enhances the NGF-promoted elongation and branching of cultured postnatal mouse SCG neuron processes, over a narrow postnatal developmental window (P1 to P3), by activating ERK1/2 dependent signalling[178]. Importantly, *Gitr* null mutant neonatal mice display a significant reduction in the density of sympathetic target field innervation compared to wild type neonates[178]. Unlike TNF-α, neither LIGHT/HVEM, RANKL/RANK nor GITRL/GITR signalling regulate the survival of developing sensory or sympathetic neurons[176-178]. The expression of FN14 mRNA, but not its ligand, TWEAK, is dramatically increased in adult mouse

dorsal root ganglion (DRG) neurons following sciatic nerve transection[238]. Although viral overexpression of FN14 in PC12 cells increases neurite outgrowth, the physiological significance of this is unclear, since overexpression of FN14 does not promote process outgrowth from cultured adult mouse DRG neurons[238]. Fas expression has been detected in neonatal mouse DRG neurons[239]. Cross linking of Fas with anti-Fas antibody increases the extent of NGF independent neurite outgrowth in explant and dissociated cultures of neonatal mouse DRG. The ability of Fas to promote neurite outgrowth from DRG neurons appears to depend on ERK activation. Interestingly, ligation of Fas improves functional repair after sciatic nerve lesion in adult mice and functional repair after sciatic nerve lesion is significantly impaired in Fas mutant mice compared to wild type mice[239].

Neuromodulatory roles for TNFSF and TNFRSF members have also been identified in the CNS. For example, FasL and its receptor are expressed in the hippocampus of embryonic and neonatal mice and FasL, or an activating anti-Fas antibody, increases the number of axonal and dendritic branches in 4DIVs cultures of E15 mouse hippocampal neurons without affecting neuronal survival[240]. Importantly, neonatal mice deficient in functional *Fas* or *FasL* exhibit reduced dendritic branching in CA1 *in vivo* compared to normal mice[240]. Interestingly, as mentioned previously, TNF-α has the opposite effect to FasL/Fas signalling by negatively regulating the length and branching of hippocampal pyramidal neurons via a signalling mechanism involving RhoA[166]. The TRAIL receptor, DR5 is expressed in the developing CNS, particularly in the developing hippocampus, cerebellum and olfactory bulb[241]. DR5 expression appears to be highest in proliferating progenitor cells and, although still persisting in newborn neurons, DR5 expression decreases as development proceeds, thereby suggesting that DR5 may play a role in modulating proliferation and/or differentiation within the developing CNS[241]. TWEAK and its receptor, FN14 are expressed by microglia, astrocytes, neurons and endothelial cells within the adult rodent CNS[242]. It has been reported that TWEAK/FN14 signalling increases neuronal death in the mouse middle cerebral artery occlusion (MCAO) model of stroke via activation of NF-κB signalling[243].

Conversely, enhanced TWEAK/FN14 signalling has been claimed to account for the ability of a preconditioning, sub-lethal hypoxic insult to ameliorate neuronal death following MCAO in mice[244]. TWEAK/FN14 signalling also promotes the expression of pro-inflammatory cytokines and matrix metalloproteinases within the CNS and neutralization of TWEAK or FN14 has shown therapeutic potential in rodent models of ischemia and multiple sclerosis[242].

Whilst certain TNFSF and TNSFR members have been shown to regulate some aspects of neuronal development in the developing PNS and CNS, and others appear to modulate neuronal function in the adult CNS under normal and pathophysiological conditions, putative roles for the many other members of these large protein families in the developing and adult nervous system remain to be investigated.

1.4. TGF-β superfamily

TGF-β1 is the prototypic molecule of a superfamily with more than 50 members characterised to date. In 1980, the "autocrine secretion" hypothesis tried to explain the mechanism by which a growth factor could cause the malignant transformation of cells. This hypothesis suggested that transformed cells could produce their own growth factor as well as the receptor for this transforming factor, thereby regulating their own proliferation, survival and malignant transformation without the need for an exogenous supply of growth factors[245]. "Transforming growth factor" was initially extracted from transformed cell lines and characterised by the ability to confer a "transformed" phenotype on rat kidney fibroblasts[246,247]. Later, scientists understood that the "transformed" phenotype reflected cell growth and not necessarily malignant transformation. Moreover, TGF-β was also purified from numerous normal tissues and further studies implicated this factor in promoting wound healing[248] and inhibiting cell growth[249]. It soon became apparent that the biological activity of TGF-β was multifunctional and it was involved in regulating a number of biological activities. The TGF-β superfamily is a wide-ranging group of cytokines involved in regulating proliferation, differentiation, apoptosis, extracellular matrix formation, hematopoiesis, angiogenesis, chemotaxis, immune and nervous system function. During embryogenesis TGF-β superfamily members are involved in pattern formation and tissue specification and in the adult they are involved in disease and tissue repair[250].

1.4.1. TGF-β superfamily Ligands

The TGF-β superfamily has been grouped in subfamilies according to DNA sequence similarities (Fig.11). These groups include: TGF-βs, activins/inhibins, decapentaplegic (Dpp) and vegetal-1 (Vg1)-related (DVR) group (also known as bone morphogenetic proteins (BMPs)/growth and differentiation factors (GDFs)) and GDNF subfamily (the most distantly related group to TGF-βs). Furthermore, there are other more distantly related members, such as the inhibin α-chain and Mullerian inhibiting substance (MIS)[250].

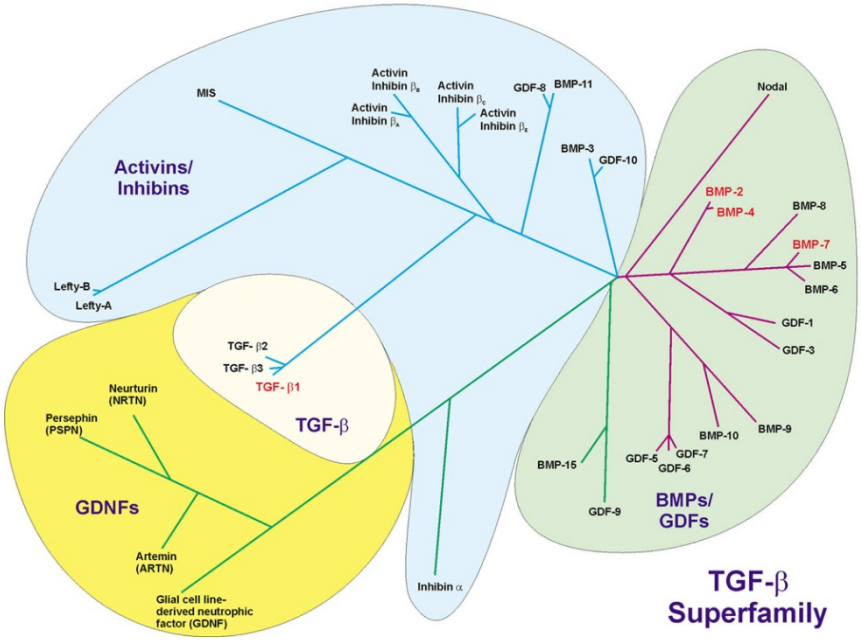

Figure 11: The TGF-β superfamily.

Members are traditionally subdivided into TGF-β, activins/inhibins, DVR or bone morphogenetic proteins (BMPs)/growth and differentiation factors (GDFs) and the most distantly related group of GDNF family ligands[251].

The majority of TGF-β superfamily ligands are synthesized as dimeric pre-proproteins. The large precursor molecule comprises an amino-terminal signal peptide that targets the molecule to the secretory pathway, a prodomain of variable size responsible for correct protein folding and dimerization of subunits and a carboxy-terminal domain constituting the mature protein. Homo or hetero-dimerization of the C-terminal domain produces biologically active molecules[252]. Because dimerization of the C-terminal domain requires the prodomain, it occurs within the cell before cleavage of the precursor protein. The cleavage of the prodomain is mediated by proteases of the subtilisin-like proprotein convertase (SPC) family, such as furin, and this mechanism is required for the release of the mature and bioactive protein[253,254]. The cleavage occurs at a dibasic cleavage site (RXXR motif) immediately preceding the bioactive domain that then is released as a fragment of 110-140 amino acids[252,255]. However, there are few exceptions and variations of this mechanism. For example, the nodal precursor has been shown to bind to activin receptors and initiate signalling from them without being processed[256].

TGF-β subfamily members are secreted as a large latent complex (LLC) in which their propeptide, or latency associated peptide (LAP), prevents the activity of the mature protein. Dissociation from the LAP requires the cleavage of the mature domain that consequently becomes biologically active[257,258]. Other exceptions are GDF-8 and GDF-11, which are capable of forming a latent complex with their cleavable prodomains[259].

Whereas the prodomain is usually poorly conserved among TGF-β superfamily members, the mature domain is highly conserved and contains characteristic features of the superfamily. A common feature is the cysteine knot motif that is also shared by other growth factors, such as NGF and the platelet-derived growth factor (PDGF), suggesting a common ancestor among these molecules[260]. The cysteine knot motif is formed by three intramolecular disulphide bonds among six strictly conserved cysteine residues (Fig.12). Two cysteine bonds build an eight-member ring structure through which the third cysteine bond passes. A seventh cysteine residue makes an intermolecular disulfide bond that link two monomers into a functional dimer. In addition, this disulfide bond provides additional stabilization of hydrophobic interactions responsible for maintaining the dimer[250]. Curiously, TGF-β superfamily members, GDF-3 and GDF-9 lack the seventh cysteine residue, suggesting a different form of interaction between their monomers[261]. Although homodimers are most commonly formed, heterodimers can also occur between monomers of different TGF-β superfamily members. For example, nodal ligand can inhibit BMP signalling by heterodimerizing with some BMP monomers[262].

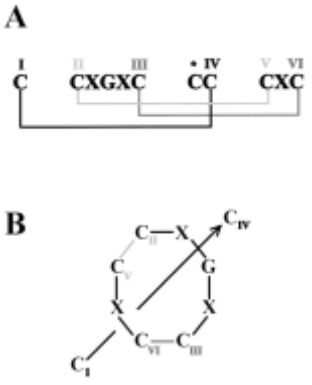

Figure 12: The cysteine knot motif is conserved among members of the TGF-β superfamily: (A) The mature domains share seven characteristic cysteine residues in each monomeric subunit. Three intramolecular disulphide bonds are formed between six cysteine residues. (B) Two cysteine bonds (C_{II}—C_V and C_{III}—C_{VI}) form an eight-member ring structure through which the third cysteine bridge (C_I—C_{IV}) passes[250].

1.4.2. TGF-β superfamily Receptors

The receptors of the TGF-β superfamily are serine/threonine kinases that are divided into two subfamilies, type I and type II receptors. However, this feature is not shared by GDNF subfamily receptors, which consist of the Ret tyrosine kinase together with a GPI-linked alpha subunit[263]. Both type I and II receptors are glycoproteins of about 500 amino acids comprising a short extracellular N-terminal cysteine rich domain that is responsible for ligand binding, a transmembrane region and a highly conserved intracellular serine/threonine kinase domain that initiates signal transduction following ligand binding[264]. Although both receptors have the capacity to bind ligands and initiate signal transduction, binding of ligand to either homodimeric receptor is not sufficient to activate signalling and, a functional interaction between type I and II receptors is necessary for signal transduction to occur. Pre-formed homodimers of type I receptors and type II receptors come together to form a heterotetrameric, active receptor complex. Although ligand binding brings both receptor types into close proximity, they do not interact directly with each other[265-267]. Type II receptor dimers are thought to be constitutively active and potentially could induce autophosphorylation of their own intracellular residues, however, signalling from type II receptors in the absence of type I receptors does not appear to occur[268,269]. Following ligand binding to the heterotetrameric receptor complex, type II receptors phosphorylate type I receptors at the GS domain, a conserved sequence upstream of the kinase domain that is rich in glycine and serine residues (SGSGSG). This sequence is conserved among all type I receptors, and its phosphorylation enables the activation of intracellular signalling pathways[270].

There are two possible mechanisms of ligand-receptor interactions amongst TGF-β superfamily members. TGF-βs and activins have a much higher affinity for type II receptors than type I receptors and first bind to homodimers of type II receptors, thereby allowing the subsequent incorporation of type I receptor homodimers into an active heterotetrameric receptor complex. These ligands cannot bind to isolated type I receptor homodimers[271]. TGF-β2, however, needs a heterotetrameric complex to be pre-formed to be able to bind

to its type II receptors and initiate intracellular signalling[272]. Like TGF-βs and activins, BMP subfamily ligands also bind to type II receptors in the absence of type I receptors. However, high affinity binding of BMPs to the heterotetrameric receptor complex, and the subsequent initiation of signal transduction requires, cooperative binding between both type I and II receptors[273].

There are five type II receptors and seven type I receptors in mammals and different combinations of type I and type II receptors can form functional receptor complexes (Fig.13). Individual receptor complexes can bind different ligands and individual ligands can bind different receptor complexes, with the result that can be reflected in the differential signalling pathway that is activated[271,272,274]. For example, the type II receptors, activin receptor II (ActRII) and ActRIIB can interact with the type I receptors, activin receptor-like kinase 4 and 7 (ALK-4 and ALK-7) to mediate activin signalling. ActRII and ActRIIB can also interact with the type I receptors, BMPR-Ia (ALK-3) and BMPR-Ib (ALK-6) to mediate BMP/GDF signalling. As mentioned above, heterodimeric TGF-β superfamily ligands provides another layer of complexity to the system[271,272,274].

A class of TGF-β superfamily co-receptors, sometimes called type III receptors, have also been characterised. Type III receptors are not capable of signal transduction, but can modulate the affinity of certain ligands to their signalling receptors. For example, the membrane-anchored proteoglycan, betaglycan binds TGF-βs and presents them to the TGF-β type II receptor enhances the responsiveness of cells expressing TβRII to TGF-β1 and lets them respond to TGF-β2, a TGF-β that otherwise cannot initiate signal transduction[275]. The betaglycan-related glycoprotein, endoglin can also facilitate the binding of TGF-β superfamily ligands to their receptors. However, endoglin cannot bind ligands in the absence of TGF-β superfamily receptors. For example, endoglin binds to TβRII, thereby allowing it to interact with TGF-β1 and TGF-β3[276]. The interaction of endoglin with Activin A and BMP-7 is facilitated by prior association of endoglin with ActRII or ActRIIB[277]. Endoglin can also associate with the type I receptors, BMPR-Ia and BMPR-Ib allowing them to bind to BMP-2. Endoglin does not appear to increase the affinity of

ligands to their receptors and further studies are required to understand the role of this glycoprotein[276,277].

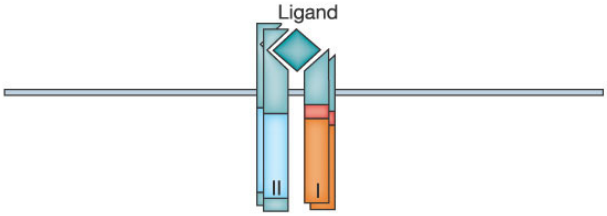

Type II	Type I	R-Smad
BMPRII	ALK-2 (ActRI) ALK-3 (BMP-RIA) ALK-6 (BMP-RIB)	Smad1, Smad5, Smad8
ActRII, ActRIIB	ALK-4 (ActRIB)	Smad2
ActRIIB	ALK-7	Smad2
TβRII	ALK-5 (TβRI) ALK-1 ALK-2	Smad2, Smad3 Smad1, Smad5
AMHR	ALK-3 ALK-2 ALK-6	Smad1, Smad5

Figure 13: **Interactions of type II and type I receptors define downstream signalling mechanisms.** The table shows known interactions of type II and type I transmembrane serine/threonine kinases and the respective R-Smads activated[274].

1.4.3. Cell Signalling

1.4.3.1. The Smad pathway

Smad proteins interact directly with activated type I receptors to initiate intracellular signalling following ligand binding to type I/type II receptor complexes. Smads were first identified in *D.melanogaster* and *C.elegans* and termed Mad and Sma, respectively. Vertebrate homologues of these proteins were termed Smads after their identification[278,279]. According to structural and functional properties, the Smad family can be subdivided in three groups. The first group are the receptor regulated Smads (R-Smads) which become phosphorylated on two serine residues at their C-terminal by specific type I receptors kinases following ligand binding. The R-Smads comprise Smad1, Smad2, Smad3, Smad5 and Smad8. The main Smad signalling pathways are initiated by the phosphorylation of Smad2 and Smad3 that associated with activin and TGF-β receptors[280] and Smads1, 5 and 8 that specifically interact

with ALK-1, ALK-2, BMPR-Ia and BMPR-Ib[274,281,282] (Fig.13). The phosphorylation of R-Smads allows them to form heteromeric complexes with the common mediator Smad or co-Smad, Smad4 that is the only member of the second group of Smads. Smad4 allows activated R-Smads to translocate to the nucleus where they regulate transcription[280]. Negative feedback of Smad signalling is mediated by the induction of the third group of Smads, the inhibitory Smads (I-Smads), which are Smad6 and Smad7. Smad6 and Smad7 are induced in response to TGF-β superfamily ligands in a Smad-dependent way and can inhibit the signalling activity of R-Smads at three different levels. I-Smads can inhibit the phosphorylation of R-Smads by stable association with activated type I receptors[283]. Alternatively, I-Smads can compete with Smad4 for binding to activated R-Smads[284]. Finally, I-Smads can interact with proteins that target TGF-β receptors for degradation[285].

Structurally, Smads have two conserved domains, the N-terminal Mad homology 1 (MH1) and the C-terminal MH2 domains, which are separated by a less conserved proline-rich linker region[286]. The MH1 domain regulates nuclear translocation, interaction with nuclear proteins, DNA binding and transcriptional activity. Smad4 and all R-Smads, except Smad2, share this domain, while the divergent I-Smads have only a weak sequence homology to other Smads in the MH1 domain. All 7 Smads share the MH2 domain that regulates Smad oligomerization, recognition by type I receptors and interaction with cytoplasmic and nuclear proteins[286]. In the nucleus, R-Smad complexes recruit transcriptional co-activators or co-repressors to regulate the transcription of target genes. The identity of target genes and the choice between transcriptional activation or repression depends on the cell type, the TGF-β receptor complex initially activated and the activating ligand. In addition, R-Smads can integrate signals from other signal transduction pathways[274] (Fig.14).

1.4.3.1.1. Cross-talk between R-Smads and other signalling pathways

Other kinase signalling pathways can regulate Smad signalling and such signalling cross-talk is important to control the growth and differentiation of many cell types. The Smad linker region can be phosphorylated by MAPKs, GSK-3β and cyclin-dependent kinases (CDKs), effectively integrating inputs from other signalling pathways[274]. For example, activated Ras can phosphorylate the linker regions of Smad2 and Smad3 in transformed epithelial cells, thereby preventing their nuclear localisation and antagonizing TGF-β signalling[287]. MAPK pathways can also enhance TGF-β signalling. For instance, JNK phosphorylates Smad3 in endothelial cells, facilitating its phosphorylation by type I receptors, its subsequent nuclear translocation and its transcriptional regulatory activity[288].

Smad signalling can also be modulated by changes in cytoplasmic Ca^{2+} levels. Activation of CaMKII by elevated levels of intracellular Ca^{2+} leads to phosphorylation of Smad2 preventing its accumulation into the nucleus[289]. Similarly, phosphorylation of Smad3 by PKC prevents Smad3 from binding to the promoters of its target genes, thereby abrogating the ability of TGF-β to inhibit the proliferation and promote the apoptosis of Mv1Lu cells[290].

Moreover, synergy has been identified between Notch and TGF-β dependent signalling pathways. Ligand binding induces the proteolytic cleavage of the transmembrane receptor Notch, resulting in the release of the Notch intracellular domain (NICD) into the cytoplasm. Cytoplasmic NICD is translocated to the nucleus where it binds to CSL (also known as RBP-Jk and CBF-1), a transcription factor that normally suppresses transcription. The NICD/CSL complex induces the transcription of target genes involved in cell fate, such as the basic helix-loop-helix (bHLH) family transcription factors Hes1 and Hey1[291]. In the myogenic cell line, C2C12, BMP-4 initiates a signalling cascade that leads to Smad1 and NICD interaction, subsequent transcription of Hey1 and Hes1 and the inhibition of myogenic differentiation[292]. BMP-2 can also promote the transcription of Hey1 leading to the inhibition of osteoblast maturation[293].

TGF-β and Wnt dependent signalling pathways can also interact in a synergistic manner to regulate biological processes. Wnt signalling promotes the stabilization and accumulation of β-catenin in the cytoplasm of cells resulting in increased nuclear translocation of β-catenin. Nuclear β-catenin is a co-activator of the transcription factors of the lymphoid enhancer binding factor 1/T cell-specific factor (LEF1/TCF) family, which transcribe genes responsible for tissue specification during development. Treatment of several cell lines with TGF-β leads to the interaction of phosphorylated Smad3 with LEF1/TCF and enhanced transcription of LEF1/TCF target genes, independently of nuclear β-catenin[294].

1.4.3.2. Non-Smad pathways

In addition to the Smad pathway, other non-Smad signalling pathways have been proposed to be activated downstream of TGF-β superfamily serine/threonine kinase receptors (Fig.14). The addition of TGF-β1 to Mv1Lu cells induces a rapid and transient Smad-independent increase in JNK activity followed by a sustained increase in JNK activity that is dependent on Smad phosphorylation[288]. In addition, Smad-independent p38 MAPK activation is required for TGF-β induced apoptosis in mouse mammary gland epithelial cells[295]. JNK and p38 MAPK are thought to be activated by several upstream MAPK kinase kinases (MAPKKK), such as TGF-β activated kinase 1 (TAK1), that can be activated by both TGF-β and BMP-4[296], and MEKK1[274]. However, further studies are necessary to fully characterise the interactions between TGF-β superfamily receptors and MAPK pathways.

TGF-β1 treatment of PC-3U human prostate carcinoma cells induces the rapid formation of lamellipodia that is dependent upon the activation of the Rho GTPases, Cdc42 and RhoA in a Smad-independent manner[297]. Moreover, TGF-β1 promotes accumulation of the monomeric GTPase, RhoB by antagonising its normal proteolytic destruction by the 26S proteasome. RhoB appears to be a negative regulator of TGF-β signal transduction, since it antagonises TGF-β mediated transcriptional activation[298]. Furthermore, TGF-β1 induced activation of PI3K/Akt signalling promotes the epithelial to mesenchymal transition of NMuMG mammary epithelial cells and the migration of 4T1 and EMT6 breast

tumour cells[299]. In addition, TGF-β1 ligation of the type I receptor ALK-5 leads to Smad-independent activation of protein phosphatase-2A (PP2A) which in turn dephosphorylates p70s6k kinase, thereby leading to G1 cell cycle arrest of EpH4 epithelial cells[300].

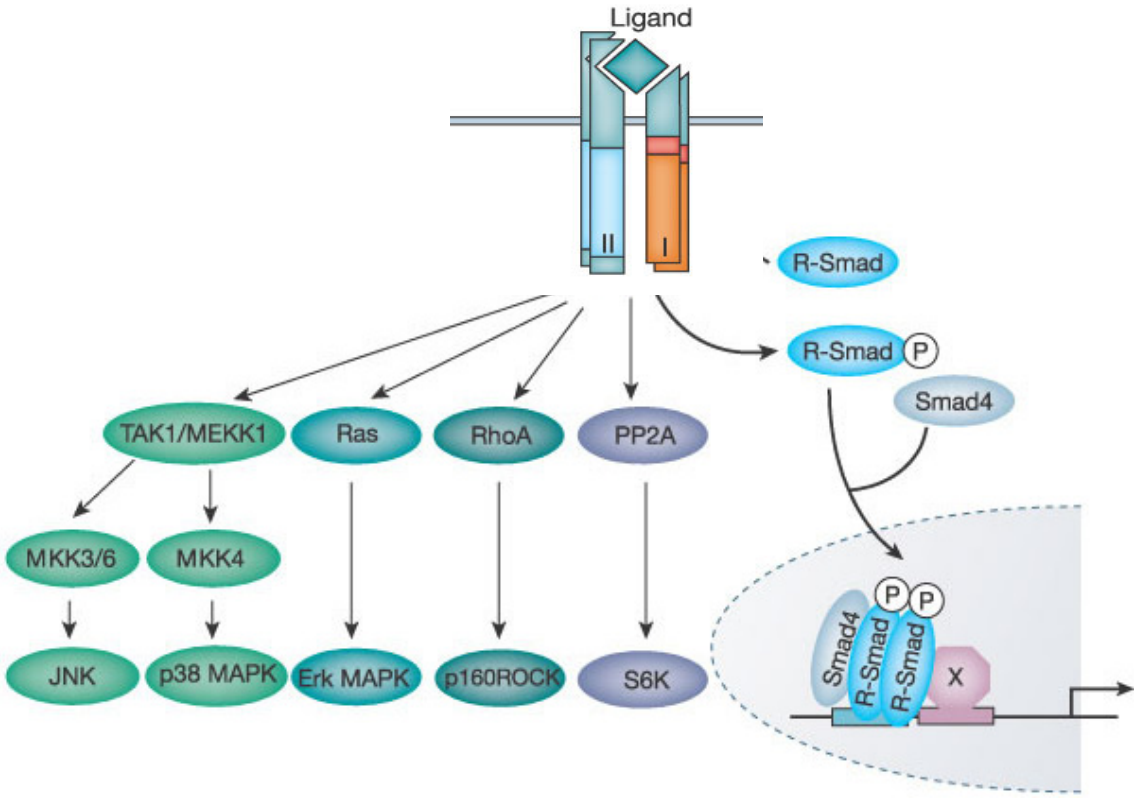

Figure 14: **TGF-β superfamily receptor signalling through Smad and non-Smad dependent pathways.** The TGF-β superfamily signals through R-Smads and non-Smad signalling pathways, such as TAK1/MEKK1, MAPK, RhoA and PP2A/p70[S6K 274].

1.4.4. Physiological roles of the TGF-β superfamily

TGF-β superfamily members regulate many biological processes from tissue development to tissue homeostasis. Processes that TGF-β superfamily members modulate include DNA replication, cell differentiation, cell adhesion, extracellular matrix composition and remodelling.

TGF-β superfamily members play crucial roles in the early development of mouse embryos. Mice that are deficient for functional BMP-4, Nodal, lefty-2, ALK-2, ALK-3, ALK-4, BMPR-II, Smad2 or Smad4, either fail to initiate gastrulation or have defects in mesoderm differentiation[301-303]. *Bmpr-II* KO embryos stop developing at around E9.5 before gastrulation is complete and have a similar phenotype to *Alk-3* deficient embryos[301]. In addition, double null

mutants for *Bmp-5* and *Bmp-7* display deficits in chorio-allantoic fusion and abnormalities in heart, branchial arch, somite and forebrain development, leading to embryonic lethality[304]. In the developing mouse embryo, morphological asymmetry of the left-right axis starts to occur at around E8. The TGF-β superfamily members, lefty-1 and lefty-2 are expressed on the left side of developing mouse embryos and are involved in the formation of the left-right axis. In the absence of lefty-1, mouse embryos display positional defects in visceral organs[302].

Heart development is regulated by TGF-β superfamily members at multiple developmental stages. *Bmp-6*/*Bmp-7* double null mutants die from cardiac insufficiency during embryonic development due to multiple defects in heart formation, such as abnormal valve morphogenesis and a delay in cardiac cushion (the precursor of mature valves and septa in the heart) f formation[305]. The use of a conditional KO strategy in mice has demonstrated that ALK-3 plays a crucial role in the normal formation of cardiac cushions, septa and valves[306]. Moreover, heterozygous mutations in BMPR-II appear to underlie familial primary pulmonary hypertension[307]. TGF-β superfamily signalling also plays an important role in vascular development and angiogenesis, particularly in the differentiation of arteries and veins and the maintenance of vessel wall integrity. Transgenic mice lacking functional *endoglin*[308] or *ALK-1*[309] show deficits in angiogenesis, and mutations in these genes commonly occur in patients with hereditary hemorrhagic telangiectasia, a disease characterised by vascular malformations[310].

TGF-β superfamily members also regulate aspects of craniofacial development, in particular tooth and eye development. For example, blocking BMP-4 signalling with Noggin induces an incisor to molar transformation demonstrating that BMP-4 is a key factor in the regulation of odontogenic gene expression[311]. BMP-4 also plays a role in the development of the eye being a critical factor for lens development. On a mixed genetic background, approximately 30% of mice with a homozygous null mutation in the *Bmp-4* gene survive until E10.5[312]. At E10.5, the lens placode containing cells that will give

rise to the lens is not formed in mutant mice, although it is present in wild type littermates. Explant culture of placode primordia from wild type mice leads to the *in vitro* formation of lens, retina and pigmented epithelium after 4 days, but these structure are absent from 4 day explant cultures of placode primordia established from *Bmp-4* null embryos. Significantly, Exogenous BMP-4 ligand rescues lens induction in explant cultures of *Bmp-4* deficient mice, defining a requirement for BMP-4 in lens induction[312].

TGF-β superfamily members also regulate skeletal morphogenesis by participating in skeletal patterning and the differentiation and maintenance of chondrocytes, osteoblasts and osteoclasts. For example, TGF-β2 participates in many steps of skeletal morphogenesis. *Tgf-β2* null mutant mice die almost immediately after birth due to collapsed airways in the lungs. E18.5 mutants display many skeletal abnormalities, such a reduction in the size of limbs, abnormal limb and rib morphology and a failure of the neural arches of the spinal column to fuse[313]. In addition, GDF-11 regulates segmental skeletal pattern along the anterior/posterior axis. Homozygous mutant mice for *Gdf-11* show an increased number of thoracic and lumbar vertebrae and ribs, and a posterior displacement of the hindlimbs[314]. The important roles that GDF-5 plays in regulating skeletal patterning and morphogenesis will be discussed in detail in Chapter 5.

Many TGF-β superfamily ligands, such as BMP-8b, BMP-2, GDF-9 and activins, have been shown regulate aspects of sexual differentiation, particularly germ cell and gonadal development[258]. In addition, TGF-β has been implicated in modulating tissue repair and inflammation. In an experimental rat model of wound healing, daily injection of TGF-β has been shown to increase fibroblast proliferation, promote the influx of mononuclear cells and enhance the formation of collagen, thereby accelerating wound healing[248,315].

Deregulation of TGF-β superfamily signalling can cause developmental abnormalities and directly lead to cardiovascular, fibrotic, reproductive and skeletal disorders[303]. Hereditary or sporadic mutations in genes encoding TGF-β superfamily ligands or receptors can also result in oncogenesis[316]. For

example, Juvenile Polyposis syndrome (JPS) predisposes young individuals to gastrointestinal tract cancers. Germ-line mutations in *Smad4*, *Alk-3* and *endoglin* genes have been identified in JPS patients. Moreover, TGF-β1 polymorphisms or sporadic *Tgf-βRII* mutations appear to underlie breast, colon, lung, pancreatic and prostate cancers[316].

1.4.5. TGF-β superfamily in the nervous system

Members of the TGF-β superfamily are widely expressed both in the developing and adult peripheral and central nervous systems, reflecting their essential functions in neuronal development, survival, morphogenesis and maintenance[258]. Importantly, an increasing amount of data has emerged to suggest that certain TGF-β superfamily members may potentially be neuroprotective against some neurological diseases.

Some members of the TGF-β superfamily family play important roles in regulating the induction of neural tissue and the determination of neural phenotypes during embryogenesis. In vertebrates, the dorsal ectoderm of the embryo forms neural tissue following induction by factors secreted by the dorsal mesoderm. Dorsal mesoderm-derived Noggin has been shown to induce anterior neural tissue[317] by suppressing the activity of epidermal inducer, BMP-4[318]. TGF-β superfamily members can also regulate the fate of neural crest cells, determining whether they become PNS neurons, melanocytes or cranial skeletal elements. For instance, BMP-4 and BMP-7 induce the expression of the adrenergic marker enzyme, tyrosine hydroxylase in neural crest cell cultures reflecting the differentiation of sympathetic neurons[319]. Moreover, TGF-β1 stimulates the proliferation of astrocytes[320] and regulates oligodendrocyte differentiation[321]. Loss of function studies, using siRNA against Smad4, have shown that TGF-β/BMP signalling is required to regulate neuronal specification, pattern formation and progenitor cell proliferation within the developing chick dorsal neural tube. TGF-β/BMPs regulate progenitor cell proliferation indirectly by promoting the expression of members of the Wnt family that act as mitogens for neural progenitor cells[322]. The regulation of neural tube progenitor cell proliferation and subsequent progenitor differentiation appears to be dependent on the identity of the BMPR-I receptor that is expressed by progenitors[323].

Mouse CNS progenitors initially express BMPR-Ia and respond to BMPs with enhanced proliferation. However, BMP induced activation of BMPR-Ia induces the expression of BMPR-Ib. When BMPR-Ib expression levels become high, proliferating progenitors respond to BMPs by ceasing proliferation. During the early embryonic period, mitotically arrested progenitors are removed by apoptosis, but as development proceeds the cessation of proliferation results in neuronal differentiation[323].

TGF-β3 potentiates the survival promoting effects of the neurotrophins, NT-3 and NT-4 on cultured E8 chick DRG neurons and a blocking antibody to TGF-β reduces NT-3 and NT-4 promoted survival of these neurons, suggesting that endogenous TGF-β3 normally acts in an autocrine/paracrine manner to enhance the actions of these neurotrophins on cultured chick DRG neurons[324]. GDNF, a divergent member of the TGF-β superfamily, is a well-established neurotrophic factor for developing PNS and CNS neurons *in vitro* and *in vivo*[93]. GDNF was initially characterised as a neurotrophic factor based on its ability to promote the survival and morphological differentiation of dopaminergic neurons in cultures established from rat embryonic midbrain[325]. Administration of GDNF prior to nigrostriatal lesion has been shown to be neuroprotective in a mouse MPTP lesion model of Parkinson's disease, reducing the loss of substantia nigra dopaminergic neurons and ameliorating the reduction in dopaminergic innervation of the striatum. Moreover, the administration of GDNF following MPTP lesion promotes re-innervation of the striatum by nigral dopaminergic neurons, raising the prospect that GDNF may have therapeutic potential in Parkinson's disease[326]. The neurotrophic effects of GDNF on developing sympathetic, sensory and dopaminergic midbrain neurons, at least in culture, appear to be dependent on a synergistic interaction between neuron-derived TGF-β and exogenous recombinant GDNF[327]. The GDNF subfamily of the TGF-β superfamily includes neurturin and artemin, both of which have been shown to play important roles in regulating the development of enteric, sympathetic and parasympathetic autonomic neurons and some subgroups of sensory neurons[93].

Several studies have shown that members of the TGF-β superfamily have an important role in axon guidance by providing neurons with chemotactic cues. For example, GDF-7 and BMP-7 are both expressed in the roof plate of the developing spinal cord and GDF-7 heterodimers act as a chemo-repellent to drive the initial ventral trajectory of commissural axons. In support of this, many commissural axons are misrouted in E11.5 *Gdf-7*/*Bmp-7* double null mutant mouse embryos[328]. TGF-β superfamily members have also been shown to regulate neuritic process outgrowth. TGF-β1 and TGF-β2 promote neurite sprouting and enhance axon elongation in cultures of embryonic rat hippocampal neurons[329]. BMP-7 induces dendritogenesis in sympathetic, cortical and hippocampal neuron cultures[330-332]. In the case of cortical neurons, dendritogenesis is mediated in a Smad-independent manner by the binding of LIM kinase 1 (LIMK1) to the BMPR-II receptor. LIMK1 is a downstream effector of Rho GTPases that regulates actin dynamics by phosphorylating and inactivating cofilin, an actin depolymerizing factor[333]. The importance of LIMK1 in regulating dendrite formation, spine morphology and synaptic plasticity has been demonstrated in *Limk1* null mice, which display abnormal dendritic spines and enhanced LTP compared to wild type mice[334].

Several studies have suggested that members of the TGF-β superfamily may be neuroprotective following neuronal damage and may ameliorate the development of damage-associated neuropathology. For example, TGF-β1 protects motor neurons from axotomy and glutamate induced apoptosis and can restore motor function in a mouse model of amyotrophic lateral sclerosis (ALS)[335]. Moreover, TGF-β1 administration before induction of focal ischemia in mice reduces lesion size and the extent of cell death, and TGF-β1 limits apoptosis in cultures of embryonic rat hippocampal neurons following trophic factor deprivation[336]. Perhaps more importantly, TGF-β1 ameliorates Aβ induced apoptosis in cultures of rat cortical neurons by a signalling mechanism that involves activation of the PI3K pathway[337]. More recently, TGF-β1 has been shown to protect cultured mouse hippocampal neurons against Aβ-induced apoptosis, in a similar manner to NGF, by inducing the expression of the transcription factor, Hes1[175].

TGF-β family members regulate the development of many cell and tissue types and play important roles in disease modulation in the adult. TGF-β family members have also been shown to play vital roles in the developing and adult nervous system including regulating neurogenesis and gliogenesis, modulating neuritic process outgrowth, promoting the establishment of functional synaptic connections, protecting against neuronal trauma and the onset of neurological diseases. However, several members of the TGF-β superfamily have yet to be fully investigated to determine whether they have neuroregulatory and/or neurotrophic roles in the developing or adult nervous system, leaving important questions unanswered.

1.5. Aims

1.5.1. Hypothesis

In this project, it was hypothesised that APRIL and GDF-5, members of the TNF-α and TGF-β superfamilies, respectively, and their cognate receptors are expressed in developing hippocampal pyramidal neurons and that APRIL and GDF-5 dependent signalling regulate some aspects of hippocampal neuron development. The characterised expression patterns of APRIL, GDF-5 and their receptors suggested that APRIL may play a role in regulating axonal elongation and GDF-5 may play a role in regulating dendrite growth.

1.5.2. Specific aims

1. Characterise the expression of APRIL and GDF-5 in developing hippocampal neurons at the mRNA and protein levels.
2. Determine the cellular location of APRIL, GDF-5 and their respective receptors in cultured hippocampal neurons and in the developing hippocampus.
3. Evaluate the morphological changes of axons and dendrites in cultures of developing hippocampal neurons following exposure to recombinant APRIL and GDF-5.
4. Determine the receptors by which the ligands exert their effects.
5. Investigate the intracellular signalling pathways that transduce the morphological changes of APRIL and GDF-5 on hippocampal neurons.
6. Validate the physiological relevance of *in vitro* findings using *in vivo* models.

Chapter 2

Material and Methods

2.1. Animal husbandry

All animals in this study were handled and kept under conditions that respected the guidelines of the Home Office Animals (Scientific Procedures) Act, ASPA, 1986. Embryonic and postnatal CD1 wild type mice and transgenic strains were obtained from timed overnight matings. Breeding was confirmed by the presence of a vaginal plug. The fertilization day was considered as embryonic day one (E1) and the day of birth as postnatal day zero (P0).

April and *Alk-6* transgenic mice, were genotyped using conventional polymerase chain reaction (PCR) (see Appendix II). *Gdf-5*$^{bp-J}$ (Growth differentiation factor 5, brachypodism-Jackson), obtained from The Jackson Laboratory), which will be referred to as *Gdf-5*^{bp} below and carry a spontaneous point mutation. Since homozygous *Gdf-5*^{bp} mice have shorter limbs than wild type or heterozygous mice, they were identified by their phenotype. All animals were fed rodent global diet pellets (Harlan) and given water *ad libitum*.

2.2. Cell culture

Cell culture was used to grow neurons under controlled conditions in order to study the effect of different recombinant ligands, mutated forms of proteins and chemical compounds on the normal physiology and biochemistry of neurons.

2.2.1. Preparation of Tungsten needles

Tungsten needles were made from pieces of 0.5mm diameter, 5cm long tungsten wire held in needle holders (InterFocus). The tip of each wire was bent into a 90° angle and placed vertically in a solution of 2M NaOH. The tip was electrolytically sharpened with a 3-12V AC current passing though the NaOH solution. Sharpened needles were sterilized using 70% ethanol and a Bunsen burner flame before and after each use.

2.2.2. Preparation of culture dishes

Neurons were cultured on a poly-L-lysine hydrobromide substratum. Four-well dishes or 35mm dishes (Greiner bio-one) were coated with 2ml of 0.5mg/ml poly-L-lysine (Sigma-Aldrich) and incubated at 37°C overnight (see Appendix II for preparation details of Poly-L-lysine solution). The dishes were then washed twice with autoclaved milli-Q water and left to dry in a laminar flow hood.

2.2.3. Preparation of culture media

Hippocampal cultures were maintained in Neurobasal-A culture media containing 2% B-27 Supplement, 500μM of Glutamax and 1% Penicillin-Streptomycin (Life technologies).

2.2.4. Hippocampal dissection

Dissection tools (InterFocus) were flamed in 70% ethanol before and after use. All dissections were performed in a sterile environment within a laminar flow hood that had been previously cleaned with 70% ethanol.

Postnatal mice at P0, P5 and P10 were killed by decapitation, whilst pregnant females were sacrificed by cervical dislocation to obtain E18 embryos. In the latter case, the female abdomen was rinsed with 70% ethanol before removing the embryonic sac by laparotomy and placing it in a Petri dish containing PBS. Next, embryos were removed from the embryonic sac, washed in PBS and placed in a fresh Petri dish containing PBS. The correct stage of development was determined according to Theiler's criteria[338].

Brains were gently harvested from E18 mouse embryos using a dissecting microscope (Nikon) and a fibre-optic light source (Schott). With the ventral side of the brain facing up, the cerebral hemispheres were separated by moving the forceps through the midline and making a saggital cut. Next, the meninges and the choroid plexus were carefully removed from both hemispheres. Each hemisphere was placed with its inner surface facing upward and the hippocampus was identified as a thicker portion lining the curved medial edge of the cortex. The hippocampus was separated from the cortex using

sharp forceps and, finally, tungsten needles were used to remove the fimbria and the remaining cortex[339] (Fig.15).

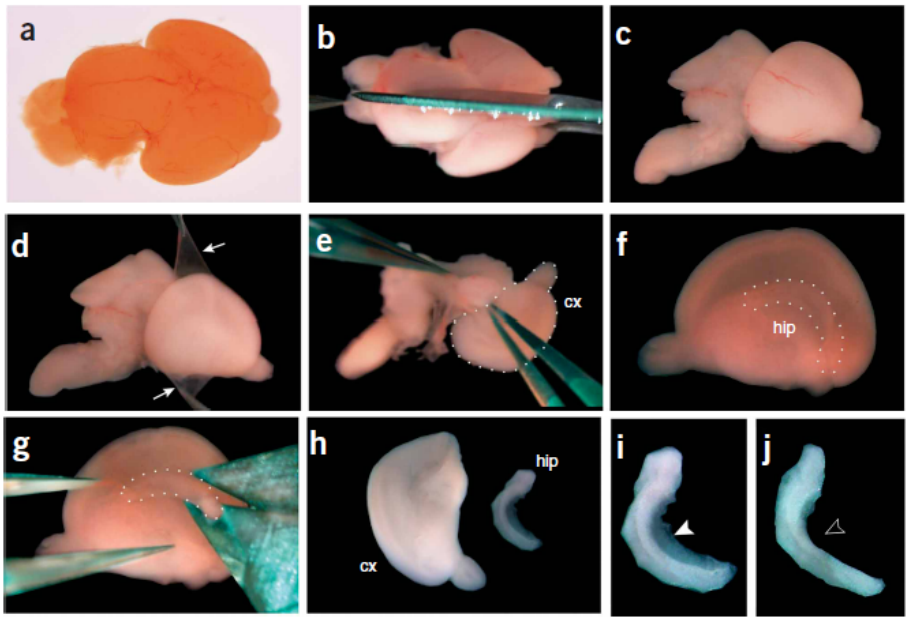

Figure 15: Hippocampus dissection at E16.5.

(a) The mouse brain was removed and (b) cut along the medial saggital plane (c). For each half (d) the meninges were removed and (e) the cortex clipped off the midbrain. (f) The hippocampus was identified on the inner surface of the forebrain (g) and dissected from the cortex. (h) Cortex (cx) and Hippocampus (hip). (i) The fimbria was removed (j) and hippocampus collected[339].

2.2.4.1. Hippocampal primary cultures

For each culture, up to 12 hippocampi were collected and placed into a 15ml tube (Greiner bio-one) containing 1800μl of 1X HBSS without Ca^{2+} and Mg^{2+} (Life technologies). For enzymatic dissociation of the hippocampi, trypsin (Worthington) (see Appendix II for details of stock solution) was added to the HBSS to give a final concentration of 1mg/ml. The mixture was next incubated in a 37°C water bath for 20min. To quench trypsin activity, trypsin inhibitor (Sigma-Aldrich) (see Appendix II for stock solution preparation) was added to a final concentration of 1mg/ml and the hippocampi were then mechanically dissociated into single cells by gentle pipetting through a 1ml tip. Finally, DNase I (Roche) (see Appendix II for stock solution) solution was gently mixed into the cell suspension, to a final concentration of 0.05mg/ml, to digest DNA liberated

from damaged cells and avoid clumping of tissue. Subsequently, the cell suspension was centrifuged for 10min at 700rpm to pellet cells. After careful removal of the supernatant, the cell pellet was gently resuspended in 1ml of hippocampal neuron complete culture medium.

To assess the number of viable cells in the cell suspension, 20μl of the suspension was diluted in 20μl of trypan blue solution (0.4%) (Sigma-Aldrich) and viable cells that excluded trypan blue were counted using a Neubauer hemacytometer. The number of cells plated onto Poly-L-lysine coated tissue culture dishes varied according to the purpose of individual experiments, and hence the type of culture dishes used (from 40,000 cells up to 500,000 cells). Up to 2ml of the cell suspension was plated in 35mm dishes, whereas only 55μl of cell suspension was plated into each well of 4-well dishes. In the latter case, 2ml of culture medium was added to 4-well dishes after allowing 2 hours for plated cells to attach to the substratum.

Cells were incubated at 37°C, with 5% CO_2, for 3 or 7DIVs according to the purpose of the experiment. Recombinant ligands or compounds were added after either 2DIVs or 6DIVs (Table 2).

2.2.4.2. Explants in 3D Matrigel cultures

Explants in 3D Matrigel cultures were use to mimic *in vivo* conditions. Using the technique described above, 350μm thick hippocampal sections were obtained using a tissue chopper. Next, the region of interest (for example CA1) was carefully isolated from each slice using tungsten needles.

Matrigel (BD Biosciences) was kept on ice prior to use to avoid polymerization. 20μl of Matrigel was pipetted into the bottom of each well of a 4-well dish, which was subsequently placed in a 37°C incubator for 15min until the gel had become polymerized. After each hippocampal explant had been transferred onto a Matrigel base in the 4-well dishes, a further 20μl of Matrigel was pipetted on top of it. Dishes were then incubated at 37°C for a further 15min until the Matrigel covering the explants had become polymerized. Finally, 2ml of complete neurobasal medium was added to each dish and the dishes were incubated at 37°C, in 5% CO_2, until further use[340].

2.2.5. Cell lines cultures

Frozen cell lines were obtained from a commercial collection (the American Type Culture Collection - ATCC, Manassas, VA, USA). The BHK-21 cell line was originally derived from baby hamster kidneys while 293T cell line was derived from human embryonic kidney. Frozen cells were thawed on ice, resuspended in Dulbecco's modified Eagle's medium (DMEM) supplemented with 10% heat-inactivated foetal bovine serum (FBS), 2mM GlutaMAX I, 100units/ml penicillin and 100µg/ml streptomycin (Life technologies) and cultured in Corning cell culture flasks (Thermo Scientific), at 37°C, in an humidified atmosphere containing 5% CO_2 and 20% O_2. After 3DIVs, the culture medium was removed and replaced with 5ml of Trypsin-EDTA (Life technologies). After 5min incubation at 37°C, the BHK-21 or 293T cells had become detached from the bottom of the tissue culture flask, allowing them to be aspirated into fresh culture medium. Following centrifugation of the cell suspension, for 5min at 1000rpm, the supernatant was removed from the cell pellet and the cells were resuspended in fresh culture medium and used to seed two new tissue culture flasks.

The IM-9 cell line was derived from human B lymphoblasts, while the Jurkat cell line was derived from human acute T cell leukaemia. In the case of both these non-adherent cell lines, frozen cells were thawed on ice, resuspended in RPMI-1640 medium (Life technologies) containing 10% FBS and 1% Penicillin-Streptomycin and cultured in Corning cell culture flasks, at 37°C, in an humidified atmosphere containing 5% CO_2 and 20% O_2. After 3DIVs, the culture medium containing suspended cells was removed and centrifuged, for 5min at 1000rpm, to pellet the cells. The cell pellet was resuspended in fresh culture medium and used to seed two new tissue culture flasks.

Cells from different cells lines were collected for RNA or protein extraction. In addition, $2x10^6$ cells of each cell line were resuspended in complete growth medium and 5% DMSO and frozen at -80°C.

Table 2: Recombinant ligands and compounds.

Ligands/Compounds	Company	Concentration
Recombinant APRIL (human)	Enzo Life Sciences	10ng/ml, 100ng/ml, 1μg/ml
Recombinant APRIL (mouse)	Enzo Life Sciences	10ng/ml, 100ng/ml, 1μg/ml
PD98059	Sigma-Aldrich	10μM
LY294002	Sigma-Aldrich	10μM
AKT1/2 kinase inhibitor	Sigma-Aldrich	5μM
LPA (Oleoyl-L-α-lysophosphatidic acid sodium salt)	Sigma-Aldrich	10μM
Recombinant GFD5/BMP-14 (mouse)	R and D systems	10ng/ml, 100ng/ml, 1μg/ml

2.3. Transfection

Transfection is the process of introducing a nucleic acid into a cell. Hippocampal neurons have to be cultured at a very high density to support their survival, thereby confounding the morphological analysis of individual neurons within cultures. To circumvent this problem, transfection of cDNA expression constructs was used to direct the expression of fluorescent proteins to individual neurons, thus allowing the morphology of individual hippocampal neurons to be analysed with fluorescence microscopy.

2.3.1. Transfection vectors

The vector expressing copGFP (pCDH-CMV-MCS-EF1-copGFP) (Fig.16) was provided from System Bioscience (see Appendix II). Flag-hAPRIL-A88 vector was kindly provided by Pascal Schneider[341]. The flag tagged hAPRIL sequence was cloned into the HindIII and EcoRI sites of the expression vector pCDNA3.1 (Life technologies). Following this, pCDH-CMV-hAPRIL-A88-EF1-copGFP was generated by excising the flag tagged hAPRIL sequence from pCDNA3.1 and inserting it into the NheI and NotI sites of the pCDH-CMV-MCS-EF1-copGFP vector.

Vectors encoding murine (m) BCMA and mBCMA ΔC83 were kindly provided by Adrian T. Ting[342]. mBCMA and mBCMA ΔC83 sequences were cloned into the HindIII and NotI sites of the vector pCDNA3.1. pCDH-CMV-mBCMA-EF1-copGFP and pCDH-CMV-mBCMA ΔC83-EF1-copGFP were made by excising the respective cDNA encoding sequences from pCDNA3.1 and inserting them into the NheI and NotI sites of the vector pCDH-CMV-MCS-

EF1-copGFP.

A constitutively active (CA), BMPR-Ib-Q203D, and dominant negative (DN), BMPR-Ib-Q203D/D265A, form of BMPR-Ib were kindly provided by Daniel J. Bernard[343]. The vector pCDH-CMV-MCS-EF1-copGFP was modified to allow the subcloning of these mutants BMPR-Ib cDNAs into it by creating additional restriction sites. Double stranded DNA was generated by annealing the following oligos: 5'-GCT AGC CGA GCT CGG ATC CGA ATT CCT CGA GGG GCC CTT CGA ATG AGC GGC CGC-3' and 5'-GGC CGC TCA TTC GAA GGG CCC CTC GAG GAA TTC GGA TCC GAG CTC GG-3'. This double stranded DNA product, containing terminal NheI and NotI sites and internal EcoR1 and BstB1 sites, was subcloned into pCDH-CMV-MCS-EF1-copGFP, thereby generating pCDH-CMV-MCS-EF1-copGFP version 1. Following this, pCDH-CMV-BMPR-Ib-Q203D-EF1-copGFP and pCDH-CMV-BMPR-Ib-Q203D/D265A-EF1-copGFP were made by inserting the respective BMPR-Ib cDNA encoding sequences into the EcoRI and BstBI sites of pCDH-CMV-MCS-EF1-copGFP version 1.

Vectors encoding pGFP-N1 BMPR-II-WT and pGFP-N1 BMPR-II-D485G (DN) were kindly provided by Nicholas W. Morrell[344]. The vector expressing EGFP (pEGFP-N1) was obtained from Clontech. pCDH-CMV-MCS-EF1-copGFP was modified a second time, by creating additional restriction sites, to allow the cloning of the BMPR-II cDNAs into it. Double stranded DNA was generated by annealing the following oligos: 5'- CTA GAG CTA GCG AAT TCG AAT TTA AAT GGA TCC ATG AGC-3' and 5'- GGC CGC TCA TGG ATC CAT TTA AAT TCG AAT TCG CTA GCT-3'. The double stranded DNA product, flanked by XbaI and NotI sites and internal EcoR1 and BamH1 sites, was subcloned into pCDH-CMV-MCS-EF1-copGFP, thereby generating pCDH-CMV-MCS-EF1-copGFP version 2. Finally, pCDH-CMV-BMPR-II-WT-EF1-copGFP and pCDH-CMV-BMPR-II D(485)G-EF1-copGFP were made by inserting the respective BMPR-II cDNA encoding sequences into the EcoRI and BamHI sites of pCDH-CMV-MCS-EF1-copGFP version 2.

The reporter plasmid pGL3-BRE-Luciferase was kindly provided by Xiao-Fan Wang[345]. pGL3-BRE-Luciferase contains the BMP responsive elements of

the mouse Id1 gene cloned into the pGL3 firefly luciferase vector. Reporter plasmids pHes5-pGL3-Luc and pHes5SM-pGL3-Luc were kindly provided by Tetsuya Taga[346]. pHes5-pGL3-Luc contains a fragment of the Hes-5 promoter (nucleotides ±179 to +72) cloned into the pGL3 firefly luciferase vector. pHes5SM-pGL3-Luc was constructed by introducing mutations (taaatcgcc) into a Smad-binding site (SBS) (±161 to ±153: gcccgcgcc) of the Hes5 promoter in pHes5-pGL3-Luc .

The vector pIRES-Hes6 was kindly provided by Phil Jones[347]. A Myc-tagged form of Hes6 was generated by inserting the Hes6 cDNA encoding sequence from pIRES-Hes6 into the NcoI/StuI sites of pCS2 (addgene). pRK-DPC4-deltaC-Flag, encoding a C-terminal truncated form of Smad4 (aa 1-511), pCS2-Flag-Smad6, encoding Smad6, and pCMV5-Smad7-HA, encoding Smad7, were obtained from addgene (Addgene plasmid 12628[348], Addgene plasmid 14960[284] and Addgene plasmid 11733[349] respectively).

Vector encoding WT form of Hes5 (pCLIG-Hes5) was kindly provided by Ryoichiro Kageyama[350]. To obtain pCDH-CMV-Hes5-EF1-copGFP, corresponding cDNA encoding sequence was subcloned into the EcoRI site of pCDH-CMV-MCS-EF1-copGFP. To obtain pCDH-CMV-t-Hes5-EF1-copGFP, the first 28 amino-terminal amino acids of the molecule, containing the DNA-binding domain, were deleted by PCR, using pCLIG-hes5 as template and the following primers: 5'-AAA TCT AGA TGG AAC AAA AAC TTA TTT CTG AAG AAG ATC TGG ACC GCA TCA ACA GCA GCA T-3' and 5'-ATT CGA ATT CGG TCG AGG CAT-3'. The resultant cDNA was subcloned into the XbaI and EcoRI sites of pCDH-CMV-MCS-EF1-copGFP.

For shRNA experiments, the vector pGFP-VRS was obtained from Origene Technologies (Rockville, MD, USA). For pGFP-VRS shRNA Hes5 construction, the targeting sequence 5'- GAC ACG CAG ATG AAG CTG CTT TAC CAC TT-3' was inserted into BamHI/HindIII sites of pGFP-VRS. For the scramble construction, the 5'-GCA CTA CCA GAG CTA ACT CAG ATA GTA CT-3' was used.

Subcloning of cDNA fragments between vectors was performed using standard molecular biology procedures. After digestion with appropriate restriction enzymes, DNA fragments were separated by running them in a 1% low-melting point agarose gel (Sigma-Aldrich). Following electrophoretic separation, desired DNA fragments were cut from the gel under UV light and purified using a QIAquick Gel Extraction Kit (Qiagen) according to the manufacturer's instructions. Vector DNA fragments were dephosphorylated by Alkaline Phosphotase (Roche) to promote efficient ligation with cDNA encoding fragment. Finally, DNA fragments were ligated using the Rapid DNA ligation kit (Roche).

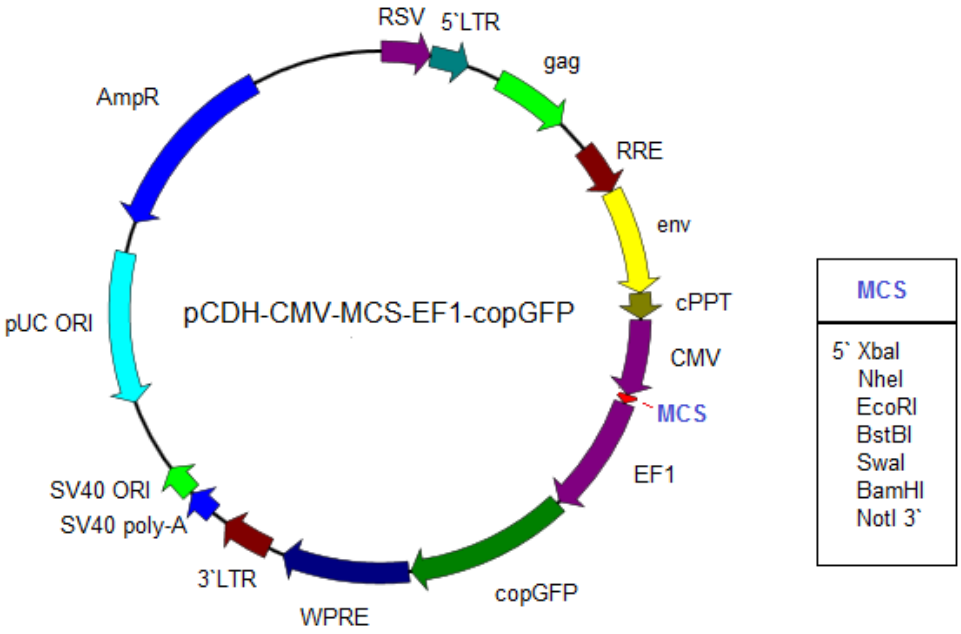

Figure 16: Schematic representation of pCDH-CMV-MCS-EF1-copGFP dual-expression vector. Of interest: CMV promoter (constitutive human cytomegalovirus promoter), MCS-multiple cloning site for cloning the coding sequence of interest into the vector downstream of the CMV promoter, EF-1 promoter (constitutive elongation factor 1α promoter) drives the expression of copGFP (copepod green fluorescent protein) as a reporter for transfected cells (see Appendix II).

Table 3: Plasmid description.

Plasmid	Company	Resistance Gene	Sequence of interest
pCDH-CMV-MCS-EF1-copGFP	SBI – System Biosciences	Ampicillin	_____
pCDH-CMV-hAPRIL-A88-EF1-copGFP	see section 2.3.1.	Ampicillin	human APRIL
pCDH-CMV-mBCMA-EF1-copGFP	see section 2.3.1.	Ampicillin	mouse BCMA
pCDH-CMV-mBCMA ΔC83-EF1-copGFP	see section 2.3.1.	Ampicillin	mouse BCMA ΔC83 (truncated mutant)
pCDH-CMV-mBMPR-Ib-QD-EF1-copGFP	see section 2.3.1.	Ampicillin	mouse BMPR-Ib-QD (constitutively active)
pCDH-CMV-m BMPR-Ib-QD D265A-EF1-copGFP	see section 2.3.1.	Ampicillin	mouse BMPR-Ib-QD D265A (dominant negative)
pCDH-CMV-BMPR-II WT-EF1-copGFP	see section 2.3.1.	Ampicillin	BMPR-II WT
pCDH-CMV-BMPR-II D(485)G -EF1-copGFP	see section 2.3.1.	Ampicillin	BMPR-II D(485)G (dominant negative)
pRK-DPC4-deltaC-Flag	addgene	Ampicillin	DPC4
CS2-Flag-Smad6	addgene	Ampicillin	Smad6
pCMV5-Smad7-HA	addgene	Ampicillin	Smad7
pGL3-BRE-Luc	Gift from Professor Xiao-Fan Wang	Ampicillin	BMP responsive element
pHes5-pGL3-Luc	Gift from Professor Tetsuya Taga	Ampicillin	Hes5 promoter
pHes5SM-pGL3-Luc	Gift from Professor Tetsuya Taga	Ampicillin	Smad binding site mutation
phRL-TK-Luc	Promega	Ampicillin	Renilla luciferase
pCS2	addgene	Ampicillin	_____
pIRES-Hes6	Gift from Professor Phil Jones	Ampicillin	Hes6
pGFP-scramble-VRS	see section 2.3.1.	Ampicillin	scramble shRNA
pGFP-shRNA-Hes5-VRS	see section 2.3.1.	Ampicillin	Hes5 shRNA
pCDH-CMV-Hes5-EF1-copGFP	see section 2.3.1.	Ampicillin	Hes5 WT
pCDH-CMV-t-Hes5-EF1-copGFP	see section 2.3.1.	Ampicillin	t-Hes5 (truncated mutant)

2.3.2. Plasmid preparation

2.3.2.1. Transformation

E.coli JM109 Competent Cells (Promega) were thawed on ice and 100μl of the bacteria were transferred into a 1.5ml microfuge tube. Sequentially, 50ng of plasmid or 20μl of ligation mixture was added to the bacteria and, following gentle mixing, the bacteria were incubated on ice for 30min. After this, bacteria were heat-shocked, at 42°C for 90sec, and then immediately incubated on ice for 5min. Following this incubation, 900μl of LB (Luria Bertani) medium (Fisher scientific) without antibiotics was added to the mixture and incubated, at 37°C for 1h, with agitation. LB agar (Fisher scientific) plates containing either 100μg/ml Ampicillin (Sigma-Aldrich) or 50μg/ml Kanamycin (Sigma-Aldrich) were prepared previously. In accordance with the resistance gene of the plasmid, 100μl of the mixture was spread onto a selective agar plate and the remainder was centrifuged, resuspended in 100μl of LB medium and spread onto a second agar plate. Agar plates were incubated overnight at 37°C.

2.3.2.2. Mini and Midi plasmid preps

The next day, 10 bacterial colonies were randomly selected from agar plates containing bacteria that had been transformed with the products of ligation reactions. Each colony was grown overnight, at 37°C with agitation, in 10ml of LB medium containing the appropriate antibiotic (LB selection medium). The following day, each overnight culture was centrifuged to pellet the bacteria and plasmid DNA was extracted from the bacterial pellet using the QIAprep Spin Miniprep Kit (Qiagen) according to the manufacture's protocol. Each plasmid was sequenced and the vector with the correct DNA sequence was selected to be used in further experiments.

Colonies derived from bacteria transformed with either commercially obtained plasmids or sequenced verified newly constructed plasmids were incubated in 3ml of LB selection medium, at 37°C with agitation, during the day. Then, 1ml of the culture was added to 200ml of LB selection medium and was incubated, at 37°C with agitation, overnight. The next day, plasmid DNA was extracted from overnight bacterial cultures using the Hipure Plasmid filter Purification kit Midiprep (Life technologies) according to the manufacture's

protocol. Briefly, cells were centrifuged, and the bacterial pellet was resuspended in Resuspension buffer containing 20mg/ml of RNase A. Next, cells were lysed under alkaline conditions (sodium hydroxide/SDS), followed by neutralization and precipitation of proteins and cellular debris with a high salt concentration buffer (potassium acetate). The mixture was then passed through a column that contained a membrane that selectively binds plasmid DNA. Plasmid DNA was eluted from the membrane in a low-salt buffer (sodium chloride and Tris-HCl), before being precipitated with isopropanol. Precipitated plasmid DNA was recovered by 30min of centrifugation, at 13,000 rpm and at 4°C. Following aspiration of the supernatant, the DNA pellet was washed for 5min with 70% ethanol, left to air dry, and finally resuspended in 100µl of nuclease free water. The concentration and purity of the plasmid DNA was measured using a Nanodrop spectrophotometer (Thermo Scientific).

2.3.3. Liposome-mediated transfection

For each 4-well dish to be transfected, 1.2µg of plasmid was mixed with 250µl of Opti-MEM (Life technologies) in a microfuge tube. In a separate microfuge tube, 4µl of Lipofectamine 2000 transfection reagent (Life technologies) was added to 250µl of Opti-MEM. The two mixtures were incubated for 5min at room temperature (RT) before combining them, mixing, and incubating for 30min at RT. During this incubation, spheroid liposomes interact with DNA, encapsulating it and allowing its delivery to cells by endocytosis when in contact with a cell membrane.

Meanwhile, neurons cultured for either 2DIVs or 6DIVs were washed with pre-warmed Opti-MEM reduced serum medium and were added a final volume of 2ml of Opti-MEM. After, 500µl of the lipofectamine mixture was added drop wise to each 4-well dish, and dishes were gently agitated, to allow a uniform distribution of the liposomes, before being incubated, for 3 hours, at 37°C. After incubation, neurons were washed twice with neurobasal complete medium and incubated in this medium overnight, either with or without compounds or cytokines. The next day, neurons were fixed with 4% paraformaldehyde (PFA) (see Appendix II), for 30min at RT, washed twice in PBS and stored at 4°C until further use.

2.3.4. Non-liposomal-mediated transfection

For each 4-well dish to be transfected, 1.2μg of plasmid was mixed with 120μl of EC buffer or DNA condensation buffer followed by 3.2μl of Enhancer. The mixture was vortexed for 1sec before being incubated for 5min at RT. This step allows Enhancer promoted DNA condensation. Next, 10μl of Effectene Transfection Reagent (Qiagen) was added and the mixture was vortexed for 10sec before being incubated for 20min at RT. Effectene reagent spontaneously forms micelle structures that coat the highly condensed DNA. Meanwhile, 400μl of medium was removed from neurons that had been cultured for 6DIVs in 4-well dishes. Following the 20min RT incubation, 635μl of neurobasal medium without antibiotics was added to the Effectene/micelle coated DNA mixture and 710μl of the resultant mixture was added drop wise per 4-well dish. Following gently agitation, to allow a uniform distribution of the micelles, neurons were incubated for 3 hours at 37°C. Finally, neurons were washed twice with neurobasal complete medium and incubated in this medium overnight, either with or without compounds or cytokines. The next day, neurons were fixed with 4% PFA, for 30min at RT, washed twice in PBS and stored at 4°C until further use.

2.3.5. Imaging

Hippocampal neurons transfected with GFP-plasmids were imaged at 20x magnification with an inverted microscope (Zeiss) to analyze axonal length. Neurons transfected with GFP-plasmids to analyze dendritic outgrowth were imaged with a 63x water immersion objective of a confocal microscope (Zeiss). Explants were imaged at 10x magnification using a confocal microscope.

2.4. Luciferase assays

Luciferase assays were carried out using the Dual-Luciferase® Reporter Assay kit (Promega). Briefly, a 12-well plate was seeded with 200,000 cells/well and transfected after 6DIVs with 1.25ug of the firefly luciferase reporter plasmid and 125ng of the control renilla luciferase reporter plasmid, phRL-TKluc. Following transfection, the neurons in some wells were incubated with 100ng/ml of GDF-5 for 16h, whereas control wells contained no GDF-5. At 7DIVs the

plate was washed with 1X PBS followed by the addition of 100µl of 1X passive lysis buffer to each well. The plate was placed on an orbital shaker, for 15min at RT, to allow cell lysis. Cell lysates were centrifuged, to remove debris, and the supernatant was collected and maintained on ice. Finally, a GloMax® 20/20 manual luminometer (Promega) was used to measure luciferase activity in the lysates. For each sample, 20µl of lysate was mixed with 100µl of LAR II reagent prior to measuring firefly luciferase activity. Then, 100µl of Stop and Glo reagent was added to the mixture and the renilla luciferase activity was measured.

2.5. Quantification of neurite outgrowth

Hippocampal neurons were transfected with GFP-plasmids at 2DIVs or 6DIVs and fixed, with 4% PFA for 20min, at 3DIVs and 7DIVs respectively. Next, 50 images were randomly taken per condition using the 20x objective of an inverted fluorescent microscope (Zeiss) for axonal analysis and a 63x water immersion objective of a confocal microscope (Zeiss) for dendritic analysis. Axonal length was measured using ImageJ software and dendritic outgrowth and complexity was analysed with Adobe Photoshop software. Briefly, a 50µm radius was projected from the cell soma of a transfected neuron. The dendrite length was expressed as the percentage of the ratio between the number of dendrites longer than 50µm and the total number of dendrites.

To analyse dendrite outgrowth in Golgi preparations, approximately 50 neurons were randomly imaged, using a 2x objective, by bright light microscopy (Zeiss) and analysed by Sholl simplified method. Briefly, a simple Matlab script takes in account the relative position of terminal and branching points relative to the cell soma[351].

2.6. Quantification of hippocampal area and neuron survival

Serial 5µm frozen sections from P10 *Gdf5*$^{bp\text{-}J}$ and C57/Black6 mice were stained with MAP-2 and nuclear marker 4',6-diamidino-2-phenylindole (DAPI) as described in sections 2.9.3. and 2.9.3.1. The hippocampal, CA fields and DG areas were obtained through ImageJ software. To calculate the cell number per CA field, 40x amplification images were obtain for each field, and cells stained with DAPI and positive for MAP-2 were counted, using ImageJ Cell Counter Plugin, within an area of 20,000µm^2.

2.7. Reverse transcription

2.7.1. Principle

The reverse transcriptase-polymerase chain reaction (RT-PCR) is a rapid and sensitive method for analysing gene expression that combines the production of a single-stranded complementary DNA copy (cDNA) of the RNA through the reverse transcriptase with PCR amplification of the cDNA.

cDNA can be synthesized using random hexamers, oligo dT or target specific primers. Random primers hybridize in multiple origins along the RNA template allowing the enzyme reverse transcriptase to attach, generating multiple single stranded cDNA molecules. This enzyme is also a DNA-dependent DNA-polymerase therefore can synthesize a second strand of cDNA using the first cDNA molecule as a template after degrading the original mRNA with its RNaseH activity (Fig.17).

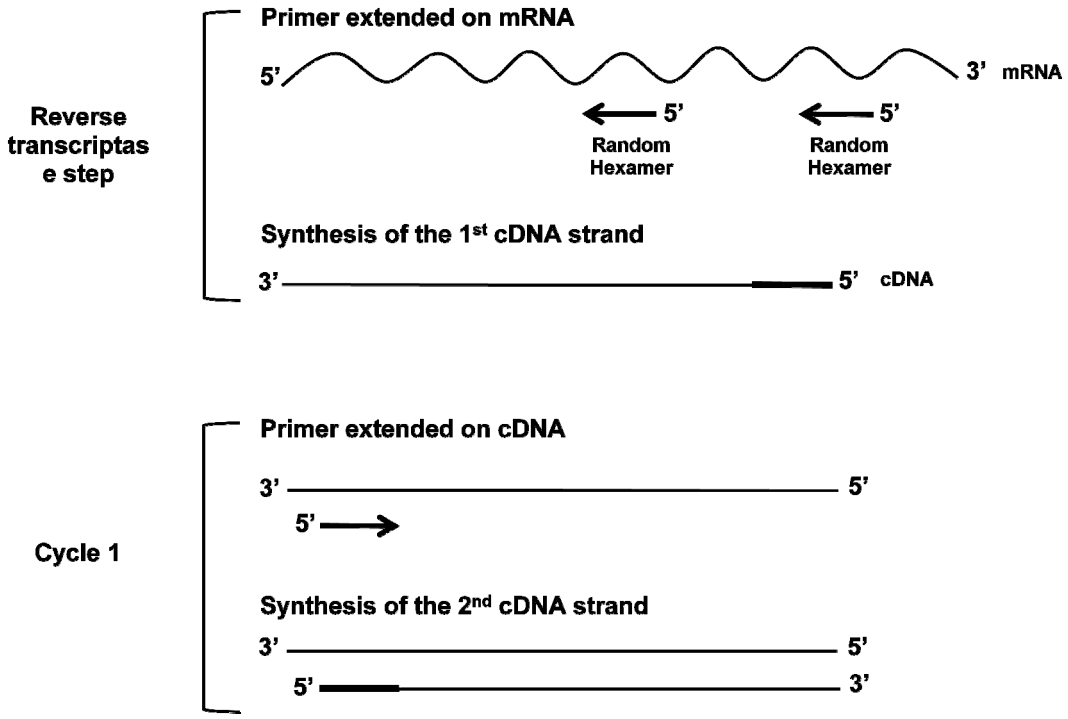

Figure 17: Reverse Transcription.

Random primers bind to mRNA allowing the reverse transcriptase to synthesize the 1st cDNA strand. After, the enzyme can produce a second strand of cDNA using the first cDNA molecule as a template.

2.7.2. Total RNA extraction

RNA from cells or tissue samples was extracted using the RNeasy Mini kit (Qiagen) and the RNeasy Lipid Tissue Mini kit (Qiagen), respectively. Briefly, cells or tissue were homogenized in RLT buffer containing 1% β-mercaptoethanol. One volume of 70% ethanol was added to each sample and mixed by pipetting up and down several times. Up to 700μl of the sample was transferred to an RNeasy spin column placed in a 2ml collection tube (both provided by the kit). The RNeasy columns contain a nucleic acid binding membrane that preferentially binds RNA as opposed to DNA. The columns were centrifuged at 13,000rpm for 15sec and the flow-through discarded. Next, 80μl of DNaseI, in DNaseI reaction buffer, (Qiagen) was added to the nucleic acid binding membrane of the columns and the columns were incubated for 15min at RT. Following this, columns were washed sequentially, by centrifugation, with 350μl of buffer RW1 and 500μl of buffer RPE. After a second wash with buffer RPE, RNA was eluted from the columns by the addition of 50-100μl of RNase-free water followed by centrifugation, at 13,000rpm for 1min. RNA was quantified as described below and stored at -80°C until further use.

2.7.3. RNA quantification

After purification, the RNA samples were kept on ice whilst the concentration of RNA and its purity were measured using a Nanodrop ND-1000 Spectrophotometer (LabTech international). The Nanodrop measures the RNA concentration (ng/ml) per 1μl of sample and calculates the 260/280nm ratio. If this ratio is between 1.8 and 2.0 this suggests that the RNA is free from protein contamination. Samples outside this interval were discarded.

2.7.4. cDNA synthesis

Total extracted RNA (400ng-1μg) was reverse transcribed using the Affinity Script Multiple temperature Reverse Transcriptase kit (Agilent Technologies). Briefly, for a 40μl reaction, 26.4μl of RNA (of a defined quantity) was mixed with 2μl of 10mM Random Hexamer Primers (Fermentas), 4μl of Affinity script 10x Buffer, 4μl of 100mM DTT, 1.6μl of 100mM of dNTPs (Roche)

and 2μl of Reverse Transcriptase. The mixture was incubated in a thermocycler for 90min at 42°C. Negative controls (reaction mix with RNase-free water instead of RNA) were also performed. Samples were stored at -20°C until further use.

2.8. Real-time PCR

2.8.1. Principle

The Polymerase Chain Reaction (PCR), invented by Kary Mullis in 1983, entails the logarithmic amplification of a specific DNA sequence *in vitro*. The starting template of a PCR reaction is either DNA or cDNA from reverse transcribed RNA. PCR is a sensitive and specific method that can discriminate between closely related mRNAs.

To amplify the target DNA sequence it is necessary to perform multiple cycles of 3 defined steps at different temperatures: denaturation (separation of double stranded DNA into single strands), primer annealing and primer extension (Fig.18).

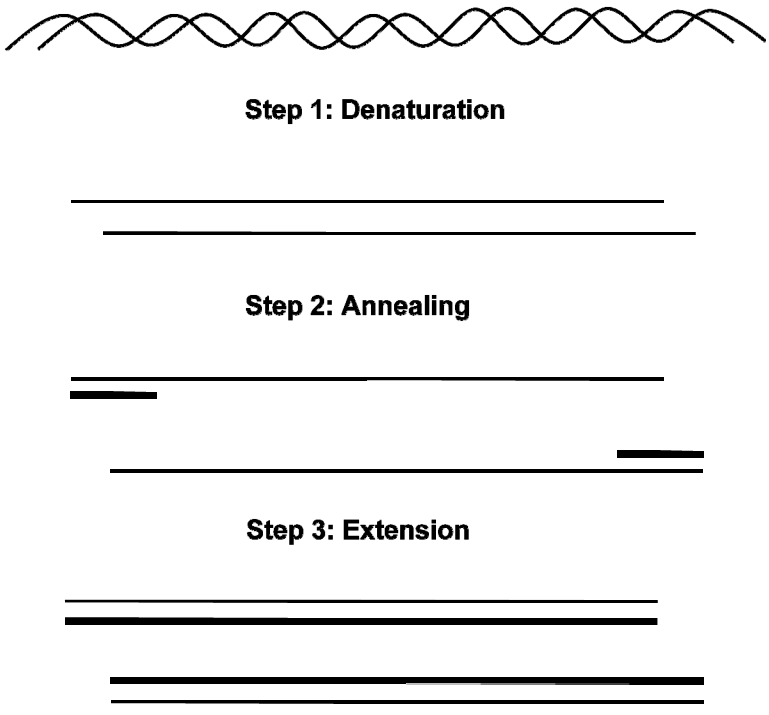

Figure 18: Polymerase Chain Reaction.
Taq polymerase allows extension of primers during repeated cycles of heat denaturation, primer annealing and primer extension.

PCR starts with a 95^{o}C denaturation step. The high temperature induces the separation of complementary DNA strands by disrupting the hydrogen bonds holding them together (Step 1: Denaturation). Next, cooling the temperature of the PCR reaction mix to 49-60^{o}C allows sequence specific primers to anneal to the single stranded DNA template (Step 2: Annealing). The annealing temperature (Ta) is usually 5-10^{o}C bellow the melting temperature (Tm) of the primer. Specific primers anneal to complementary sequences on the template strand, thereby defining the DNA fragment that is going to be amplified by the PCR process. The annealing of primers to the template allows a thermostable DNA Polymerase to attach to its 3' end and, by increasing the temperature to 72^{o}C, a copy of the DNA template is made, synthesizing new DNA in a 5' to 3' direction (Step 3: Extension) (Fig.18).

PCR is an exponential process, since newly generated double stranded DNA serves as a template for the next amplification cycle. Consequently, there is an exponential increase of copies of the target DNA template throughout time. Both original DNA strands serve as a template for synthesis of complementary strands. Therefore, if the reaction starts with 1 DNA template molecule, after the first cycle there will be 2 template copies, then after the next cycle 4 and after the third cycle 8. The degree of amplification of specific target DNA molecules can be simplified to 2^{n} where n is the number of cycles. After the target sequence has been amplified for between 20 to 40 cycles, depending on the original number of target template copies, it is possible to visualize the targeted PCR product on an ethidium bromide stained gel under UV light. Products appear as a single band with the size of the amplified sequence.

In Real-time PCR or quantitative-PCR (Q-PCR), the amplification of the target DNA is quantified whilst the PCR reaction is running by employing fluorescent detection methods. The fluorescence accumulation during thermocycling is directly proportional and reflects the amount of target DNA product present after each cycle. Real-time PCR uses the exponential phase of the PCR reaction for quantification. Quantitative analysis is based on the cycle number where accumulated fluorescence increases above a threshold level (Ct value) that is itself determined by the point where the accumulation of fluorescent PCR products at successive cycles becomes exponential. The lower

the Ct value of a sample is, the higher the number of copies of target DNA/cDNA that were present before PCR amplification. Figure 19 shows a representative amplification plot of a real-time PCR reaction.

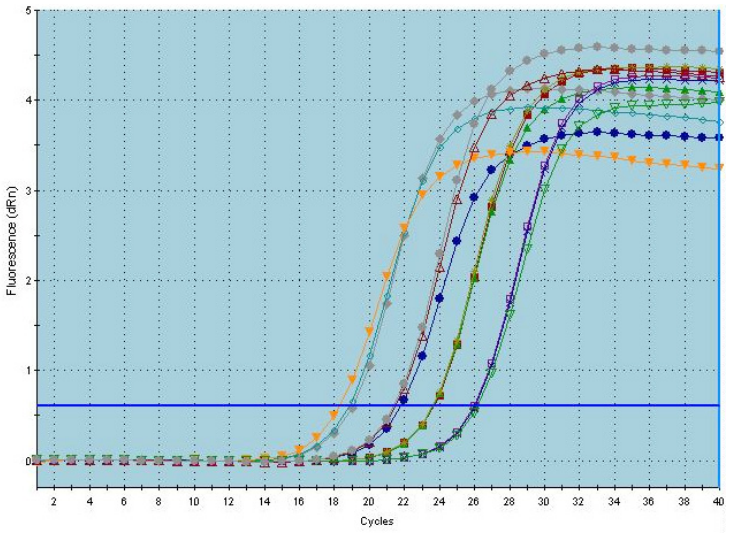

Figure 19: Real-time PCR Amplification Plot on a Stratagene Mx3000P Thermocycler. Amplification plot of five-fold serially diluted cDNA using the SYBR Green fluorescence detection method.

In this thesis, two different fluorescence detection methods were used to quantify PCR products: SYBR Green and Taqman probes.

SYBR Green is an intercalating dye that fluoresces once bound to double-stranded DNA. The amount of dye incorporated, and hence the level of fluorescence, is proportional to the amount of amplified product. However, this dye can bind to both specific target DNA amplification products and non-specific PCR products. Non-specific PCR products are generated either as a result of PCR primers binding to incorrect templates or due to self-amplification of primers (primer artefacts). The generation of high levels of non-specific PCR products in SYBR Green real-time PCR can confound the accurate quantification of correct PCR products. To overcome this problem, the purity of generated PCR products can be measured by incorporating a melting curve analysis step after the final PCR cycle. In melting curve analysis, the PCR reaction is heated up from 65°C at a rate of 1 degree per minute whilst continuously monitoring the fluorescence level of each sample. At 65°C, the vast majority of DNA in each sample is double-stranded and the fluorescence level of the sample is high. As the temperature is slowly increased, there is little

change in fluorescence levels until the melting temperature of the PCR products is reached. At this point, the individual DNA strands of the PCR products separate, thereby leading to a rapid and dramatic loss of fluorescence. A plot of rate of change of fluorescence against temperature reveals the melting temperature of the PCR products (Fig.20). Each PCR product has a unique dissociation temperature that can be calculated based on its length and sequence. For a SYBR Green real-time PCR assay to be valid, each sample must display a single, defined melting peak of the correct temperature. The presence of a peak at the wrong temperature and/or an ill-defined peak with a shoulder indicates the presence of incorrect PCR products and signals that the data from the sample cannot be used.

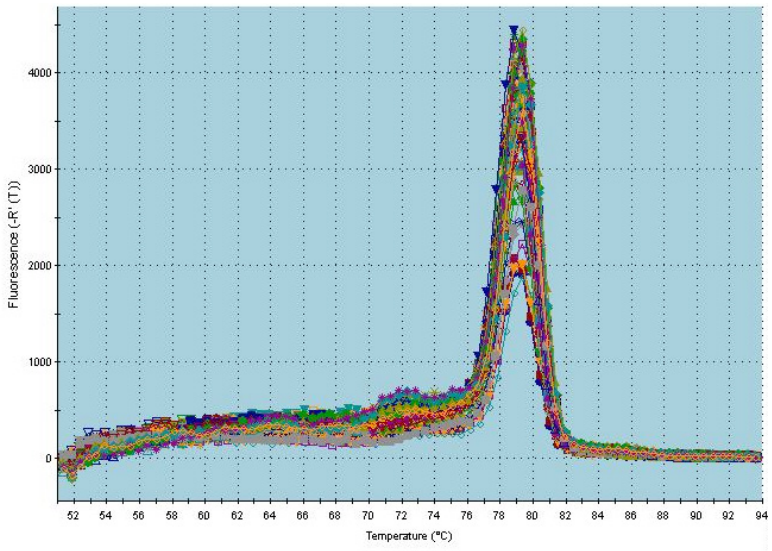

Figure 20: Graph showing the melting temperature of GAPDH real-time PCR products on a Stratagene Mx3000P Thermocycler. The clean, well-defined peak at 79°C demonstrates that the real-time PCR products correspond to GAPDH and contain insignificant amounts of non-specific amplification products.

The use of Taqman probes or double dye Probes entails using a third oligonucleotide, a fluorogenic probe, in the PCR reaction. A reporter fluorescent dye (ex: FAM or 6-carboxyfluorescein) is attached to the 5' end of the probe and a quencher dye (ex: TAMRA or tetramethylrhodamine) on the 3' end. While the probe is intact, FAM does not fluoresce as it passes its energy onto TAMRA by fluorescence resonance energy transfer (FRET). The sequence specific probe

binds to the DNA template in the annealing step of the PCR, downstream from one of the primer sites. When Taq polymerase extends from the primers, it displaces the 5' end of the probe which is subsequently degraded by the 5'-3' exonuclease activity of the Taq polymerase. This process allows primer extension to continue to the end of the DNA template and separates the reporter dye from the quencher dye, leading to an irreversible increase in fluorescence from FAM (Fig.21). As in the case of SYBR Green, the increase in fluorescence intensity as the real-time PCR reaction progresses is proportional to the amount of amplified product.

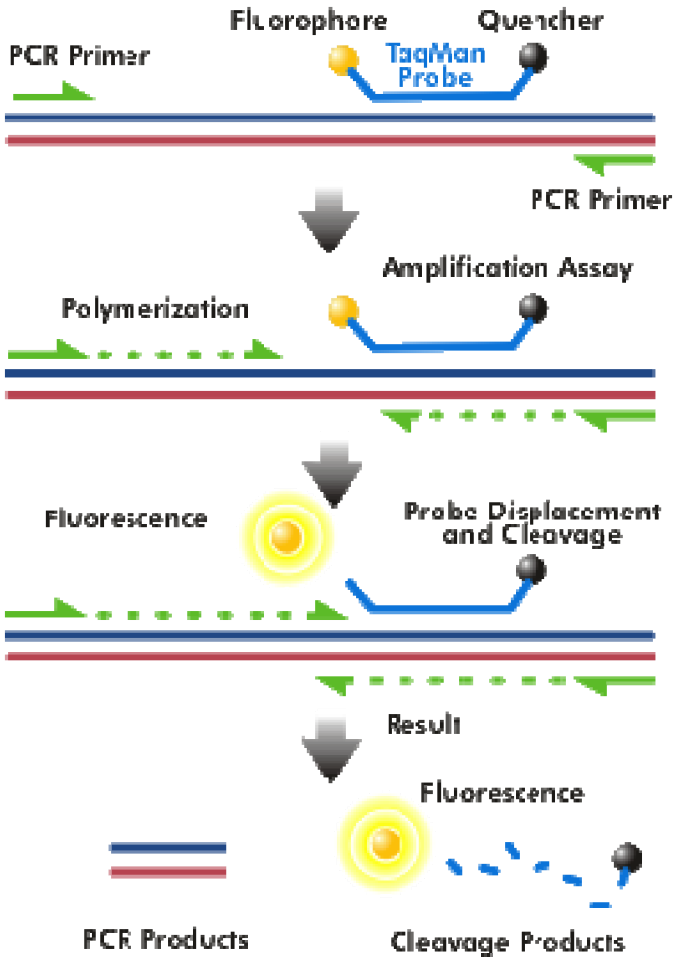

Figure 21: Taqman probe mechanism.

Taq polymerase allows the release of the reporter dye from the quencher dye, following the cleavage of the dual-labeled probe due to 5´–3´nuclease activity of Taq DNA polymerase.

2.8.2. Design of primers and probes

Primers are single stranded oligonucleotides that serve as a starting point for DNA amplification. Primers are designed to have a sequence that is the reverse complement of the template region. Probes are also small oligonucleotides that hybridize within the region flanked by the Forward (Fwd) and Reverse (Rev) primers. A good design of primers and probes allows real-time PCR to be a sensitive and specific method to quantify gene expression. There are several criteria that one must consider while designing small oligonucleotides to be used as primers and probes.

Primers and probes should have between 18-30bp length and the optimal Tm of primer and probes with template DNA is 55-60°C. Furthermore, the difference in Tm between the Fwd and Rev primers should be ≤4°C. Probes should have a Tm that is 8-10°C higher than the primers. Given the fact GC base paring (Guanine and Cytosine) involves 3 hydrogen bonds a higher GC content requires more energy for disruption than AT base paring. Consequently, the GC content of primers and probes should be around 40-60%. It is also important to avoid base paring complementarities between the Fwd and Rev primers, or between the primers and the probe, to prevent primer/primer and primer/probe dimers that can severely reduce the efficiency of real-time PCR reactions. Base paring complementarities within individual primers and probes will lead to the formation of stable hairpins that will reduce the efficiency of the real-time PCR reaction, and therefore should be avoided. Interactions between primers and probes, and secondary structures within primers and probes, are measured by the ∆-G (change in Gibbs free energy) parameter. The ∆-G value should be high (close to zero) because low (more negative) ∆-G values mean that it takes more energy to dissociate secondary structures and prevent primer/primer and primer/probe interactions.

The probe should be placed as close as possible to one of the primers without overlapping it and the Fwd and Rev primers should be either intron spanning or intron flanking, when possible, to prevent amplification of any contaminating genomic DNA. Furthermore, the amplicon lengths should be between 80 and 150bp. Finally, to determine that primers and probes are

unique and specific for their target DNA, they should be checked for off target interactions using BLAST software.

To design primers and probes for this thesis (Table 4 and 5), sequences for the various genes were obtained from the Ensembl database: http://www.ensembl.org/index.html. Sequences were then copied into Primer3 software: http://frodo.wi.mit.edu/primer3/, and oligos that matched the criteria above were selected. Primers dimers, secondary structures and Δ-G values were analyzed using the Oligo Analyzer software: http://eu.idtdna.com/analyzer/Applications/OligoAnalyzer/. Primers with Δ-G value greater than -1 were selected. Finally, to check if designed primers and probes were unique and specific for their target DNA, each sequence was checked using a BLAST search: www.ncbi.nlm.nih.gov/BLAST/.

Table 4. Syber Green QPCR amplification. Primer set for each gene and corresponding optimal annealing temperature.

Gene	Oligo	Sequence (5' to 3')	Annealing Temperature (°C)
GAPDH	Forward Reverse	TCCCACTCTTCCACCTTC CTGTAGCCGTATTCATTGTC	51

Table 5: Taqman probe real-time PCR amplification. Primer and probe set for each gene and corresponding optimal annealing temperature.

Gene	Oligo	Sequence (5' to 3')	Annealing Temperature (°C)
TNFSF13 (APRIL)	Forward Reverse Probe	CTGTCCTTCCTAGATAATG CTAGTGACACTCTGACAC CACCAAATTCTCCTGAGGCT	55
TNFRSF17 (BCMA)	Forward Reverse Probe	TGACCAGTTCAGTGAAAGG GGGTTCATCTTCCTCAGC CGTACACGGTGCTCTGGATCTTCTT	57
TNFRSF13B (TACI)	Forward Reverse Probe	CTCAAGGAAATCCTGTGT GAATTTGCAGAAGTCTGTAC CGCTGGCTCCTCTGGCTG	56
GDF-5 (BMP-14)	Forward Reverse Probe	TAATGAACTCTATGGACC GATGAAGAGGATGCTAAT TGAATCCACACCACCCACTTG	51
BMPR-Ib (Alk-6)	Forward Reverse Probe	AGTGTAATA AAGACCTCCA AACTACAGACAGTCACAG CCACTCTGCCTCCTCTCAAG	51
BMPR-II	Forward Reverse Probe	ACTAGAGGACTGGCTTAT CCAAAGTCACTGATAACAC CACAGAATTACCACGAGGAGA	49
SDHA	Forward Reverse Probe	GGAACACTCCAAAAACAG CCACAGCATCAAATTCAT CCTGCGGCTTTCACTTCTCT	57

2.8.3. Real-time PCR procedure

Standard curves were generated for every real-time PCR run by using serial five-fold dilutions of reverse transcribed RNA from spleen (for TNF-α superfamily members) or from total adult brain (for all the other genes) (Fig.22). All values obtained were normalized to the geometric mean of the reference genes GAPDH and SDHA. Four separate samples were analyzed for each age.

Real-time PCR was used to amplify 2.5μl of the reverse transcription reaction in a 25μl reaction. To amplify GAPDH FastStart Universal SYBR Green Master (Rox) (Roche) was used and the PCR was followed by melting curve analysis. For the amplification of other genes (Table 5) FastStart Universal Probe Master (Rox) (Roche) and Taqman probes were used. Primers and probes were acquired from Eurofins – MWG-Operon and used at a final concentration of 200nM each. Primers and probes for Hes1 and Hes5 were purchased from Applied Biosystems.

PCR was performed using a Stratagene Mx3000P thermocycler with an initial step at 95^{o}C for 10min, to activate the Taq polymerase, followed by 45 cycles consisting of the denaturation step of 95^{o}C for 1min, the annealing step at 49-60^{o}C, depending on the gene, for 1min, and the extension step at 72^{o}C for 30sec. TaqMan probes and primers for Hes1 and Hes5 and the housekeeping gene ribosomal (r)RNA 18S were selected as the Assay-on-Demand gene expression products (Applied-Biosystem-Invitrogen Life Technologies, Paisley, UK).

2.8.4. Data analysis

The real-time PCR data were analysed using an absolute quantification assay. The value for each gene in each sample was determined by placing its Ct value on the standard curve (Fig.22). GAPDH and SDHA were used as reference genes (stable throughout the different samples) and the geometric mean of these genes was calculated and used as a normalisation factor. The raw values of each gene of interest were then standardised to the normalisation factor.

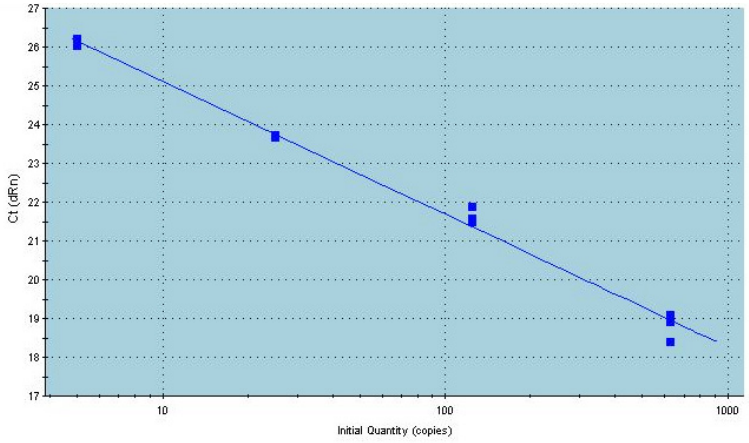

Figure 22: Standard curve.

Example of a 5 times-serially diluted cDNA standard curve for GAPDH. Amplification was performed using SYBR Green reagents and a Stratagene Mx3000P thermocycler.

2.9. Immunohistochemistry

2.9.1. Principle

Immunohistochemistry is a technique that allows the visualization of a specific protein or proteins in cells or tissues by using an antibody. The antibody-antigen complex is then observed using either chromogenic detection, in which an enzyme conjugated to the antibody cleaves a substrate to produce coloured deposits at the sites of antibody-antigen binding, or fluorescent detection, in which a fluorophore is conjugated to the antibody and can be visualized using fluorescence microscopy.

2.9.2. Immunocytofluorescence of dissociated cultures

Dissociated cultures were prepared in 4-well dishes as described in section 2.2.4.1. Cultures at 7DIVs were fixed with 4% PFA, for 30min, at RT. After this, they were washed twice with PBS and permeabilised for 15min with 0.5% Triton X-100/PBS. Cells were washed three times, for 5min each, with 0.1% Triton X-100/PBS before being incubated for 1 hour with blocking buffer (10% Goat serum in 0.1% Triton X-100/PBS). Cells were then incubated with the primary antibody in blocking buffer (see dilution and incubation time in table 7). Subsequently, cells were washed three times, incubated with the appropriate secondary antibodies in blocking buffer for 1h at RT (see dilution and incubation time in table 8), and then washed three times with PBS. In all cases,

counterstaining off the nuclei was performed using either DNA stain 4',6-diamidino-2-phenylindole (DAPI, 1:10000, Invitrogen) or TOTO®-3 Iodide staining (1:10000 Invitrogen). Negative controls (no primary antibody staining) were also set up.

2.9.3. Preparation of brain frozen sections

Mouse brains were collected at different ages (E18, P0, P5 and P10) and fixed in 4% PFA, at 4°C (Table 6). Next, brains were cryo-protected in 30% sucrose, at 4°C, either overnight or until they sank. Each brain was then washed in water, dried and embedded in Tissue-Tek O.C.T. compound (Sakura) in a disposable mold (Polysciences, Inc.). The molds were placed in an ice cold 2-methylbutan/iso-Pentan (Fisher scientific) holder surrounded by dry ice, and were slowly frozen. Once frozen, the molds were stored at -80°C. Frozen sections 15µm thick were obtained with a cryostat (Leica) and placed directly into X-tra adhesive slides (Leica). After the sections had been allowed to dry, they were stored at -80°C until further use.

Table 6: Incubation time in 4% PFA for mouse brains.

Age	4% PFA incubation time
E18	1 hour
P0	2 hours
P5	4 hours
P10	4 hours, after perfusion

2.9.3.1. Immunohistofluoroscence staining of frozen sections

Frozen sections were incubated at RT with PBS for 5min, followed by 1 hour incubation with blocking buffer (10% Goat serum/0.1% Triton X-100/PBS). Sections were then incubated, at 4°C overnight, with the primary antibody in 2% Goat serum/PBS (see antibody dilutions in table 7). To avoid sections drying out, they were covered by a piece of Parafilm during incubation. Subsequently, sections were washed three times in PBS, and incubated with the appropriate secondary antibodies, in 2% Goat serum/PBS, for 1 hour at RT (see antibody dilutions in table 8) covered with a piece of parafilm. Finally, sections were

washed three times with PBS and mounted with Hydromount (National Diagnosis).

2.9.4. Golgi staining

Modified Golgi-Cox impregnation of neurons was performed using the FD Rapid GolgiStain kit (FD NeuroTechnologies, Ellicott City,MD) according to the manufacturer's instructions. Briefly, P10 mouse brains from *Gdf-5* WT, *Gdf-5* Het and *Gdf-5*^{bp}, mice were incubated in impregnation solution (solution A + solution B) for 2 weeks at RT in the dark. Brains were transferred to solution C for 1 week at 4°C in the dark, and cut at 80μm on the cryostat. Sections were mounted on polylisine-coated slides with solution C and dried before staining with silver nitrate solution (solution D + solution E). Sections were dehydrated in increasing ethanol solutions, cleared in xylene and mounted with DPX mounting medium (VWR Scientific, West Chester, PA).

2.9.5. Imaging

Cells and sections were imaged using an inverted or confocal microscope (Zeiss). In some experiments 10x, 20x or 40x objectives were used, whereas for in other experiments a 63x water immersion objective was used for confocal microscopy.

Table 7: Primary antibodies used in the study.

Primary Antibody	Antibody Type	Company	Concentration	Incubation time
GFP	polyclonal	abcam	1:500	4°C overnight
copGFP	polyclonal	evrogen	1:500	1 hour at RT
TNFSF13 (APRIL)	polyclonal	abcam	1:100	4°C overnight
TNFRSF17 (BCMA)	polyclonal	abcam	1:100	4°C overnight
TNFRSF13B (TACI)	polyclonal	abcam	1:100	4°C overnight
TAU	monoclonal	abcam	1:500	4°C overnight
GDF-5	polyclonal	abcam	1:100	4°C overnight
BMPR-Ib	polyclonal	abcam	1:100	4°C overnight
BMPR-II	polyclonal	abcam	1:100	4°C overnight
MAP2 (2a+2b)	monoclonal	Sigma	1:500	4°C overnight
β-III Tubulin	monoclonal	R and D Systems	1:500	4°C overnight

Table 8: Secondary antibodies used in the study.

Secondary Antibody	Company	Concentration	Incubation time
Alexa Fluor 488 anti-mouse IgG	Invitrogen	1:1000	1 hour at RT
Alexa Fluor 488 anti-rabbit IgG	Invitrogen	1:1000	1 hour at RT
Alexa Fluor 488 anti-chicken IgG	Invitrogen	1:1000	1 hour at RT
Alexa Fluor 546 anti-mouse IgG	Invitrogen	1:1000	1 hour at RT
Alexa Fluor 546 anti-rabbit IgG	Invitrogen	1:1000	1 hour at RT
Alexa Fluor 633 anti-mouse IgG	Invitrogen	1:1000	1 hour at RT
Alexa Fluor 633 anti-rabbit IgG	Invitrogen	1:1000	1 hour at RT

2.10. Western blotting

2.10.1. Principle

Western blotting, or immunoblotting, is a widely used technique to detect and quantify specific proteins in a complex protein mixture. This is achieved by using high-quality antibodies directed against the proteins of interest. Initially, proteins are separated by their size through SDS-polyacrylamide gel electrophoresis (SDS-PAGE). Next, the negatively charged, separated proteins are transferred by electric current from the SDS-gel to a positively charged

nitrocellulose or polyvinylidene fluoride (PVDF) membrane. Finally, the transferred protein is detected on the membrane by using a specific primary antibody, followed by a secondary enzyme-conjugated antibody (e.g., horseradish peroxidase (HRP)) that is used to visualize the protein.

2.10.2. Protein extraction

Neurons were plated in 24-well plate or 35mm dishes and incubated for 3DIVs or 7DIVs. Two hours before neuron stimulation by trophic factors, the culture medium was replaced by Neurobasal A medium without additives. After neuron stimulation, the medium was removed before adding 30μl of RIPA lysis buffer (see Appendix II) containing a 1:100 dilution of Protease Inhibitor Cocktail and 1mM of sodium orthovanadate (Sigma-Aldrich). Using a cell scraper, neurons were removed from each well, collected in a microfuge tube, and incubated on ice for 30min. Following this, insoluble debris was removed from the lysates by centrifuging the samples, for 5min at 12,000g, in a pre-cooled (4^{o}C) centrifuge. Supernatants were stored at -80°C in a microfuge tube whilst awaiting further analysis.

Tissue samples (spleen, midbrain, thymus and aorta) were minced and homogenized in 100μl of complete RIPA lysis buffer using a pellet pestle motor (VWR international). The lysates were centrifuged, for 5min at 12,000g, in a pre-cooled (4^{o}C) centrifuge and the supernatants were collected and stored on ice. Protein levels in the lysates were quantified, as described below, and used for Western blotting on the same day.

2.10.3. Protein quantification

Protein was quantified using the Bradford protein assay. The Bradford assay is a colorimetric method based on an absorbance shift of the dye Coomassie Brilliant Blue G-250. Under acidic conditions, the dye is predominantly in the double-protonated, red cationic form (maximum absorbance at 470nm). However, when the dye binds to protein, it is converted to a stable non-protonated blue form (maximum absorbance at 595nm). A commercially available version of the Bradford assay, the Bio-Rad Protein Assay (Bio-Rad), was used to determine protein concentrations in cell lysates,

and BSA (Sigma-Aldrich) was used to generate a protein standard curve. Prior to performing the assay, a standard curve was prepared according to table 9 and samples of lysate were diluted 1:100 in distilled water. The Bio-Rad Protein Assay reagent was diluted 5-fold in water to its working concentration. After, 200μl of each standard and each unknown sample were pipetted, in triplicate, into a 96-well plate. Following this, 50μl of diluted Bio-Rad reagent was added to each well and, following thorough mixing, The absorbance of each sample was measured at 595nm using a microplate reader. The protein concentration in each diluted lysate sample was quantified using the standard curve.

Table 9: Standard curve dilutions for Bradford assay.

Curve standards	Concentration	BSA (0.1mg/ml)	distilled H_2O
1	0μg/ml	0μl	200μl
2	2μg/ml	5μl	195μl
3	4μg/ml	10μl	190μl
4	6μg/ml	15μl	185μl
5	8μg/ml	20μl	180μl
6	10μg/ml	25μl	175μl

2.10.4. Western blotting procedure

Protein extracts were boiled for 5min with Laemmli buffer (see Appendix II) to denature the proteins. Protein extracts were then allowed to cool on ice before equal amounts of each sample were loaded into the wells of a 10% SDS-polyacrylamide mini gel with a 5% stacking gel (see Appendix II). A molecular weight marker was loaded into one well of each gel to confirm the molecular weights of unidentified proteins. The gels were assembled (Mini-Protean Tetra Cell (Bio Rad)), submerged in running buffer (see Appendix II) and run for 20min at 80V, followed by 50min at 130V. Laemmli buffer also served as an indicator dye to observe the migration front that runs ahead of the proteins in the gel.

Following electrophoresis, proteins in the gel were electrophoretically transferred onto a PVDF membrane (Millipore), for 1 hour at 100V, whilst submerged in transfer buffer (see Appendix II). To confirm the transfer of proteins, the membrane was stained with Ponceau S (see Appendix II).

Subsequently, the membrane was washed with PBS containing 0.1% Tween 20 (PBS-T) and incubated, for 1 hour at RT, with blocking solution (3% (w/v) BSA and 5% (w/v) milk (Bio Rad) in PBS-T) whilst being gently agitated on an orbital shaker. The membrane was then rinsed in PBS-T and incubated with the primary antibody in 3% BSA/PBS-T (see dilution and incubation time in table 10).

Next, the membrane was washed three times, for 10min each, in PBS-T followed by 1 hour incubation, at RT with gentle agitation, on an orbital shaker with the appropriate peroxidase-linked secondary antibody that had been diluted in blocking solution (see dilution and incubation time in table 11). Membranes were washed after the incubation with secondary antibodies and protein complexes were visualized with Western blot Luminol Reagent (Santa Cruz). Membranes were incubated with luminol for 1min and then were put in contact with a chemiluminescence film (GE Helthcare) in an autoradiography cassette. The film was developed and fixed (Kodak GBX developing and fixing solution Sigma-Aldrich), and the membrane was then stripped of antibodies by 15min incubation, at RT, with stripping buffer (Thermo Scientific). The membrane was then washed before being re-probed with antibodies to detect other proteins.

2.10.5. Protein densitometry

Chemiluminescence films were scanned and GelPro Analyzer software was used to perform densitometry and quantify the amount of protein in bands.

Table 10: Primary antibodies used in the study.

Primary Antibody	Antibody Type	Company	Concentration	Incubation time
TNFSF13 (APRIL)	polyclonal	abcam	1:500	4°C overnight
TNFRSF17 (BCMA)	polyclonal	abcam	1:500	4°C overnight
TNFRSF13B (TACI)	polyclonal	ProSci Incorporated	1:400	4°C overnight
Phospho-p44/p42 MAPK (Erk1/2) (Thr202/Tyr204)	monoclonal	Cell Signaling	1:2000	4°C overnight
p44/p42 MAPK (Erk1/2)	monoclonal	Cell Signaling	1:2000	4°C overnight
Phospho-Akt (Ser473)	monoclonal	Cell Signaling	1:1000	4°C overnight
Akt	monoclonal	Cell Signaling	1:1000	4°C overnight
Phospho-GSK-3α/β (Ser21/9)	polyclonal	Cell Signaling	1:2000	4°C overnight
GSK-3β	monoclonal	BD Transduction Laboratories	1:3000	4°C overnight
GDF-5	polyclonal	abcam	1:50	4°C overnight
BMPR-Ib	polyclonal	Thermo Scientific	1:50	4°C overnight
BMPR-II	polyclonal	Thermo Scientific	1:50	4°C overnight
Phospho-Smad1 (Ser463/465)/ Smad5(Ser463/465)/ Smad8(Ser426/428)	polyclonal	Cell Signaling	1:1000	4°C overnight
Smad1	polyclonal	Cell Signaling	1:1000	4°C overnight
Hes5	polyclonal	abcam	1:200	4°C overnight
copGFP	polyclonal	evrogen	1:500	1 hour at RT
GAPDH	polyclonal	abcam	1:2500	1 hour at RT
β-actin	polyclonal	abcam	1:2500	4°C overnight
β-III Tubulin	monoclonal	R and D systems	1:5000	1h at RT

Table 11: Secondary antibodies used in the study.

Secondary Antibody	Company	Concentration	Incubation time
anti-rabbit IgG HRP conjugate	Promega	1:5000	1 hour at RT
anti-mouse IgG HRP conjugate	Promega	1:5000	1 hour at RT
anti-chicken IgG HRP conjugate	Abcam	1:2000	1 hour at RT

2.11. Elisa

2.11.1. Principle

The ELISA (Enzyme-Linked Immunosorbent Assay) assay is a specific and highly sensitive method for quantitative measurements of proteins, in particular cytokines. This assay is usually performed in a 96-well plate that is coated with a specific monoclonal antibody able to capture the cytokine of interest. A detection enzyme or other tag can be either linked directly to the primary antibody, or introduced through a secondary antibody that recognizes the primary antibody. Detection is accomplished by assessing the conjugated enzyme activity via incubation with a chromogenic substrate to produce a coloured product whose concentration can be measured on a plate reader.

2.11.2. Sample collection

Hippocampal cultures were plated in 6 wells of a 96-well plate with a density of 75,000 cells per well. After 3DIVs, the supernatant was collected, centrifuged to remove debris, and stored at -80°C until further use. Cells were collected in distilled water, centrifuged to remove debris, and stored at -80°C until further use.

2.11.3. Procedure

Standards and samples (100μl) were added to a microtiter plate pre-coated with an antibody specific for APRIL (Uscn Life Science inc.). The plate was covered with a plate sealer and incubated, for 2 hours, at 37°C. Next, the liquid was removed from each well and 100μl of a biotin-conjugated antibody specific for APRIL was added to each well, followed by incubation, for 1 hour, at 37°C. After this, the plate was washed three times with wash solution and 100μl of avidin conjugated to HRP was added to each well. Following incubation, for 30min at 37°C, the plate was washed three times with wash solution and 90μl of TMB (3,3'5'5'-tetramethylbenzidine base) substrate solution was added to the wells. TMB was incubated with the avidin-HRP in the dark, for 25min at 37°C, prior to the addition of 50μl of Stop solution (a sulphuric acid solution) to terminate the colorimetric reaction. The absorbance of each well was immediately read in a plate reader at a wavelength of 450nm. The concentration

of APRIL in each well was then determined by comparison with a standard curve set up in the same plate with known concentrations of APRIL (0ng/ml, 0.625ng/ml, 1.25ng/ml, 2.5ng/ml, 5ng/ml, 10ng/ml, 20ng/ml and 40ng/ml).

2.12. Statistical analysis

To determine whether or not data was normally distributed, the D´Agostino-Person test was used. To determine whether or not data had equal or different variances an F-test test was used. For normal distributed data, statistical significance was determined by the Student´s *t* test. If the data was not normally distributed, statistical significance was calculated using the Mann–Whitney U test. The minimum level of significance accepted for all tests was $p<0.01$.

Chapter 3

Expression pattern of APRIL and its receptors in the developing hippocampus

3.1. Introduction

APRIL is a type II membrane protein cytoplasmic domain, a hydrophobic transmembrane region and an extracellular domain of 201 amino acids. To be biologically active, APRIL needs to be processed by a furin convertase in the Golgi apparatus prior to its secretion[352]. Although APRIL was initially characterised as a new member of the TNFSF with tumourigenic activity, it has since been shown to be expressed predominantly in cells of the immune system, namely monocytes, macrophages, dendritic cells and T cells[353-355]. Several cytokines, such as IFNα, IFNγ and CD40L, can stimulate the production of APRIL by macrophages and dendritic cells[355]. APRIL is also expressed in osteoclasts[356], various tumour derived cell lines, human thyroid and colorectal carcinomas and lymphomas[353]. The two APRIL receptors, BCMA and TACI, are predominantly expressed in mature B cells and activated T cells[357,358]. BCMA is also expressed by germinal centre B cells and plays a role in later stages of B cell maturation and survival[359]. Additionally, BCMA mRNA is detectable in malignant T cell lymphoma[358] and myeloma[360]. Intriguingly, *Bcma* deficient mice do not display an abnormal B cell phenotype[361], although they show impairment in the survival of bone marrow plasma cells compared to wild type mice[362]. Within the spleen and lymph nodes of mice, TACI is expressed by marginal zone B cells and activated B cells, but not by germinal centre B cells[359]. *Taci* deficient mice show normal B cell maturation and T-dependent antibody production, but the responses to T-independent type II antigens are impaired, with a significant reduction in secretion of both immunoglobulin M (IgM) and IgG compared to wild type mice[363]. *Taci* null mice also display increased B cell accumulation and splenomegaly[364].

APRIL has been reported to be important in immune regulation by stimulating IgM production by peripheral blood B cells[365], as well as enhancing the proliferation of primary B and T cells *in vitro*[354]. APRIL binding to BCMA also induces the expression of co-stimulatory molecules on splenic B cells, thereby enhancing their capacity to present antigen to T cells[342]. *In vivo* injection of recombinant APRIL results in splenomegaly due to the expansion of the B cell population and increased T cell activation[354]. Moreover, transgenic mice

specifically overexpressing APRIL in T cells, display enhanced T cell survival both *in vitro* and *in vivo* that correlates with elevated levels of Bcl-2[366]. Two groups have generated *April* deficient mice with different results. The first group reported normal lymphoid development and normal B and T cell proliferation[367]. Whilst the second group also reported normal B and T cell development and proliferation, their mice had an increased number of effector memory T cells and enlarged germinal centres[368].

APRIL has been linked to the establishment and maintenance of autoimmune diseases. For example, patients with systemic lupus erythematosus (SLE) have higher levels of APRIL in their serum compared to healthy control patients[369]. This observation raises the possibility that APRIL could play a role in the aetiology of the disease. In support of this, an APRIL polymorphism, *APRIL* 67G, has been found to be correlated with susceptibility to SLE in humans[370]. Importantly, APRIL blockade in a SLE mouse model delays the development of the disease as well as ameliorating some of its symptoms[371]. APRIL and its related ligand, BAFF, have also been detected in the synovial fluid of patients with inflammatory arthritis[372]. These ligands are thought to be produced locally in the inflamed joints, thereby aiding the survival and/or expansion of B cells that produce pathogenic autoantibodies, and potentially promoting local T cell activation, actions that can both consequently promote joint destruction[372]. In a mouse model of rheumatoid arthritis, TACI-Fc treatment significantly reduces joint inflammation, bone and cartilage destruction and inhibits disease progression[224]. Increased levels of APRIL have also been found in the plasma and cerebrospinal fluid of patients with multiple sclerosis[373].

In addition to potential roles in the aetiology of autoimmune disease, APRIL has emerged as a potent enhancer of tumourigenesis. APRIL is produced in large quantities within malignant tumours and stimulates the survival and proliferation of transformed cells[353]. For example, APRIL increases the proliferation of cultured glioblastoma cell lines, an effect that can be blocked by the addition of a soluble BCMA-Fc fusion protein to cultures[374]. In addition, multiple myeloma cell lines and primary myeloma cells from patients express

APRIL and its receptors, and exogenous APRIL can rescue myeloma cells lines from IL-6 withdrawal induced apoptosis and prevent dexamethasone induced apoptosis of primary myeloma cells[360] rather than by the transformed cells themselves[375]. High levels of APRIL are found in the serum of patients with B-cell chronic lymphocytic leukaemia (B-CLL)[376]. Moreover, patients with B-CLL express APRIL within leukemic B cells and there is an inverse relationship between the percentage of leukemic B cells expressing APRIL and patient survival[377]. Together, this suggests that inhibiting APRIL or its receptors may present a valuable therapeutic approach for B-CLL and related B cell lymphomas. In support of this, the addition of either a BCMA-Fc fusion protein or anti-APRIL antibodies enhances apoptosis in cultures of leukemic B cells[378], and neutralization of endogenous APRIL (or BAFF) by soluble TACI and BCMA decoy receptors reduces the survival of cultured, patient-derived non-Hodgkin's lymphoma B cells[379].

Prior to this current study, there has been little evidence showing that APRIL and its receptors are either expressed in the nervous system or play a role in regulating nervous system development or function. APRIL has previously been shown to be expressed in a number of glioblastoma cell lines[374]. In addition, flow cytometry has suggested that specific APRIL receptors are expressed by glioblastomas, human embryonic neural progenitors and human embryonic and adult astrocytes. In accordance with this, recombinant APRIL increases the proliferation of cultured human adult astrocytes and glioblastoma cells, an effect that can be blocked by the addition of soluble BCMA-Fc to cultures[374]. Likewise, APRIL is expressed by adult human astrocytes and, multiple sclerosis patients show increased expression of APRIL within reactive astrocytes[380]. This chapter provides novel data on the expression of APRIL and its receptors in the nervous system, in particular in the developing hippocampus.

3.2. Aims

The aims of this chapter were to characterise the expression levels of APRIL and its receptors at the mRNA and protein levels in the developing hippocampus and to determine which cell types within the hippocampus predominantly express these molecules.

3.3. Results

3.3.1. Stage specific development of cultured hippocampal neurons

E18 hippocampal neurons were cultured as described in Chapter 2 and fixed after 0.25, 0.5, 1.5, 4 and 7DIVs. Following fixation, β-III tubulin immunofluorescence staining was performed to visualise the neurons and axonal and dendritic processes. Because later stage cultures become complex due to precocious axonal and dendritic outgrowth, cultures were transfected with pCDH-CMV-MCS-EF1-copGFP at 3DIVs and 6DIVs and fixed 24h later to allow the visualisation of single neurons at 4DIVs (stage 4) and 7DIVs (stage 5).

In accordance with previously published data[22], hippocampal cultures show 5 distinct stages of development (Fig.23). At stage 1 (0.25DIVs), it is possible to observe growing lamellipodia around neuronal cell bodies that are organized in patches where the first neurites will arise. Stage 2 (0.5DIVs) is characterized by the transformation of lamellipodia into minor processes. By 1.5DIVs (stage 3), neurons have few processes, but it is possible to identify one major process forming which is the axon. At 4DIVs (stage 4), dendrites become discernible. The final stage of hippocampal neuron development, stage 5, corresponds to 7 or more DIVs and is characterised by neuronal maturation (Fig.23).

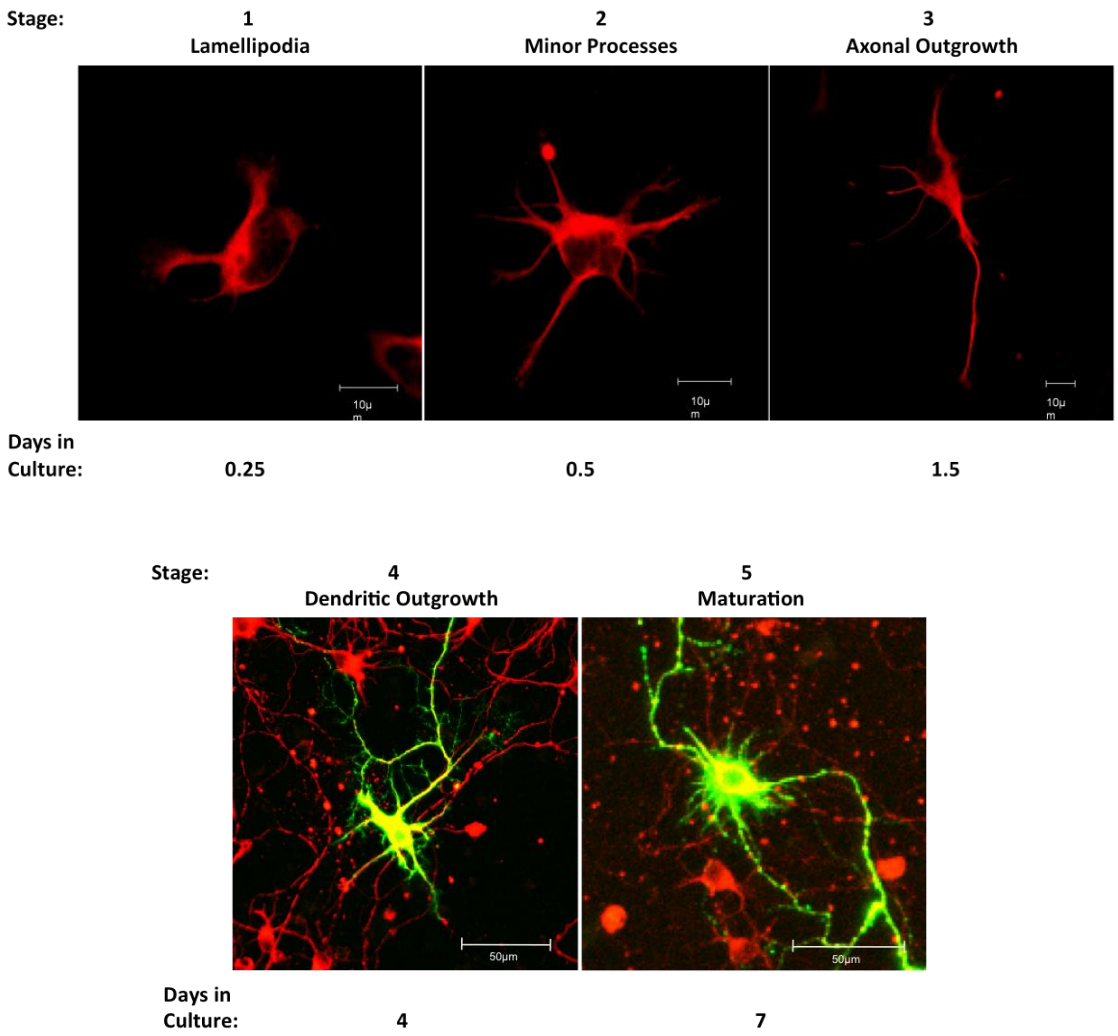

Figure 23: The stages of hippocampal neuron development *in vitro*.

E18 hippocampal pyramidal neurons were cultured and fixed at 0.25, 0.5, 1.5, 4 and 7DIVs, time points that correspond to Dotti[22] stages 1 to 5 of hippocampal neuron development. Neurons were stained for β-III tubulin (red). Cultures were transfected with pCDH-CMV-MCS-EF1-copGFP (green) at 3DIVs and 6DIVs and fixed 24h later to allow clear visualisation of single neurons at stages 4 and 5. Stages 1, 2 and 3; scale bar 10µm. Stages 4 and 5; scale bar 50µm.

3.3.2. The expression of APRIL, BCMA and TACI mRNAs in the developing hippocampus and in hippocampal cultures

In order to study the relative expression of transcripts encoding APRIL and its receptors in the developing hippocampus, reverse transcriptase real-time PCR was performed on total RNA extracted from hippocampi of different developmental ages from E18 to adult. The levels of APRIL, BCMA and TACI transcripts were normalised to the expression levels of the reference mRNAs, GAPDH and SDHA. As shown in Fig.24.A, APRIL mRNA levels in the developing hippocampus remain relatively constant from E18 to adult. In contrast, BCMA mRNA expression levels increase 2.5 fold between E18 and P10, before dropping by a similar amount between P10 and adult (Fig.24.B). Real-time PCR was not able to reliably quantify the very low levels of TACI mRNA expressed in the developing and adult hippocampus. The levels of APRIL and BCMA mRNAs were also quantified in total RNA extracted from adult mouse thymus and spleen, reservoirs of T and B cells, respectively, in order to calibrate the levels of hippocampal APRIL and BCMA transcript expression with tissues that are known to express very high, functional levels of these mRNAs[190,353,358,359,381]. Not surprisingly, both APRIL and BCMA mRNA expression levels are significantly higher in the thymus and spleen compared to the adult hippocampus (Fig.24.C and D).

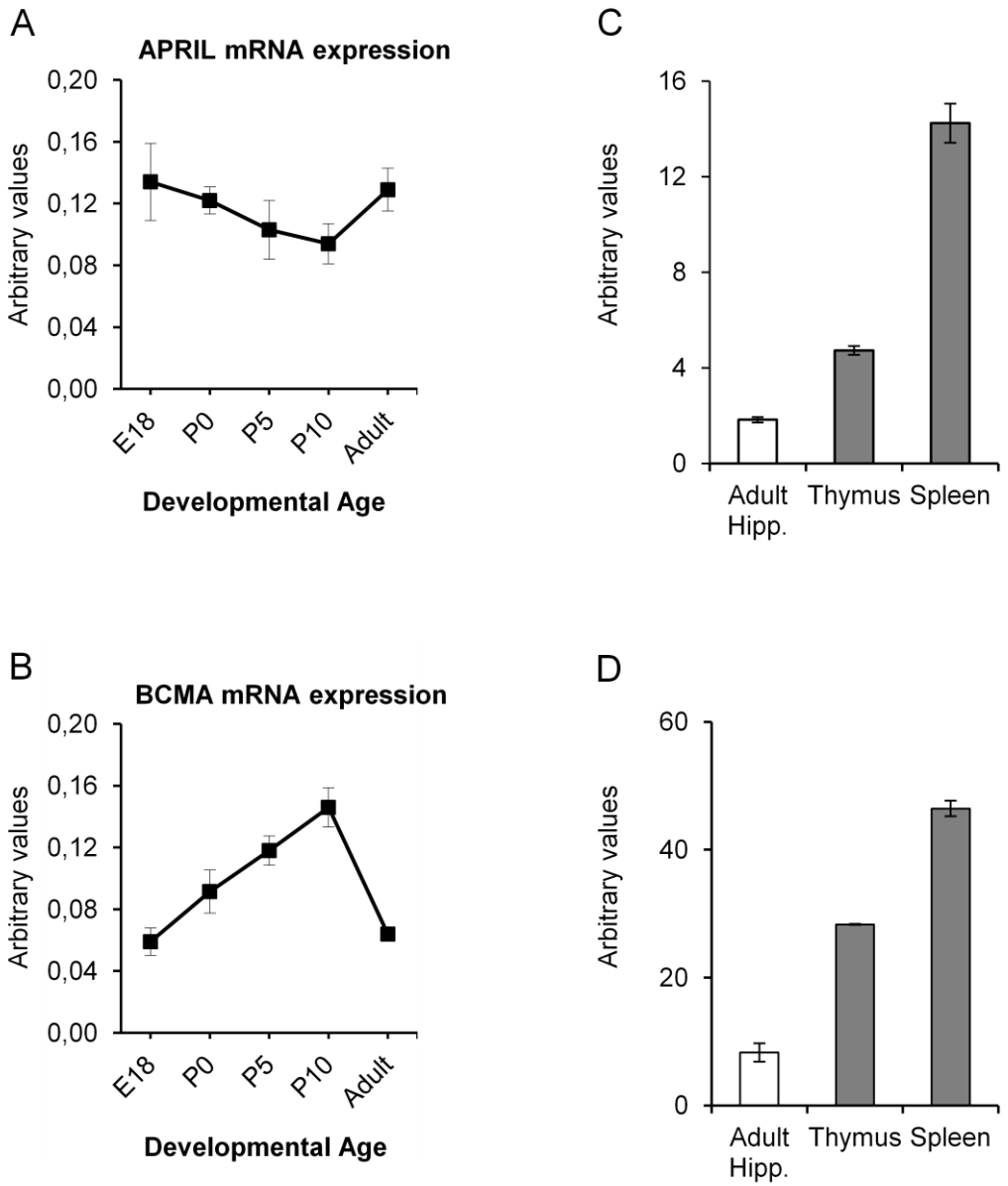

Figure 24: The relative expression levels of APRIL and BCMA mRNAs in the developing and adult mouse hippocampus and adult mouse thymus and spleen. Total RNA was extracted from E18, P0, P5, P10 hippocampus and adult hippocampus, thymus and spleen. The expression of APRIL and BCMA mRNAs were analysed by reverse transcriptase real-time PCR and quantified relative to the expression levels of mRNAs for the reference genes, GAPDH and SDHA. The data represents mean and SEM of four separate experiments. Graphs show: (A) APRIL and (B) BCMA mRNA levels in the hippocampus at different developmental ages and (C) APRIL and (D) BCMA mRNA levels in adult hippocampus compared with thymus and spleen. Data represent the mean and sem of four separate experiments.

Reverse transcriptase real-time PCR was also used to examine the expression of APRIL, BCMA and TACI mRNAs in E18 hippocampal cultures after 2 hours (0DIVs), 2, 5 and 7DIVs. APRIL mRNA levels fall by 50% during the first two days in culture. Thereafter, APRIL transcript levels remain unaltered from 2DIVs to 7DIVs (Fig.25.A). BCMA mRNA levels are maintained over the first two days in culture, but decrease by 50% between day 2 and day 5 to reach a level that is maintained until day 7 (Fig.25.B). TACI transcript levels increase 3-fold from 2 hours in culture to reach a peak at 2DIVs, before falling 4-fold to reach a lower level by 5DIVs that is maintained until 7DIVs (Fig.25.C). During the whole culture period, TACI mRNA levels are at the lower limit of reliable quantification by real-time PCR.

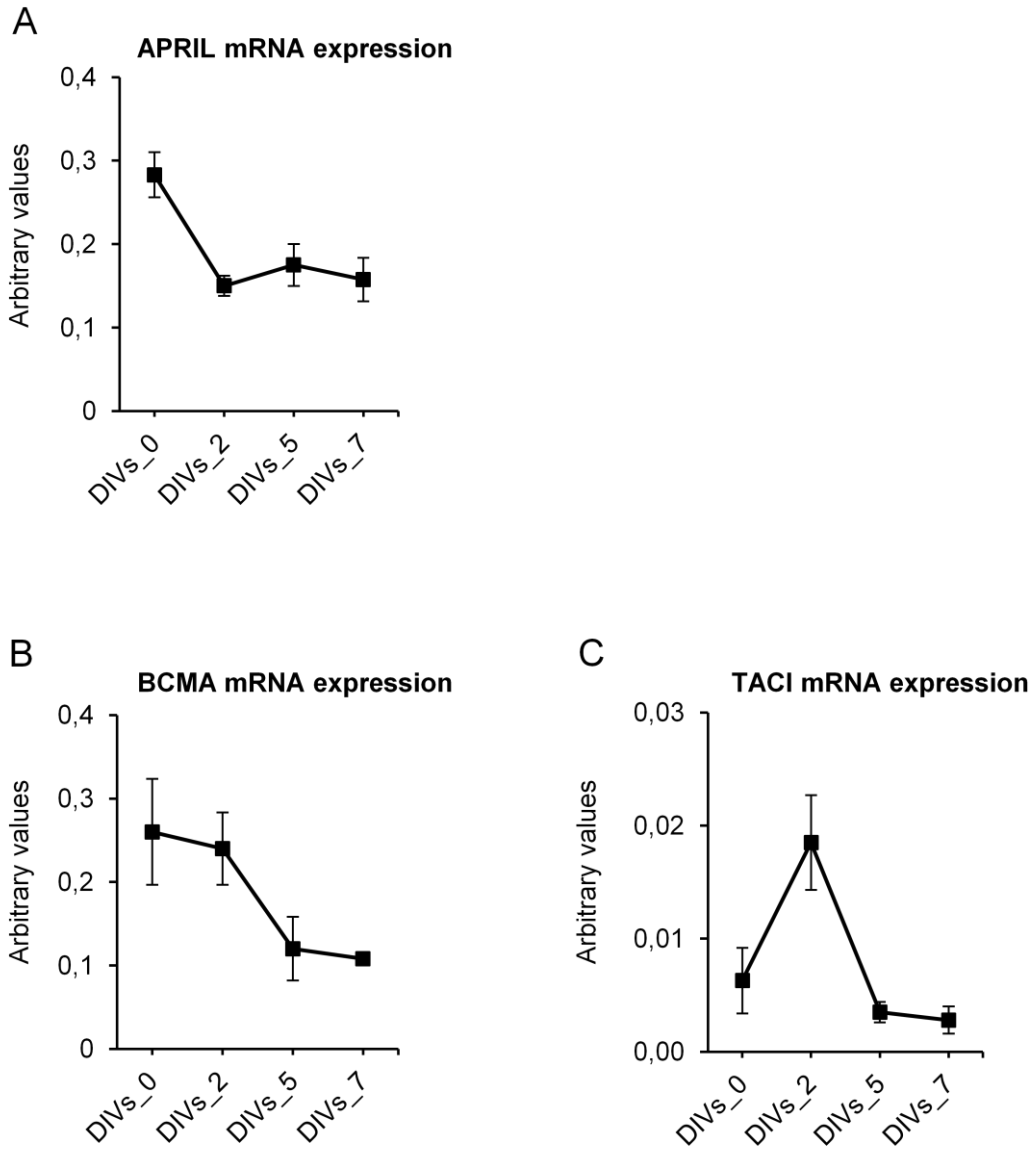

Figure 25: The relative expression levels of APRIL, BCMA and TACI mRNAs at different time points in E18 hippocampal cultures. Total RNA was extracted from E18 hippocampal cultures after 2 hours (0DIV) and 2, 5 and 7DIVs. The levels of (A) APRIL, (B) BCMA, and (C) TACI mRNAs were determined by reverse transcriptase real-time PCR and are relative to mRNAs for the reference genes, GAPDH and SDHA. Data represent the mean and sem of four separate experiments.

3.3.3. Expression of APRIL, BCMA and TACI proteins in 7DIVs hippocampal cultures

Western blotting was used to assess the levels of APRIL, BCMA and TACI proteins in E18 hippocampal neurons that had been cultured for 7DIVs. The levels of these three proteins were also analysed by Western Blotting in protein extracts from spleen and thymus, tissues that are known to express high levels of these proteins[190,353,358,359,381]. In addition, the expression of APRIL, BCMA and TACI proteins were analysed in the BHK cell line. Western blots were also probed with antibodies against β-III tubulin (a neuronal marker) and β-actin (a protein expressed in all cell types). As shown in Fig.26.A, two immunoreactive bands of approximately 17KDa and 32KDa, corresponding to mature and precursor (pro) forms of APRIL, respectively, are detected in lysates from hippocampal cultures, thymus, spleen and BHK cells. Relative to the pro form, the mature form of APRIL is expressed at lower levels in hippocampal neurons than it is in the other tissues analysed. BCMA protein, with a molecular weight of 35KDa, is also expressed in all the tissues analysed (Fig.26.B). Similarly, a 45KDa band corresponding to TACI is detectable in the lysates of all tissues (Fig.26.C). It is notable that hippocampal neurons express similar or higher levels of BCMA, relative to β-actin, compared to the other tissues tested, whereas hippocampal neurons express low levels of TACI compared to spleen, thymus and BHK cells.

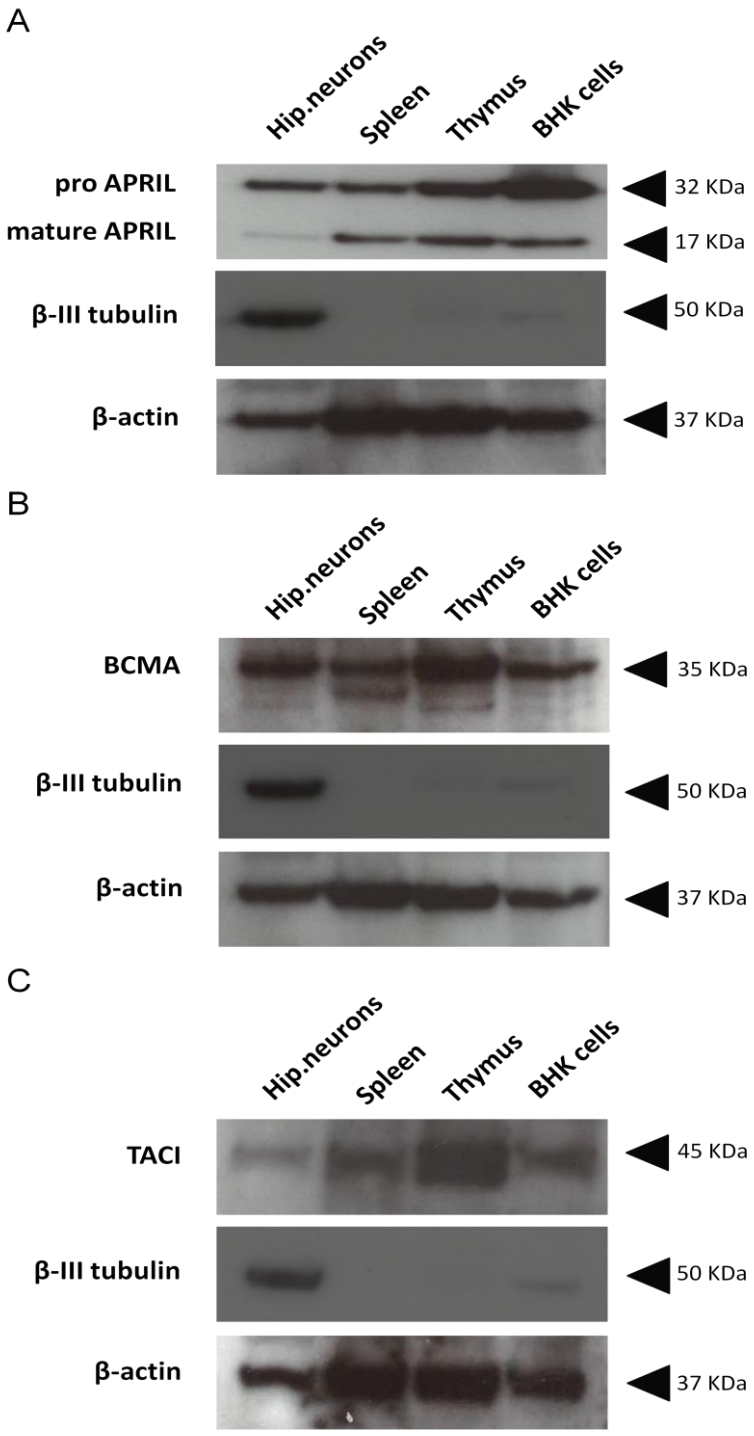

Figure 26: Western blots showing APRIL, BCMA and TACI protein expression in 7DIVs hippocampal neurons. β-III tubulin was used as a neuronal marker and β-actin as an endogenous control. Protein extracts from spleen, thymus and BHK cells were used as positive controls. (A) 17KDa mature and 32KDa pro forms of APRIL are expressed in all tissues analysed. Similarly, the lysates of all tissues contain (B) 35KDa BCMA and (C) 45KDa TACI proteins. 50KDa β-III tubulin expression in restricted to hippocampal neurons, whereas 37KDa β-actin is expressed in all tissues (A, B and C).

3.3.4. Cellular localisation of APRIL, BCMA and TACI proteins in hippocampal neurons

To investigate the cellular distribution of APRIL and its receptors in hippocampal neurons, E18 neurons were transfected with a GFP expression plasmid after 6DIVs, fixed 24 hours later and labelled using antibodies that recognise either APRIL, BCMA or TACI. Antibodies that recognise TAU were also used to identify the axons of hippocampal neurons. Photomicrographs of stained neurons reveal that APRIL is expressed in the cell soma as well as in the axon of cultured hippocampal neurons (Fig.27.A). BCMA immunoreactivity is distributed over the soma and processes, although it is more evident in axons rather than dendrites (Fig.27.B). TACI is expressed at very low levels in the soma of hippocampal neurons and is not detectable in the processes (Fig.27.C). Although E18 hippocampal cultures contain very few non-neuronal cells after 7DIVs, occasionally non-neuronal cells expressing APRIL or BCMA were observed (data not shown).

Macrophages and lymphocytes were used as positive control cells for the APRIL antibody (Fig.28 and 29) and lymphocytes were used as a positive control for BCMA and TACI antibodies (Fig.29). Macrophages and lymphocytes were kindly provided by Luke Davies from the Department of Infection, Immunity and Biochemistry at Cardiff University School of Medicine.

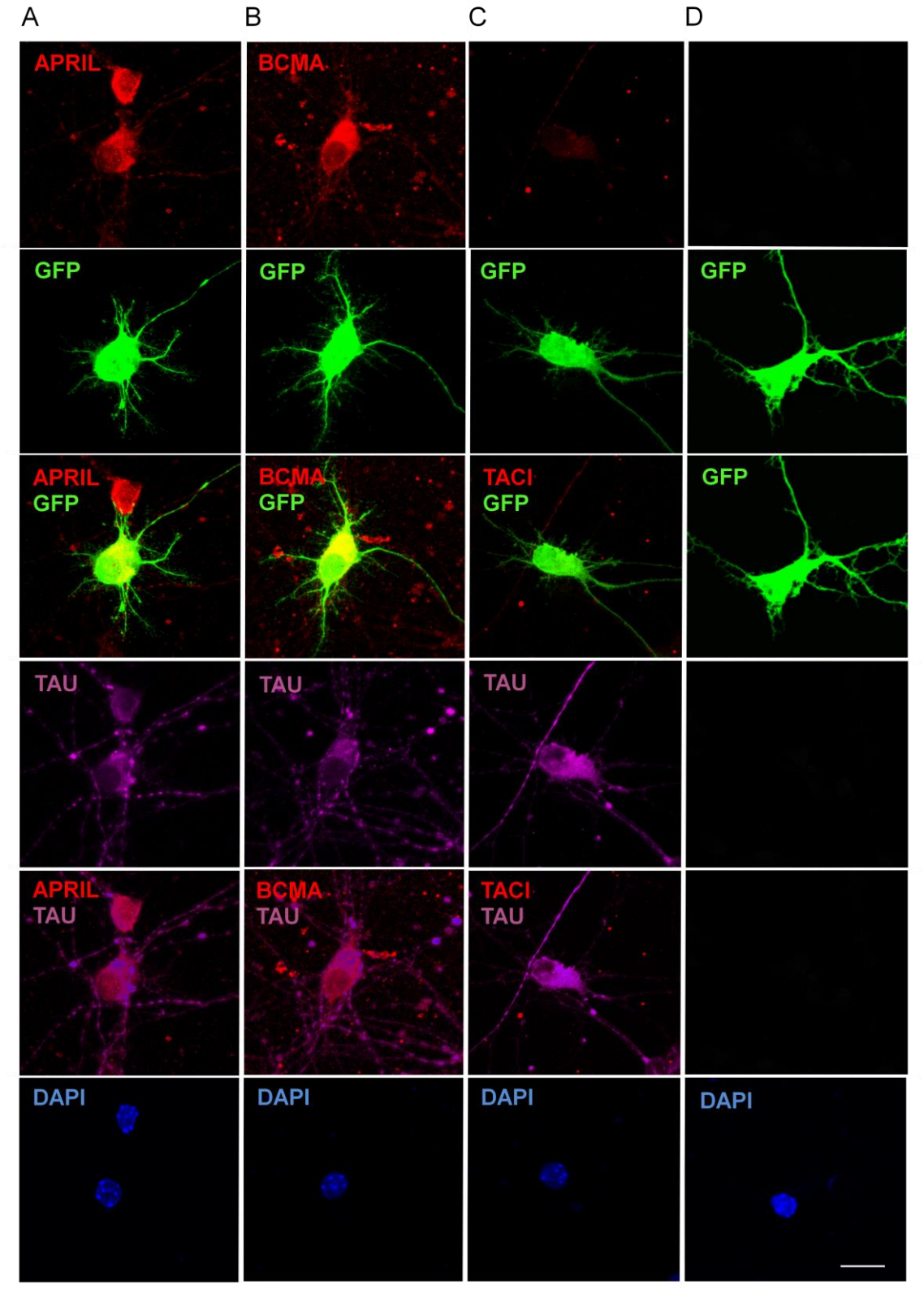

Figure 27: The cellular localisation of APRIL, BCMA and TACI proteins in 7DIVs hippocampal neurons. Hippocampal neurons were transfected with pCDH-CMV-MCS-EF1-copGFP (green) after 6DIVs and fixed 24h later. Fixed neurons were stained with antibodies against (A) APRIL, (B) BCMA, (C) TACI (all red) or (D) no primary antibody. Fixed neurons were also stained using an antibody against the axonal marker, TAU (purple in A, B and C) and with the nuclear marker DAPI (blue in A, B, C and D). Scale bar: 20μm.

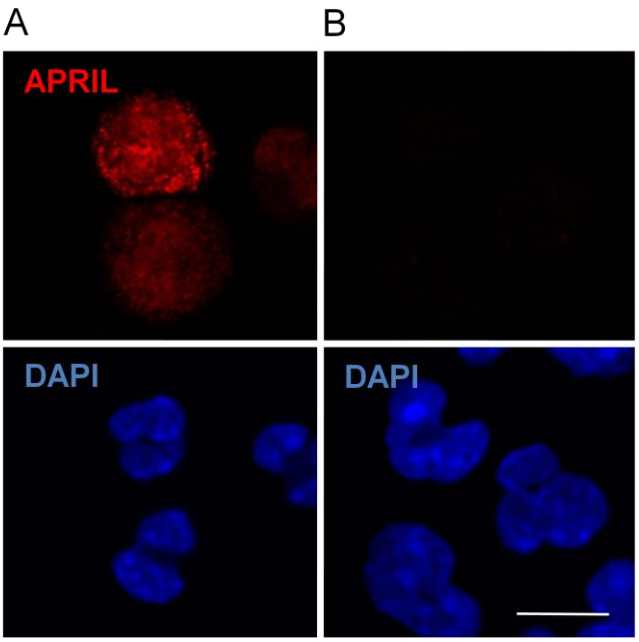

Figure 28: APRIL expression in macrophages.
Fixed macrophages were stained with antibodies recognising (A) APRIL (red) or (B) no primary antibody and nuclear marker DAPI (blue). Scale bar: 50μm.

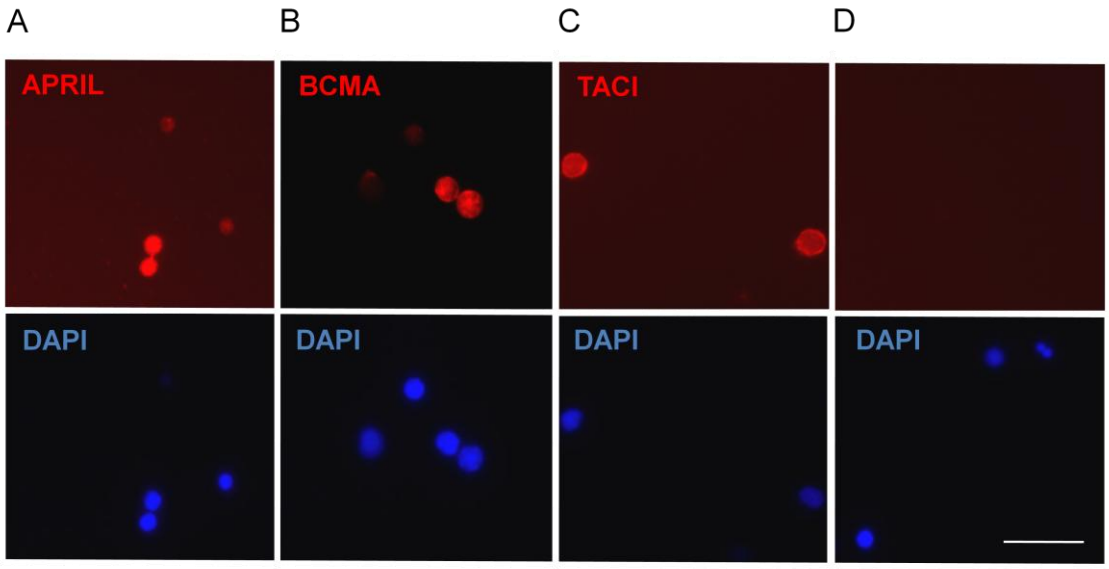

Figure 29: APRIL, BCMA and TACI expression in lymphocytes.
Fixed lymphocytes were stained with antibodies recognising (A) APRIL, (B) BCMA, (C) TACI (red) or (D) no primary antibody and nuclear marker DAPI (blue). Scale bar: 50μm.

3.3.5. Localisation of APRIL, BCMA and TACI proteins in the hippocampus

Immunohistochemistry was used to investigate the distribution of APRIL, BCMA and TACI in the developing mouse hippocampus at E18, P0, P5 and P10. At E18, there is diffuse, low level APRIL staining in the developing hippocampus, but BCMA staining is absent (Fig.30). By P0, APRIL and BCMA are beginning to be localised to the stratum pyramidale and the granule layer of the DG and the expression of both proteins is more prominent in these cell layers at P5 and P10. In accordance with the data from 7DIVs E18 hippocampal cultures (Fig.27 above), TACI protein is not detectable at any age examined in the developing hippocampus (Fig.30 below).

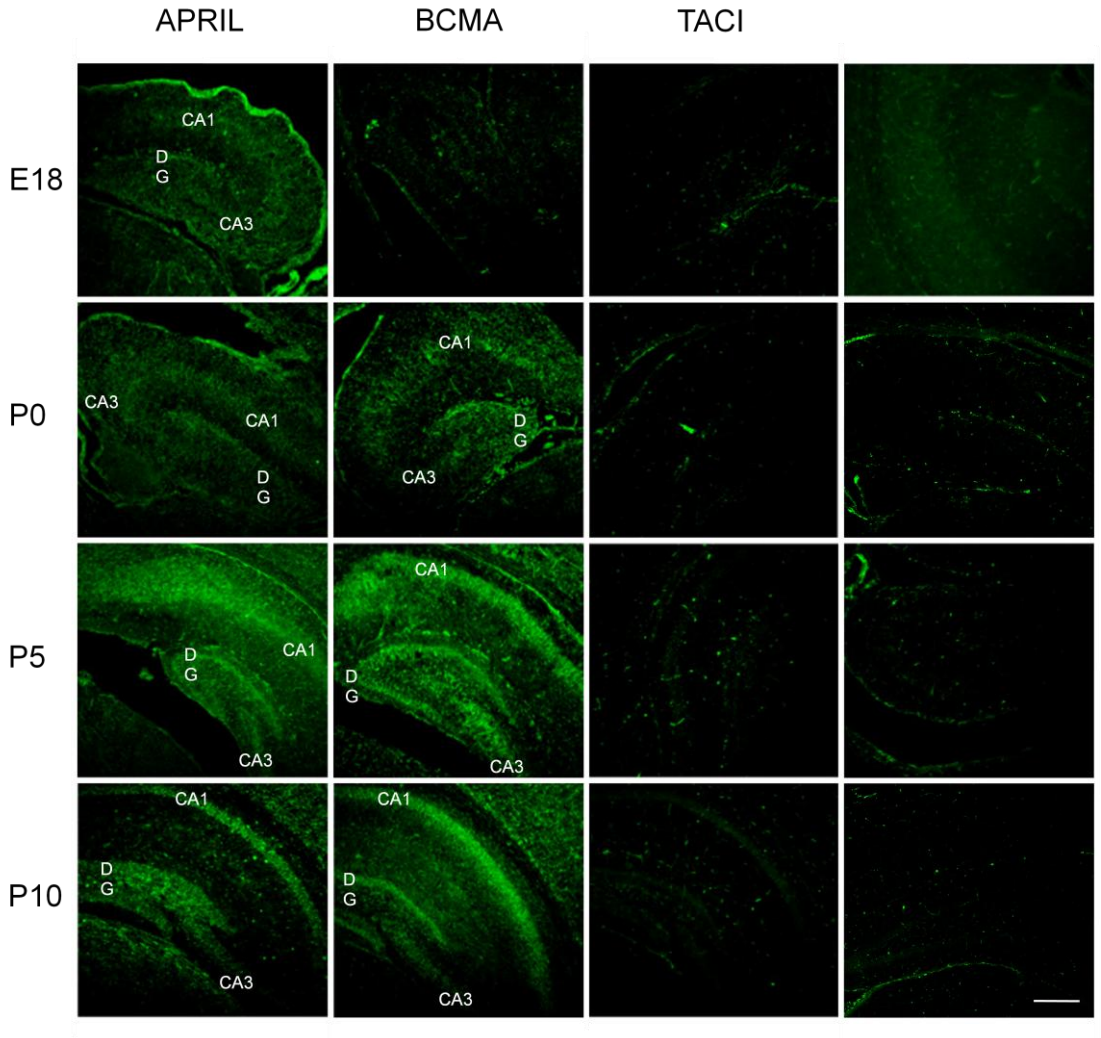

Figure 30: Localisation of APRIL, BCMA and TACI proteins in the developing mouse hippocampus. E18, P0, P5 and P10 hippocampal sections were stained with antibodies against APRIL, BCMA, and TACI (green). The column of panels on the right shows staining in the absence of primary antibodies. Scale bar: 200μm. (DG: dentate gyrus, CA1 and CA3 layer).

3.3.6. APRIL is secreted by cultured hippocampal neurons

To determine if cultured hippocampal neurons release soluble APRIL into the culture medium, an APRIL ELISA was performed on culture medium after E18 neurons had been in culture for 3 days. To allow a comparison between the levels of secreted APRIL and the total amount of APRIL expressed by cultured hippocampal neurons, protein extracts of 3DIVs cultures were also analysed by an APRIL ELISA alongside culture medium samples. Medium samples and protein extracts were obtained from both high (100,000cells/cm^2) and low-density (20,000cells/cm^2) hippocampal cultures. Soluble APRIL was clearly present in the culture medium from 3DIVs hippocampal cultures and the level of APRIL was higher in medium from high-density cultures (1.9ng/ml) compared to low-density cultures (1.5ng/ml). In high-density cultures, the culture medium contained more APRIL than cell lysates, a situation that was reversed in low-density cultures (Fig.31). The high levels of APRIL in culture medium suggest that APRIL is actively released from hippocampal neurons rather than being a consequence of leakage following neuronal death.

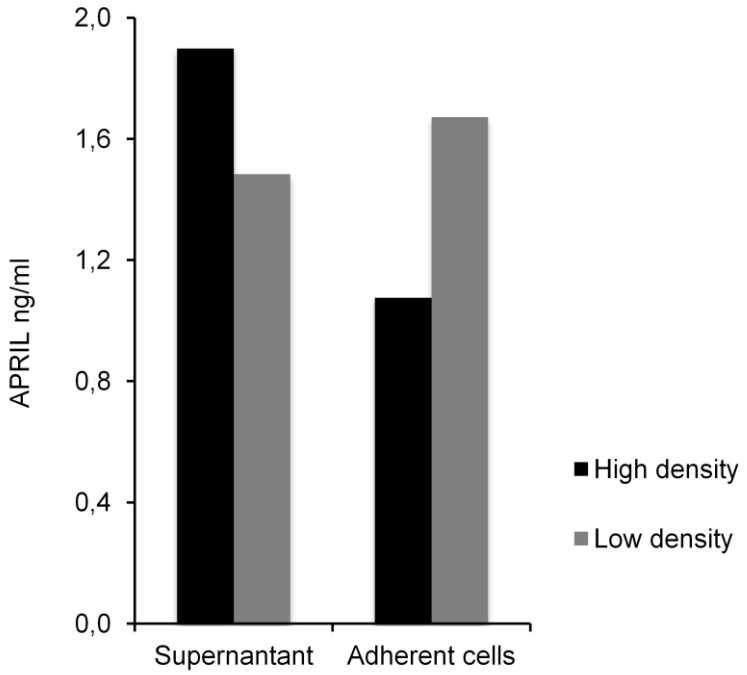

Figure 31: Hippocampal neurons secrete APRIL.

The amount of APRIL in culture medium and cell lysates of high (100,000cells/cm^2) and low density (20,000cells/cm^2), 3DIVs E18 hippocampal cultures was quantified by ELISA.

3.4. Discussion

In order to lay the ground work for the research presented in Chapters 4 and 6, E18 hippocampal neuron cultures needed to be established and confirmed they progressed clearly through the 5 stages of development that have previously been documented[22]. This was important so analyses on axons (stage 3) and dendrites (stage 4-5) could be performed. Figure 23 shows that Dotti stages 1-5 were all clearly identifiable these cultures.

As the expression of APRIL, BCMA and TACI have not previously been reported in the developing or adult hippocampus, a wide range of techniques was used to examine the expression of these TNFSF and TNFRSF members at the mRNA and protein level. Reverse transcriptase real-time PCR was utilised to quantify the levels of APRIL, BCMA and TACI transcripts in the developing hippocampus and in E18 hippocampal neurons cultured for between 0 and 7DIVs. Since APRIL and its receptors are mainly expressed by cells of the immune system[190,353,358,359,381], the transcripts encoding these proteins were also quantified in adult mouse thymus (where thymocytes mature into T cells) and spleen (reservoir of monocytes, B and T lymphocytes), both to act as a positive control for the real-time PCR and to allow a judgement to be made regarding the physiological relevance of APRIL, BCMA and TACI transcript levels in the developing hippocampus. Both APRIL and BCMA mRNAs are readily detectable and quantifiable throughout hippocampal development. Whilst APRIL mRNA expression levels are fairly constant during hippocampal development, BCMA transcript levels increase linearly from E18 to reach a peak at P10, before decreasing 2.5-fold between P10 and adult (Fig.24). This expression pattern suggests a possible role for BCMA in the early stages of neuronal maturation and hippocampal circuit development. In contrast to APRIL and BCMA, TACI mRNA levels are too low to be reliable quantified in the developing hippocampus, suggesting that it is unlikely to be a functional receptor for APRIL in the developing hippocampus. APRIL and BCMA mRNAs are readily detectable and quantifiable in cultures of E18 hippocampus, but TACI mRNA, although just about quantifiable, is expressed at very low levels in these cultures (Fig.25).

As future work it would be interesting to analyse the expression levels of BCMA mRNA at ages between P10 and adult, to determine whether the decrease in BCMA transcript levels between P10 and adult is gradual or whether a pronounced drop in expression occurs at a specific postnatal age. If the latter is the case, the drop in expression may be correlated with a specific developmental/maturation process.

The analysis of mRNA expression in hippocampal cultures aimed to understand how the expression of BCMA and APRIL transcripts varied during the culture periods when hippocampal neurons were projecting their first minor processes, specifying a single axon and undergoing axon elongation. High levels of APRIL and BCMA transcripts at 0DIVs (2hrs after plating) might reflect a transcriptional reaction to hippocampal dissociation and the new culture environment. Alternatively, it may reflect the levels of these mRNAs in the intact hippocampus *in vivo.* This could be addressed by analysing the expression of BCMA and APRIL mRNAs in RNA extracted from freshly dissected hippocampi and comparing expression levels to those in RNA extracted from hippocampal neurons that had been cultured for 2 hours. Importantly, BCMA transcript levels remain elevated in hippocampal neurons at 2 DIVs, a period of axonal extension, and are reduced at 7DIVs, a period characterised by the beginning of dendrite maturation (Fig.25). This suggests that APRIL/BCMA signalling may play a role in regulating axon elongation and is less likely to play a role in modulating dendrite outgrowth and branching.

Western blotting of lysates from E18 hippocampal cultures after 7DIVs revealed that hippocampal neurons express BCMA and APRIL proteins. Two isoforms of APRIL are evident in Western blots of hippocampal neurons, spleen and thymus lysates: one of 17KDa corresponding to mature APRIL and the other, 32KDa, corresponding to precursor APRIL. Whilst the ratio of mature to precursor protein is lower in hippocampal neurons than in thymus and spleen, mature APRIL is clearly detectable in hippocampal neurons. The expression levels of BCMA protein relative to β-actin appears to be higher in cultured hippocampal neurons compared to the thymus and spleen. In contrast, the levels of TACI are much lower in hippocampal neurons than in thymus and spleen (Fig.26). Once again this suggests that BCMA may play an important

role in hippocampal neuron development and that TACI is unlikely to be a receptor for APRIL in the developing hippocampus.

Immunocytochemistry has revealed that 7DIVs cultured hippocampal neurons express the ligand APRIL and the receptor BCMA, but not the alternative APRIL receptor, TACI. Double staining for APRIL and the axonal marker TAU has shown that the ligand is expressed in the soma and axon of hippocampal neurons. Likewise, BCMA is detected in the cell soma and co-localises with TAU in axons. In addition BCMA is also expressed in the initial segments of dendritic processes (Fig.27). These observations suggest a possible role for APRIL/BCMA signalling in promoting initial neurite formation and potentially enhancing axon elongation. The expression of both APRIL and its receptor, BCMA, in neurons raises the possibility that APRIL/BCMA signalling may act in an autocrine manner to regulate some aspect of hippocampal neuron development. Whilst E18 hippocampal cultures contain few glia by 7DIV, some non-neuronal cells in the cultures express APRIL and BCMA as previously reported[380]. Given that hippocampal non-neuronal cells also express APRIL, there is a possibility that paracrine signalling between neurons and glia could modulate neuronal development in the hippocampus.

Immunohistochemistry for APRIL, BCMA and TACI in the hippocampus at different developmental ages, validated the expression data obtained from real-time PCR, Western Blotting and immunocytochemistry. Whilst APRIL is detectable in sections of E18 hippocampus, expression is diffuse. By P0, APRIL expression appears to become localised to the DG granule cell layer and the stratum pyramidale, and these structures become more clearly delineated by APRIL expression as development proceeds. BCMA protein is not detectable in sections of E18 hippocampus, but from P0 onwards BCMA staining co-localises with APRIL staining in the stratum pyramidale and granule cell layer of the DG (Fig.30). DG granule cells are not present in hippocampal cultures established from E18 mouse embryos, because at E18 putative granule cells are still migrating towards the hippocampus[4]. As may be expected from real-time PCR, Western blot and immunocytochemistry data, TACI is not detectable in the hippocampus by immunohistochemistry at any developmental stage. BCMA

protein levels increase from E18 to P10 and this observation correlates with the mRNA expression data. However, the same is not observed for APRIL. APRIL protein levels increase from E18 to P10, but mRNA levels remain constant, or even slightly decrease over this developmental period. This may reflect an increase in the efficiency of translation of the APRIL message as hippocampal development proceeds and/or an increase in the stability of the APRIL protein over this time period.

The fact that Western blot analyses of cultured hippocampal neurons detect both the mature and pro forms of APRIL suggests that APRIL might be synthesised and processed by hippocampal neurons before secretion as the mature form. A specific ELISA for APRIL detects the protein in both cell lysates and culture medium of low and high-density hippocampal neuron cultures (Fig.31). This result demonstrates that hippocampal neurons not only express APRIL, as shown by the expression of its mRNA and protein in the developing hippocampus and in hippocampal cultures, but are also able to process it in their Golgi apparatus and release it exogenously in a mature and functional form to the culture environment *in vitro*, and presumably the extracellular matrix *in vivo*.

In summary, the data presented in this chapter provides the first demonstration that APRIL and one of its receptors, BCMA, are expressed by neurons in the developing mouse hippocampus. TACI, the alternative cognate TNF superfamily receptor for APRIL, is detected at significantly lower levels than BCMA in developing hippocampal neurons, suggesting that it does not mediate potential trophic effects of APRIL on these neurons. Since APRIL and BCMA are both expressed by neurons, and APRIL is secreted from cultured hippocampal neurons, it is possible that APRIL regulates some aspect of hippocampal neuron development via an autocrine route. The data provided the bases for further studies that aimed to determine if APRIL was a novel neurotrophic factor for developing hippocampal pyramidal neurons.

Chapter 4

APRIL promotes the growth of hippocampal axons through MAPK and PI3K/Akt/GSK-3β signalling pathways

4.1. Introduction

The *April* gene encodes a 250 amino acids protein that is most closely related to BAFF amongst TNFSF members, sharing 30% amino acid sequence identity and a similar tertiary structure[382]. APRIL and another TNFSF member, TWEAK, are both mapped in close proximity on the same chromosome (chromosome 17 in humans and 11 in mice) and alternative splicing of the locus leads to the generation of TWE-PRIL, a protein that comprises APRIL exons 2-6 fused with TWEAK exons 1-6. TWE-PRIL is a membrane bound protein sharing the cytoplasmic and transmembrane domains of TWEAK and the extracellular portion of APRIL[383,384]. APRIL can also form heterotrimers with the TNFSF member, BAFF that is detected in the serum of patients with systemic immune-based rheumatic diseases[385].

In addition to forming heterotrimers, APRIL and BAFF both signal through BCMA and TACI, although the affinity of BCMA for BAFF is significantly lower than that for APRIL[365,386]. BAFF, but not APRIL, also binds to and signals through BAFF-R[387]. Curiously, contrary to the majority of TNF receptors, BCMA and TACI only have a single CRD that contact APRIL or BAFF[388]. TWE-PRIL is hypothesized to bind to BCMA and TACI[383,384] while APRIL/BAFF heterodimers appear to bind more efficiently to TACI[385]. Interestingly, neither BCMA nor TACI appear to be involved in the tumour promoting effects of APRIL on some cell types. For example, whilst APRIL induces the proliferation of Jurkat T leukaemia, HT29 colon carcinoma and A549 lung epithelial cells, these tumour cells do not express BCMA or TACI[357]. Therefore, it was suggested that a third specific APRIL receptor, that was responsible for the tumour promoting effects of APRIL, existed in these cell lines[357]. A consensus motif in the N-terminal basic region of mature APRIL that is important for the binding of heparan sulphate proteoglycans (HSPG) has been identified[389]. As this region is different from the one that APRIL uses to bind to TNF receptors, APRIL is able to bind to HSPG and BCMA or TACI at the same time. It is possible that HSPG may mediate APRIL/BCMA or APRIL/TACI interactions in some cell types; however, it seems likely that APRIL can signal directly through proteoglycans in some tumour cell lines[389].

The signalling pathways that are initiated by APRIL binding to its receptors differ between BCMA and TACI. Immunoprecipitation studies have shown that BCMA associates with TRAF1, 2 and 3[390]. Overexpression of BCMA in human embryonic kidney (HEK) 293 cells results in the activation of MAPK, JNK, p38 kinase, NF-κB and Elk-1. Moreover, a 25 amino acid sequence in the cytoplasmic domain of BCMA is crucial for its association with TRAFs and the subsequent activation of NF-κB, Elk-1 and JNK[390]. Ligand bound TACI associates with TRAFs 2, 5 and 6 in B cells, leading to the promotion of NF-κB and JNK activity[391]. TACI has also been shown to activate the nuclear factor of activated T cells transcription factor (NF-AT) in T lymphocytes[392].

4.2. Aims

The previous chapter revealed that APRIL and BCMA are both expressed by developing hippocampal neurons *in vitro* and *in vivo*, suggesting that APRIL/BCMA signalling regulates some aspect of hippocampal neuron development. This chapter aimed to identify and clarify the role of APRIL/BCMA signalling in developing hippocampal neurons. After establishing that APRIL enhances axonal elongation from cultured hippocampal neurons, further work identified BCMA as the receptor that mediates this effect and revealed the signalling pathways downstream of BCMA that lead to increased axonal growth.

4.3. Results

4.3.1. APRIL increases hippocampal neuron axon length

To determine whether APRIL regulates the extent of axon outgrowth from cultured E18 hippocampal neurons, neurons were cultured for 2DIVs before being transfected with pCDH-CMV-MCS-EF1-copGFP and supplemented with different concentrations of recombinant APRIL for a further 16 hours. Cultured neurons were fixed, stained with an antibody against GFP and analysed at 3DIVs, a time point that precedes the growth of dendrites[22] (3.3.1. above). Figures 32 and 33 show that recombinant APRIL significantly increases the length of axons projecting from 3DIVs hippocampal neurons compared to control cultures. The enhancement of axonal growth is highly significant at 10ng/ml APRIL and the degree of enhancement is slightly

increased at 100ng/ml and 1000ng/ml APRIL. In addition to dissociated cultures of hippocampal neurons, P0 explants of the hippocampal CA area were cultured for 2 days in the presence or absence of 100ng/ml of APRIL to investigate the effects of APRIL on axon outgrowth. Figure 32.B clearly demonstrates that APRIL promotes axonal outgrowth from P0 hippocampus explants.

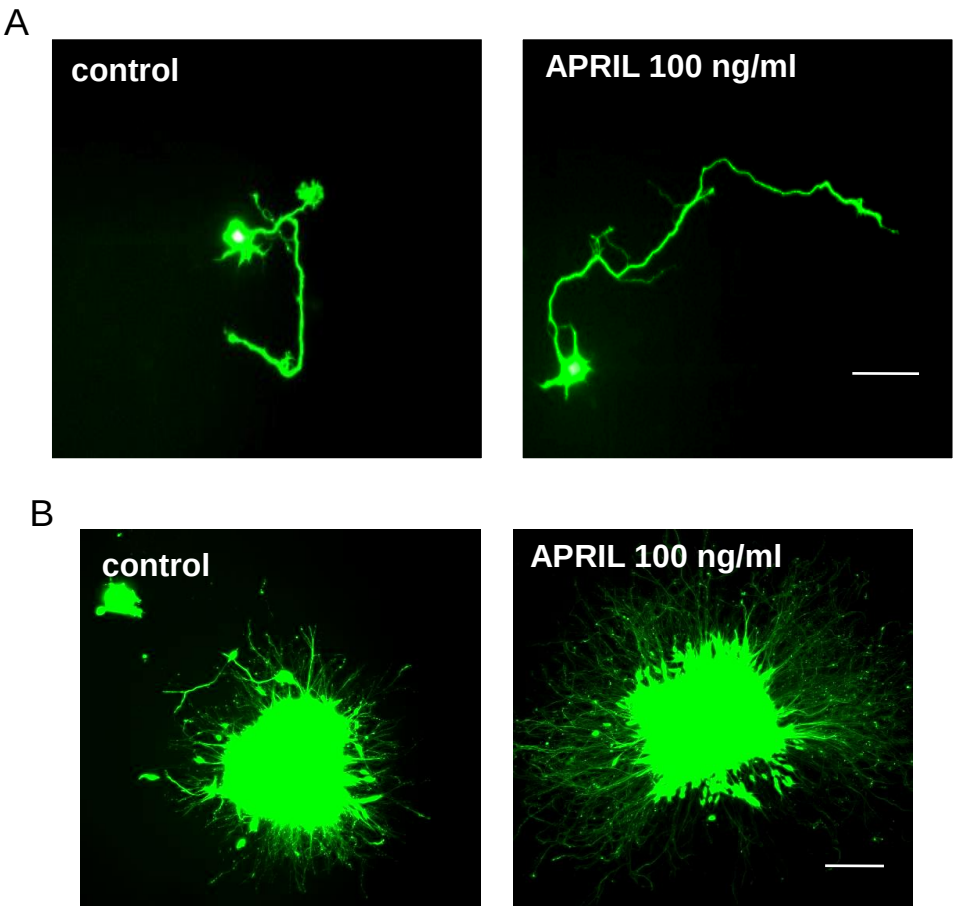

Figure 32: APRIL promotes axonal outgrowth from cultured hippocampal neurons.
(A) Representative photomicrographs of typical cultured hippocampal neurons that were grown for 2DIVs before being transfected with pCDH-CMV-MCS-EF1-copGFP and cultured for a further 16 hours, either with no factors or with 100ng/ml recombinant APRIL, and then fixed and stained for GFP. Scale bar: 100µm. (B) Representative photomicrographs of P0 hippocampal explants that were cultured for 2 days, either in the absence of factors or with 100ng/ml APRIL, before being stained with Calcein AM. Scale bar: 200µm.

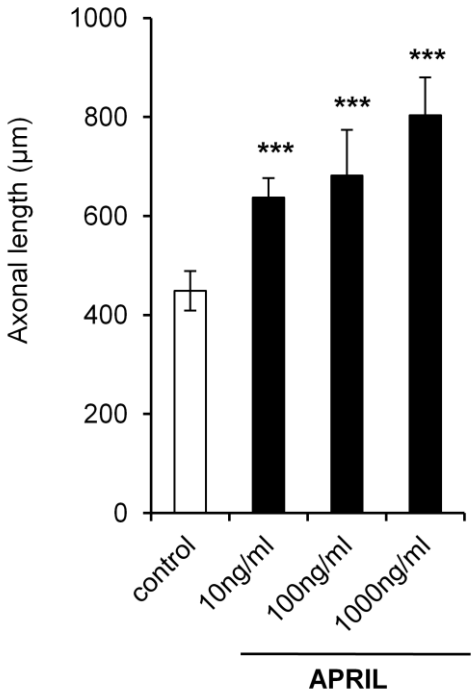

Figure 33: APRIL promotes axonal outgrowth from cultured hippocampal neurons.
E18 hippocampal neurons were cultured for 2DIVs before being transfected with pCDH-CMV-MCS-EF1-copGFP, and cultured for a further 16 hours in medium containing no factors (control) or medium containing either 10ng/ml, 100ng/ml or 1000ng/ml recombinant APRIL. Cultures were fixed at 3DIVs and stained with an anti-GFP antibody, before being imaged using a fluorescence microscope. Images were analysed using ImageJ software. Graph corresponds to mean of total axonal length. Data represent the mean and sem of 150 neurons for each condition from 3 separate experiments. ***indicates $p<0.0001$, statistical comparison with control, (Mann–Whitney U test).

4.3.2. APRIL does not increase hippocampal dendritic outgrowth

To evaluate whether APRIL could enhance dendrite outgrowth in addition to axon elongation, 6DIVs E18 hippocampal neuron cultures were transfected with pCDH-CMV-MCS-EF1-copGFP and cultured for a further 16 hours in medium containing, either no factors (control) or 10ng/ml, 100ng/ml or 1000ng/ml APRIL. After fixation and staining for GFP, neurons were imaged using a fluorescence microscope and the images analysed with Photoshop. The addition of APRIL to cultures does not increase the number of dendrites projecting from GFP stained neurons that are greater than 50µm in length compared to control cultures (Fig.34.A and B) Similarly, APRIL does not increase the mean number of primary dendrites arising from GFP stained neurons above that of control cultures (Fig.34.A and C).

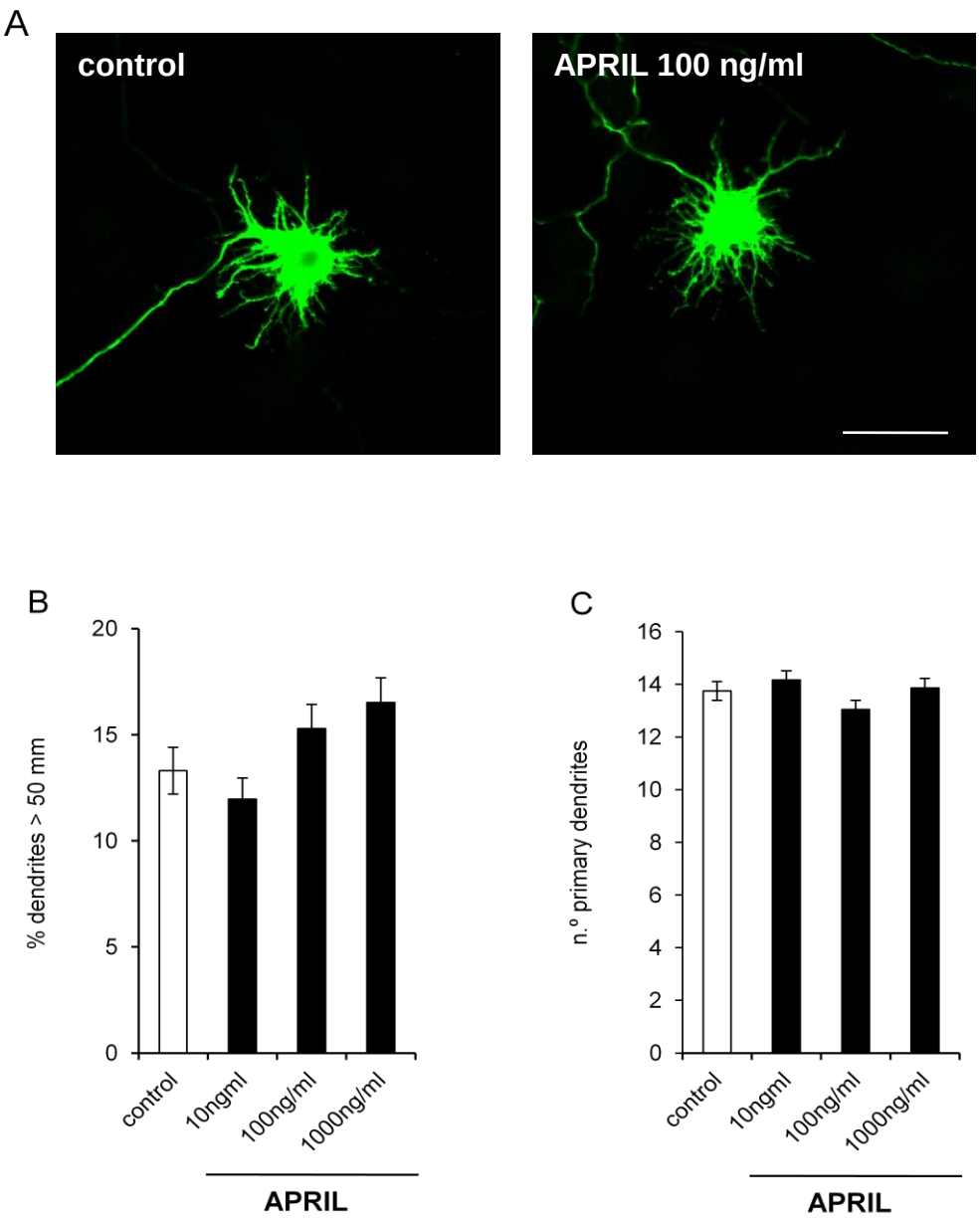

Figure 34: APRIL does not promote dendritic outgrowth from cultured hippocampal neurons. 6DIVs E18 hippocampal neurons were transfected with pCDH-CMV-MCS-EF1-copGFP, and cultured for a further 16h in medium containing, either no factors (control) or 10ng/ml, 100ng/ml or 1000ng/ml recombinant APRIL. Cultures were fixed at 7DIVs, stained with an anti-GFP antibody and imaged on a fluorescence microscope. Images were analysed using Photoshop. (A) Representative photomicrographs of typical hippocampal neurons cultured either in the absence of factors (control) or in medium containing 100ng/ml APRIL. Scale bar: 50μm. Graphs correspond to the (B) % of dendrites > 50μm and the (C) mean number of primary dendrites. Data represent the mean and sem of 150 neurons for each condition from 3 separate experiments.

4.3.3. BCMA mediates APRIL-promoted axonal elongation from cultured hippocampal neurons

Transfection of bicistronic expression plasmids encoding either WT BCMA and GFP (pCDH-CMV-BCMA-EF1-copGFP), or GFP together with a signalling-defective BCMA mutant lacking 83 C-terminal residues (pCDH-CMV-BCMA-ΔC83-EF1-copGFP), were used to investigate the role of BCMA in APRIL promoted axon growth. Compared to control transfected neurons (transfected with pCDH-CMV-MCS-EF1-copGFP), the overexpression of WT BCMA increases axon length by the same order as magnitude as the addition of 100ng/ml recombinant APRIL to cultures. The addition of 100ng/ml APRIL to cultures containing neurons transfected with WT BCMA does not further increase axon length compared to neurons transfected with WT BCMA cultured in the absence of APRIL. Conversely, the expression of truncated BCMA significantly decreases axon length compared to control transfect cultures and prevents exogenous APRIL from promoting axonal elongation (Fig.35.A and B).

Taken together, these data demonstrates that APRIL signals via BCMA to mediate axonal growth in hippocampal cultures.

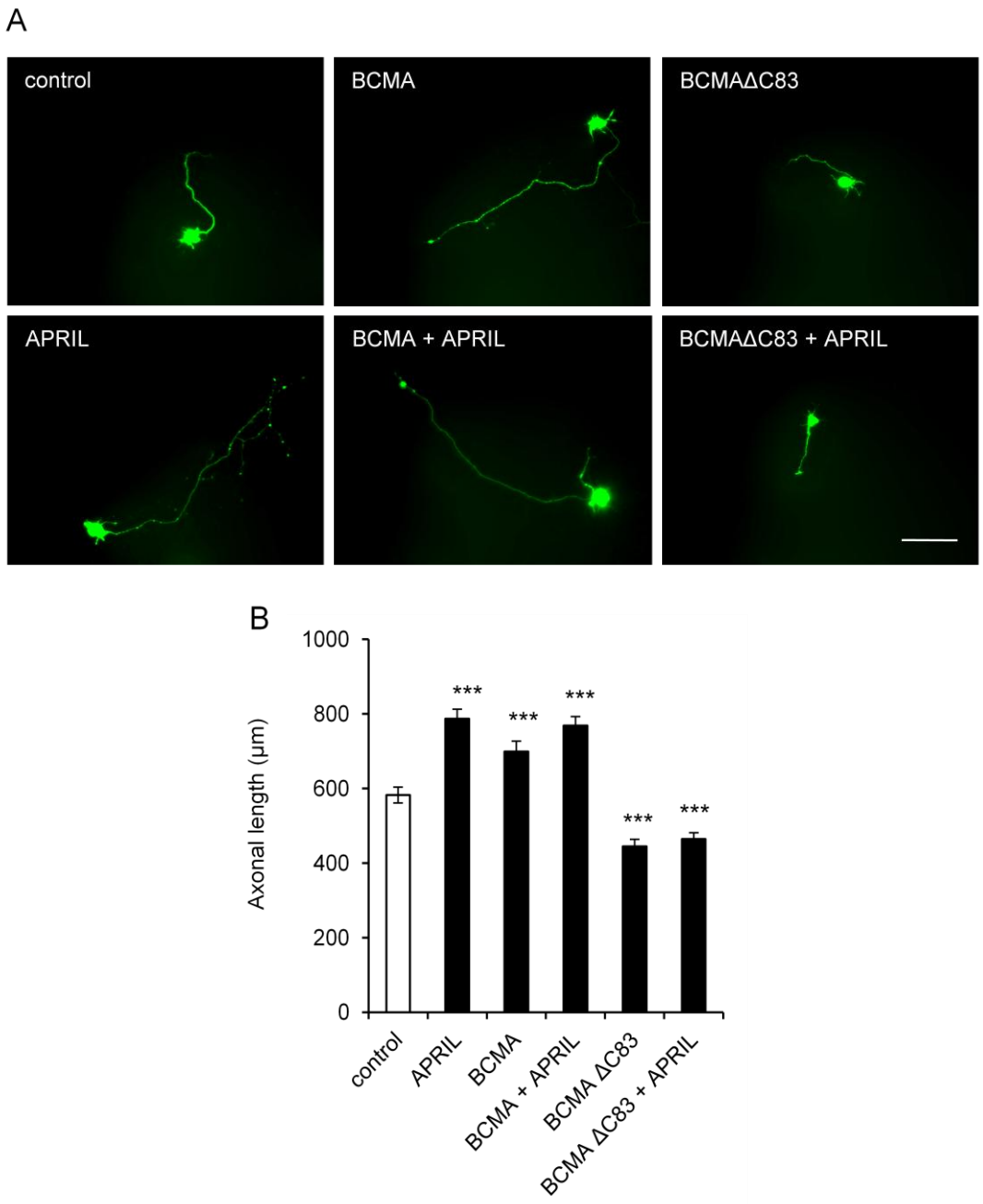

Figure 35: BCMA mediates APRIL promoted-axonal outgrowth from cultured hippocampal neurons. E18 hippocampal neurons that had been cultured for 2DIVs were transfected with either pCDH-CMV-MCS-EF1-copGFP (control), pCDH-CMV-BCMA-EF1-copGFP or pCDH-CMV-BCMA-ΔC83-EF1-copGFP. Transfected neurons were culture for a further 16h in medium containing either no factors or medium containing 100ng/ml APRIL before being fixed, stained for GFP and imaged under a fluorescence microscope. Images were analysed by ImageJ software. (A) Representative photomicrographs of typical cultured neurons under different conditions. Scale bar: 100µm. Graph corresponds to (B) mean of total axonal length. Data represent the mean and sem of 150 neurons for each condition from 3 separate experiments. ***indicates $p<0.0001$, statistical comparison with control, (Mann–Whitney U test).

4.3.4. Heparan sulphate proteoglycans are not essential for APRIL-promoted axon growth from cultured hippocampal neurons

To evaluate whether HSPGs were required for BCMA mediated enhancement of axon elongation by APRIL, E18 hippocampal neurons were transfected with pCDH-CMV-MCS-EF1-copGFP after 2DIVs and cultured for a further 16 hours in medium containing either no factors (control) or medium containing recombinant mutant APRIL (APRIL H89) that lacks the capacity to bind HSPGs. APRIL H89 promotes a dose-dependent increase in axonal growth. However, whilst the extent of axon elongation promoted by APRIL H89 and WT APRIL are similar at APRIL concentrations of 100ng/ml and 1000ng/ml, 10ng/ml of APRIL H89, unlike WT APRIL, is not able to significantly increase the length of hippocampal neuron axons compared to control cultures (Fig.36.A and B). This data suggests that although APRIL H89 promotes axon elongation from cultured hippocampal neurons, it may be slightly less potent than WT APRIL.

The efficacy of APRIL H89 in enhancing axon growth was further investigated in a second series of experiments. Hippocampal neurons that had been cultured for 2DIVs were transfected either with a control plasmid expressing GFP alone (pCDH-CMV-MCS-EF1-copGFP) or a plasmid expressing GFP together with WT APRIL (pCDH-CMV-APRIL-EF1-copGFP). Following transfection, control transfected neurons were cultured for a further 16 hours either in the absence of factors (control) or in medium containing 100ng/ml of either WT APRIL or APRIL H89. Figure 37.A and B demonstrates that overexpressing WT APRIL is as effective as the addition of 100ng/ml APRIL to cultures in terms of enhancing axon elongation from hippocampal neurons. Interestingly, 100ng/ml APRIL H89 appears to be more potent than 100ng/ml WT APRIL in promoting axon growth. Taken together, the data indicate that the binding of APRIL to HSPGs is not required to mediate axon elongation from cultured hippocampal neurons.

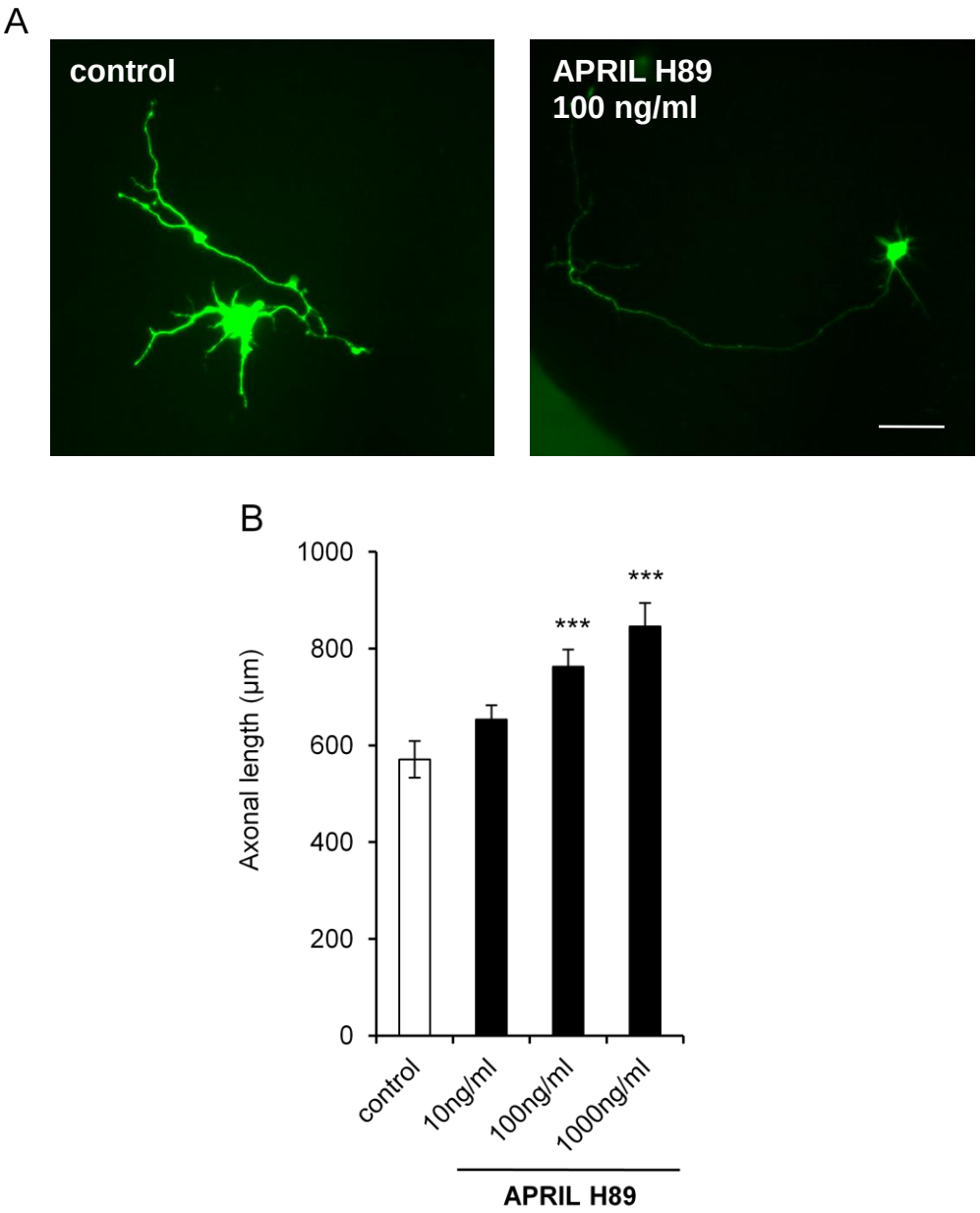

Figure 36: APRIL does not require HSPGs to promote axonal outgrowth from cultured hippocampal neurons. E18 hippocampal neurons were cultured for 2DIVs before being transfected with pCDH-CMV-MCS-EF1-copGFP, and cultured for a further 16h in medium containing no factors (control) or medium containing either 10ng/ml, 100ng/ml or 1000ng/ml recombinant APRIL H89. Cultures were fixed at 3DIVs and stained with an anti-GFP antibody, before being imaged using a fluorescence microscope. Images were analysed using ImageJ software. (A) Representative photomicrographs of typical hippocampal neurons cultured either in the absence of factors (control) or in medium containing 100ng/ml APRIL H89. Scale bar: 100µm. Graph corresponds to (B) mean of total axonal length. Data represent the mean and sem of 150 neurons for each condition from 3 separate experiments. ***indicates p<0.0001, statistical comparison with control, (Mann–Whitney U test).

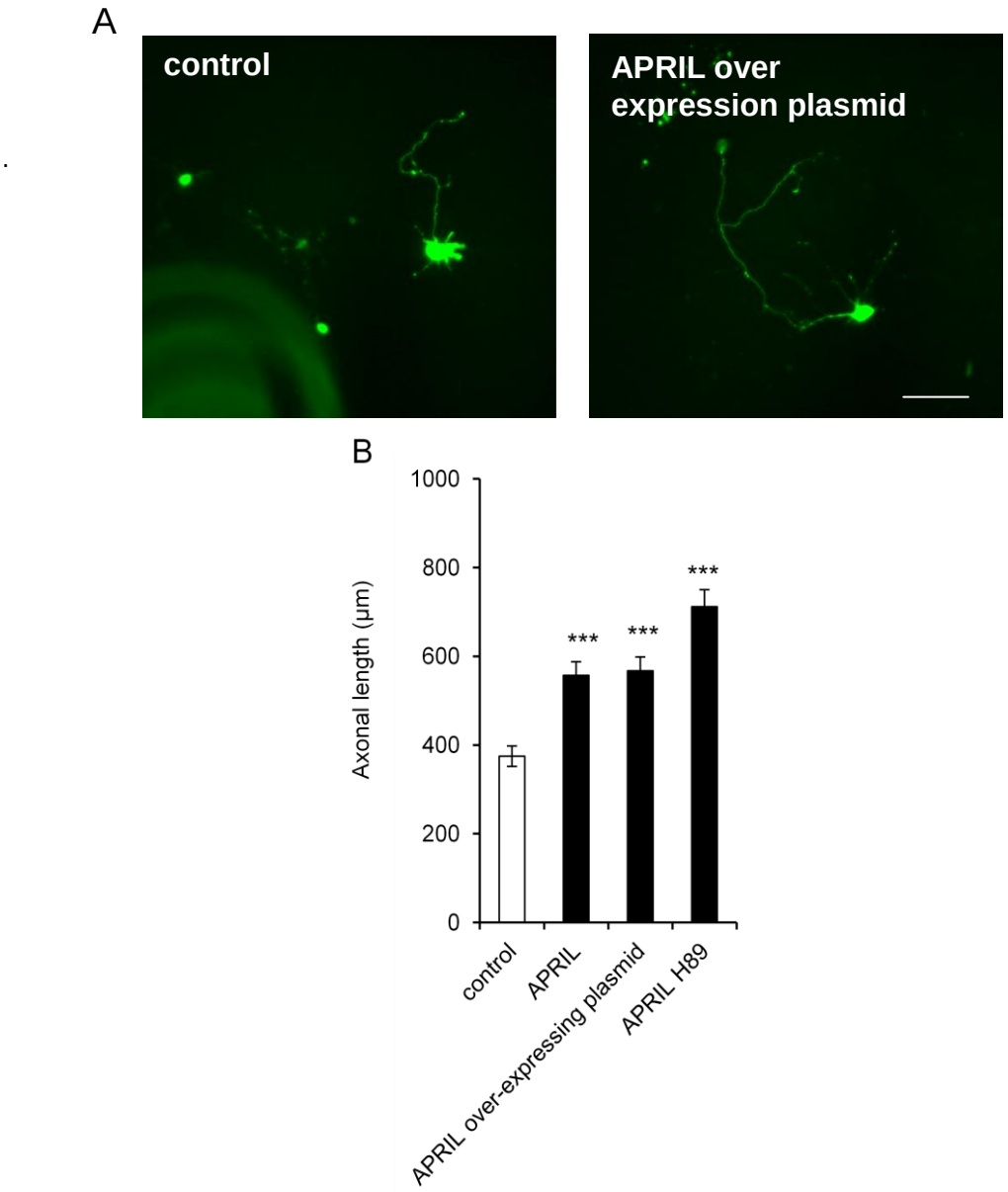

Figure 37: APRIL does not require HSPGs to promote axonal outgrowth from cultured hippocampal neurons. E18 hippocampal neurons were cultured for 2DIVs before being transfected with either pCDH-CMV-MCS-EF1-copGFP (control) or pCDH-CMV-APRIL-EF1-copGFP. Control transfected neurons were cultured for a further 16h in medium containing no factors (control) or medium containing either 100ng/ml of WT APRIL or APRILH89. Neurons transfected with pCDH-CMV-APRIL-EF1-copGFP were cultured for a further 16h in the absence of trophic factors. Cultures were fixed at 3DIVs and stained with an anti-GFP antibody, before being imaged using a fluorescence microscope. Images were analysed using ImageJ software. (A) Representative photomicrographs of typical hippocampal neurons transfected with either pCDH-CMV-MCS-EF1-copGFP (control) or pCDH-CMV-APRIL-EF1-copGFP and cultured for a further 16h in the absence of factors. Scale bar: 100µm. Graph corresponds to (B) mean of total axonal length. Data represent the mean and sem of 150 neurons for each condition from 3 separate experiments. ***indicates p<0.0001, statistical comparison with control, (Mann–Whitney U test).

4.3.5. Signalling transduction induced by APRIL in hippocampal neurons: activation of MAPK and PI3K/Akt-PKB/GSK-3β pathways

To elucidate the molecular mechanism underlying the selective influence of APRIL on promoting axonal growth from hippocampal neurons, potential common links in intracellular signalling were explored. To assess the importance of ERK1/2 activation on APRIL-promoted axonal growth, PD98059, a selective MEK1 and MEK2 inhibitor that prevents the phosphorylation, and hence activation, of ERK1/2[393], was added to hippocampal neuron cultures. Hippocampal neurons that had been cultured for 2DIVs were transfected with pCDH-CMV-MCS-EF1-copGFP and cultured for a further 2 hours either in the absence or presence of 10μM PD98059. After, cultures were incubated for a further 16 hours either in the presence or absence of 100ng/ml APRIL. Whilst PD98059 does not reduce the length of axons compared to control cultures when hippocampal neurons are cultured without APRIL, it totally blocks the axon growth promoting ability of APRIL (Fig.38.A and B). Further evidence that ERK1/2 activation forms part of the signalling mechanism that mediates APRIL promoted axonal elongation can be seen in figure 39. The addition of 100ng/ml APRIL to 3DIVs hippocampal cultures results in a rapid and sustained increase in the levels of phospho-ERK1/2 (phosphorylation of residues Thr202 and Tyr204 in ERK1 and 2, respectively) in hippocampal neurons, as determined by Western blotting.

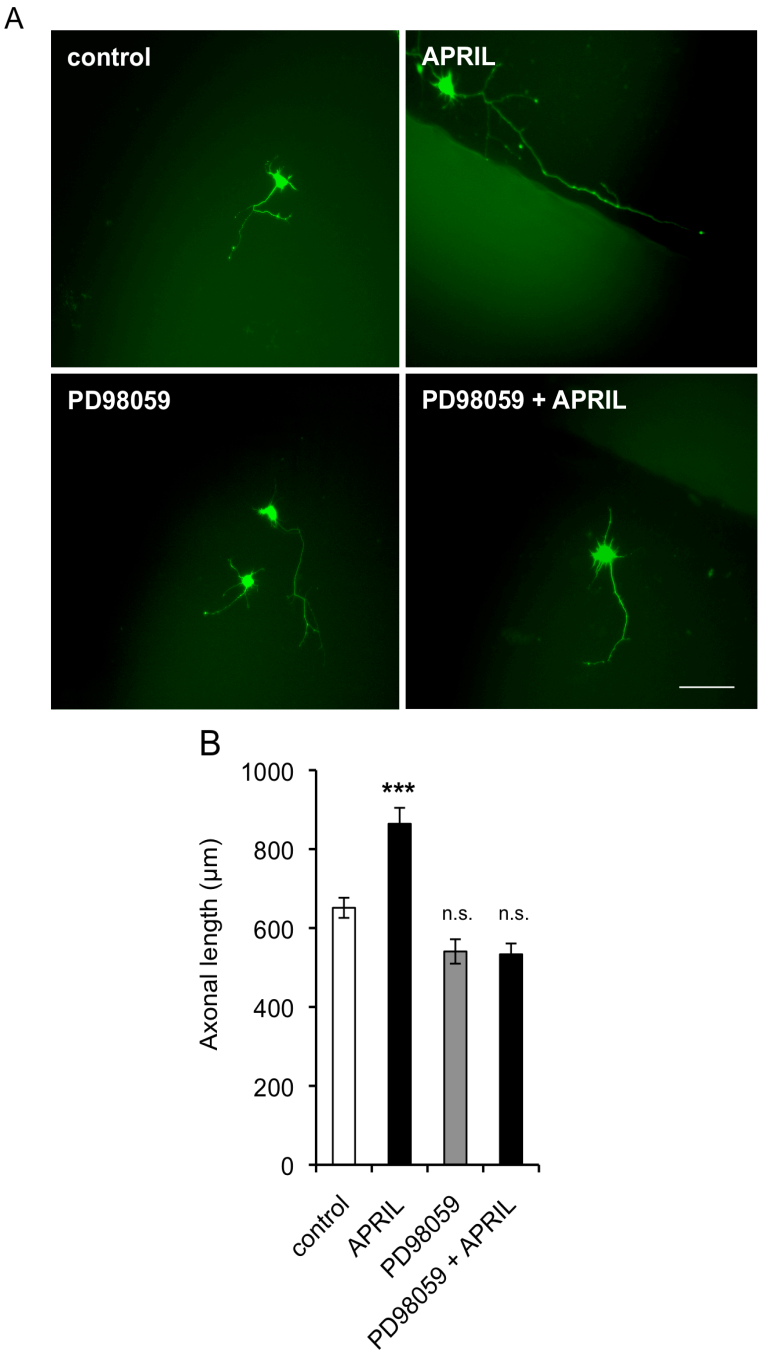

Figure 38: ERK activation is required for APRIL-promoted axonal growth.

E18 hippocampal neurons that had been cultured for 2DIVs were transfected with pCDH-CMV-MCS-EF1-copGFP prior to 2h incubation either in the presence or absence of 10µM PD98059. Following this, neurons were cultured for a further 16h, either in the presence or absence of 100ng/ml of recombinant APRIL, before being fixed at 3DIVs, stained with an antibody against GFP and imaged under a fluorescence microscope. Images were analysed with ImageJ. (A) Representative photomicrographs of typical hippocampal neurons cultured under the stated conditions. Scale bar: 100µm. Graph corresponds to (B) mean of total axonal length. Data represent the mean and sem of 150 neurons for each condition from 3 separate experiments. ***indicates $p \leq 0.0001$, statistical comparison with control, n.s. non-significant (Mann-Whitney U test).

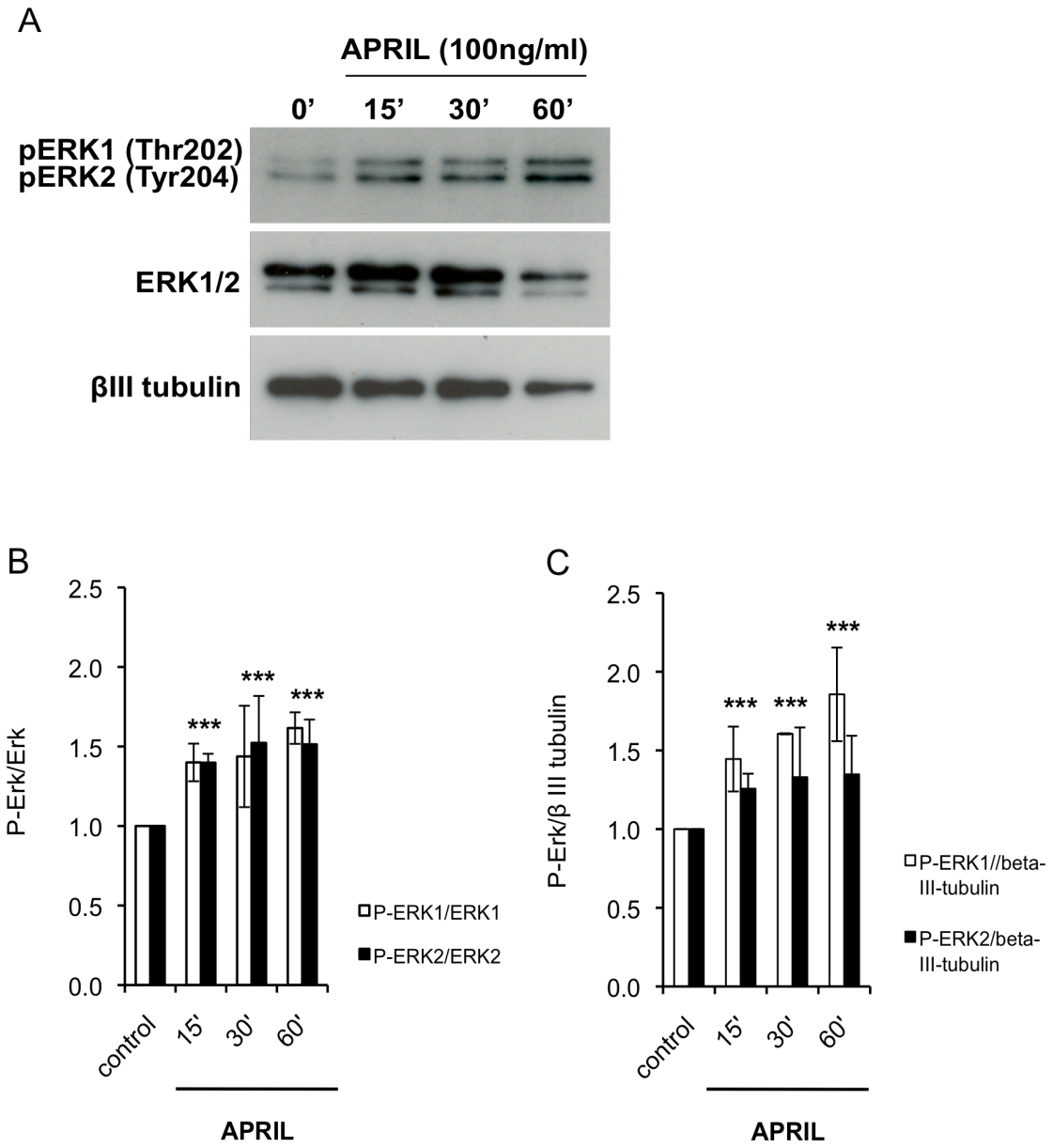

Figure 39: APRIL increases ERK phosphorylation.

E18 hippocampal neurons that had been cultured for 3DIVs were treated with 100ng/ml of recombinant APRIL for 15, 30 or 60min before being lysed. Western blots of lysates were probed with antibodies against ERK1/2, phospho-ERK1/2 and β-III tubulin. (A) Representative scans of Western blots. Graphs correspond to densitometry measurements from films and show (B) P-Erk/Erk and (C) P-Erk/β-III tubulin ratios. Data represent the mean and sem of 3 separate experiments. ***indicates $p<0.0001$, statistical comparison with control and refers to both Erk1 and Erk2 (Mann-Whitney U test).

Having established that the addition of recombinant APRIL to cultures of hippocampal neurons leads to the phosphorylation of ERK1/2, and that inhibiting ERK1/2 phosphorylation abolishes APRIL promoted axonal growth, the roles that PI3K and Akt play in mediating APRIL promoted axon elongation were examined. LY294002 is a selective pharmacological blocker of PI3K activity that prevents the phosphorylation and activation of Akt1/2[394]. Hippocampal neurons that had been cultured for 2DIVs were transfected with pCDH-CMV-MCS-EF1-copGFP and cultured for a further 2 hours either in the absence or presence of 10μM LY294002. After, cultures were incubated for a further 16 hours either in the presence or absence of 100ng/ml APRIL. Whilst LY294002 does not reduce the length of axons compared to control cultures in the absence of APRIL, it totally prevents APRIL from enhancing the growth of hippocampal neuron axons (Fig.40.A and B).

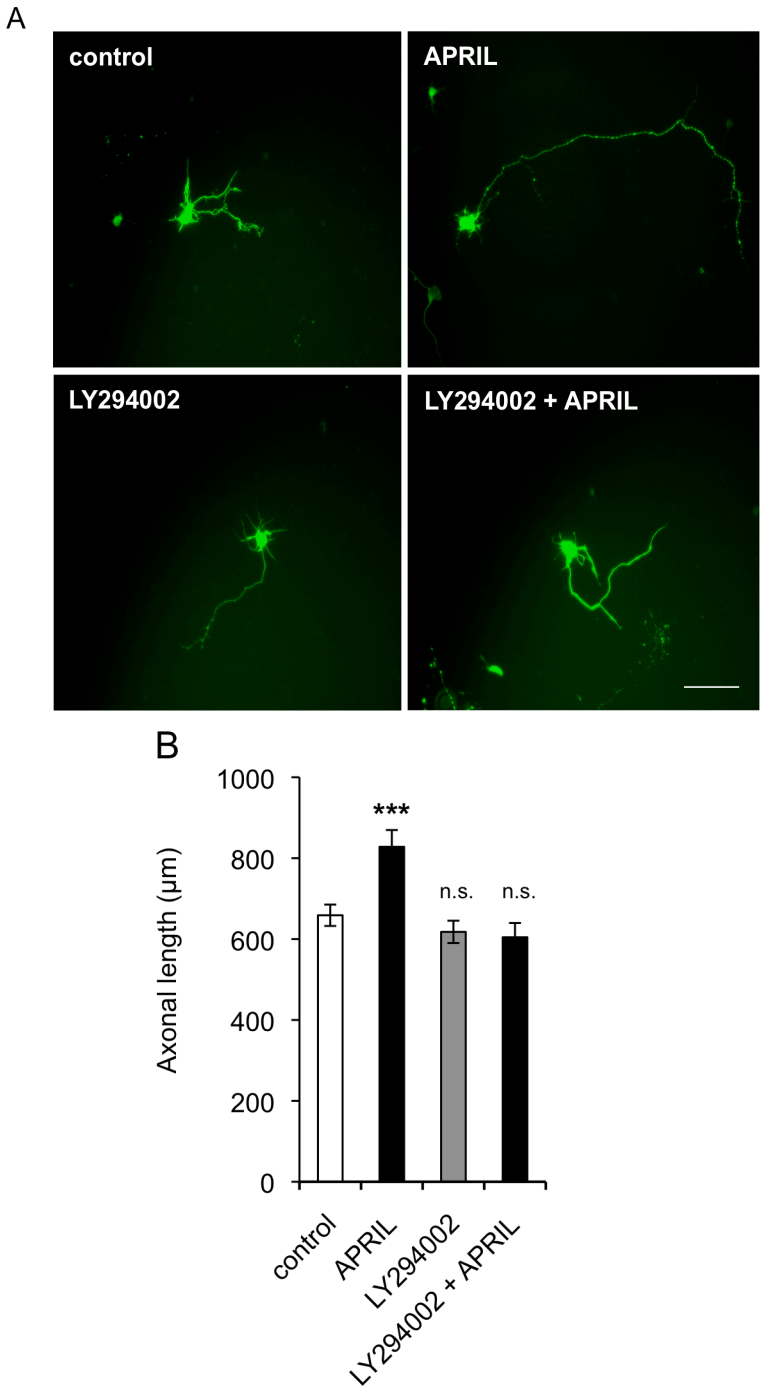

Figure 40: PI3K activity is required for APRIL-promoted axonal growth.

E18 hippocampal neurons that had been cultured for 2DIVs were transfected with pCDH-CMV-MCS-EF1-copGFP prior to 2h incubation either in the presence or absence of 10µM LY294002. Following this, neurons were cultured for a further 16h, either in the presence or absence of 100ng/ml of recombinant APRIL, before being fixed at 3DIVs, stained with an antibody against GFP and imaged under a fluorescence microscope. Images were analysed with ImageJ. (A) Representative photomicrographs of typical hippocampal neurons cultured under the stated conditions. Scale bar: 100µm. Graph corresponds to (B) mean of total axonal length. Data represent the mean and sem of 150 neurons for each condition from 3 separate experiments. ***indicates $p<0.0001$, statistical comparison with control, n.s. non-significant (Mann-Whitney U test).

Blocking the activity of PI3K, and potentially the subsequent phosphorylation and activation of Akt1/2, clearly prevents APRIL from promoting the elongation of hippocampal axons. To address whether Akt1/2 activity is essential for APRIL promoted axonal growth, an Akt1/2 inhibitor was added to cultures using a similar experimental paradigm to that used for MEK1/2 and PI3K inhibitors. In the absence of exogenous APRIL, the Akt inhibitor does not change mean axon length compared to control cultures. However, the inhibitor abolishes APRIL-mediated axonal growth (Fig.41.A and B). The role of activated Akt in transducing APRIL promoted axon outgrowth was further investigated by examining the phosphorylation status of Akt after the addition of 100ng/ml APRIL to hippocampal neurons that had been in culture for three days. The addition of APRIL induces a rapid and sustained phosphorylation of Akt serine residue 473, and hence activation of Akt (Fig.42).

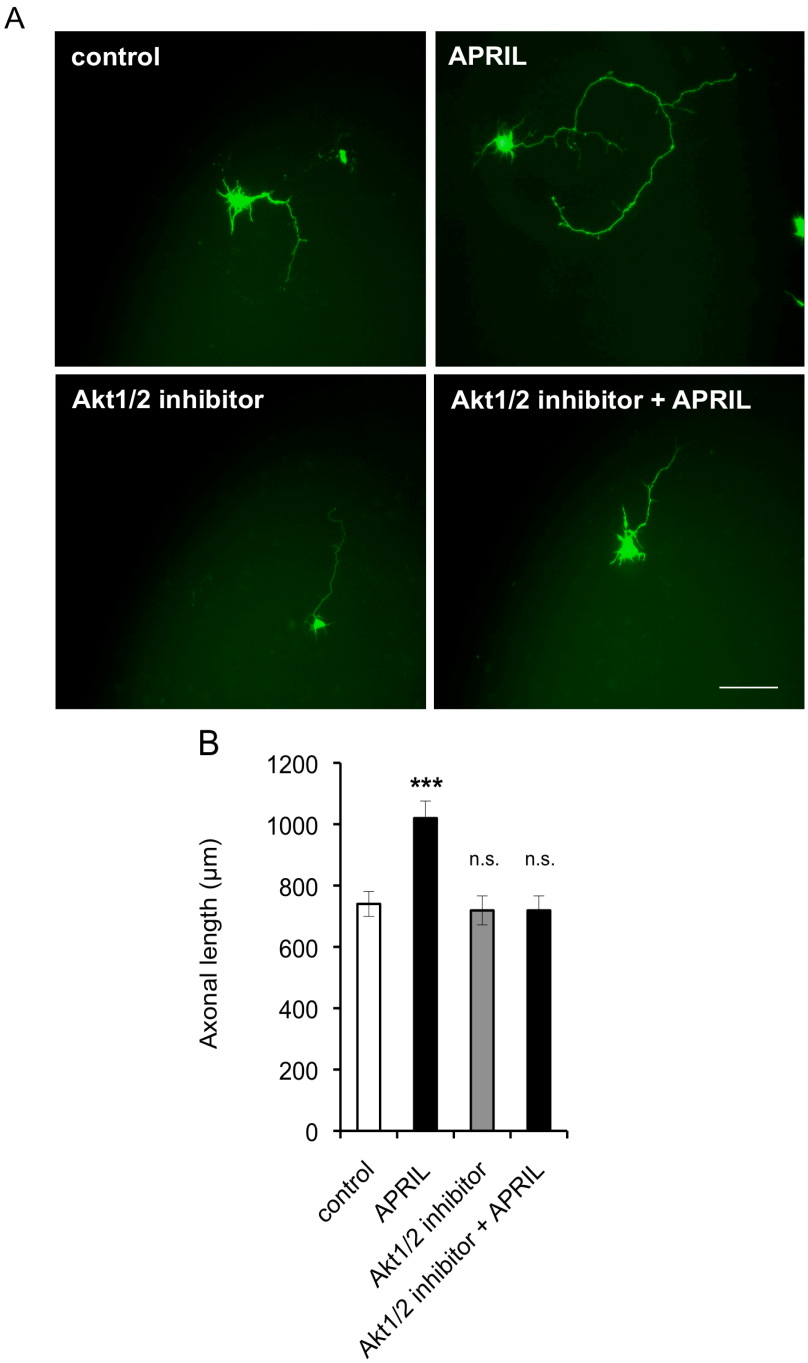

Figure 41: Akt activity is required for APRIL-promoted axonal growth.
Hippocampal neurons that had been cultured for 2DIVs neurons were transfected with pCDH-CMV-MCS-EF1-copGFP prior to 2h incubation either in the presence or absence of 5µM of Akt1/2 inhibitor. Following this, neurons were cultured for a further 16h, either in the presence or absence of 100ng/ml of recombinant APRIL, before being fixed at 3DIVs, stained with an antibody against GFP and imaged under a fluorescence microscope. Images were analysed with ImageJ. (A) Representative photomicrographs of typical hippocampal neurons cultured under the stated conditions. Scale bar: 100µm. Graph corresponds to (B) mean of total axonal length. Data represent the mean and sem of 150 neurons for each condition from 3 separate experiments. ***indicates $p \leq 0.0001$, statistical comparison with control, n.s. non-significant (Mann-Whitney U test).

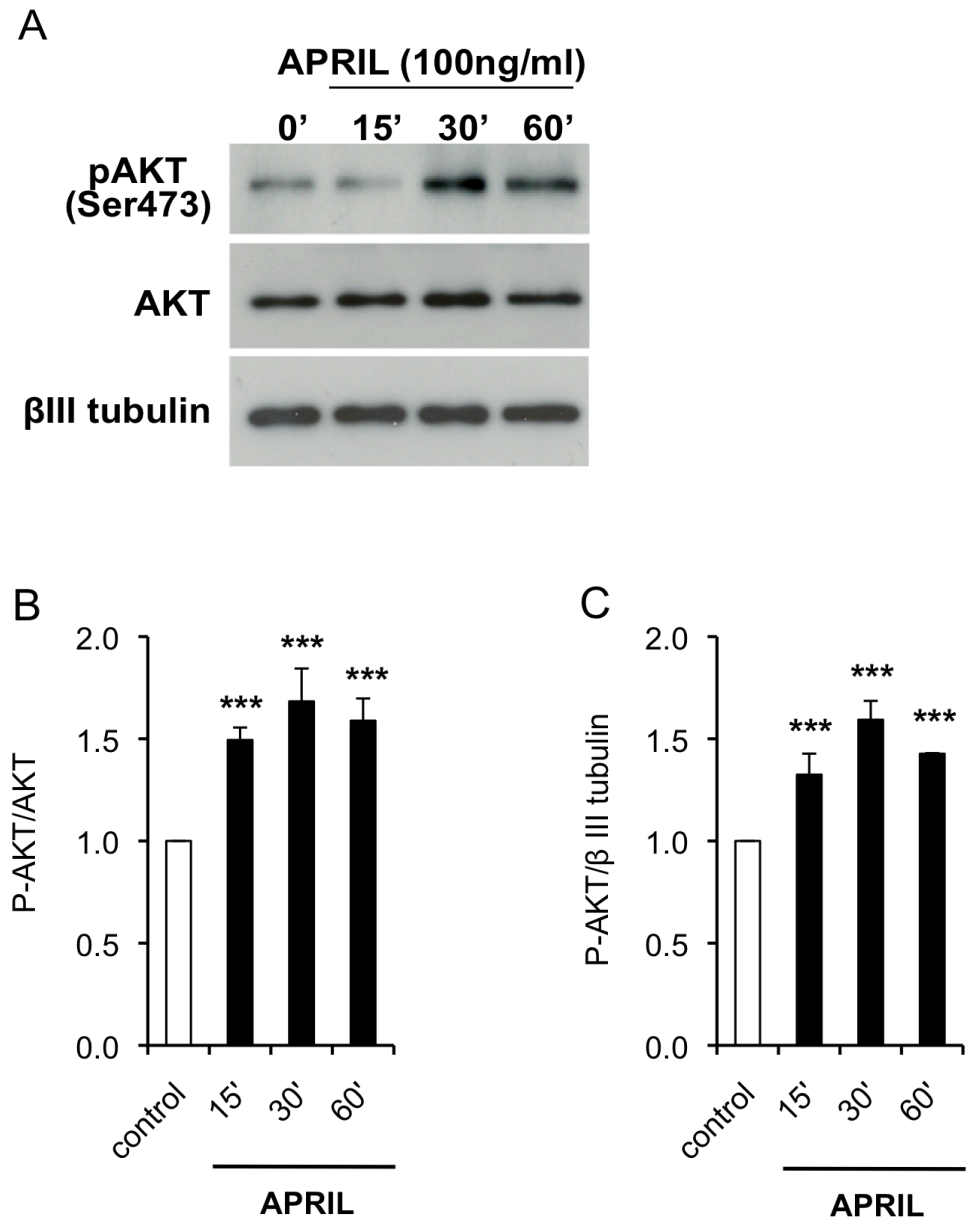

Figure 42: APRIL enhances the phosphorylation of Akt.

E18 hippocampal neurons that had been cultured for 3DIVs were treated with 100ng/ml of recombinant APRIL for 15, 30 or 60min before being lysed. Western blots of lysates were probed with antibodies against Akt, phospho-Akt and β-III tubulin. (A) Representative scans of Western blots. Graphs correspond to densitometry measurements from films and show (B) P-Akt/Akt and (C) P-Akt/β-III tubulin ratios. Data represent the mean and sem of 3 separate experiments. ***indicates $p<0.0001$, statistical comparison with control (Mann-Whitney U test).

One of the downstream targets of activated Akt is GSK-3β, a protein kinase that acts to inhibit axon growth in its non-phosphorylated, kinase active state. Phosphorylation of GSK-3β abolishes its kinase activity, thereby removing its ability to inhibit axon growth[395]. To try to ascertain whether the modulation of GSK-3β activity is part of the signalling cascade that leads to APRIL-induced axonal extension, hippocampal neurons were cultured in the presence or absence of APRIL and/or lysophosphatidic acid (LPA), a known activator of GSK-3β activity[396], using a similar experimental paradigm to that used above for MEK, PI3K and Akt inhibitors. In the absence of exogenous APRIL, LPA does not change mean axon length compared to control cultures. The addition of LPA to cultures, and hence the promotion of GSK-3β kinase activity, does, however, prevent APRIL from enhancing axonal outgrowth (Fig.43). Moreover, Western blotting reveals that the addition of 100ng/ml recombinant APRIL to E18 hippocampal neurons that had been in culture for 3 days leads to a rapid and sustained increase in the phosphorylation of GSK-3β (Fig.44).

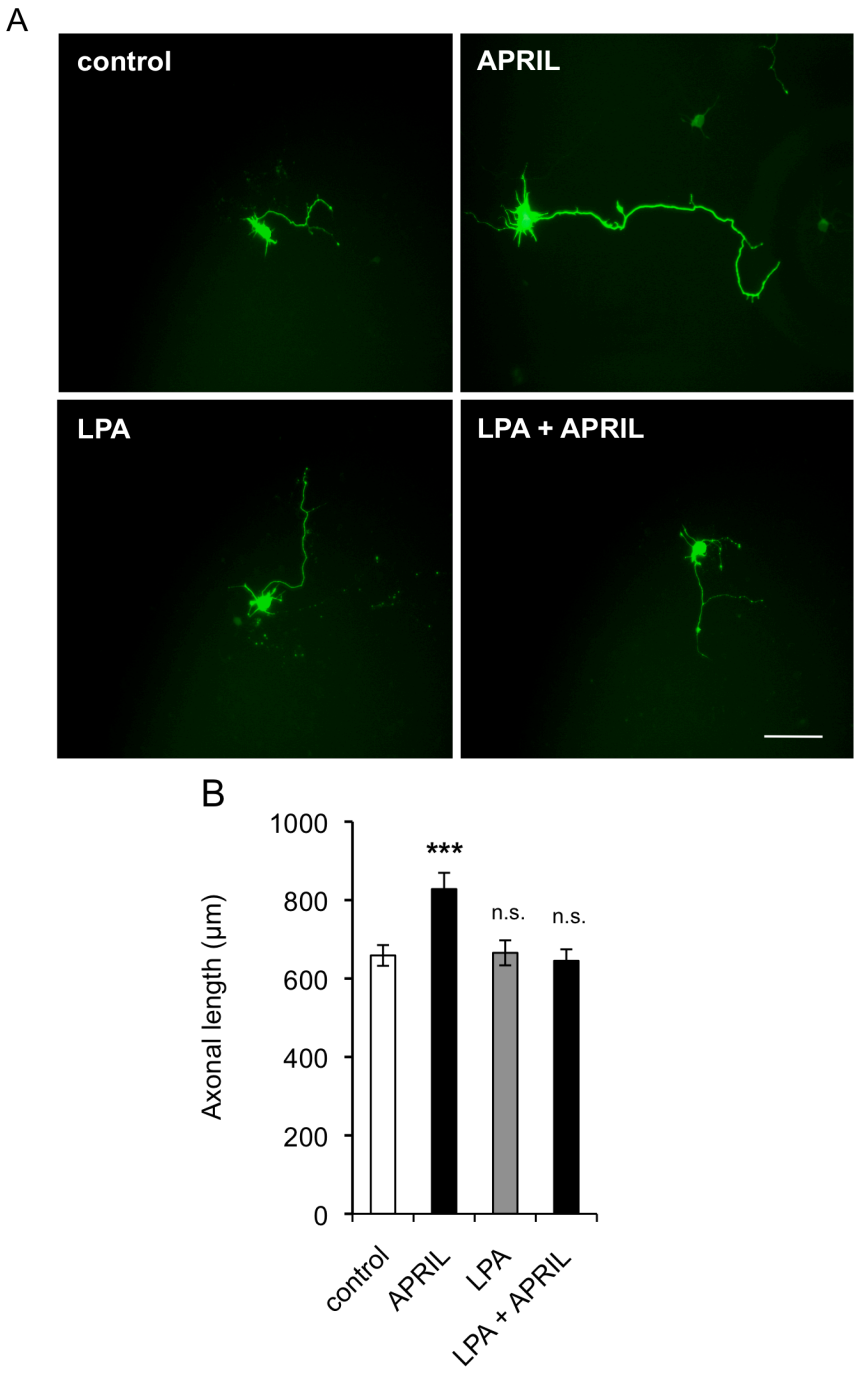

Figure 43: Enhancing GSK-3β kinase activity prevents APRIL-promoted axonal growth. E18 hippocampal neurons that had been cultured for 2DIVs were transfected with pCDH-CMV-MCS-EF1-copGFP prior to 2h incubation either in the presence or absence of 10µM LPA. Following this, neurons were cultured for a further 16h, either in the presence or absence of 100ng/ml of recombinant APRIL, before being fixed at 3DIVs, stained with an antibody against GFP and imaged under a fluorescence microscope. Images were analysed with ImageJ. (A) Representative photomicrographs of typical hippocampal neurons cultured under the stated conditions. Scale bar: 100µm. Graph corresponds to (B) mean of total axonal length. Data represent the mean and sem of 150 neurons for each condition from 3 separate experiments. ***indicates $p<0.0001$, statistical comparison with control, n.s. non-significant (Mann-Whitney U test).

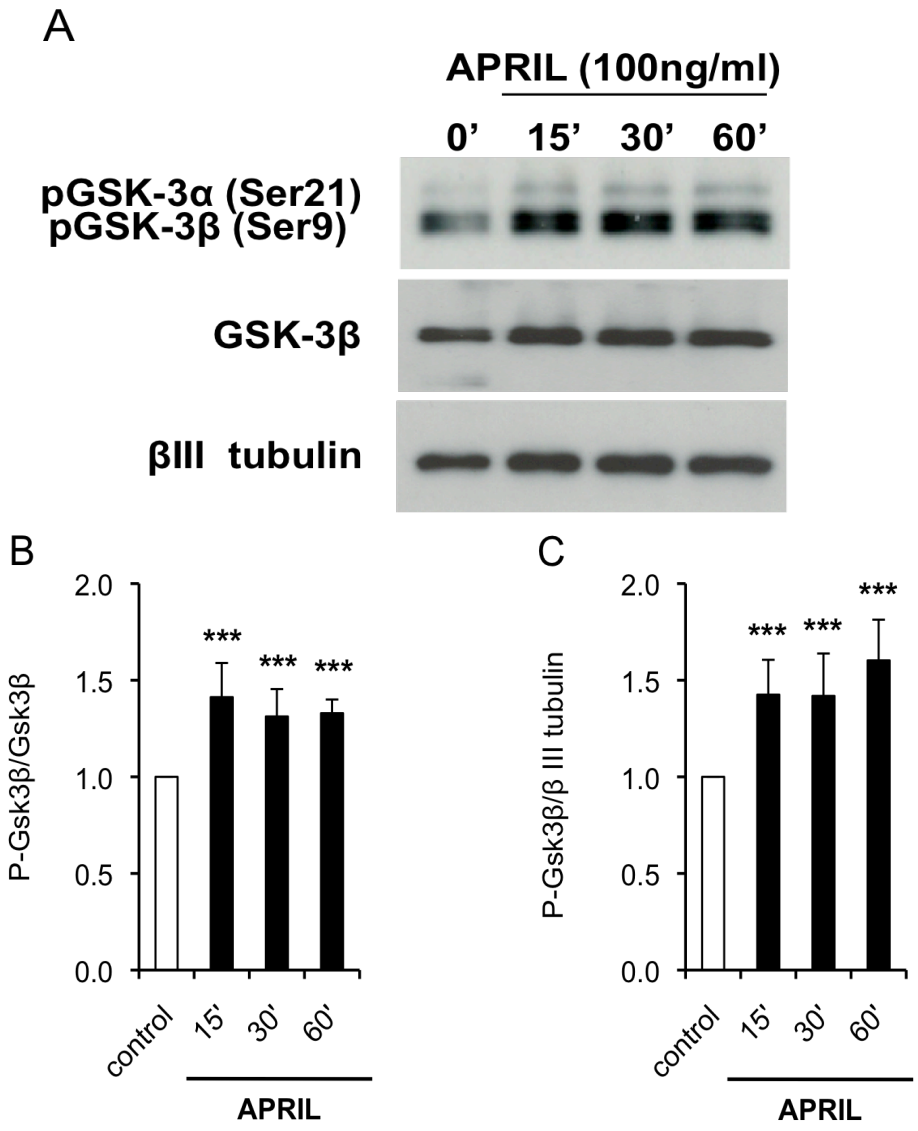

Figure 44: APRIL enhances the phosphorylation of GSK-3β.

E18 hippocampal neurons that had been cultured for 3DIVs were treated with 100ng/ml of recombinant APRIL for 15, 30 or 60min before being lysed. Western blots of lysates were probed with antibodies against GSK-3β, phospho-GSK-3 (recognises phosphorylated GSK-3α and GSK-3β) and β-III tubulin. (A) Representative scans of Western blots. Graphs correspond to densitometry measurements from films and show (B) P-GSK-3β/GSK-3β and (C) P-GSK-3β/β-III tubulin ratios. Data represent the mean and sem of 3 separate experiments. ***indicates $p<0.0001$, statistical comparison with control (Mann-Whitney U test).

4.4. Discussion

Novel roles for TNFSF members in the developing nervous system have recently been characterised. In particular, TNFSF members have been shown to regulate the elongation and branching of the processes of developing neurons from peripheral sensory and sympathetic ganglia[176-178,397]. TNFSF members have also been shown to either promote or inhibit neurite outgrowth from developing hippocampal and cortical neurons[166,240].

This chapter describes a novel role for APRIL in promoting axonal growth from cultured embryonic mouse hippocampal neurons. APRIL's ability to promote axonal growth is mediated by BCMA dependent activation of MAPK and PI3K/Akt/GSK-3β signal pathways. The co-expression of APRIL and BCMA in hippocampal neurons described in Chapter 3, together with the release of APRIL into the medium in hippocampal cultures, raised the possibility of autocrine and/or paracrine APRIL-BCMA signalling in these neurons. To investigate the potential significance of this signalling, the effect of exogenous recombinant APRIL was examined on neurite outgrowth from cultured embryonic hippocampal neurons. APRIL significantly increased hippocampal axon length in a dose-dependent manner. In addition to enhancing axonal outgrowth from E18 dissociated cultures of hippocampal neurons, APRIL also induced profuse axonal outgrowth from P0 explants of the hippocampal CA region (Fig.32 and 33). In contrast to its efficacy in promoting axonal growth, APRIL had no effect on the length or number of primary dendrites projecting from the soma of hippocampal neurons (Fig.34).

Since Chapter 3 demonstrated that the APRIL receptor, BCMA is expressed at much higher levels in the developing hippocampus than the alternative APRIL receptor, TACI, the role of BCMA was examined in mediating the axon growth enhancing effects of APRIL. BCMA overexpression mimicked the effect of adding recombinant APRIL to hippocampal cultures by increasing axon length, presumably by potentiating signalling by hippocampal neuron secreted APRIL. Adding recombinant

APRIL to neurons overexpressing BCMA did not further increase axonal length (Fig.35).

Overexpression of signalling deficient BCMA significantly decreased axonal length in the absence of exogenous APRIL and totally prevented recombinant APRIL from promoting axonal elongation (Fig.35). The reduction in axonal length in the absence of exogenous APRIL, may mean that expression of signalling deficient BCMA interferes with endogenous APRIL/BCMA autocrine/paracrine signalling, either by being incorporated into functional BCMA signalling trimers, thereby rendering them non-functional, or acting as a decoy receptor. Alternatively, the possibility exists that autocrine BAFF/BAFFR signalling may act in hippocampal cultures to promote axon elongation and mutant BCMA may sequester autocrine/paracrine released BAFF and interfere with this putative signalling loop. Taken together, these data indicate that BCMA mediates APRIL induced axonal growth from hippocampal neurons and suggests that endogenous autocrine and/or paracrine signalling normally plays a role in regulating the growth of hippocampal axons. APRIL autocrine/paracrine signalling has previously been described in other cell types. For example, APRIL confers resistance to apoptosis in B-CLL cells via an autocrine signalling route[378]. APRIL, BCMA and TACI are expressed by B-CLL leukemic cells and the addition of APRIL to cultures protects these cells from spontaneous, and flavopiridol induced apoptosis. In contrast, neutralizing APRIL-BCMA signalling, using either a soluble BCMA-Fc fusion protein or a function blocking APRIL antibody increases B-CLL cell death[378]. Similarly, Hodgkin lymphoma is initiated by the clonal expansion of malignant Hodgkin and Reed-Sternberg cells (HRS cells). HRS cells express APRIL, BAFF, BCMA and TACI and exogenous BAFF or APRIL enhances their survival and proliferation. Conversely, siRNAs against APRIL, BAFF, BCMA or TACI reduce the survival and proliferation of HRS cells, suggesting HRS cell expansion is as a result of autocrine/paracrine signalling between these TNFSF members and their receptors[398]. APRIL can also act as an autocrine growth factor during megakaryocytopoiesis, a developmental hematopoietic process responsible for progenitor cell differentiation to megakaryoblasts and megakaryocytes, leading to platelet formation[399]. APRIL, but not BCMA or TACI, is expressed in differentiating

megakaryocytes and cDNA driven overexpression of APRIL promotes increased proliferation of immature megakaryocytes in culture. In accordance with this, sequestering megakaryocyte produced APRIL with a TACI-Fc fusion protein reduces megakaryocyte expansion and reduces platelet formation in culture[399]. A similar approach of using soluble receptor-Fc fusion proteins or APRIL blocking antibodies would be useful in future experiments designed to further investigate APRIL-BCMA signalling in cultures of hippocampal neurons.

To assess the role of HSPGs in APRIL signalling, hippocampal neurons were cultured in medium containing a recombinant mutant APRIL (APRIL H89) that lacks 10 basic amino acids preceding the TNF homology domain and cannot bind HSPGs[341]. Surprisingly, mutant APRIL promoted robust axonal growth demonstrating that this cytokine does not require HSPGs for functional signalling in hippocampal neurons. However, unlike WT APRIL, APRIL H89 was not able to promote axon elongation at a concentration of 10ng/ml, suggesting that, although not necessary for APRIL signalling in hippocampal neurons, HSPGs may act to potentiate APRIL signalling (Fig.36). HSPGs play important roles in several biological processes in several tissue types, such as proliferation, cell adhesion, differentiation and cell migration. HSPGs can either be extracellular (example: perlecan or agrin) or plasma membrane bound (example: syndecans or glypicans) and can bind to growth factors, cytokines, proteases and proteases inhibitors[400,401]. Rat primary hippocampal neuron cultures have been shown to express agrin, glypican, syndican-3 and perlecan[402] and HSPGs have previously been shown to play a role in regulating the extent of process outgrowth from cultured hippocampal neurons[402,403]. For example, heparin promotes the polarization of cultured E18 rat hippocampal neurons and enhances the elongation of their axons. The Wnt signalling antagonist, Sfrp1 prevents heparin promoted axon elongation, suggesting that heparin stimulates axon growth by potentiating endogenous Wnt signalling[402]. Whilst soluble GDNF does not enhance neurite outgrowth from cultured E17 rat hippocampal neurons, immobilised GDNF dramatically increases the percentage of hippocampal neurons bearing processes in these cultures

through a signalling mechanism that does not require an interaction with cognate GDNF receptors, Ret and GFRα1[403]. The neurite growth promoting effects of immobilised GDNF are significantly reduced in the presence of heparinase III, suggesting that immobilised GDNF promotes neurite outgrowth by interacting with neuron expressed HSPGs. The HSPG that mediates immobilised GDNF signalling appears to be syndecan-3, since immobilised GDNF promotes neurite outgrowth from hippocampal cultures established from wild type E16 mouse embryos but not *syndecan-3* null mutant embryos. The data presented in this chapter suggest that, whilst HSPGs are not required for APRIL mediated promotion of axon elongation, they may enhance APRIL-BCMA signalling at low concentrations of APRIL. This is in line with previous data demonstrating that APRIL does not require HSPG binding to promote B-cell proliferation, but that binding to HSPGs enhances the multimerisation of APRIL and thereby potentiates its ability to signal through BCMA and TACI[404]. To further investigate the potential roles that HSPGs play in APRIL mediated promotion of axon growth, further experiments need to be performed to examine APRIL promoted axon elongation in cultures of hippocampal neurons supplemented with different heparinases.

To determine the intracellular signalling pathways that induce axon elongation following APRIL mediated activation of BCMA, several intracellular signalling pathways that have previously been linked to the regulation of neuronal process growth were investigated. ERKs have being widely described as signalling mediators that are important for regulating axonal growth. For instance, neurotrophins, netrin-1, Sema7A and members of the TNFSF induce axonal growth that is mediated by the phosphorylation, and hence activation, of ERKs[397,405-408]. ERK activation has also been directly linked to the regulation of axon microtubule dynamics. For example, MAP-2 is a substrate of ERK[409]. ERK signalling also regulates actin filament dynamics in the growth cones of sympathetic SCG neurons and blocking this signalling causes actin depolymerization and growth cone collapse[410]. Exactly how these processes are regulated is not yet well understood, but it is thought that ERK regulates local protein production within growth cones, thereby maintaining a balance between protein synthesis and degradation. Campbell

and Holt have shown that inhibiting ERK1/2 signalling blocks the synthesis of proteins such as netrin-1 and Sema3A that are necessary for growth cone guidance[411]. The importance of ERK signalling in regulating axon growth is further exemplified by the observation that specific targeting of ERK1/2 to the proteasome following distal axotomy or neurotrophic factor deprivation appears to play a role in regulating Wallerian degeneration and local axon pruning, respectively[412]. APRIL has previously been shown to activate ERK signalling in myeloma cells, thereby protecting them from dexamethasone induced apoptosis[360], and the ability of APRIL to increase the proliferation of cultured human adipose-derived stem cells is mediated by ERK activation[413]. The data in this chapter demonstrates that APRIL induces the phosphorylation and activation of ERK1/2, and suggests that ERK1/2 activation is essential for APRIL promoted growth of hippocampal neuron axons (Fig.38 and 39). However, one caveat of the data is that ERK1/2 activity was inhibited pharmacologically by the compound PD98059. Although PD98059 is claimed to be a specific inhibitor of MEK1/2, it is likely to have at least some off target affects. To confirm the essential role of ERK1/2 activation in APRIL promoted axon growth, further experiments should be performed using transfection of expression vectors encoding signalling deficient, dominant-negative ERKs. It is unclear at present how APRIL binding to BCMA leads to the induction of ERK1/2 signalling in hippocampal neurons. In a human kidney cell line, BCMA associates with TRAF1, 2 and 3 and these adaptor proteins mediate the activation of the p38 and JNK, but not ERK1/2, MAPK pathways[390]. The association of BCMA with TRAFs has not been verified in the nervous system, but the possibility clearly exists that APRIL binding to hippocampal neuron BCMA induces the association of TRAFs with BCMA and, ERK1/2 is activated as a result of this association. Further investigation is required to determine which, if any, TRAFs can associate with ligand bound BCMA in hippocampal neurons and whether TRAFs are an essential mediator of APRIL induced ERK1/2 activation and axonal growth. One way this could be addressed would be by analysing axon length in cultures of hippocampal neurons transfected with cDNA expression constructs coding for either GFP together with WT BCMA or GFP together with mutated versions of BCMA that lack TRAF binding sites. Transfection of hippocampal

neurons with expression vectors encoding either WT or DN TRAFs would also be informative. In addition to characterising the upstream signalling pathways that lead to APRIL mediated ERK1/2 activation, it would also be interesting to identify the downstream targets of activated ERK1/2 and determine how they contribute to APRIL promoted axonal elongation.

In addition to investigating whether ERK1/2 activation mediates APRIL promoted axonal growth in hippocampal cultures, the experiments in this chapter also aimed to determine whether PI3K/Akt signalling plays a role in transducing the growth enhancing properties of APRIL. APRIL has previously been reported to activate PI3K in myeloma cells[360], B-cell lymphoma[414] and human adipose-derived stem cells[413]. The PI3K signalling pathway is well established as being crucial for nervous system development, in particular with respect to axonal and dendritic morphogenesis[415]. Neurotrophins have been shown to activate the PI3K signalling pathway in a number of different neuron types. For example, NGF-induced PI3K activity at the growth cone promotes rapid axon growth through the inactivation of GSK-3β in cultured mouse DRG neurons[416]. BDNF binding to exogenously expressed TrkB in sympathetic neurons promotes sympathetic neuron survival and axonal growth by stimulating PI3K activity[405]. The pharmacologic inhibition of PI3K activity using LY294002 was shown to prevent APRIL-mediated axon elongation, thereby identifying PI3K as an essential signalling molecule for APRIL promoted axon growth (Fig.40). However, once again the data comes with the limitation that PI3K activity was inhibited pharmacologically by the compound LY294002. Although LY294002 is claimed to be a specific inhibitor of PI3K, it is likely to exert at least some inhibitory activity on other closely related kinases. To confirm the essential role of PI3K activity in APRIL promoted axon growth, further experiments should be performed using transfection of expression vectors encoding signalling deficient, dominant-negative PI3K.

Downstream of activated PI3K, several other kinases are phosphorylated to regulate different aspects of axonal growth. One of these kinases is the serine/threonine kinase, Akt. Overexpression of Akt is sufficient to induce the formation of multiple axons from cultured embryonic rat

hippocampal neurons[417] and enhance the regeneration of axotomized adult rat hypoglossal motor neurons[418]. In agreement with these observations, pharmacological inhibition of Akt prevented APRIL from promoting axon growth in cultures of E18 mouse hippocampal neurons and the addition of APRIL to these cultures induced a rapid and sustained phosphorylation of Akt (Fig.41 and 42). Curiously, the use of pharmacological inhibitors for MEK (PD98059), PI3K (LY294002) or AKT (Akt inhibitor) did not affect axonal outgrowth in the absence of exogenous APRIL. Baseline axonal growth should be affected by these inhibitors, given the fact, that, axonal growth appears to be dependent on ERK and PI3K/Akt signalling pathways (395) and dense cultures of hippocampal neurons are likely to be secreting a number of axon growth promoting trophic factors. This anomaly can perhaps be explained by the use of sub-optimal concentration of signalling inhibitors. Dose response analysis of the ability of each inhibitor to inhibit axon growth should have been performed.

GSK-3β is one of the downstream targets of activated Akt. GSK-3β, an isoform of GSK-3, is a serine/threonine kinase that regulates tubulin polymerization and microtubule stability by phosphorylating several microtubule associating proteins[395,416,417]. A second GSK-3 isoform, GSK-3α appears to have a similar function to GSK-3β, and both are localized in axon growth cones[395]. Curiously, despite the wealth of data implicating GSK-3β as an important regulator of axon growth, *Gsk-3β* null mice do not display obvious differences in neuronal development or axonal growth, presumably because of a functional redundancy with GSK-3α[419]. However, the use of GSK-3 inhibitors or shRNA directed against both GSK-3α and 3β isoforms blocks neurotrophin-induced axonal growth from both DRG and hippocampal neurons[109,419,420]. PI3K/Akt mediated phosphorylation of GSK-3β on serine residue 9 has been shown to result in the inactivation of GSK-3β activity, increased microtubule stability and enhanced axon growth[109,416,417]. LPA is a known activator of GSK-3β activity[396]. The addition of LPA to hippocampal cultures prevents APRIL from promoting axonal growth (Fig.43), suggesting that the activation of PI3K/Akt signalling by APRIL increases axon elongation by inhibiting GSK-3β activity. Further support for this hypothesis comes from

the observation that the addition of APRIL to hippocampal neuron cultures leads to the rapid and sustained phosphorylation of GSK-3β and, therefore, its inactivation (Fig.44).

Whilst the data in this chapter suggest that APRIL promotes axonal elongation by a mechanism that involves the sequential activation of PI3K and Akt followed by Akt mediated phosphorylation and inactivation of GSK-3β, it is not clear how the binding of APRIL to BCMA results in the phosphorylation and activation of PI3K. There are some clear avenues to explore in future studies. For example, activated Trk receptors recruit growth factor receptor-bound protein 2 (Grb2) that in turn recruits PI3K, leading to its phosphorylation[421]. In the case of TNFRSF members, an interaction between ligand bound TNFR1 and Grb2 has been shown to be essential for the activation of c-Raf-1 kinase and subsequently ERK1/2[422]. Therefore, Grb2 may be a possible link between ligand bound BCMA and the activation of either ERK1/2 or PI3K pathways. Interestingly, ERK1/2 activation appears to mediate the phosphorylation of GSK-3β in PC12 cells and neonatal rat SCG neurons[423]. It would be interesting to analyse whether blocking ERK1/2 activation and/or PI3K/Akt activity, prevents the phosphorylation of GSK-3β in hippocampal neurons following the addition of recombinant APRIL. Although activating GSK-3β by the addition of LPA to cultures prevents APRIL from increasing axonal growth and possible phosphorylation and inactivation of GSK-3β, an essential role for GSK-3β inactivation in APRIL promoted outgrowth needs to be confirmed. Further experiments need to be performed to determine whether transfection of a constitutively active GSK-3β, were serine 9 is replaced by alanine, can prevent APRIL from increasing the length of cultured hippocampal neuron axons[424].

Taken together, the results presented above define a novel neurotrophic role for APRIL in the developing nervous system. APRIL promotes the elongation of cultured embryonic mouse hippocampal neuronal axons by a signalling mechanism that involves the activation of ERK1/2 and PI3K/Akt signalling pathways and the subsequent phosphorylation and inhibition of GSK-3β.

Chapter 5

GDF-5, BMPR-Ib and BMPR-II expression in the developing hippocampus

5.1. Introduction

The TGF-β superfamily member GDF-5 initially received particular interest because spontaneous frameshift mutations in the *Gdf-5* gene result in brachypodism (*bp*) in mice[425]. These mice have a normal axial skeleton (skull and rib cage) but have numerous alterations in the appendicular skeleton (lower and upper limbs). Skeletal abnormalities include shortening of limbs and feet, reduction of the number of bones in digits, abnormal joint formation within the limbs and sternum. Moreover, chromosome mapping of GDF-5 showed a physical proximity with a locus on mouse chromosome 2 that had previously been linked to brachypodism. In *Gdf-5*^{bp} mice, spontaneous frameshift mutations in the *Gdf-5* gene create a translational stop codon in the prodomain of the peptide that prevents the translation of the mature and bioactive form of GDF-5[425]. Mutations in the human homologue of GDF-5, cartilage-derived morphogenetic protein (CDMP1), leads to at least three different skeletal displasias. Brachydactyly type C is an autosomal dominant condition whereby heterozygous mutations in the *Cdmp1* gene are sufficient to cause the shortening or absence of phalanges[426]. Homozygous mutations in the *Cdmp1* gene result in more severe conditions, namely Hunter-Thompson type (CHTT) and Grebe type I (CGT) chondrodysplasias. CHTT is similar in appearance to the phenotype of *Gdf-5*^{bp} mice and is characterized by under developed bones in hands, feet, ankles and wrists and joints dislocations[427]. CGT is an autosomal recessive disorder that is characterised by severe limb shortening. In CGT, the bones of the hands and feet are particularly severely affected and fingers and toes lack articulation. Whilst CHTT is a consequence of mutations in the *Cdmp1* gene that result in truncation of the CDMP1 protein, CGT is caused by missense mutations in the *Cdmp1* gene that result in a single amino acid substitution in CDMP1 and impaired secretion of the protein from cells[428]. Mice that are deficient for the GDF-5 type I receptor, *Bmpr-Ib* (also known as *Alk-6*) show a similar phenotype to *Gdf-5*^{bp} mice. In addition, *Bmpr-Ib* null mice, display reduced proliferation of prechondrogenic cells in the phalanges as well as impaired chondrocyte differentiation[429].

The distinct phenotypes of *Gdf-5*^{bp} and *Bmpr-Ib* null mice are consistent with a role for GDF-5 in the developing appendicular skeleton. *In situ*-hybridization on embryonic mouse tissues has shown that GDF-5 mRNA is expressed at its highest levels within developing limbs at the sites of developing elbow and shoulder joints and at the site of future joints between the metacarpals and the proximal phalanges[430]. GDF-5 is involved in regulating cartilage formation, normal joint development and in determining the correct positioning of joints[431]. GDF-5 does this, in part, by accelerating the initial steps of chondrogenesis by increasing cell adhesion. In addition, GDF-5 regulates chondrogenic and osteogenic differentiation during later stages of skeletal development[432], thereby inducing the formation of cartilage, bone[433], tendon, ligaments[434] and teeth[435]. Similarly, the GDF-5 receptors, BMPR-Ia (also known as ALK-3) and BMPR-Ib are expressed during early chondrogenesis and play important roles in chondrocyte proliferation, survival, and differentiation *in vivo*[429,436]. Transgenic mice with a null mutation in both *Bmpr-Ia* and *Bmpr-Ib* have severe chondrodysplasia with flattened thoracic cavities and shortened limbs. These mice display impaired chondrocyte differentiation, reduced proliferation and increased apoptosis of chondrocytes and disorganization of cartilage elements due to a lack of cartilage-specific extracellular matrix[429,436]. GDF5-induced chondrogenesis is negatively regulated by the tyrosine kinase, Ror2. This kinase forms a heterodimeric complex with BMPR-Ib that results in the suppression of Smad signalling and the activation of non-Smad signalling pathways[437]. The GDF-5 type II receptor, BMPR-II is required for many different aspects of embryonic development and mice with a germ line-null mutation of the *Bmpr-II* gene die during gastrulation[301]. Mutant mice lacking part of the extracellular domain of *Bmpr-II* survive to mid-gestation and display delayed ossification of bones, rib loss and impairment of limb development[438]. However, the main defects observed in these mutants are cardiovascular in nature and include abnormalities of heart septation, interruption of the aortic arch and the absence of semilunar valves[438]. BMPR-II is expressed in pulmonary artery endothelial cells and mutations in the human gene, *Bmpr-II* are the basis of primary pulmonary hypertension (PPH), a vascular disease that is caused by increased proliferation of endothelial and smooth muscle cells in the

pulmonary arteries[439]. Furthermore, GDF-5 has angiogenic activity, inducing the formation of capillary-like structures in collagen gels *in vitro* and rabbit cornea *in vivo*[440].

GDF-5 and its receptors are also expressed in the nervous system. GDF-5 enhances the survival promoting effects of NGF and NT-3 in cultures of DRG neurons[441]. Moreover, in the presence of NGF and cell adhesion molecules, GDF-5 synergistically increases neurite outgrowth from cultured chick DRG neurons[442]. GDF-5 is widely expressed in the developing and adult brain in regions such as cortex, midbrain, striatum and cerebellum[443]. Most studies on the roles of GDF-5 in the CNS have been focused on the therapeutic potential of GDF-5 in the midbrain, particularly in Parkinson's disease. The neurotrophic potential of GDF-5 has been demonstrated by its ability to enhance the survival and differentiation of embryonic midbrain dopaminergic neurons *in vitro*[444]. Intra-striatal or intra-nigral injection of GDF-5 preserves nigral dopaminergic cell bodies, restores dopamine levels in the injured striatum and significantly reverses the behavioral consequences of 6-hydroxydomamine (6-OHDA) treatment in rats that have been subjected to the 6-OHDA partial lesion model of Parkinson's disease[445]. GDF-5 pre-treatment enhances the survival of mesencephalic grafts and their ability to compensate for 6-OHDA lesions in the same rat Parkinson's disease model to the same extent as GDNF pre-treatment of graft tissue[446]. Moreover, transplantation of CHO cells that overexpress GDF-5 has a neuroprotective and a neurorestorative effect in a rat 6-OHDA model of Parkinson's disease[447]. BMPR-Ia, BMPR-Ib and BMPR-II have all been shown to be expressed in the developing rodent nervous system and the adult rat brain[448-450]. Whilst BMPR-Ia, BMPR-Ib and BMPR-II proteins are detected in many kinds of axons in the adult rat brain, BMPR-Ib appears to be preferentially expressed in dendrites and BMPR-Ia is more highly expressed in neuronal cell bodies. All three BMP receptors are expressed in the adult hippocampus and also expressed by astrocytes[449,450].

5.2. Aims

The experimental aim of this chapter was to quantify the expression of GDF-5, BMPR-Ib and BMPR-II mRNAs and proteins in the developing hippocampus and to localise the expression of GDF-5 and its receptors, both within the hippocampus as a whole and within individual hippocampal neurons.

5.3. Results

5.3.1. The expression of GDF-5, BMPR-Ib and BMPR-II mRNAs in the developing mouse hippocampus and cultured E18 hippocampal neurons

Reverse transcriptase real-time PCR was used to determine the relative levels of GDF-5, BMPR-Ib and BMPR-II mRNAs in total RNA extracted from hippocampi dissected at different developmental ages from E18 to P10 and from adult mice. GDF-5 mRNA levels increase 2.5-fold from E18 to reach a peak at P0. After this peak, the levels of GDF-5 mRNA fall by 7.5-fold between P0 and P10 and a further 15-fold between P10 and adult (Fig.46.A). BMPR-Ib transcript levels in the developing hippocampus increase 5-fold from E18 to reach a maximum at P10. The amount of BMPR-Ib mRNA expressed in the adult hippocampus is approximately 40% lower than that at P10 (Fig.46.B). There is little change in the amount of BMPR-II mRNA expressed in the developing hippocampus between E18 and P10; however, there is an approximately 40% increase in BMPR-II transcript levels in the hippocampus between P10 and adult (Fig.46.C).

The levels of GDF-5, BMPR-Ib and BMPR-II mRNAs expressed in the adult mouse hippocampus were compared to those expressed in total RNA extracted from E18 mouse midbrain, thymus and aorta, as these tissues have previously been shown to express GDF-5 and its receptors[426,440,451]. As shown in Fig.46.D, the levels of GDF-5 mRNA expressed in adult mouse hippocampus are approximately the same as in E18 mouse midbrain, lower than in the E18 mouse thymus and much higher than in E18 mouse aorta. In contrast, BMPR-Ib transcripts are expressed at slightly higher levels in the adult mouse hippocampus compared to E18 mouse midbrain. E18 mouse

aorta and thymus express negligible levels of BMPR-Ib mRNA (Fig.46.E). The comparative levels BMPR-II mRNA expressed in the adult hippocampus and the other tissues analysed are almost identical to BMPR-Ib mRNA (Fig.46.F).

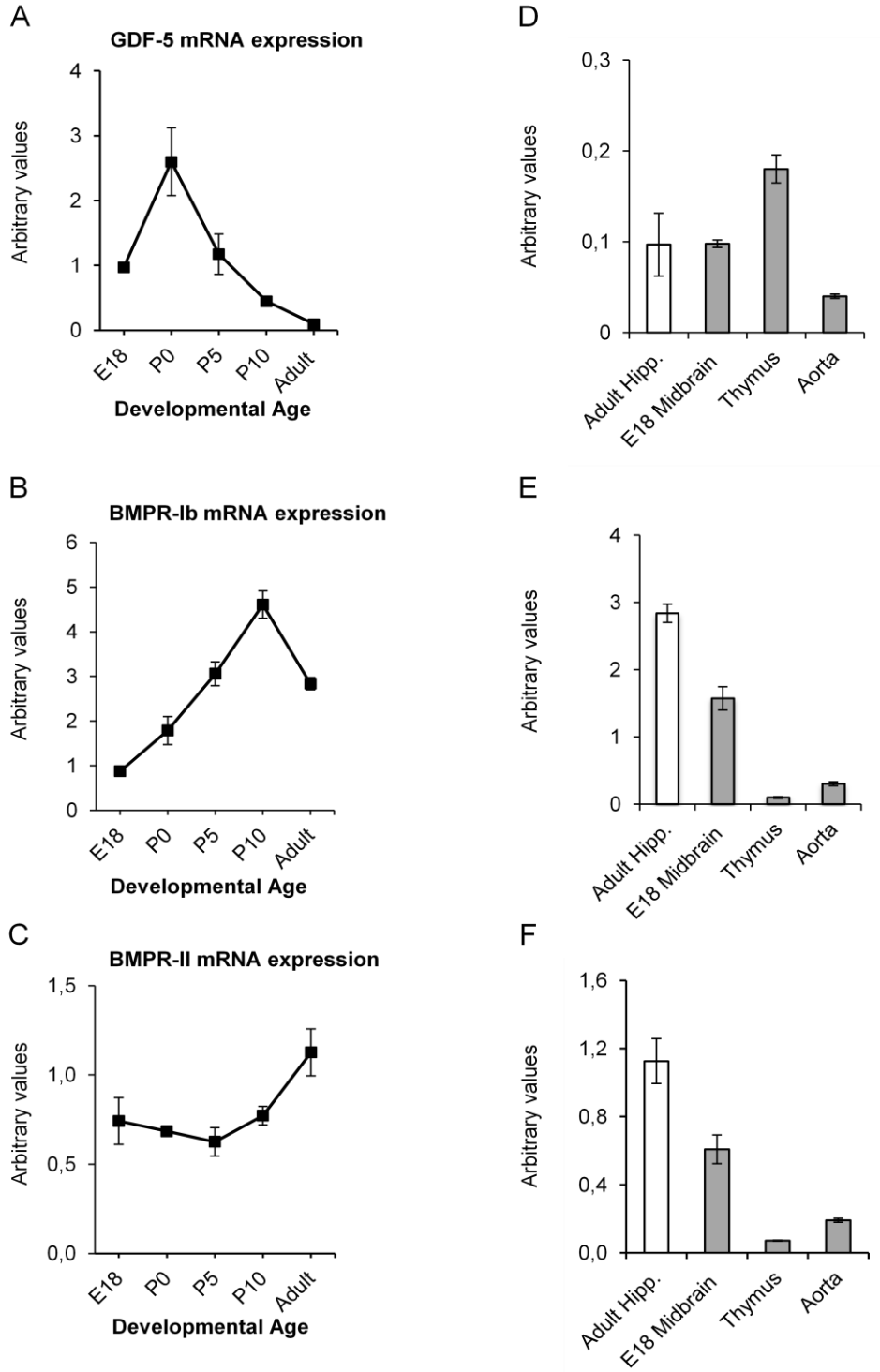

Figure 46: Relative expression of GDF-5, BMPR-Ib and BMPR-II mRNAs in the developing and adult mouse hippocampus. Total RNA was extracted from E18, P0, P5, P10 and adult mouse hippocampi, E18 mouse midbrain, thymus and aorta. Reverse transcriptase real-time PCR was used to quantify the levels of GDF-5, BMPR-Ib and BMPR-II transcripts and the levels of these mRNAs are expressed relative to the mRNAs encoding the reference genes GAPDH and SDHA. Graphs show (A) GDF-5, (B) BMPR-Ib and (C) BMPR-II mRNA expression at different developmental ages. (D) GDF-5, (E) BMPR-Ib and (F) BMPR-II mRNA expression levels in adult mouse hippocampus compared with E18 mouse midbrain, thymus and aorta. Data represent the mean and sem of four separate samples.

Reverse transcriptase real-time PCR was also used to examine the expression of GDF-5, BMPR-Ib and BMPR-II mRNAs in E18 hippocampal cultures after 2 hours (0DIVs), 2, 5 and 7 days in culture. GDF-5 mRNA expression levels initially fall by approximately 50% over the first two days in culture, but remain constant between 2 and 7DIVs (Fig.47.A). In contrast, whilst BMPR-Ib transcript levels also drop by approximately 50% over the first two days in culture, cultured hippocampal neurons increase their expression of this mRNA by almost 2-fold between 2DIVs and 7DIVs (Fig.47.B). The levels of BMPR-II mRNA expressed by cultured E18 hippocampal neurons remain fairly constant throughout the 7 days culture period (Fig.47.C).

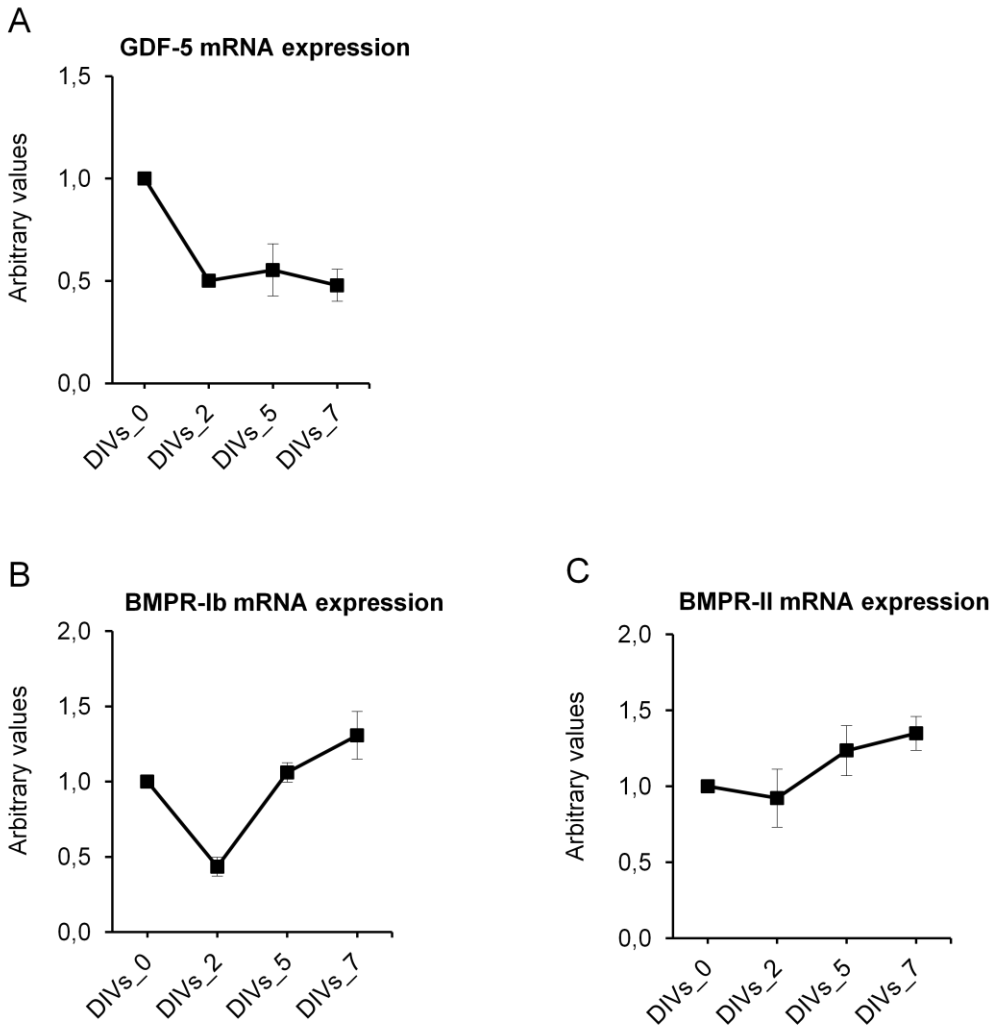

Figure 47: Relative levels of GDF-5, BMPR-Ib and BMPR-II mRNAs expressed by cultured hippocampal neurons. Total RNA was extracted from E18 hippocampal cultures after 2h (0DIV) and 2, 5 and 7DIVs. The levels of (A) GDF-5, (B) BMPR-Ib, and (C) BMPR-II mRNAs are expressed relative to the mRNAs encoding the reference genes GAPDH and SDHA. Data represent the mean and sem of four separate experiments.

5.3.2. The expression of GDF-5, BMPR-Ib and BMPR-II proteins in the developing mouse hippocampus

To assess the levels of GDF-5, BMPR-Ib and BMPR-II protein in the developing hippocampus Western blotting was performed on lysates of E18, P0, P5 and P10 hippocampi. Lysates of E18 midbrain were used as a positive control, since the embryonic rodent midbrain has previously been shown to express GDF-5 and its receptors and GDF-5 is a neurotrophic factor for embryonic midbrain neurons *in vitro*[443,444,448,450]. GDF-5 protein is expressed at a similar level to E18 midbrain in E18, P0, P5 and P10 hippocampus. Two immunoreactive bands, of approximately 27KDa and 58KDa, are present in midbrain and hippocampal lysates corresponding to mature and precursor forms of GDF-5, respectively (Fig.48.A). A 57KDa immunoreactive band corresponding to BMPR-Ib is present in the lysates from E18 midbrain and E18 to P10 hippocampus. Whilst BMPR-Ib expression in the hippocampus appears to be lower at E18 than in the E18 midbrain, hippocampal expression of BMPR-Ib increases with age, so that by P10 the hippocampus expresses comparable levels of BMPR-Ib to the E18 midbrain (Fig.48.B). In contrast, BMPR-II (115KDa) is expressed at higher levels in the E18 hippocampus than the E18 midbrain and BMPR-II expression in the developing hippocampus appears to decrease slightly with age (Fig.48.C).

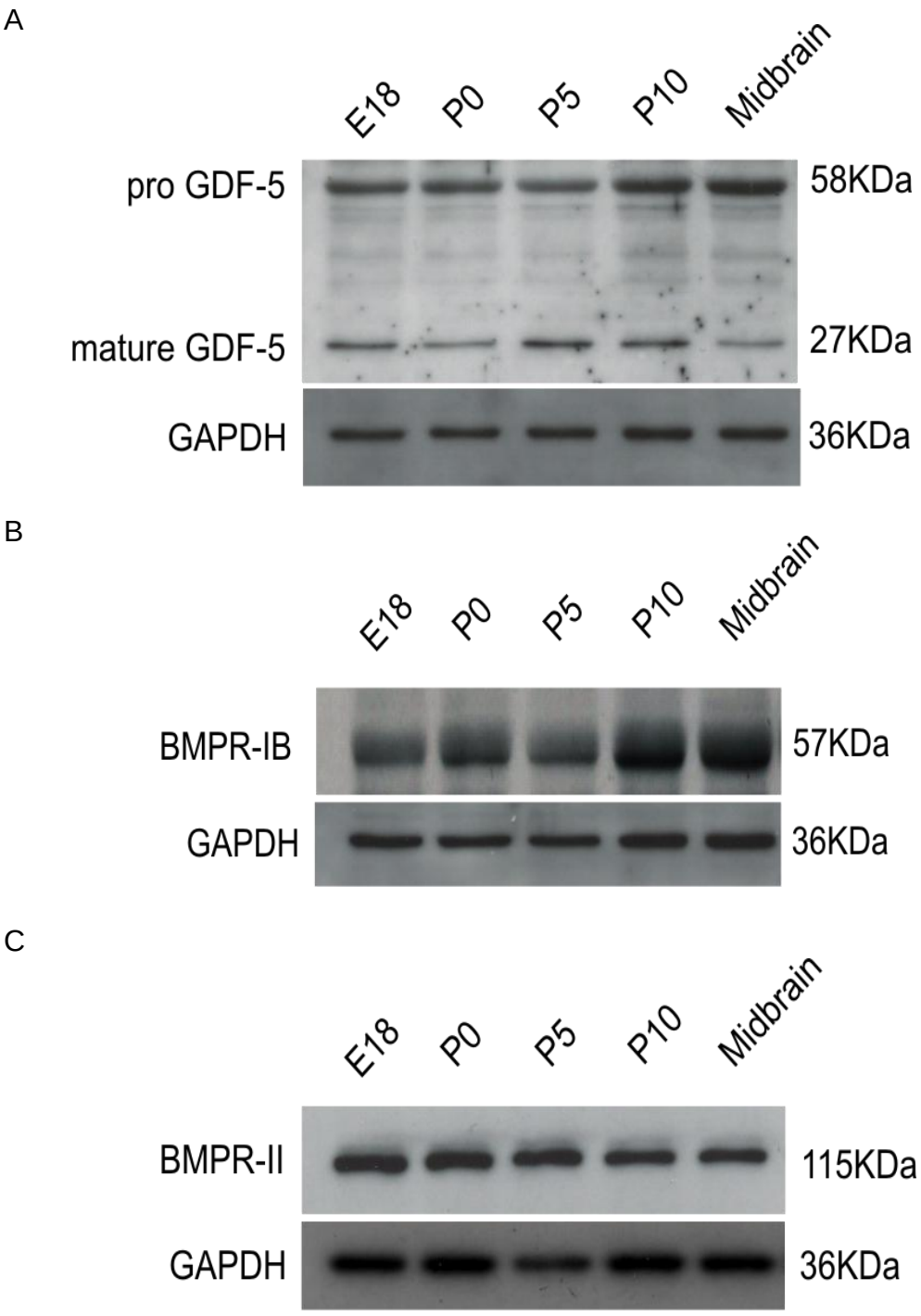

Figure 48: GDF-5, BMPR-Ib and BMPR-II protein expression in the developing hippocampus. Western blots of E18, P0, P5 and P10 hippocampus and E18 midbrain lysates were probed with antibodies against GDF-5, BMPR-Ib and BMPR-II. Panels show (A) mature (27kDa) and pro- (58KDa) GDF-5, (B) 57KDa BMPR-Ib and (C) 115KDa BMPR-II. GAPDH (36KDa) was used as an endogenous loading control.

5.3.3. Cellular localisation of GDF-5, BMPR-Ib and BMPR-II proteins in cultured pyramidal neurons

To determine the cellular location of GDF-5 and its receptors, E18 hippocampal neurons that had been cultured for 6DIVs were transfected with pCDH-CMV-MCS-EF1-copGFP, cultured for a further 24 hours and then fixed. Fixed neurons were labeled with antibodies that recognize either GDF-5, BMPR-Ib or BMPR-II. Neurons were also double-labelled with an antibody against MAP-2[452] and nuclei were stained with DAPI. GDF-5 is mainly present in the cell soma of pyramidal neurons but weak staining is also observed the dendrites (Fig.49.A). Both GDF-5 receptors were distributed in the cell soma as well as in the dendrites (Fig.49.B and C). Negative controls are shown in Fig.49.D.

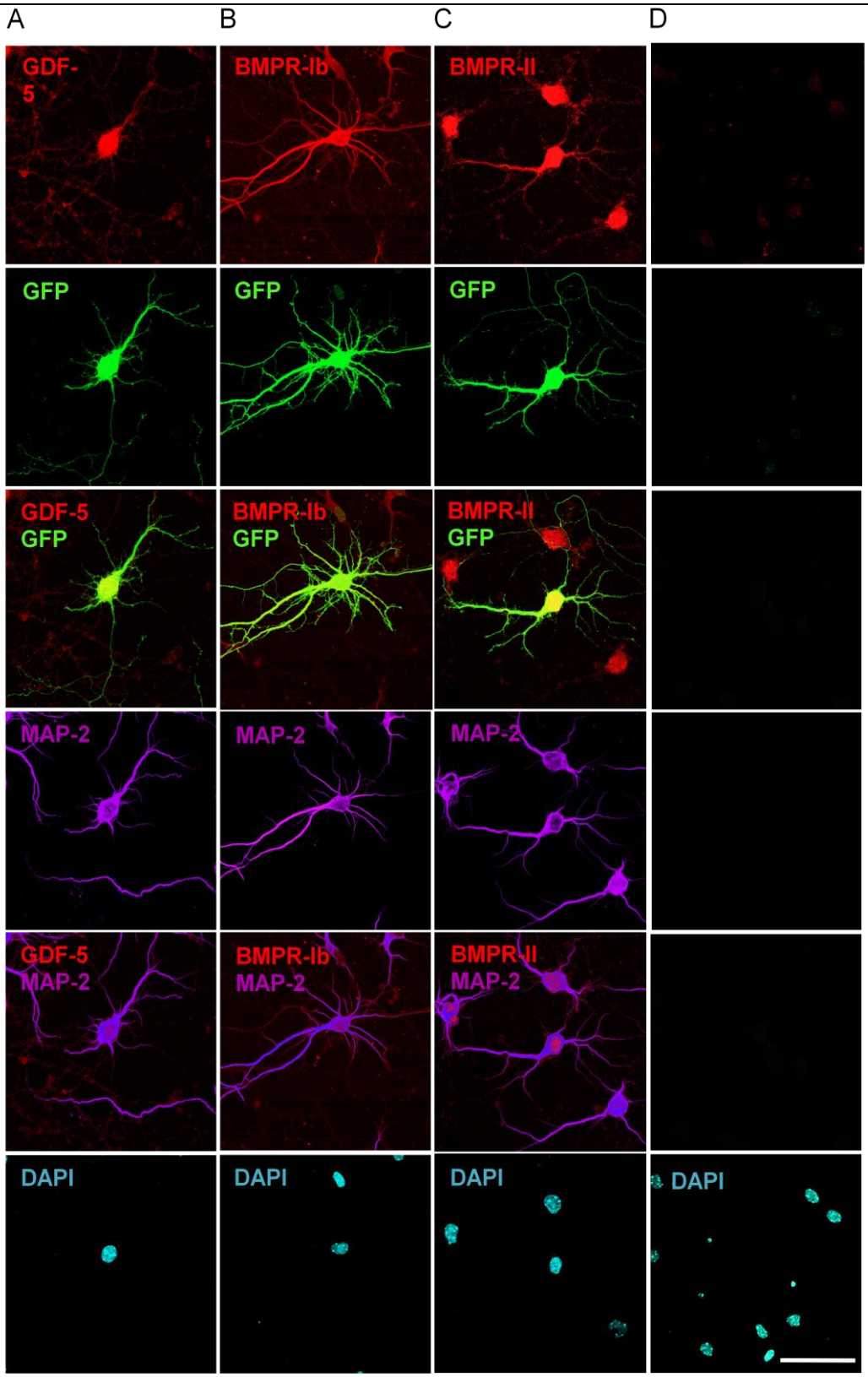

Figure 49: The cellular location of GDF-5, BMPR-Ib and BMPR-II proteins in 7DIVs hippocampal neurons. Hippocampal neurons were transfected with pCDH-CMV-MCS-EF1-copGFP (green) at 6DIVs and fixed 24h later. Fixed neurons were stained with antibodies against (A) GDF-5, (B) BMPR-Ib, (C) BMPR-II (all red) or (D) no primary antibody, as well as antibodies for the dendritic marker MAP-2 (purple) and nuclear marker DAPI (blue). Scale bar: 20μm.

5.3.4. Localisation of GDF-5, BMPR-Ib and BMPR-II proteins in the developing hippocampus

To study the distribution of GDF-5, BMPR-Ib and BMPR-II proteins in the developing hippocampus immunohistochemistry was performed on frozen sections cut from E18, P0, P5 and P10 mouse brains. Hippocampal sections were triple stained with the nuclear marker TOTO-3, the dendrite marker anti-MAP-2 and either anti-GDF-5, anti-BMPR-Ib or anti-BMPR-II.

GDF-5 expression is distributed in the CA area of the hippocampus and in the granule cell layer of the DG. Immunoreactivity is weak at E18, but increases as the hippocampus matures between P0 and P10. GDF-5 protein is detected in both CA1 and CA3 areas and localises mainly within cell soma in the stratum pyramidale (Fig.50). Like GDF-5, BMPR-Ib and BMPR-II are both expressed at all ages in the developing hippocampus and expression increases with age (Fig.51 and 52). However, compared to GDF-5, BMPR-Ib and BMPR-II are only expressed at low levels in the granule cell layer of the DG and mostly in the suprapyramidal blade. Both receptors are expressed in the cell soma within the stratum pyramidale but, unlike GDF-5, they also colocalise with MAP-2 staining, and hence the dendrites of pyramidal neurons.

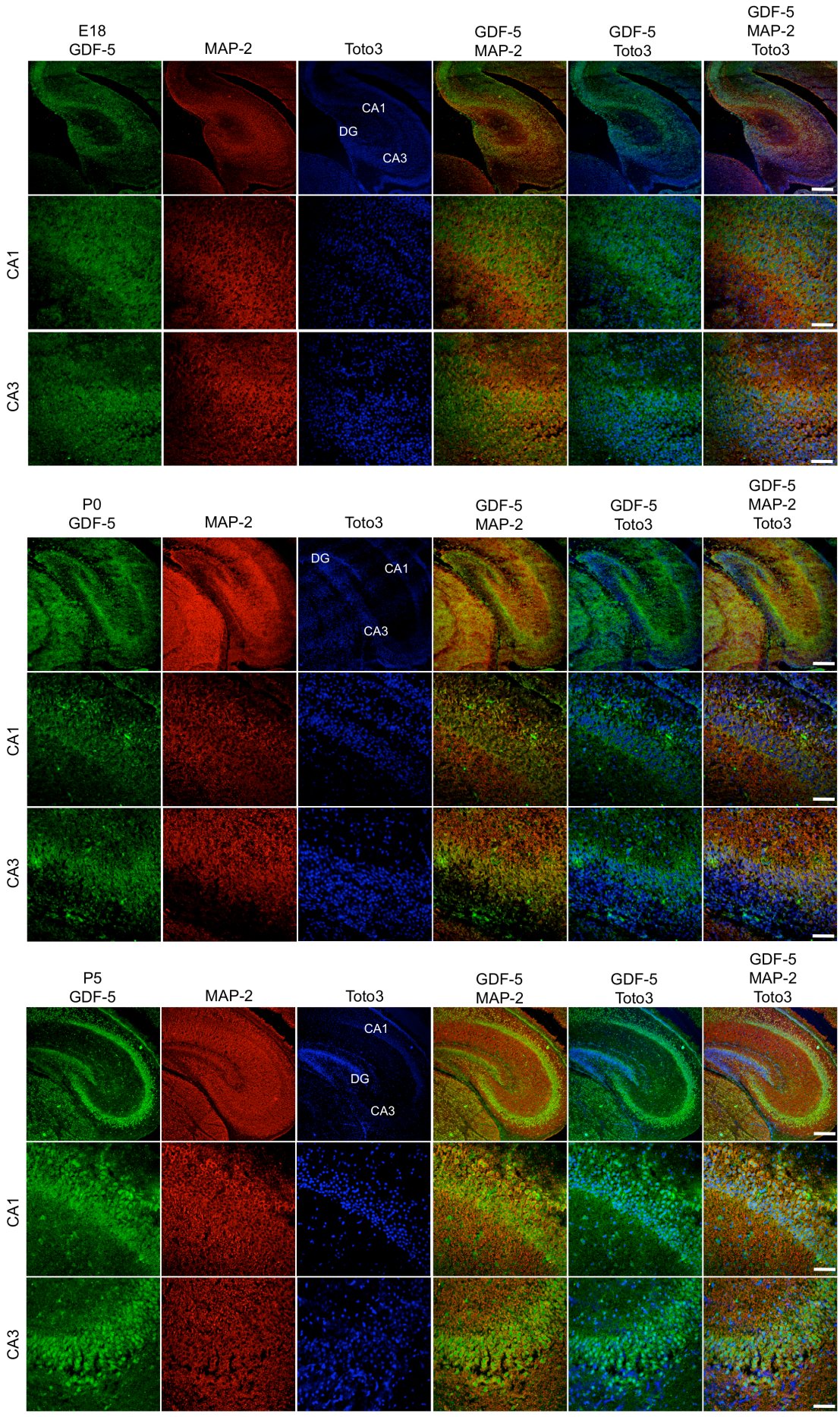
E18
GDF-5
MAP-2
Toto3
GDF-5
MAP-2
GDF-5
Toto3
GDF-5
MAP-2
Toto3
CA1
DG
CA3
CA1
CA3
P0
GDF-5
MAP-2
Toto3
GDF-5
MAP-2
GDF-5
Toto3
GDF-5
MAP-2
Toto3
DG
CA1
CA3
CA1
CA3
P5
GDF-5
MAP-2
Toto3
GDF-5
MAP-2
GDF-5
Toto3
GDF-5
MAP-2
Toto3
CA1
DG
CA3
CA1
CA3

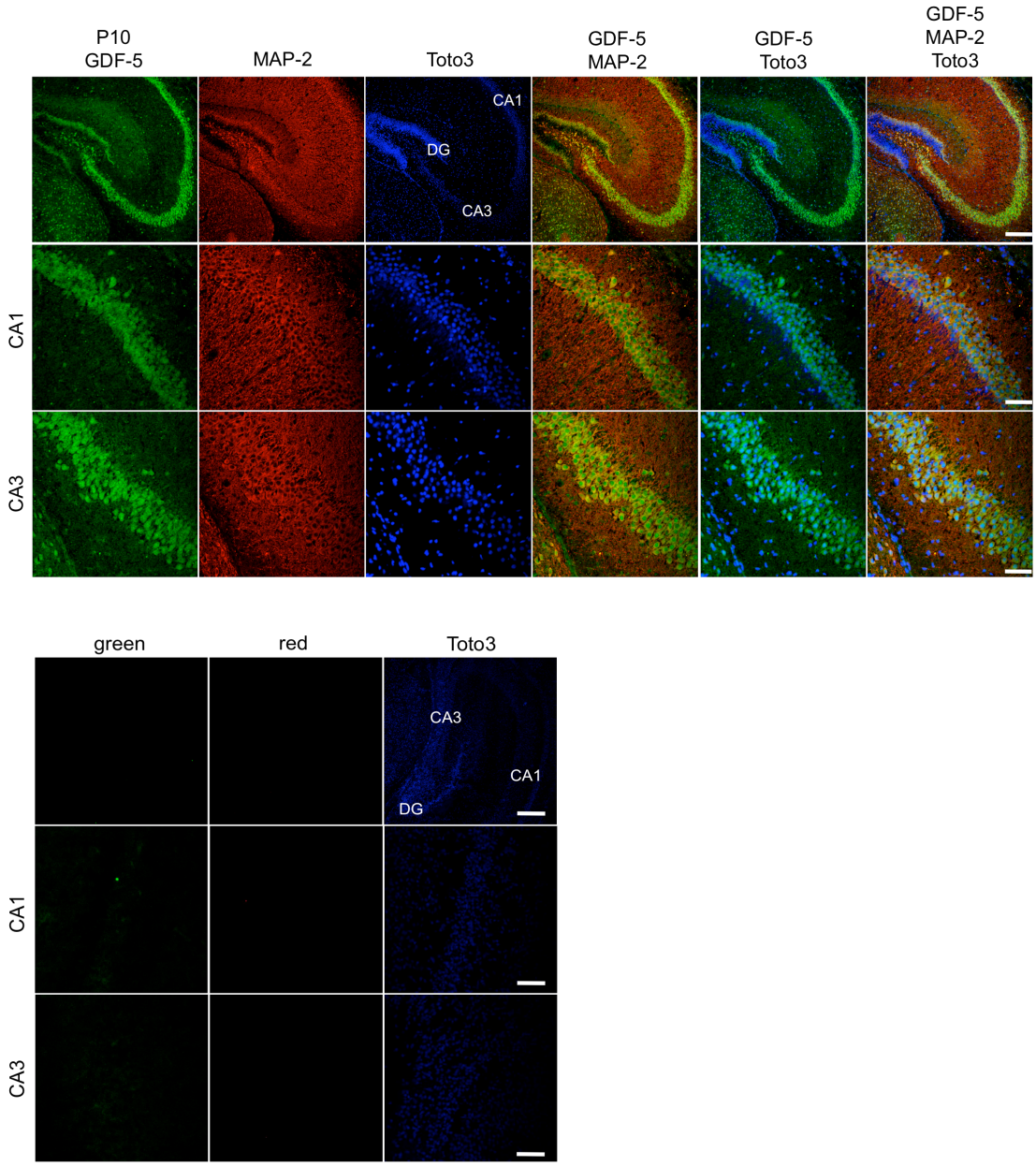

Figure 50: GDF-5 distribution in the developing hippocampus.

E18, P0, P5 and P10 hippocampal sections were stained for GDF-5 (green), MAP-2 (red) and TOTO-3 Iodide (blue). (DG: dentate gyrus; CA1 and CA3 layer). Last panel shows staining in the absence of primary antibodies. Scale bar: low magnification 200μm and high magnification 50μm.

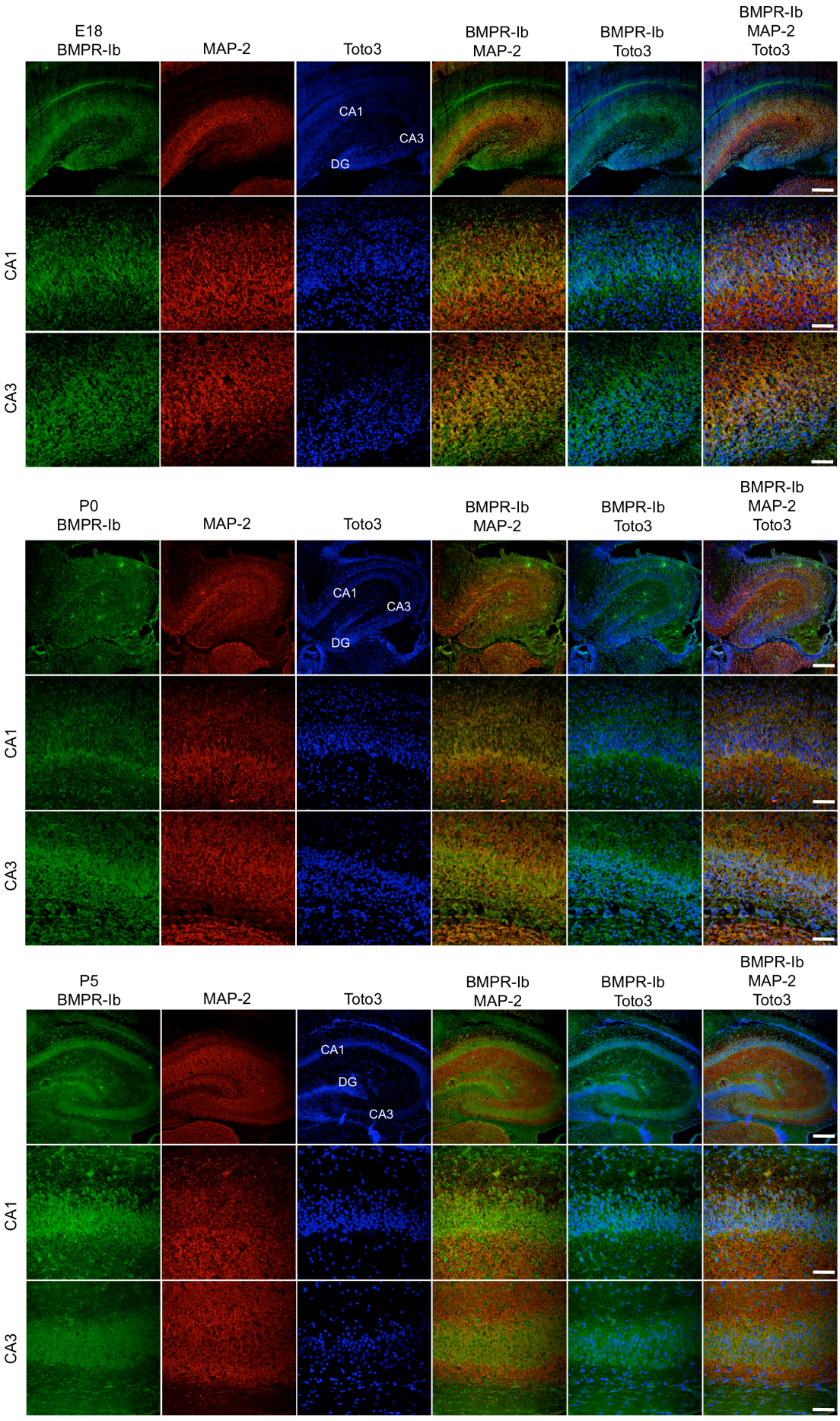
E18
BMPR-Ib
MAP-2
Toto3
BMPR-Ib
MAP-2
BMPR-Ib
Toto3
BMPR-Ib
MAP-2
Toto3
CA1
CA3
DG
CA1
CA3
P0
BMPR-Ib
MAP-2
Toto3
BMPR-Ib
MAP-2
BMPR-Ib
Toto3
BMPR-Ib
MAP-2
Toto3
CA1
CA3
DG
CA1
CA3
P5
BMPR-Ib
MAP-2
Toto3
BMPR-Ib
MAP-2
BMPR-Ib
Toto3
BMPR-Ib
MAP-2
Toto3
CA1
DG
CA3
CA1
CA3

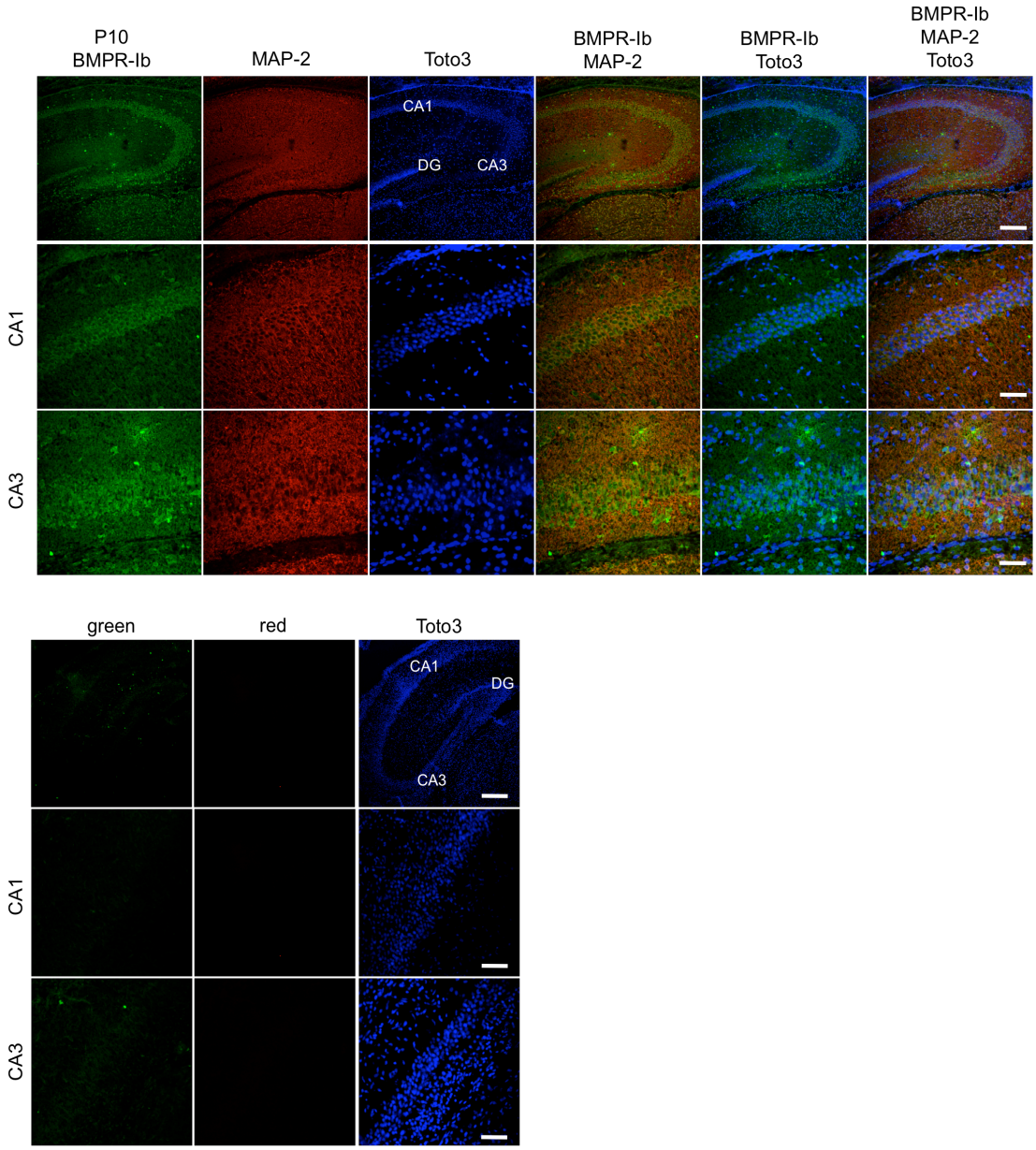

Figure 51: BMPR-Ib distribution in the developing hippocampus.

E18, P0, P5 and P10 hippocampal sections were stained for BMPR-Ib (green), MAP-2 (red) and TOTO-3 Iodide (blue). (DG: dentate gyrus; CA1 and CA3 layer). Last panel shows staining in the absence of primary antibodies. Scale bar: low magnification 200μm and high magnification 50μm.

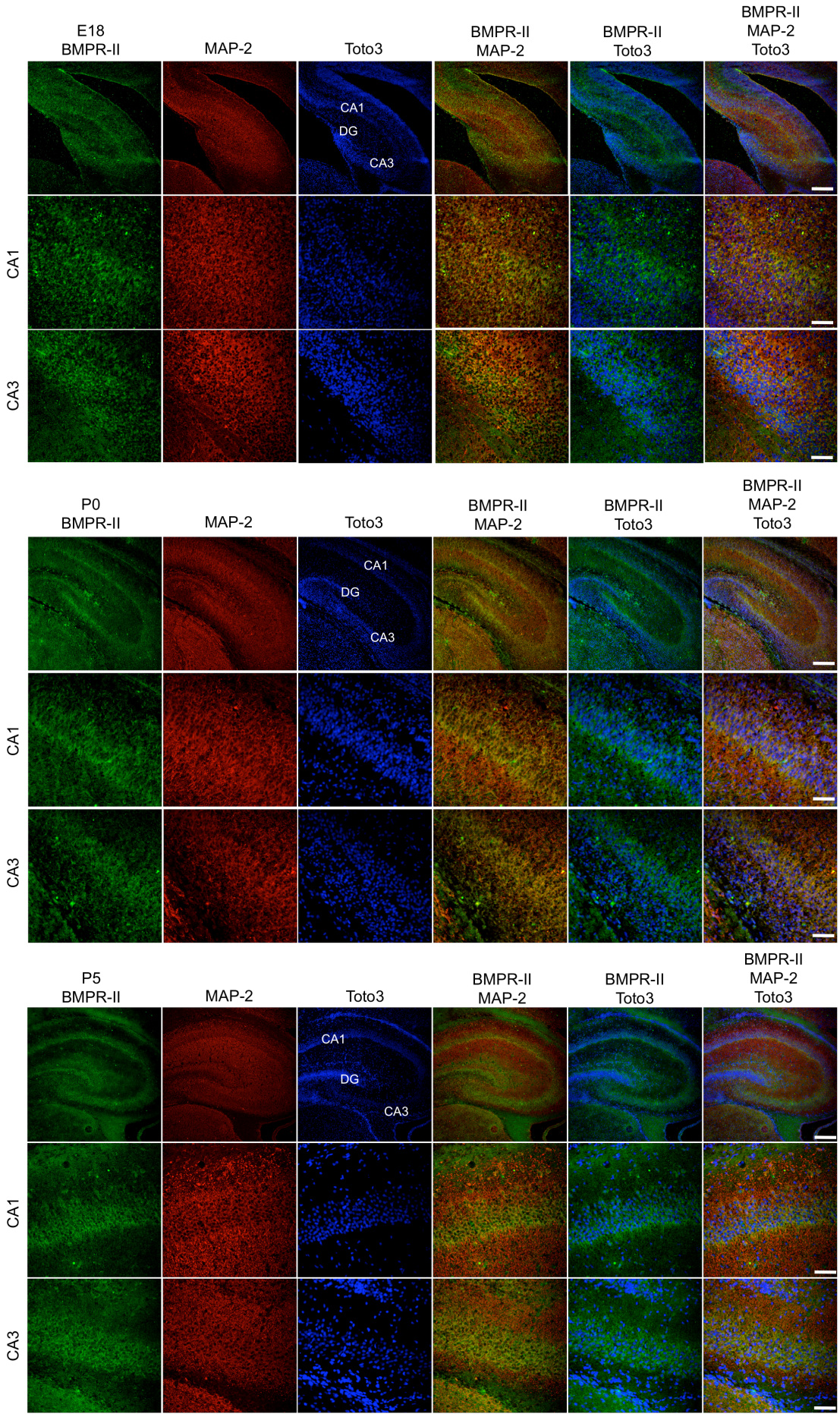
E18
BMPR-II
MAP-2
Toto3
BMPR-II
MAP-2
BMPR-II
Toto3
BMPR-II
MAP-2
Toto3
CA1
DG
CA3
CA1
CA3
P0
BMPR-II
MAP-2
Toto3
BMPR-II
MAP-2
BMPR-II
Toto3
BMPR-II
MAP-2
Toto3
CA1
DG
CA3
CA1
CA3
P5
BMPR-II
MAP-2
Toto3
BMPR-II
MAP-2
BMPR-II
Toto3
BMPR-II
MAP-2
Toto3
CA1
DG
CA3
CA1
CA3

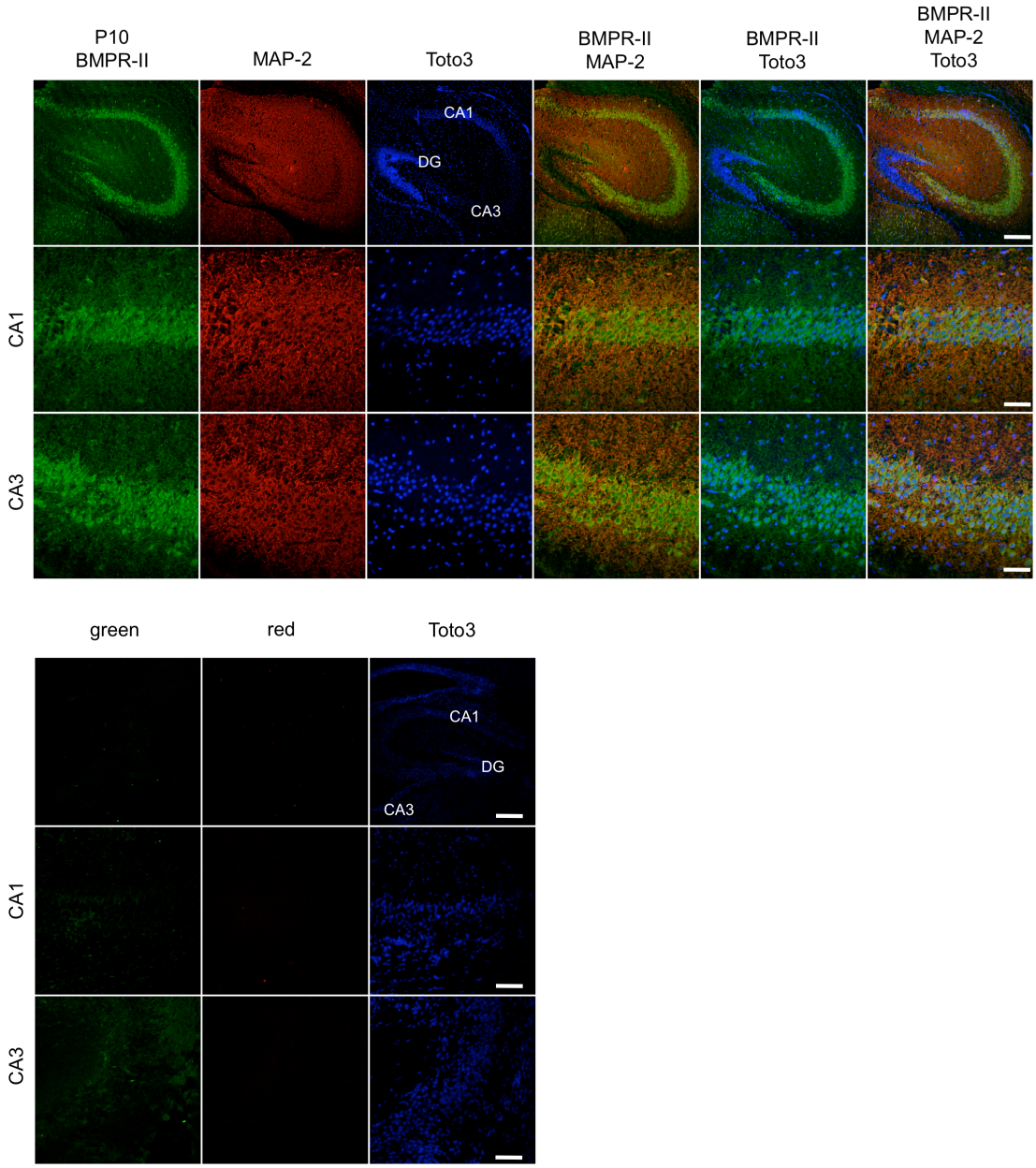

Figure 52: BMPR-II distribution in the developing hippocampus.

E18, P0, P5 and P10 hippocampal sections were stained for BMPR-II (green), MAP-2 (red) and TOTO-3 Iodide (blue). (DG: dentate gyrus; CA1 and CA3 layer). Last panel shows staining in the absence of primary antibodies. Scale bar: low magnification 200μm and high magnification 50μm.

5.4. Discussion

In this chapter, the expression of GDF-5 and its receptors, BMPR-Ib and BMPR-II were analysed at the mRNA and protein level in the developing hippocampus. Although BMPR-Ib and BMPR-II proteins have previously been detected in the adult rat hippocampus[449], it was important to verify that transcripts and protein for these two receptors are expressed in the developing mouse hippocampus. GDF-5 expression has previously not been reported in the developing or adult mouse hippocampus. Transcripts for GDF-5 and its receptors are expressed throughout hippocampal development and each shows a distinct developmental expression pattern. GDF-5 mRNA levels peak in the developing hippocampus at P0 and thereafter fall to small levels in the adult hippocampus. In contrast, the levels of BMPR-Ib mRNA gradually rise between E18 and P10 and fall only marginally between P10 and the adult. BMPR-II transcripts are expressed at relatively constant levels between E18 and P10 as hippocampal development proceeds, but expression increases modestly between P10 and adult (Fig.46). Similarly to chapter 3, it would have been interesting to analyse the mRNA expression of ligand and receptors at several postnatal ages between P10 and adult. During this period the neurons mature, dendrites become more complex and synaptogenesis takes place. It would be interesting to determine whether these events are marked by significant changes in the levels of GDF5, BMPR-Ib and BMPR-II mRNAs. The developmental expression patterns of GDF-5 and its receptors suggest that GDF-5 may play a role in regulating some aspects of hippocampus development during the early postnatal period. Although GDF-5 mRNA levels are very low in the adult hippocampus compared to the neonatal period, GDF-5 is expressed at similar levels in the adult hippocampus as the E18 mouse midbrain. Since GDF-5 is a trophic factor for embryonic rodent midbrain neurons[444], the parity of expression levels between adult hippocampus and midbrain, does not rule out a functional role for GDF-5 in the adult hippocampus. However, the relatively high levels of BMPR-Ib and BMPR-II mRNAs expressed in the adult hippocampus suggests that another member of the BMP subfamily of the TGF-β superfamily may be the functional ligand for these receptors in the adult hippocampus. The analysis of GDF-5,

BMPR-Ib and BMPR-II mRNAs in hippocampal cultures reveals that putting hippocampal neurons in culture does not dramatically alter the expression levels of these transcripts. Importantly, transcript levels after 5-7DIVs, the time that functional experiments analysing the effect of GDF-5 on dendrite size were performed, are close to those at 0DIVs (Fig.47).

Western blotting has revealed that mature and pro-GDF-5, BMPR-Ib and BMPR-II proteins are all expressed in the developing hippocampus (Fig.48). Whilst the changing levels of these proteins in the developing hippocampus do not closely follow the mRNA expression patterns, Western blotting is only a semi-quantitative measure of protein expression levels. However, the disparity between protein and transcript expression patterns observed may reflect a change in the efficiency of translation of GDF-5, BMPR-Ib and BMPR-II mRNAs as hippocampal development proceeds.

Immunocytochemistry was subsequently used to localise the proteins detected by Western blotting in cultured embryonic hippocampal neurons. GDF-5 is predominantly localised in the soma of hippocampal neurons, including the nucleus, although some weak staining is evident in the initial segments of the dendrites. GDF-5, in common with other members of the BMP subfamily of TGF-β superfamily members, can exist as a non-cleaved protein, containing the proregion and a nuclear localization signal, which is translocated to the nucleus[453]. The antibody used to detect GDF-5 in this chapter recognises the proform of GDF-5 and, therefore, detects GDF-5 that has been translocated to the nucleus. In addition to being detectable in the neuron soma, BMPR-Ib and BMPR-II are also found in dendrites where they co-localise with the dendritic marker, MAP-2 (Fig.49). The dendritic localisation of these receptors suggests that they may play a role in transducing a signal that regulates the morphology and/or molecular phenotype of developing hippocampal neuron dendrites. The detection of GDF-5 and its receptors, BMPR-Ib and BMPR-II in the same neuron raises the possibility that GDF-5 may regulate some aspect of hippocampal neuron development by autocrine and/or paracrine signalling.

Immunohistochemistry has revealed that, in the accordance with the data from Western blotting, GDF-5 expression is low in the developing hippocampus at E18 and increases as development proceeds. At postnatal ages, GDF-5 is clearly expressed in the soma of pyramidal neurons in the CA fields of the hippocampus, as well as in the granule cell layer of the DG (Fig.50). These protein expression results are not in accordance with the GDF-5 mRNA expression data at postnatal ages. This difference might be due to an increase in the efficiency of GDF-5 mRNA translation as postnatal development proceeds and/or an increased half life of the GDF-5 protein over the same period. BMPR-Ib is expressed in the developing hippocampus at all the ages examined and, like GDF-5, its expression increases as development proceeds, thereby mirroring real-time PCR and Western blot data (Fig.51). BMPR-II expression increases significantly in the developing hippocampus from E18 to P10 (Fig.52). At P5 and P10, both GDF-5 receptors are clearly expressed in the soma of pyramidal neurons and also in the surrounding lamina containing MAP-2 positive apical and basal dendrites. In contrast to GDF-5, BMPR-Ib and BMPR-II are not highly expressed in the granule cell layer of the DG. Negative controls with no primary antibodies were included in immunocytochemistry and immunohistochemistry experiments, confirming the specificity of the secondary antibodies. Ideally, the staining should be repeated using blocking peptides and/or tissues from transgenic mice lacking the expression of either GDF-5, BMPR-Ib or BMPR-II to confirm primary antibody specificity.

In conclusion, the data in this chapter demonstrates the expression of GDF-5 in the developing hippocampus for the first time. Developing hippocampal pyramidal neurons express GDF-5, BMPR-Ib and BMPR-II *in vitro* and *in vivo*. The expression of GDF-5 receptors in dendritic arbors raises the possibility that GDF-5 plays a role on regulating dendrite development. The co-expression of GDF-5 and its receptors in the same neurons may suggest that, if GDF-5 modulates dendrite development, it may do so by an autocrine and/or paracrine route. These results provide the rationale behind the functional studies described in Chapter 6.

Chapter 6

GDF-5 promotes hippocampal dendritic growth by regulating Smad1/5/8 signalling and induction of hairy enhancer of split-1 and -5 expression

6.1. Introduction

The crystal structure of recombinant human GDF-5 has confirmed that functional GDF-5 is a dimer consisting of two banana-shaped monomers[454]. Like other members of the TGF-β superfamily, GDF-5 is produced intracellularly as a large dimeric precursor that is subsequently cleaved at an RXXR (Arg, X, X, Arg) consensus sequence to release the biologically active molecule. The core of the mature dimer forms a ‘‘cysteine-knot’’ structure with seven disulfide bonds in total, comprising three intramolecular cysteine interactions per monomer and one disulfide bridge linking the GDF-5 monomers[454].

GDF-5 preferentially binds to the BMPR-Ib type I receptor with a high affinity, although it has been reported that GDF-5 can bind with a 17-fold lower affinity to BMPR-Ia and interact very weakly with ActR-I. Regarding type II receptors, GDF-5 has been shown to bind efficiently to BMPR-II and ActR-II and less efficiently to ActR-IIB1[455]. GDF-5 preference for BMPR-Ib as a type I receptor is corroborated by the phenotypic similarities of *Gdf-5*^{bp} and *Bmpr-Ib* deficient mice. However, a comprehensive analysis of the limbs of transgenic mice with a double inactivating mutation of *Gdf-5*^{bp} and *Bmpr-Ib*, and a comparison to the limbs of mice containing a single mutation in either *Gdf-5*^{bp} or *Bmpr-Ib*, has suggested that GDF-5 partially regulates limb morphogenesis through an alternative receptor to BMPR-Ib, and that, BMPR-Ib also binds other BMP ligands to modulate some aspects of limb development[456]. A single amino acid residue of GDF-5, Arg57 defines the binding specificity for BMPR-Ib[457].

GDF-5 has been shown to induce the phosphorylation and nuclear translocation of Smad1 in cultures of smooth muscle cells derived from the human umbilical cord vein[458]. The nuclear translocation of Smad1 promotes the expression of the transcriptional regulator, ID1 in cultured smooth muscle cells and induces their migration. Curiously, GDF-5 also activates ERK1/2 in cultured smooth muscle cells, although ERK1/2 activation is not required to promote the expression of ID1 and induce cell migration[458]. GDF-5 has also been shown to activate ERK1/2 signalling, together with p38 MAPK signalling,

in cultures of human ligamentum flavum (HLF) cells (a ligament that connects adjacent vertebrae in the spinal column). GDF-5 induced activation of these two MAPK pathways results in increased activity of alkaline phosphatase and increased expression of osteocalcin within HLF cells, suggesting that GDF-5 is promoting their osteogenic differentiation[459].

6.2. Aims

The data in Chapter 5 revealed that GDF-5, BMPR-Ib and BMPR-II are expressed in developing hippocampal neurons; thereby suggesting that GDF-5 regulates some aspect of hippocampal neuron development. Since BMPR-Ib and BMPR-II are expressed in the dendrites of developing hippocampal neurons, the initial aim of the experimental work presented in this chapter was to determine whether GDF-5 regulates the growth and complexity of developing hippocampal neuron dendrites *in vitro.* After establishing that GDF-5 promotes the growth of dendrites, further experiments aimed to identify the intracellular signalling pathways that GDF-5 uses to promote dendrite growth. The final aim of this chapter was to verify the physiological significance of *in vitro* data by examining hippocampal neuron dendrite development in *Gdf-5*^{bp} mice.

6.3. Results

6.3.1. GDF-5 increase dendritic but not axonal outgrowth from cultured hippocampal neurons

Functional analyses were performed to evaluate whether GDF-5 could promote axonal and/or dendritic outgrowth from E18 mouse hippocampal neuron *in vitro*. For axonal analyses, 2DIVs hippocampal neurons were transfected with pCDH-CMV-MCS-EF1-copGFP and incubated for a further 16 hours in media containing either no GDF-5 (control) or media containing different concentrations of recombinant GDF-5. Cultured neurons were fixed, stained with an antibody against GFP and analysed at 3DIVs, a time point that precedes the growth of dendrites[22]. GDF-5 did not alter the length of hippocampal neuron axons compared to control cultures (Fig.53 and Fig.54.A and B). Although 10ng/ml and 1000ng/ml GDF-5 does not alter the number of collaterals that hippocampal neuron axons have compared to control cultures, 100ng/ml GDF-5 induces a small, but statistically significant, reduction in the mean number of axon collaterals (Fig.54.A and C).

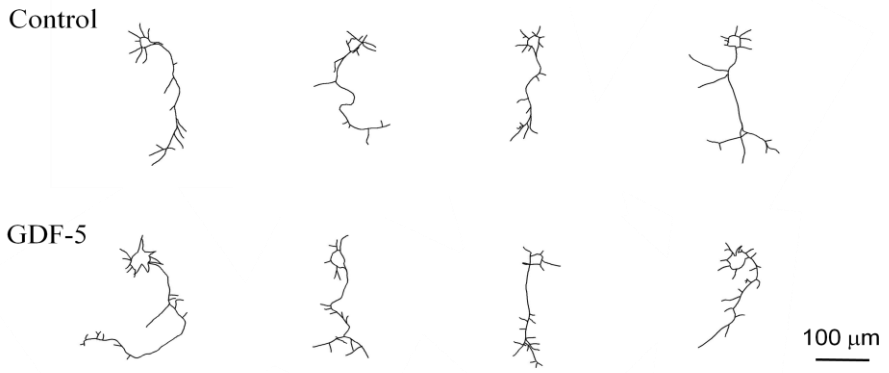

Figure 53: GDF-5 does not promote axonal outgrowth from cultured hippocampal neurons. Camera lucida drawings of representative control neurons and neurons treated with 100ng/ml GDF-5.

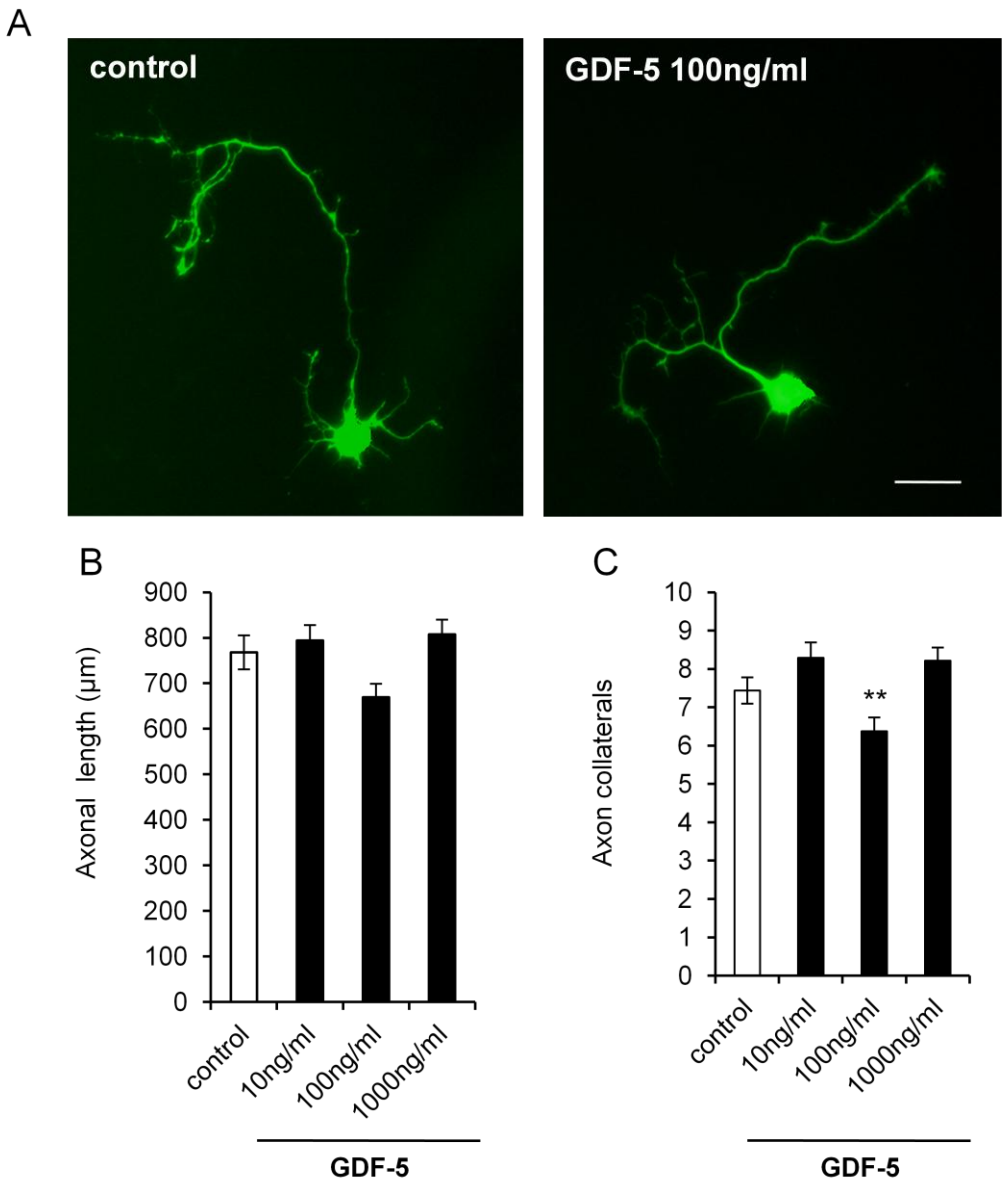

Figure 54: GDF-5 does not promote axonal outgrowth from cultured E18 hippocampal neurons. E18 hippocampal neurons were cultured for 2DIVs before being transfected with pCDH-CMV-MCS-EF1-copGFP and cultured for a further 16h in medium containing no factors (control) or medium containing either 10ng/ml, 100ng/ml or 1000ng/ml recombinant GDF-5. Cultures were fixed at 3DIVs and stained with an anti-GFP antibody, before being imaged using a fluorescence microscope. Images were analysed using ImageJ software. (A) Representative photomicrographs of typical neurons cultured under the stated conditions. Scale bar: 100µm. Graphs correspond to (B) mean axonal length and the (C) mean number of axon collaterals. Data represent the mean and sem of 150 neurons for each condition from 3 separate experiments. **indicates $p<0.001$, statistical comparison with control, (Mann–Whitney U test).

To determine whether GDF-5 regulates dendritic outgrowth from cultured embryonic hippocampal neurons, 6DIVs E18 hippocampal neuron cultures were transfected with pCDH-CMV-MCS-EF1-copGFP and cultured for a further 16 hours in medium containing either no factors (control) or 10ng/ml, 100ng/ml or 1000ng/ml GDF-5. After fixation and staining for GFP, neurons were imaged using a fluorescence microscope and the images analysed with Photoshop. Fig.55 and Fig.56.A and B demonstrate that GDF-5 increases the number of dendrites that are greater than 50µm in length in a dose dependent manner. The most effective concentration of GDF-5, 100ng/ml, increases the number of dendrites that are over 50µm in length by almost 2-fold compared to control cultures. Representative camera lucida drawing of typical neurons cultured in the absence or presence of 100ng/ml GDF-5 are shown in Figure 55. Interestingly, in addition to promoting an increase in the number of dendrites greater than 50µm in length, 100ng/ml GDF-5 significantly decreases the mean number of primary dendrites (Fig.55, Fig.56.A and C).

A

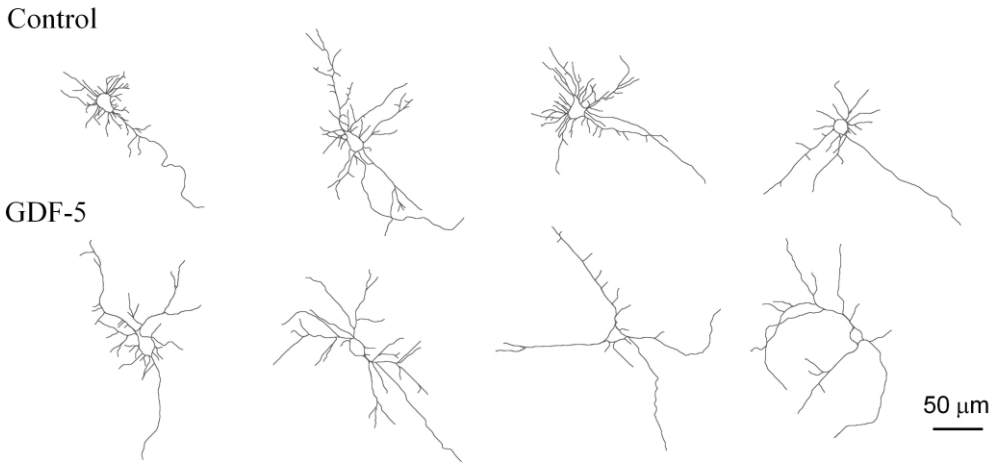

Figure 55: GDF-5 promotes dendritic outgrowth from cultured E18 hippocampal neurons. Camera lucida drawings of representative control neurons and neurons treated with 100ng/ml GDF-5.

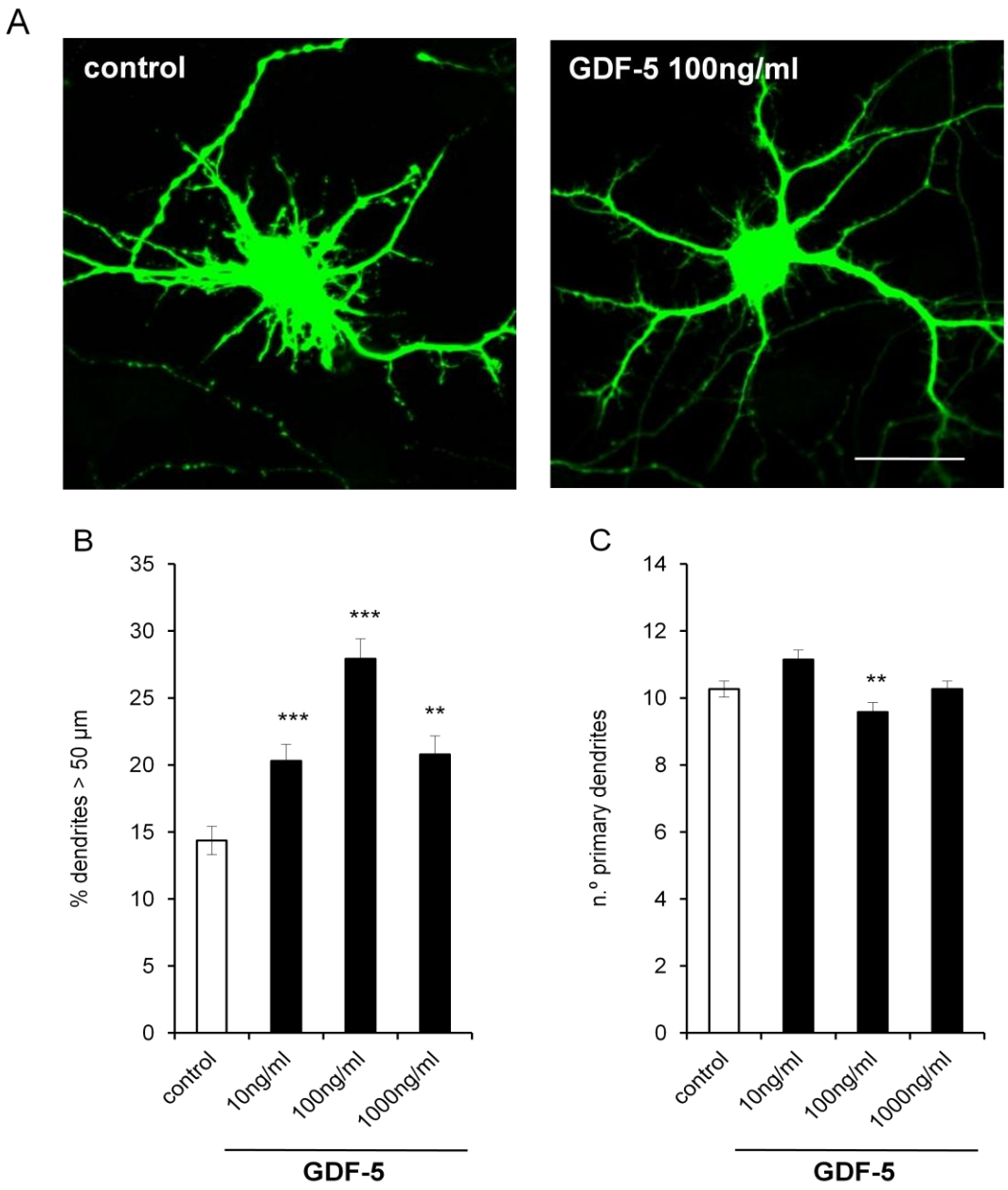

Figure 56: GDF-5 promotes dendritic outgrowth from cultured E18 hippocampal neurons. 6DIVs E18 hippocampal neurons were transfected with pCDH-CMV-MCS-EF1-copGFP and cultured for a further 16h in medium containing either no factors (control) or 10ng/ml, 100ng/ml or 1000ng/ml recombinant GDF-5. Cultures were fixed at 7DIVs, stained with an anti-GFP antibody and imaged on a fluorescence microscope. Images were analysed using Photoshop. (A) Representative photomicrographs of typical neurons cultured under the stated conditions. Scale bar: 50µm. Graphs correspond to the (A) % of dendrites > 50µm and the (B) mean number of primary dendrites. Data represent the mean and sem of 150 neurons for each condition from 3 separate experiments. **indicates $p<0.001$, ***indicates $p<0.0001$, statistical comparison with control, (Mann–Whitney U test).

6.3.2. BMPR-Ib and BMPR-II receptors mediate GDF-5 promoted dendrite growth

Next, the roles that BMPR-Ib and BMPR-II receptors play in GDF-5 promoted dendritic growth were evaluated. E18 Hippocampal neurons that had been cultured for 6DIVs were transfected with either pCDH-CMV-MCS-EF1-copGFP (control), or pCDH-CMV-MCS-EF1-copGFP containing an insert encoding either a constitutively active (CA) form of BMPR-Ib (pCDH-CMV-mAlk6QD-EF1-copGFP) or a dominant-negative (DN) form of BMPR-Ib (pCDH-CMV-mAlk6QD-D265A-EF1-copGFP). Transfected neurons were cultured for a further 16 hours in the presence or absence of 100ng/ml recombinant GDF-5. After fixation at 7DIVs, neurons were stained with an antibody that recognises GFP and imaged under a fluorescence microscope. Images were analysed using Photoshop.

In accordance with figure 56, 100ng/ml GDF-5 significantly increases the number of dendrites that are longer than 50µm and significantly decreases the number of primary dendrites compared to control cultures (Fig.57). Expression of constitutively active BMPR-Ib in hippocampal neurons increases the length of dendrites, compared to control cultures, in the absence of recombinant GDF-5, but does not alter the number of primary dendrites. The addition of 100ng/ml GDF-5 to cultures containing neurons that express constitutively active BMPR-Ib does not further increase the number of dendrites that are longer than 50µm, but it does significantly reduce the number of primary dendrites. Whilst the expression of the dominant-negative form of BMPR-Ib does not affect the length of dendrites in the absence of exogenous GDF-5, it totally prevents 100ng/ml GDF-5 from promoting the elongation of hippocampal neuron dendrites (Fig.57).

To confirm that BMPR-Ib is required to mediate the dendrite growth promoting effects of GDF-5, E18 hippocampal cultures were established from *Bmpr-Ib* (*Alk6*$^{-/-}$) deficient embryos, WT embryos (*Alk6*$^{+/+}$) and embryos that were heterozygous for functional *Alk-6* deletion (*Alk6*$^{+/-}$). After 6DIVs, cultures were transfected with pCDH-CMV-MCS-EF1-copGFP and cultured for a

further 16 hours, either in the presence or absence of 100ng/ml GDF-5. As expected, GDF-5 increases the number of dendrites longer than 50µm and reduces the number of primary dendrites, compared to controls, in cultures established from *Alk6*$^{+/+}$ embryos (Fig.58). Very similar data was obtained from cultures established from *Alk6*$^{+/-}$ embryos. In contrast, 100ng/ml GDF-5 does not increase dendrite length compared to control cultures in cultures established from *Alk6*$^{-/-}$ embryos (Fig.58.A and B). Curiously, the complete loss of functional *Alk-6* reduces the number of primary dendrites associated with cultured hippocampal neurons in the absence of exogenous GDF-5 and the addition of 100ng/ml recombinant GDF-5 to cultures of *Alk6*$^{-/-}$ hippocampal neurons does not further decrease the number of primary dendrites (Fig.58.A and C).

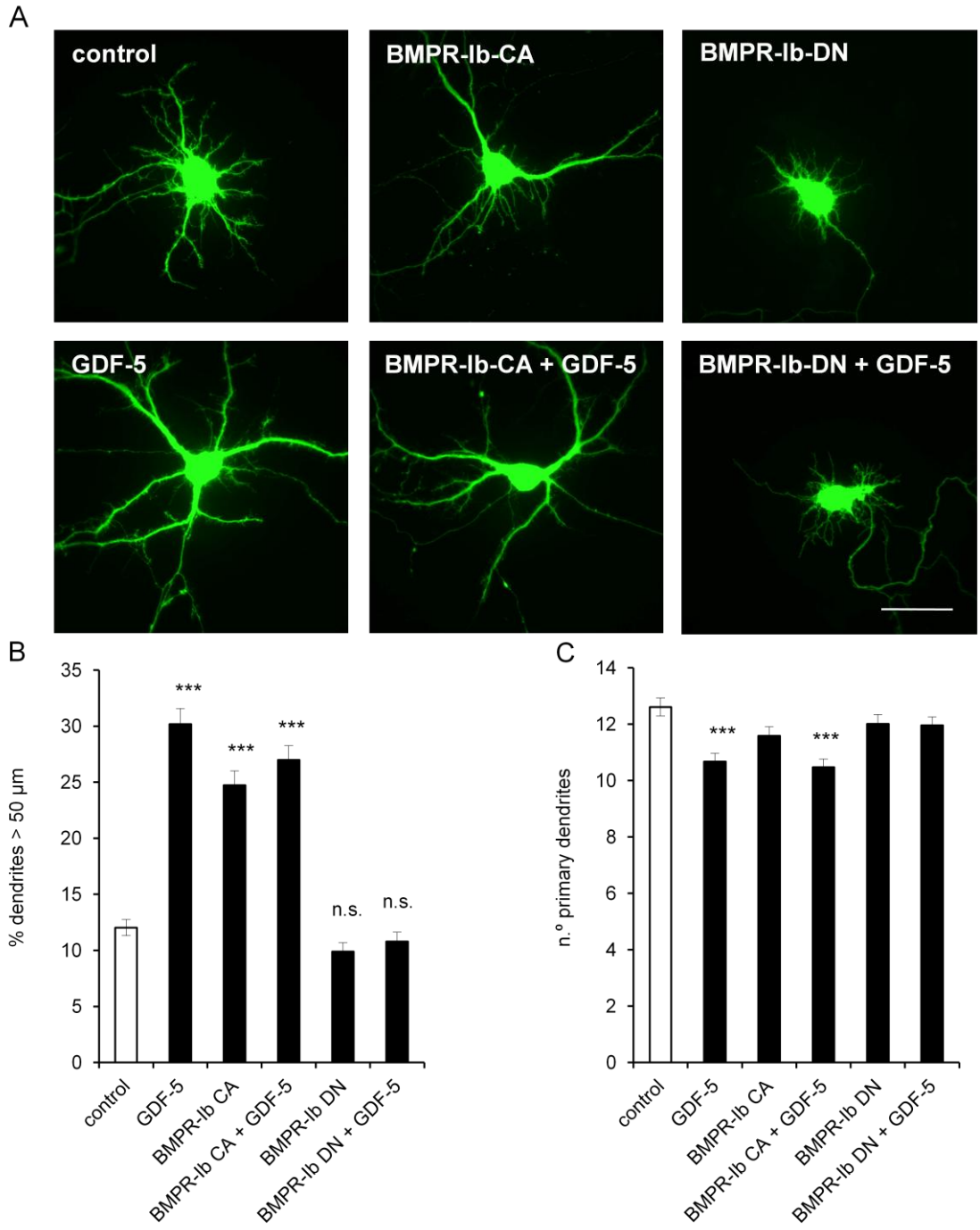

Figure 57: BMPR-Ib mediates GDF-5-promoted dendrite growth. E18 hippocampal neurons that had been cultured for 6DIVs were transfected with either pCDH-CMV-MCS-EF1-copGFP (control), pCDH-CMV-mAlk6QD-EF1-copGFP (BMPR-Ib-CA) or pCDH-CMV-mAlk6QD-D265A-EF1-copGFP (BMPR-Ib-DN). Transfected neurons were culture for a further 16h in medium containing either no factors or medium containing 100ng/ml GDF-5 before being fixed, stained for GFP and imaged under a fluorescence microscope. Images were analysed using Photoshop. (A) Representative photomicrographs of typical neurons cultured under the stated conditions. Scale bar: 50µm. Graphs correspond to the (B) % of dendrites >50µm and the (C) mean number of primary dendrites. Data represent the mean and sem of 150 neurons for each condition from 3 separate experiments. ***indicates p<0.0001, statistical comparison with control, n.s. non-significant (Mann–Whitney U test).

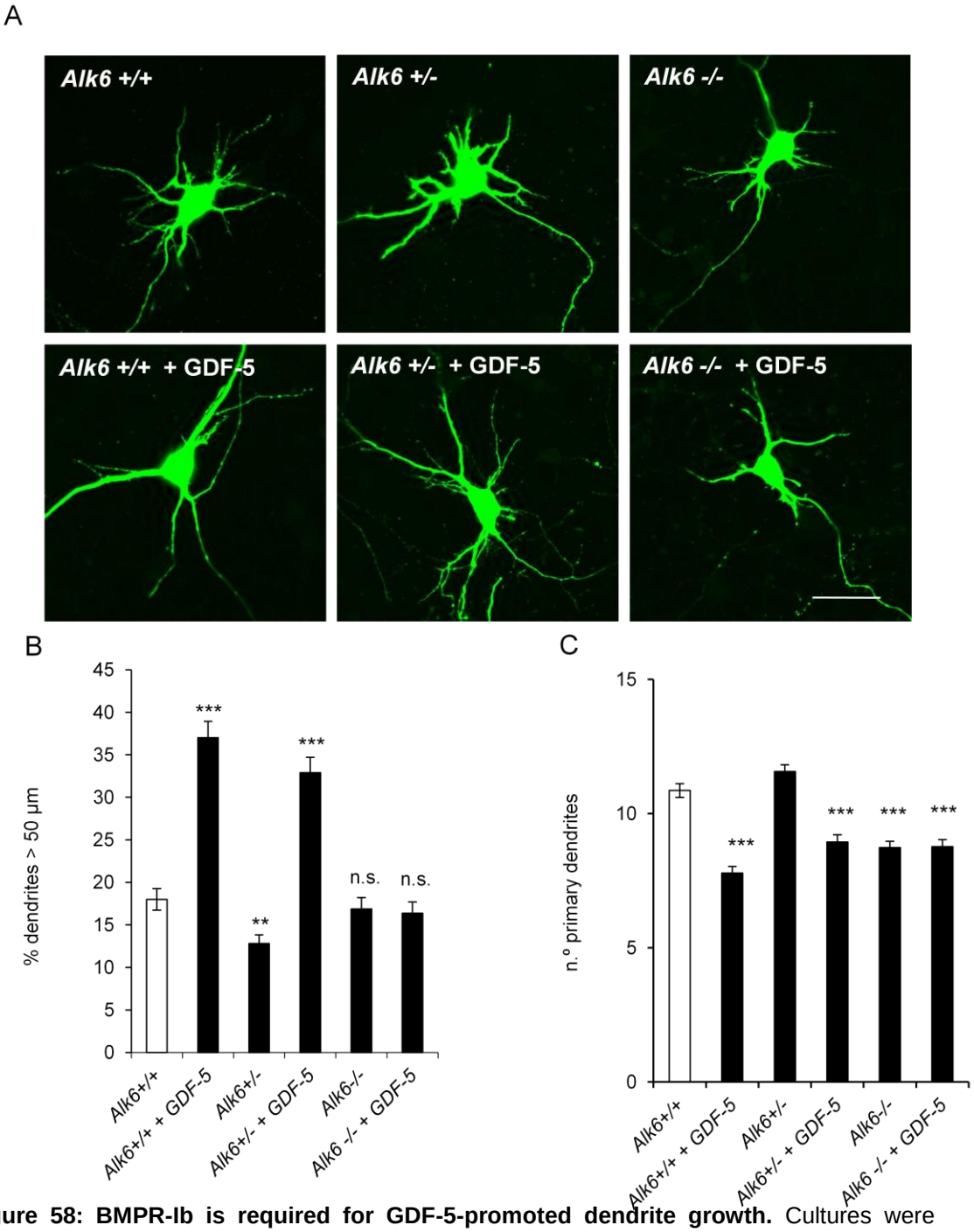

Figure 58: BMPR-Ib is required for GDF-5-promoted dendrite growth. Cultures were established from *Alk6*$^{+/+}$, *Alk6*$^{+/-}$ and *Alk6*$^{-/-}$ E18 mouse embryos. After 6DIVs, cultured were transfected with pCDH-CMV-MCS-EF1-copGFP, and cultured for a further 16h in medium containing either no factors (control) or 100ng/ml recombinant GDF-5. Neurons were fixed at 7DIVs, stained with an anti-GFP antibody and imaged on a fluorescence microscope. Images were analysed using Photoshop. (A) Representative photomicrographs of typical cultured neurons established from *Alk6*$^{+/+}$, *Alk6*$^{+/-}$ and *Alk6*$^{-/-}$ embryos and cultured with or without GDF-5. Scale bar: 50µm. Graphs correspond to the (B) % of dendrites > 50µm and the (C) mean number of primary dendrites. Data represent the mean and sem of 150 neurons for each condition from 3 separate experiments. **indicates p<0.001, ***indicates p<0.0001, statistical comparison with control, n.s. non-significant (Mann–Whitney U test).

To assess the role of the BMPR-II receptor in GDF-5 promoted dendrite growth, hippocampal neurons that had been in culture for 6DIVs were transfected with either pCDH-CMV-MCS-EF1-copGFP (control), or pCDH-CMV-MCS-EF1-copGFP containing an insert encoding either a WT form of BMPR-II (pCDH-CMV-BMPR-II WT-EF1-copGFP) or a DN form of BMPR-II (pCDH-CMV-BMPR-II-D(485)G-EF1-copGFP). Transfected neurons were cultured for a further 16 hours, either in the presence or absence of 100ng/ml GDF-5. After this period, neurons were fixed, stained with an antibody against GFP and imaged with a fluorescence microscope. Images were analysed with Photoshop.

Overexpression of WT BMPR-II mimics the effect of adding 100ng/ml of recombinant GDF-5 by increasing the percentage of hippocampal neurons with dendrites greater than 50µm in length, compared to control cultures Adding GDF-5 to neurons overexpressing WT BMPR-II does not further increase the length of dendrites. Expression of DN BMPR-II does not reduce the percentage of hippocampal neurons with dendrites greater than 50µm in length, compared to control transfected neurons, but it totally prevents GDF-5 promoted dendrite growth (Fig.59.A and B). The addition of exogenous GDF-5 to cultures and transfection of WT or DN BMPR-II, either in the presence or absence of 100ng/ml GDF-5, significantly reduces the number of hippocampal neuron primary dendrites compared to control cultures (Fig.59.A and C).

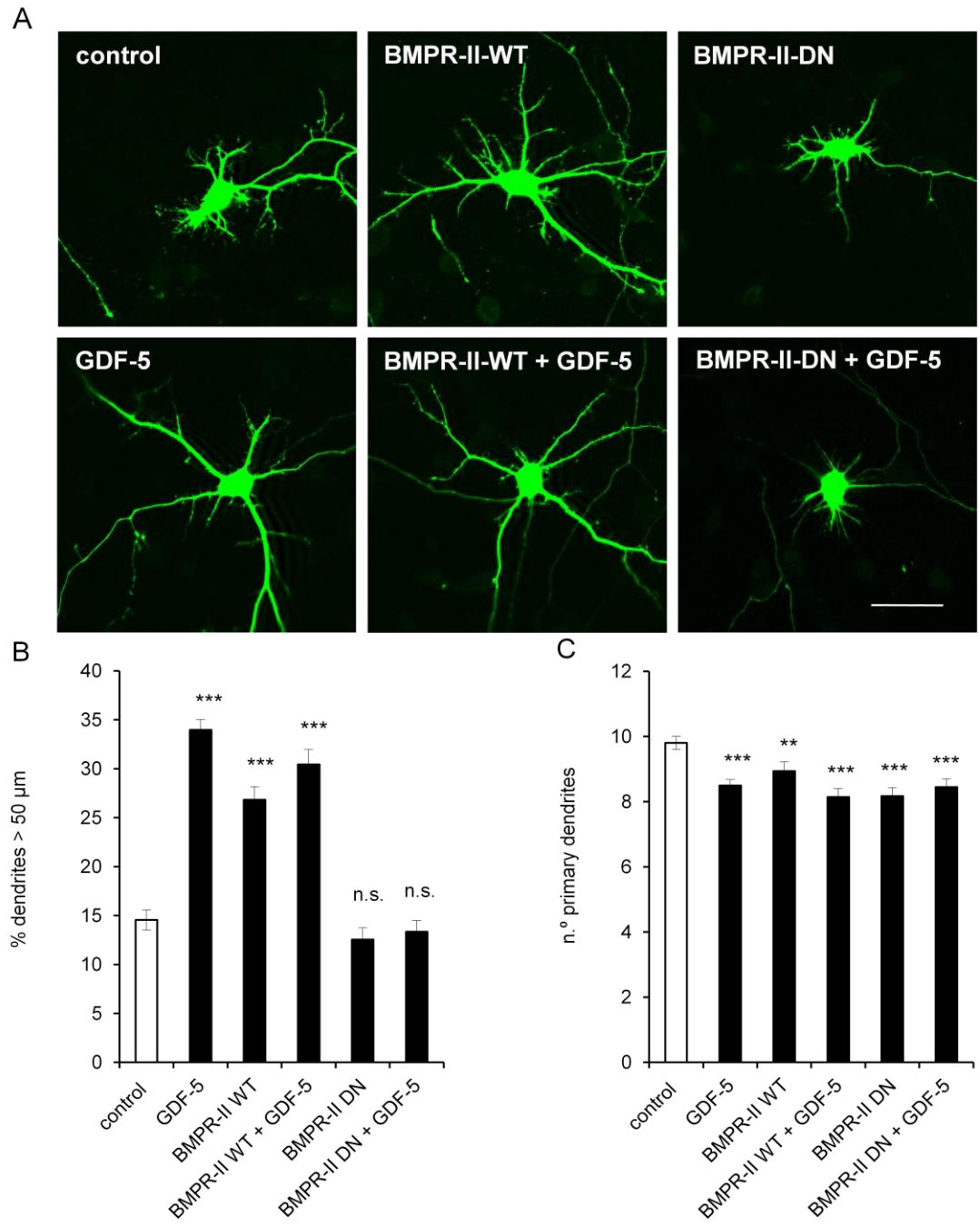

Figure 59: BMPR-II mediates GDF-5-promoted dendrite growth.

E18 hippocampal neurons that had been cultured for 6DIVs were transfected with either pCDH-CMV-MCS-EF1-copGFP (control), pCDH-CMV-BMPR-II-WT-EF1-copGFP (BMPR-II WT) or pCDH-CMV-BMPR-II-D(485)G-EF1-copGFP (BMPR-II-DN). Transfected neurons were culture for a further 16h in medium containing either no factors or medium containing 100ng/ml GDF-5 before being fixed, stained for GFP and imaged under a fluorescence microscope. Images were analysed using Photoshop. (A) Representative photomicrographs of typical neurons cultured under the stated conditions. Scale bar: 50µm. Graphs correspond to the (B) % of dendrites >50µm and the (C) mean number of primary dendrites. Data represent the mean and sem of 150 neurons for each condition from 3 separate experiments. **indicates p<0.001, ***indicates p<0.0001, statistical comparison with control, n.s. non-significant (Mann–Whitney U test).

6.3.3. Signalling pathways induced by GDF-5 in hippocampal neurons: activation of Smad1/5/8 transcription factors

To begin to elucidate the molecular mechanisms underlying GDF-5 promoted dendritic outgrowth, E18 hippocampal neurons that had been in culture for 6DIVs were treated with 100ng/ml of recombinant GDF-5 for 15, 30 and 60 minutes and lysed. Control cultures did not have recombinant GDF-5 added. Lysates were analysed by Western Blotting using antibodies against phospho-Smads 1/5/8 (that recognises the phosphorylation of ser463/465 of Smads1 and 5 and ser426/428 of Smad8), non-phosphorylated Smad1 and β-III tubulin. The addition of GDF-5 to cultures results in an increase in the levels of phospho-Smad1/5/8 within 15 minutes that is maintained until 60 minutes (Fig.60.A, B and C).

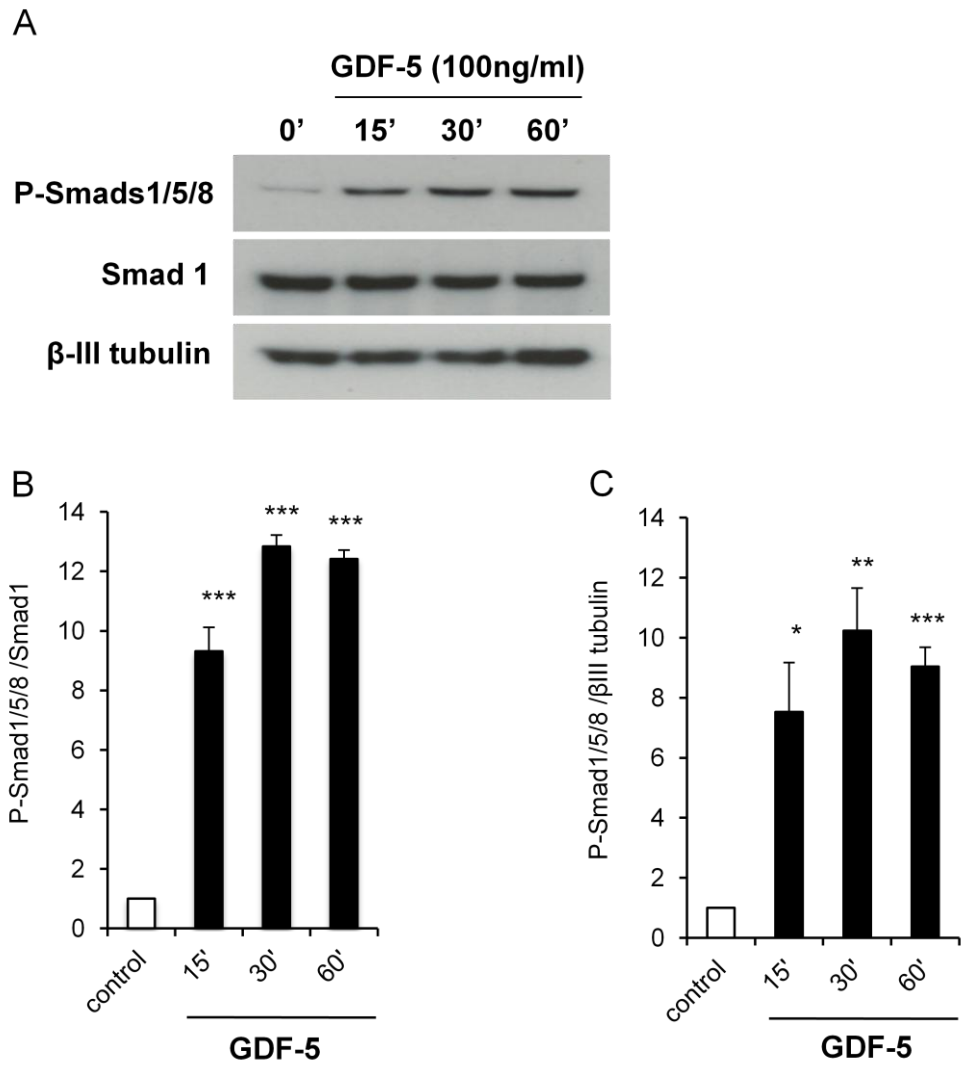

Figure 60: GDF-5 promotes the phosphorylation and activation of Smads1/5/8.

E18 hippocampal neurons that had been cultured for 6 days were exposed to 100ng/ml of recombinant GDF-5 for 15, 30 and 60min before being lysed. Control cultures were lysed without the addition of GDF-5. Lysates were analysed by Western blotting using antibodies against phospho-Smads 1/5/8, non-phosphorylated Smad1 and β-III-tubulin. (A) Representative scan of a Western blot. Graphs correspond to densitometry measured ratios of (B) P-Smad1/5/8 /Smad1 and (C) P-Smad1/5/8 /β-III tubulin. Data represent the mean and sem of 3 separate experiments. *indicates p<0.01, **indicates p<0.001, ***indicates p<0.0001, statistical comparison with control (Mann–Whitney U test).

To determine the importance of Smad signalling in GDF-5-promoted dendrite growth, 6DIVs hippocampal neurons were co-transfected with pCDH-CMV-MCS-EF1-copGFP together with either a plasmid that expresses an inhibitor of Smad signalling or an empty control plasmid that consisted of the expression vector that the Smad signalling inhibitors were cloned into. To inhibit Smad signalling, neurons were transfected with expression vectors encoding the inhibitory Smads, Smad6 (pCS2-Flag-Smad6) or Smad7 (pCMV5-Smad7-HA) or with a DN version of Smad4 (pRK-DPC4-deltaC-Flag). Transfected neurons were cultured for a further 16 hours, either in the presence or absence of 100ng/ml recombinant GDF-5, fixed, stained for GFP and imaged under a fluorescence microscope. Images were analysed using Photoshop.

Dendrite growth from neurons transfected with a plasmid expressing DN Smad4 is significantly less than that from control-transfected neurons in the absence of GDF-5, and expression of DN Smad4 completely eliminates GDF-5-promoted dendrite growth (Fig.61.A and B). In accordance with previous experiments, the number of primary dendrites is significantly reduced in control transfected neurons cultured in the presence of 100ng/ml GDF-5 compared to control transfected neurons cultured in the absence of GDF-5. The expression of DN Smad4 prevents GDF-5 from reducing the number of primary dendrites (Fig.61.A and C). As expected, the expression of inhibitory Smads6 and 7 prevents GDF-5 from promoting dendrite growth and reducing the primary number of dendrites (Fig.62.A, B and C).

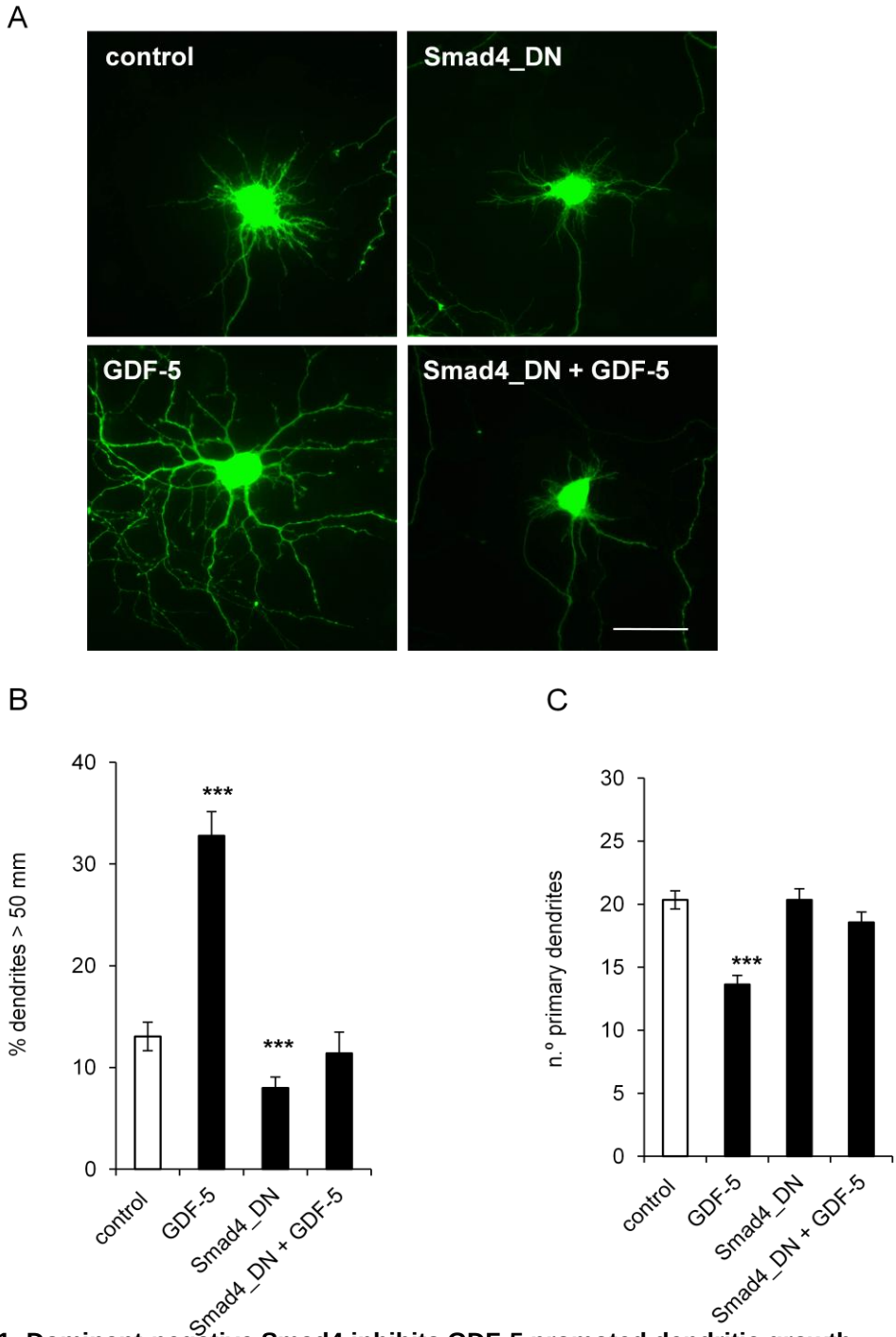

Figure 61: Dominant-negative Smad4 inhibits GDF-5 promoted dendritic growth.

E18 hippocampal neurons that had been in culture for 6 days were co-transfected with pCDH-CMV-MCS-EF1-copGFP together with either pRK-DPC4-deltaC-Flag (Smad4_DN) or pRK-Flag (control). Transfected neurons were cultured for a further 16h, either in the presence or absence of 100ng/ml recombinant GDF-5, before being fixed, stained for GFP and imaged under a fluorescence microscope. Images were analysed using Photoshop. (A) Representative photomicrographs of typical cultured neurons under the stated conditions. Scale bar: 50μm. Graphs correspond to the (B) % of dendrites > 50μm and the (C) number of primary dendrites. Data represent the mean and sem of 150 neurons for each condition from 3 separate experiments. ***indicates $p<0.0001$, statistical comparison with control (Mann–Whitney U test).

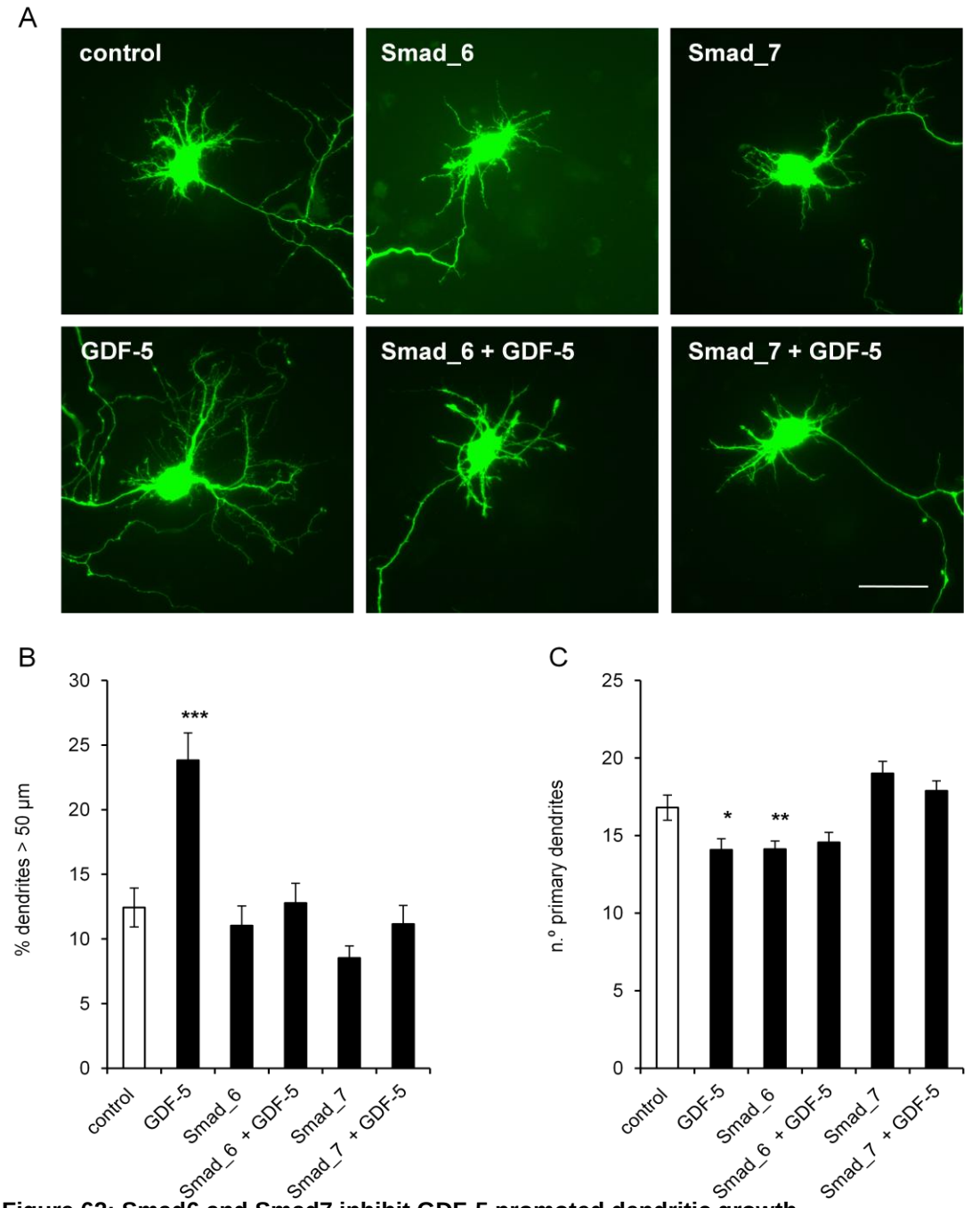

Figure 62: Smad6 and Smad7 inhibit GDF-5 promoted dendritic growth.

E18 hippocampal neurons that had been in culture for 6 days were co-transfected with pCDH-CMV-MCS-EF1-copGFP together with either pCS2-Flag-Smad6 (Smad_6), pCMV5-Smad7-HA (Smad_7) or pCS2-Flag/pCMV5-HA (control). Transfected neurons were cultured for a further 16h, either in the presence or absence of 100ng/ml recombinant GDF-5, before being fixed, stained for GFP and imaged under a fluorescence microscope. Images were analysed using Photoshop. (A) Representative photomicrographs of typical cultured neurons under the stated conditions. Scale bar: 50µm. Graphs correspond to the (B) % of dendrites > 50µm and the (C) mean number of primary dendrites. Data represent the mean and sem of 150 neurons for each condition from 3 separate experiments. *indicates p<0.01, **indicates p<0.001 and ***indicates p<0.0001, statistical comparison with control (Mann–Whitney U test).

To determine the specificity of Smad signalling, neurons were transfected with a pGL3-BRE-Luc plasmid. This construct has a BMP responsive element sequence followed by a luciferase gene. If the BRE is activated by phospho-Smads the luciferase gene is transcribed. As shown in Fig.63.A, an increase in luciferase activity is observed when cells expressing BRE-Luc are treated with GDF-5. When Smad inhibitors, Smad_6 or Smad_7, were co-transfected in the presence of GDF-5, there was a decrease of luciferase activity compared to neurons co-transfected with a control plasmid and treated with GDF-5 (Fig.63.B).

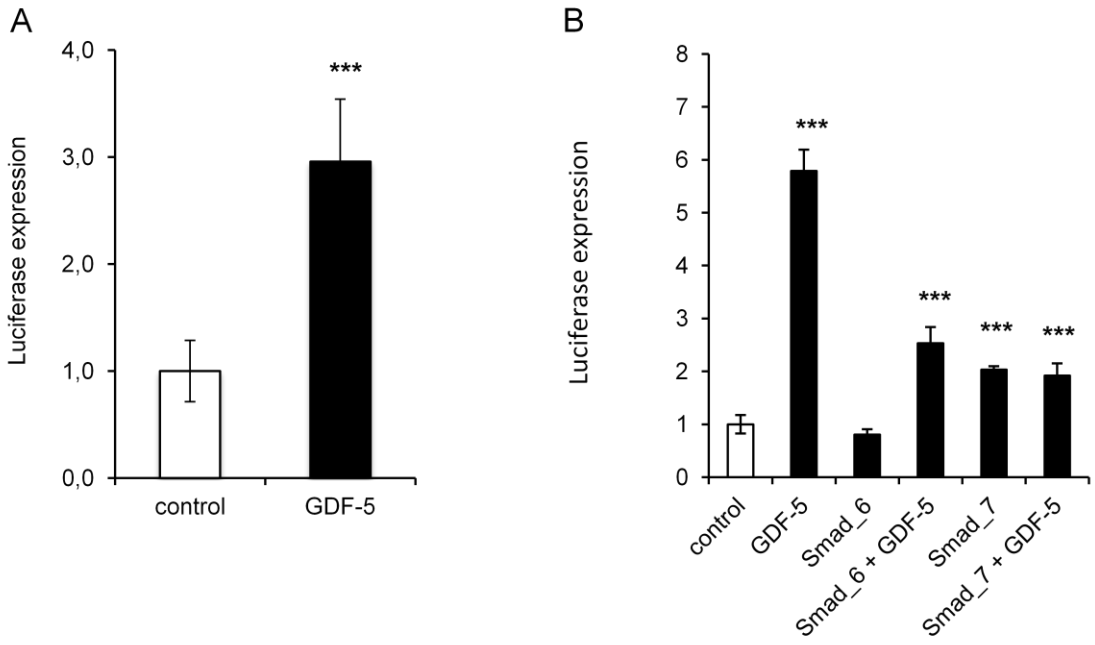

Figure 63: GDF-5 enhances Smad transcriptional activation.

(A) Hippocampal neurons that that had been in culture for 6 days were transfected with pGL3-BRE-Luc and cultured for a further 16h either without GDF-5 (control) or with 100ng/ml GDF-5. At 7DIVs neurons were lysed and processed for luciferase quantification. (B) Hippocampal neurons that that had been in culture for 6 days were co-transfected with pGL3-BRE-Luc and either pCDH-MCS-EF1-copGFP, pCS2-Flag-Smad6 (Smad_6) or pCMV5-Smad7-HA (Smad_7). Co-transfected neurons were cultured for a further 16h either without GDF-5 (control) or with 100ng/ml GDF-5. At 7DIVs neurons were lysed and processed for luciferase quantification. Data represent the mean and sem of 3 separate experiments. ***indicates $p<0.0001$, statistical comparison with control ((A) t-test and (B) Mann–Whitney U test).

6.3.4. Signal transduction induced by GDF-5 in hippocampal neurons: induction of hairy and enhancer-of-split-1 (Hes1) and -5 (Hes5) expression

NGF-enhanced dendrite elongation from cultured hippocampal neurons has previously been shown to be promoted by increasing the expression of Hes1 and Hes5 bHLH transcription factors that are nuclear targets of Notch signalling[110]. To investigate if GDF-5-promoted dendrite growth is mediated by an upregulation of Hes1 and Hes5 transcription factor expression, 7DIVs hippocampal neuron cultures were supplemented with 100ng/ml GDF-5 for either 4h or 18h. Control 7DIVs cultures were not treated with GDF-5. Rea-time PCR analysis of total RNA extracted from hippocampal neuron cultures shows that 4h of GDF-5 treatment significantly increases the expression of Hes1 and Hes5 mRNAs (Fig.64.A and B). Although the GDF-5 induced increase in Hes1 transcript expression was not maintained with prolonged exposure to GDF-5, Hes5 mRNA levels are higher after 18h culture with GDF-5 compared to after 4h (Fig.64.B).

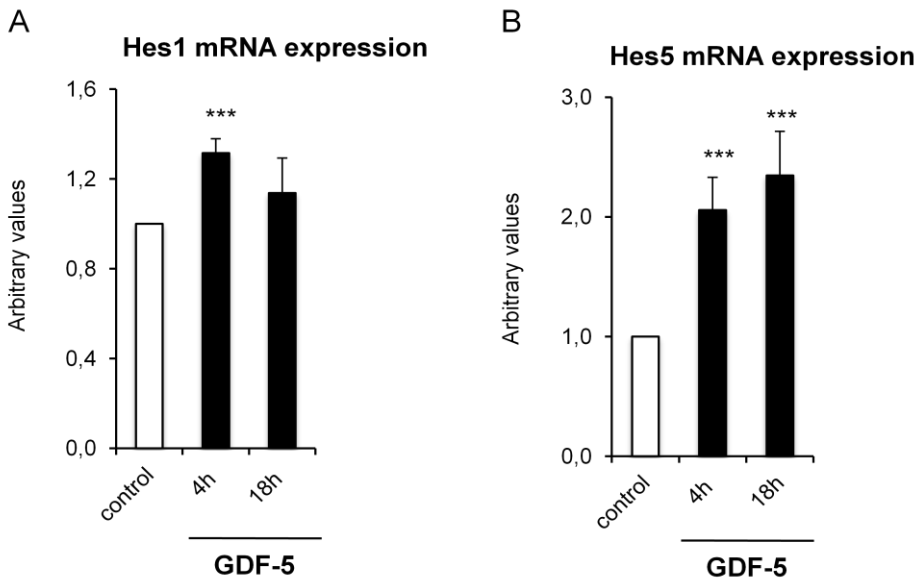

Figure 64: GDF-5 increases the expression of Hes1 and Hes5 mRNAs.

Total RNA was extracted from 7DIVs hippocampal cultures that had been exposed to 100ng/ml GDF-5 for either 4h or 18h. Control cultures were not treated with GDF-5. Graphs show the levels of (A) Hes1 and (B) Hes5 mRNAs relative to the reference mRNA, 18s. Data represent the mean and sem of five separate experiments. ***indicates $p<0.0001$, statistical comparison with control (*t* test).

Having established that GDF-5 promotes the expression of Hes1 and Hes5 mRNAs, the next step was to try and establish a direct link between Smad activation and Hes5 expression (Hes5 expression was analysed because it is more robustly upregulated by GDF-5 than Hes1). To do this, 6DIVs hippocampal neurons were transfected with the luciferase reporter constructs pHes5-pGL3-Luc or pHes5-SM-pGL3-Luc and cultured for a further 16 hours either without GDF-5 or with 100ng/ml GDF-5. pHes5-pGL3-Luc contains a fragment of the Hes5 promoter containing a Smad binding site that can be used to drive luciferase expression, while pH5-SM-pGL3-Luc contains mutations in the Smad-binding site of the Hes-5 promoter. The addition of GDF-5 to cultures transfected with pHes5-pGL3-Luc induces a robust increase in luciferase reporter signal in comparison to neurons transfected with pHes5-pGL3-Luc and cultured without GDF-5. The GDF-5 promoted increase in luciferase reporter signal does not occur in neurons transfected with pH5-SM-pGL3-Luc (Fig.65). This data suggested that GDF-5 increases the expression of Hes5 mRNA by a Smad-dependent mechanism.

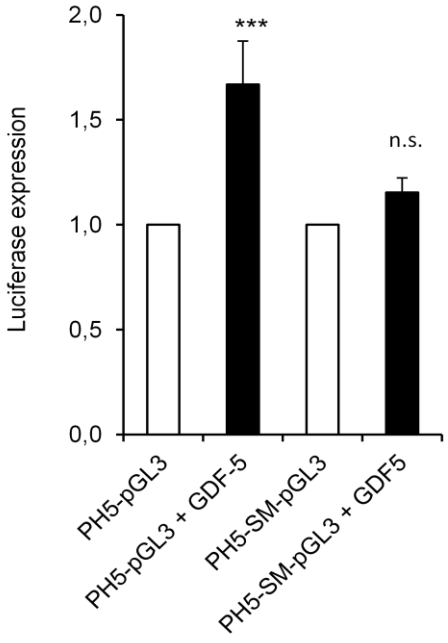

Figure 65: Activation of Hes5 promoter activity by Smads.

Hippocampal neurons that had been cultured for 6 days were transfected with pH5-pGL3-Luc or pH5-SM-pGL3-Luc. Transfected neurons were incubated for a further 16h, either in the presence or absence of 100ng/ml GDF-5, and lysed after 7DIVs and processed for luciferase activity quantification. Data represent the mean and sem of 3 separate experiments. ***indicates $p<0.0001$, n.s. non-significant, statistical comparison with control (*t* test).

To further investigate the role that Hes1 and Hes5 transcription factors play in mediating the dendrite growth promoting effects of GDF-5, 6DIVs hippocampal neurons were transfected with pCDH-CMV-MCS-EF1-copGFP alone (control) or pCDH-CMV-MCS-EF1-copGFP together with an expression plasmid encoding Hes6 (pIRES-Hes6), a transcription factor that antagonizes the functions of Hes1 and Hes5[460,461]. The overexpression of Hes6 prevents 100ng/ml GDF-5 from both promoting dendrite growth and reducing the number of primary dendrites (Fig.66). Interestingly, the overexpression of Hes6 increases the number of primary dendrites in the absence of recombinant GDF-5 and the addition of GDF-5 to cultures reverses this effect (Fig.66.A and C).

To determine whether Hes-5 upregulation is required for GDF-5 promoted dendrite growth, hippocampal neurons were transfected with a plasmid that expresses Hes5 shRNA to interfere with Hes-5 expression. The efficiency of Hes-5 knockdown by Hes5 shRNA was first confirmed in HEK 293T cells. Western blot analysis of HEK 293T cell lysates 24 hours after transfection with either Hes5 shRNA, or a plasmid containing a scrambled control RNA, reveals that cells transfected with Hes5 shRNA express significantly lower levels of Hes5 protein compared to cells transfected with scrambled RNA. (Fig.67.B). The expression of Hes5 shRNA, but not scrambled RNA, in cultured hippocampal neurons completely prevents GDF-5 promoted dendrite growth and prevents GDF-5 from reducing the number of primary dendrites (Fig.67.A, C and D).

As a final step to confirm the role that Hes5 plays in mediating GDF-5 promoted dendrite outgrowth, 6DIVs cultures of hippocampal neurons were transfected with either pCDH-CMV-MCS-EF1-copGFP (control), a plasmid that expresses WT Hes5 (pCDH-CMV-Hes5-EF1-copGFP) or a plasmid that expresses a truncated Hes5 protein that dimerises with endogenous Hes5 normally but lacks the DNA binding domain, thereby interfering with the transcriptional activity of endogenous Hes5 (pCDH-CMV-t-Hes5-EF1-copGFP). Transfected neurons were cultured for a further 16 hours, either in the absence or presence of 100ng/ml GDF-5, before being fixed, processed

and imaged. The extent of dendrite growth from neurons overexpressing Hes5 and cultured in the absence GDF-5 is comparable to that of control transfected neurons treated with GDF-5. Furthermore, GDF-5 treatment does not further increase the growth of dendrites from neurons overexpressing WT Hes5 (Fig.68.A and B). The number of primary dendrites is significantly reduced in the presence of GDF-5 in control transfected neurons compared to control transfected neurons cultured without GDF-5. Whilst, the overexpression of WT Hes5 decreases the number of primary dendrites compared to control cultures, the addition of GDF-5 to cultures transfected with WT Hes5 does not further reduce the number of primary dendrites (Fig.68.A and C). The expression of truncated Hes5 does not reduce dendrite length or increase the number of primary dendrite compared to control cultures, but it does prevent GDF-5 from promoting the growth of dendrites and reducing the number of primary dendrites (Fig.68).

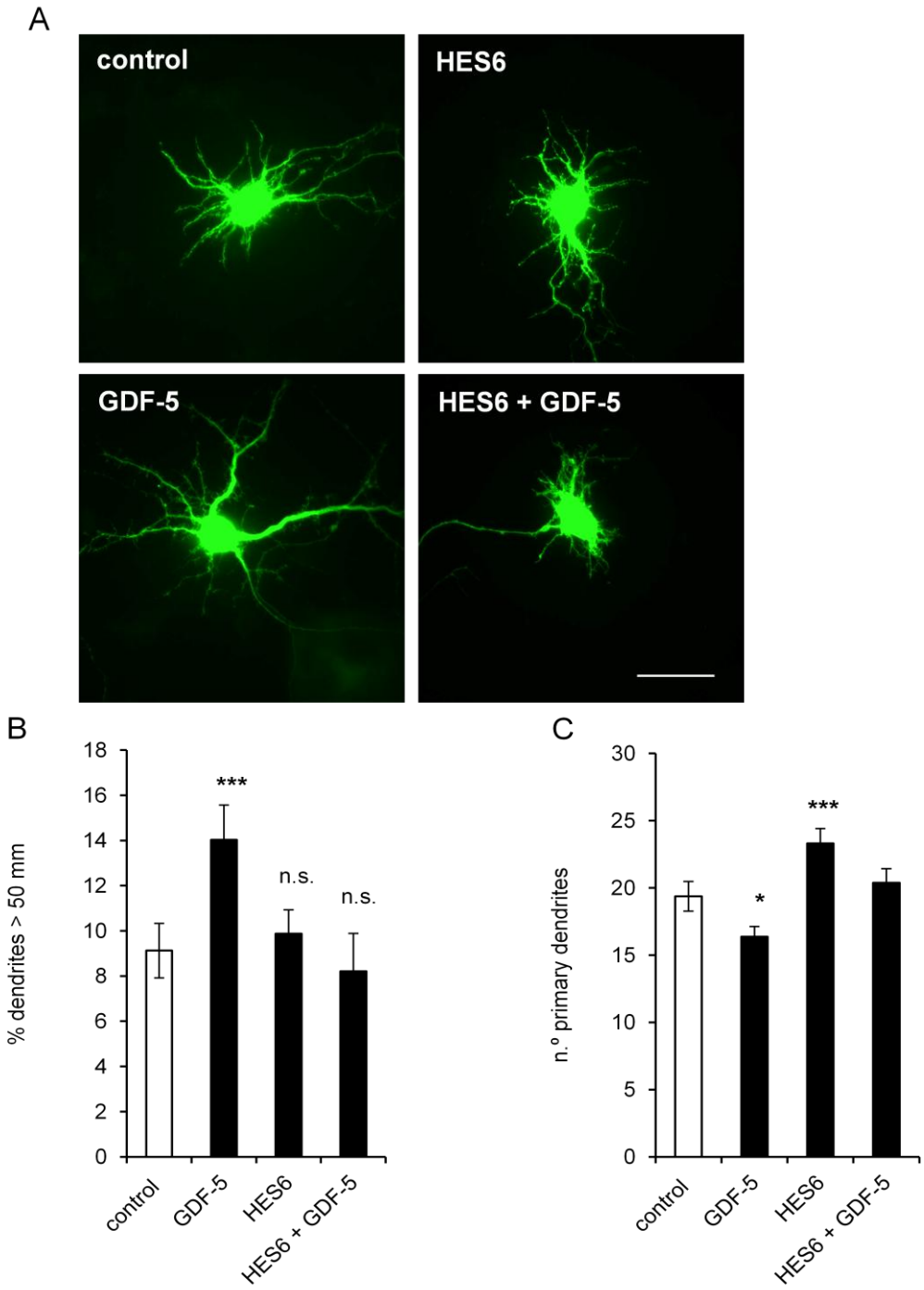

Figure 66: Hes6 overexpression prevents GDF-5 promoted dendritic growth.

Hippocampal neurons that had been cultured for 6 days were transfected with pCDH-CMV-MCS-EF1-copGFP alone or co-transfected with pCDH-CMV-MCS-EF1-copGFP plus pIRES-Hes6. Transfected neurons were incubated for a further 16h, either in the presence or absence of 100ng/ml GDF-5, fixed at 7DIVs, stained with an antibody against GFP and imaged using a fluorescence microscope. Images were analysed using Photoshop. (A) Representative photomicrographs of typical neurons cultured under the stated conditions. Scale bar: 50µm. Graphs correspond to the (B) % of dendrites > 50nm and the (C) mean number of primary dendrites. Data represent the mean and sem of 150 neurons for each condition from 3 separate experiments. *indicates $p<0.01$ and ***indicates $p<0.0001$, n.s. non-significant, statistical comparison with control (Mann–Whitney U test).

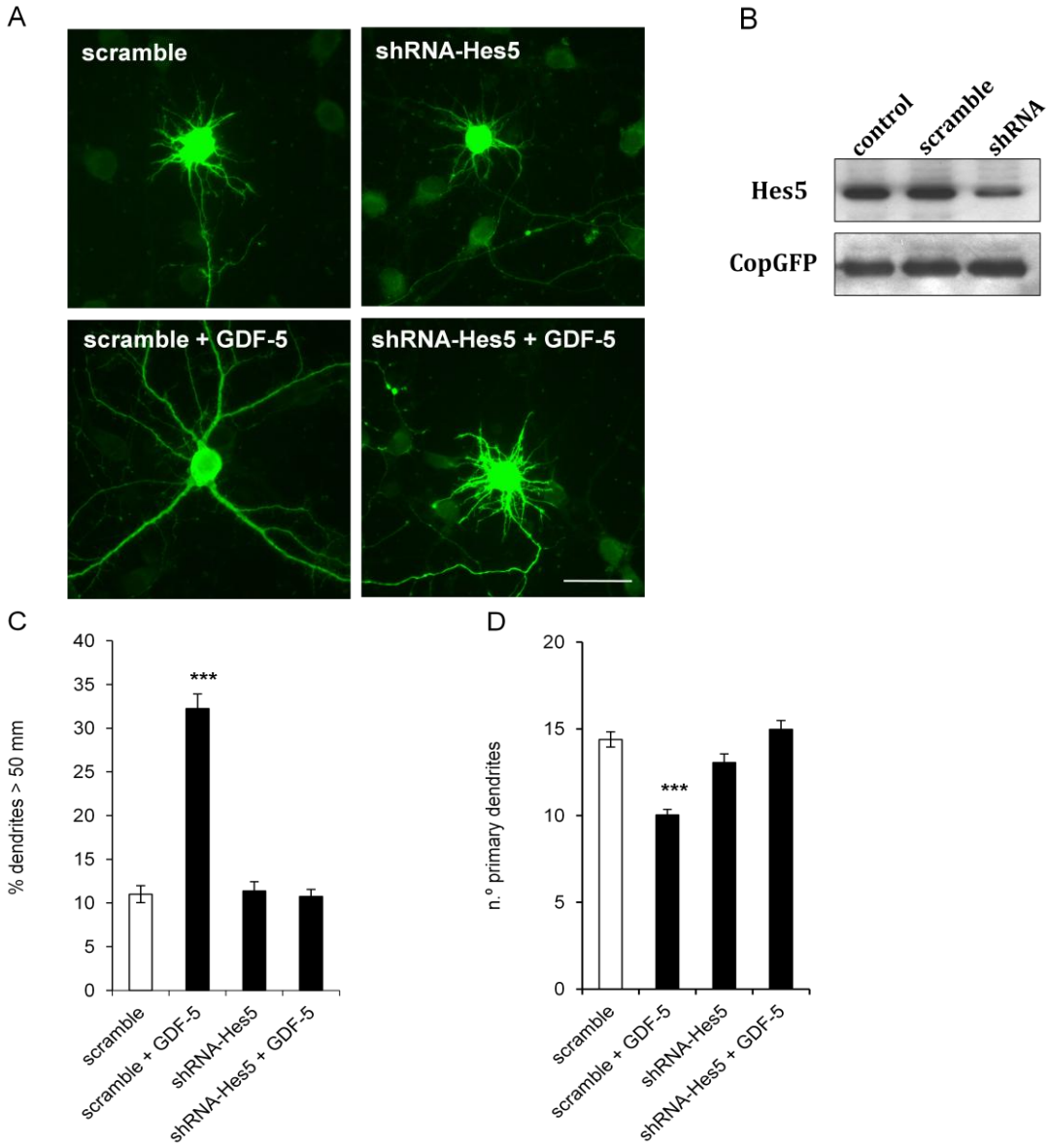

Figure 67: Hes5-shRNA prevents GDF-5 promoted dendrite growth.

Hippocampal neurons that had been cultured for 6 days were co-transfected with pCDH-CMV-MCS-EF1-copGFP containing either Hes5 shRNA (shRNA-Hes5) or a scrambled RNA. Transfected neurons were incubated for a further 16h, either in the presence or absence of 100ng/ml GDF-5, fixed at 7DIVs, stained with an antibody against GFP and imaged using a fluorescence microscope. Images were analysed using Photoshop. (A) Representative photomicrographs of typical neurons cultured under the stated conditions. Scale bar: 50µm. (B) Representative Western blot of lysates of HEK 293T cells co-transfected with pCDH-CMV-MCS-EF1-copGFP expressing Hes5 shRNA (shRNA-Hes5) or a scrambled RNA. HEK 293T cells were lysed 24h after transfection. Western blots were probed with and antibody against Hes5 and GFP. Graphs correspond to the (C) % of dendrites > 50µm and the (D) mean number of primary dendrites. Data represent the mean and sem of 150 neurons for each condition from 3 separate experiments. ***indicates p<0.0001, statistical comparison with control (Mann–Whitney U test).

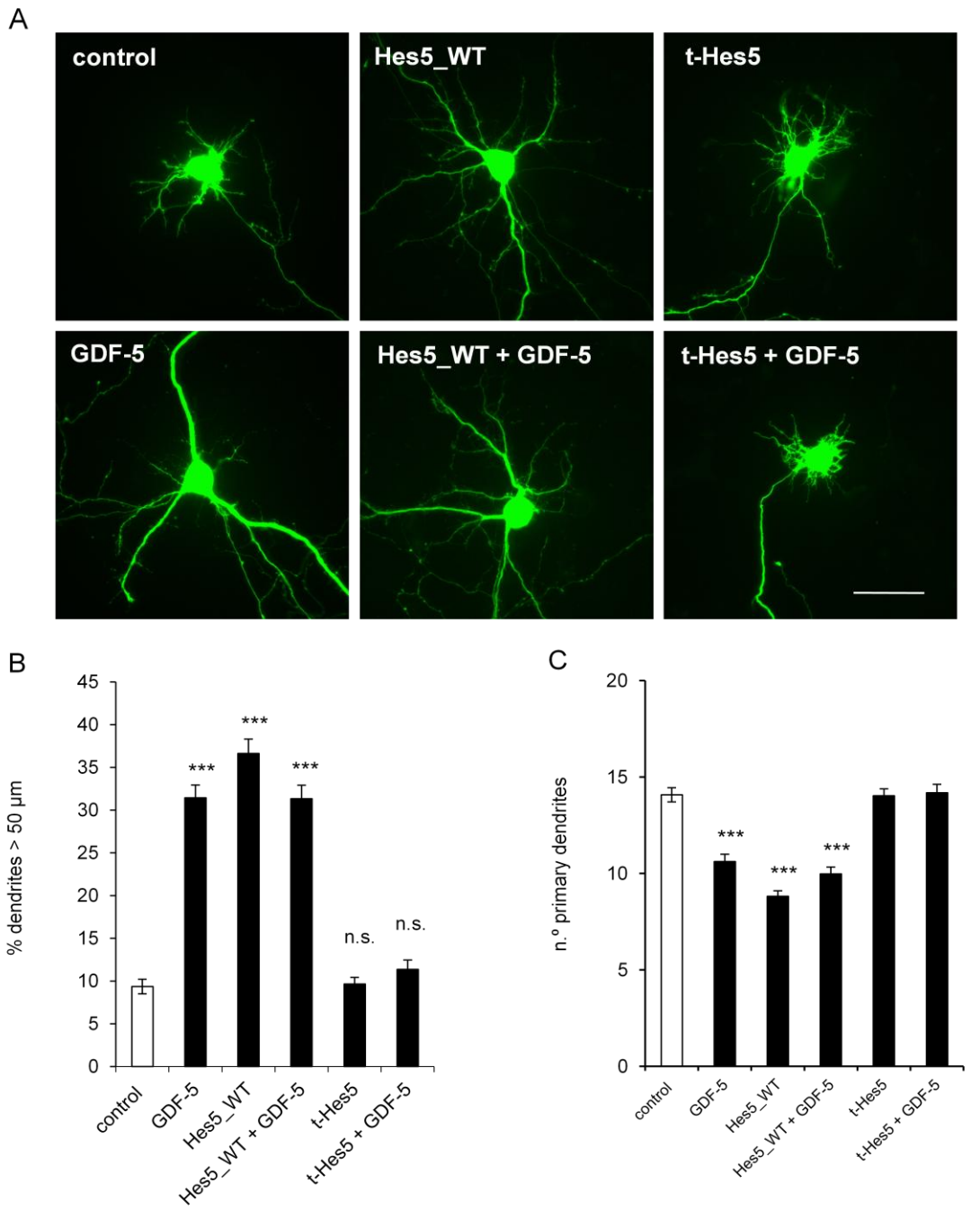

Figure 68: Hes5 regulates the growth of hippocampal neuron dendrites.

Hippocampal neurons that had been cultured for 6 days were transfected with either pCDH-CMV-MCS-EF1-copGFP (control), pCDH-CMV-Hes5-EF1-copGFP (Hes5-WT) or pCDH-CMV-t-Hes5-EF1-copGFP (t-Hes5). Transfected neurons were incubated for a further 16h, either in the presence or absence of 100ng/ml GDF-5, fixed at 7DIVs, stained with an antibody against GFP and imaged using a fluorescence microscope. Images were analysed using Photoshop. (A) Representative photomicrographs of typical neurons cultured under the stated conditions. Scale bar: 50µm. Graphs correspond to the (B) % of dendrites > 50µm and the (C) mean number of primary dendrites. Data represent the mean and sem of 150 neurons for each condition from 3 separate experiments. ***indicates p<0.0001, n.s. non-significant, statistical comparison with control (Mann–Whitney U test).

6.3.5. Hippocampal pyramidal dendrites are greatly reduced in size in brachypod mice

To assess the physiological and developmental significance of the effects of GDF-5 on dendrite growth observed *in vitro*, Golgi staining was used to visualise the dendritic arbors of pyramidal neurons in the CA1 and CA3 fields of the P10 hippocampus of WT mice and mice that are either heterozygous (Het) or homozygous (*Gdf-5*^{bp}) for the brachypod null mutation in the *Gdf-5* gene. These preparations revealed that pyramidal dendrite arbors of *Gdf-5*^{bp} mice are dramatically reduced compared with those of WT mice in both CA1 (Fig.69.A) and CA3 (Fig.69.B). Because the dendrite arbors of pyramidal neurons in CA1 are normally less exuberant than those of CA3, they were especially amenable to analysis by Sholl profiling and quantification of total dendrite length and branch point number. This analysis was carried out separately on the apical and basal parts of the dendritic arbors of large numbers of these neurons in all three genotypes. This analysis reveals highly significant reductions in total dendrite length and branch point number in both components of the dendrite arbors of both heterozygous and homozygous mice compared with WT mice (Fig.69.C and D). Accordingly, reductions in the sizes of both dendritic compartments are evident in Sholl plot, length and branching data and the Sholl profiles for heterozygous mice are intermediate between those of WT and homozygous mice.

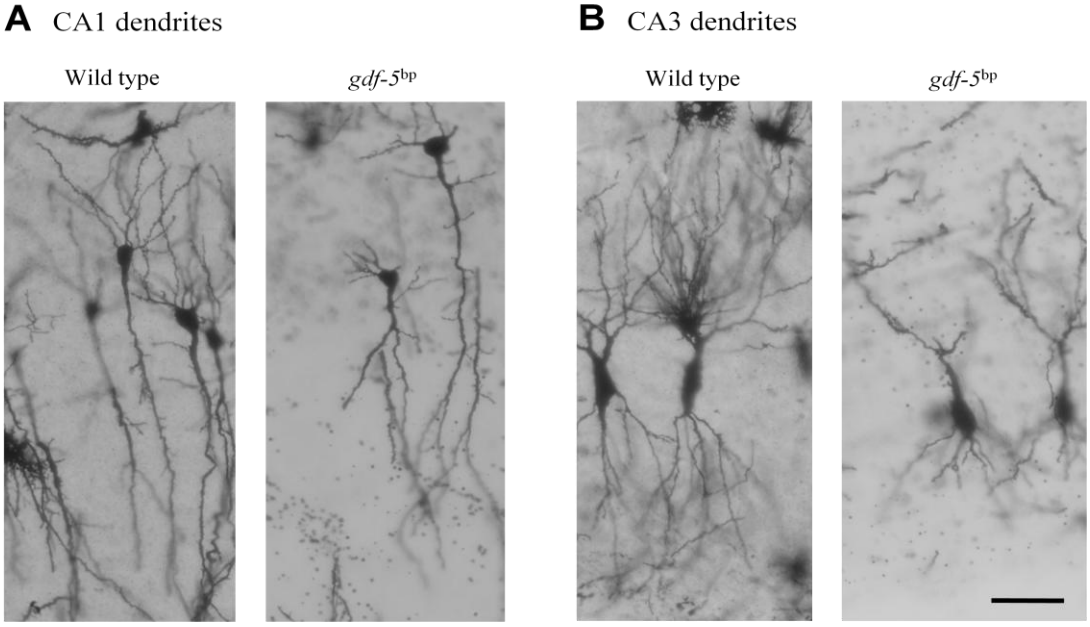

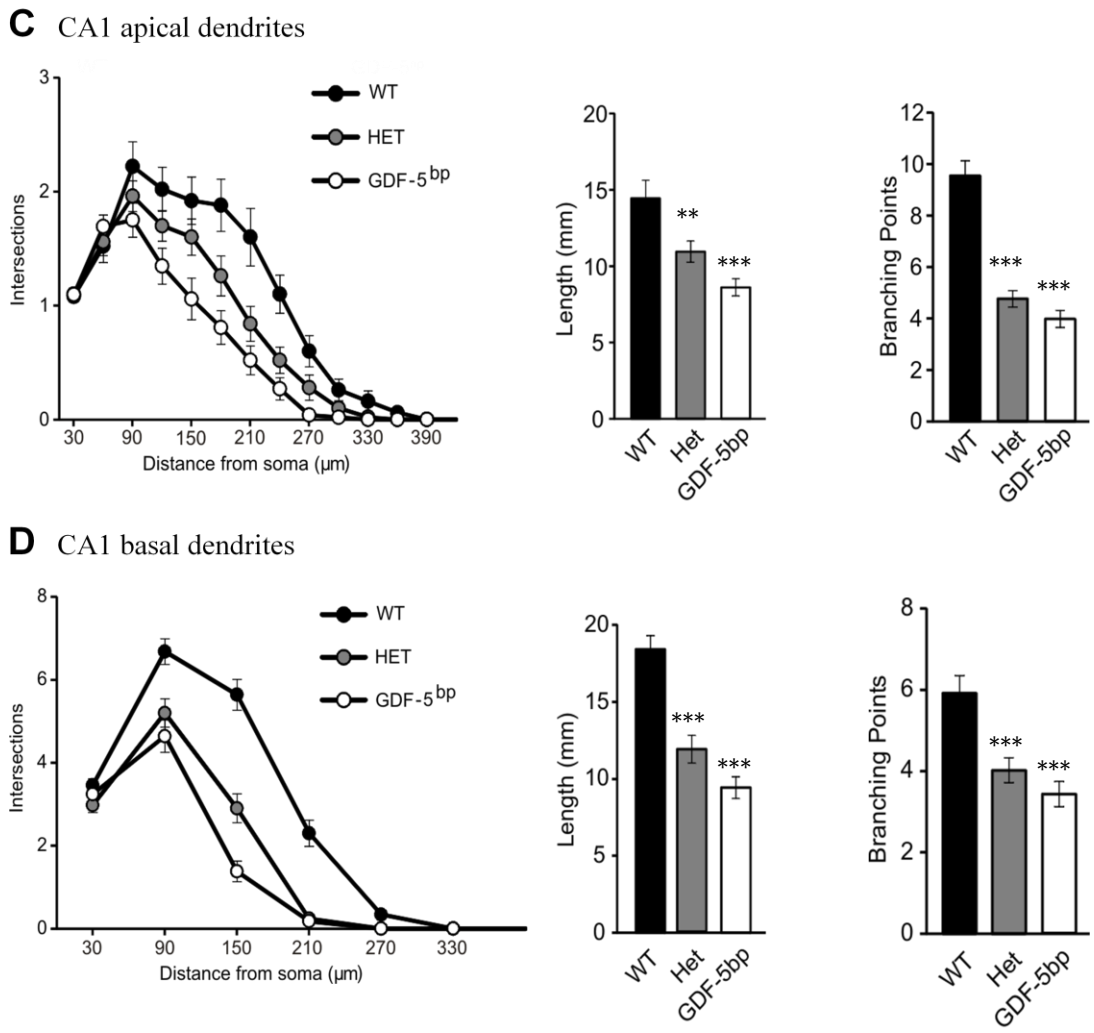

Figure 69: Reduced size and complexity of pyramidal dendrites in *Gdf-5*^{bp} mice.
Representative images of Golgi stained preparations of the hippocampi of P10 WT and *Gdf-5*^{bp} mice illustrating the typical appearance of pyramidal neurons in (A) CA1 and (B) CA3. Scale bar: 50µm. Sholl plots, total length and number of branch points in the (C) apical and (D) basal dendrites of the CA1 field of P10 hippocampi of P10 WT, *Gdf-5*^{bp} and heterozygous mice. Data represent the mean and sem of 50 neurons from at least 6 separate mice of each of each genotype. **indicates P <0.001 and ***indicates P <0.0001, statistical comparison with WT, Mann-Whitney U test).

6.4. Discussion

The data obtained in this chapter provide the first evidence that GDF-5 is a key regulator of dendritic growth in the developing nervous system and suggest that it exerts this effect by a Smad/Notch-dependent signalling mechanism.

The expression of both GDF-5 and BMP receptors in developing hippocampal pyramidal neurons raises the possibility that GDF-5 acts on these neurons by an autocrine and/or paracrine mode of action *in vivo*. Autocrine signalling is well documented in the TGF-β superfamily, and has been demonstrated for several BMPs[245,463,464]. In future work, it will be important to ascertain whether GDF-5 is constitutively synthesized and secreted by pyramidal neurons or whether its synthesis and/or release are regulated, as this has a bearing on understanding how GDF-5 participates in the regulation of dendrite growth and elaboration in the developing hippocampus.

Hippocampal neurons that have been cultured for 3DIVs in the presence of recombinant GDF-5 are morphologically indistinguishable from neurons cultured in the absence of GDF-5, demonstrating that GDF-5 does not regulate axonal outgrowth from developing hippocampal neurons (Fig.53 and 54). In contrast, 100ng/ml of recombinant GDF-5 induces significant dendrite elongation in 7DIVs cultures of hippocampal neurons, whilst simultaneously reducing the number of primary dendrites (Fig.53 and 54). Although GDF-5 does not induce changes in the length of hippocampal neuron axons, BMP family proteins have been shown to play a role in promoting axon elongation from other populations of CNS and PNS neurons. For example, BMP-7 can induce the differentiation of dorsal horn projection interneurons and initiate axonal growth from them[465]. BMP-7 can also orientate axon growth, directing growing axons away from the dorsal midline, and increase the extent of axon growth. High concentrations of BMP-7 are required to induce dorsal interneuron specification through Smad-dependent transcription. In contrast, lower concentrations of BMP-7 regulate the

orientation of growing axons via PI3K dependent signalling[465]. BMPs also promote axonal growth from cultured embryonic, but not adult, mouse DRG neurons via a Smad-dependent signalling pathway. Interestingly, reactivation of the Smad1 signalling pathway in adult mouse DRG neurons, by virally transduced overexpression of BMP-4, promotes the regeneration of ascending sensory axons in a mouse model of spinal cord injury[466]. Although recombinant GDF-5 does not promote axon elongation in cultures of embryonic mouse hippocampal neurons, it may modulate axonal growth at postnatal stages of hippocampal development or in the adult. Since it is very difficult to establish cultures from postnatal and adult hippocampus, this would need to be investigated by examining efferent and afferent hippocampal projections in transgenic mouse models, such as *Gdf-5*^{bp} and *Alk6*$^{-/-}$ mice. In addition, it will be interesting to determine whether GDF-5 has neurotrophic effects on spinal cord interneurons and DRG sensory neurons.

GDF-5 resembles NGF in its ability to promote dendrite growth and reduce the number of primary dendrites in cultures of embryonic hippocampal neurons[110]. BMP-7 has also been reported to enhance the growth of identified dendrites from cultured sympathetic[330], cortical[331] and hippocampal[332] neurons, although the physiological significance of these *in vitro* observations have not been addressed or confirmed *in vivo*. Like GDF-5, BMP-7 selectively promotes the growth of dendrites from cultured hippocampal pyramidal neurons without affecting axonal growth[332].

Having established that GDF-5 promotes the growth of hippocampal neuron dendrites, the project focused on identifying the BMP receptors that mediate this effect. In particular, the roles of the BMP receptors, BMPR-Ib/Alk6 and BMPR-II were examined. As mentioned previously, GDF-5 binds preferentially to BMPR-Ib compared to other type I BMP receptors[455,457]. However, GDF-5 can also signal via a BMPR-II/BMPR-Ia receptor complex[457] and a receptor complex consisting of BMPR-Ib and Ror2[458]. BMPR-Ib has previously been established as a regulator of nervous system development. For example, double-transgenic mice, that have a germ line null mutation in *Bmpr-Ib* together with a telencephalon specific conditional *Bmpr-Ia* null mutation, have shown that BMPR-Ib signalling is important for the generation

of the neuronal lineage within the telencephalon that gives rise to both DG granule neurons during development and stem cells that continue to generate neurons in the adult hippocampus[467]. Interestingly, adult double-transgenic mice are significantly less responsive to fear or anxiety-provoking stimuli than wild type mice[467]. Moreover, BMPR-Ib is expressed by postmitotic neurons in the E11.5 mouse dorsal spinal cord and, *in-ovo* electroporation of expression constructs encoding constitutively active forms of BMPR-Ia and BMPR-Ib has shown that BMPR-Ib mediates commissural axon outgrowth and guidance in the chicken embryo. In accordance with this, many commissural axons display an aberrant trajectory in *Bmpr-Ib* deficient mice[468]. In this chapter, transfection of cultured hippocampal neurons with expression constructs encoding either a CA or a DN forms of BMPR-Ib had identified BMPR-Ib as an essential mediator of GDF-5 promoted dendrite growth from hippocampal neurons. The expression of CA BMPR-Ib mimics the effects of adding recombinant GDF-5 to cultures by increasing the length of dendrites, whereas the expression of DN BMPR-Ib prevents GDF-5 from promoting dendrite growth and reducing the number of primary dendrites (Fig.57). The essential role of BMPR-Ib in mediating the effects of GDF-5 was confirmed by using hippocampal cultures established from *Alk6*$^{+/+}$ and *Alk6*$^{-/-}$ mouse embryos. Whilst GDF-5 increases the length of dendrites in cultures of *Alk6*$^{+/+}$ and *Alk6*$^{+/-}$ hippocampal neurons, it does not affect dendrite length in cultures of *Alk6*$^{-/-}$ hippocampal neurons. The number of primary dendrites is reduced by GDF-5 in cultures established from *Alk6*$^{+/+}$ and *Alk6*$^{+/-}$ embryos. Curiously, the number of primary dendrites is reduced in the absence of GDF-5 in cultures of *Alk6*$^{-/-}$ hippocampal neurons and the addition of recombinant GDF-5 does not reduce the number of primary dendrites further (Fig.58). This may suggest that the loss of functional BMPR-Ib induces compensatory alterations in the expression levels of other type I BMP receptors that in turn alters the response of hippocampal neurons to autocrine/paracrine GDF-5 and/or other BMPs.

Hippocampal neurons overexpressing the BMPR-II receptor display an increase in dendrite length in the absence of recombinant GDF-5, whereas neurons transfected with an expression construct encoding a DN form of

BMPR-II are unable respond to recombinant GDF-5 by increasing the length of their dendrites (Fig.59). These data clearly show that BMPR-II plays an important role in mediating GDF-5 promoted dendrite growth. The overexpression of BMPR-II or the expression of DN BMPR-II both reduce the number of primary dendrites compared to control neurons in the absence of recombinant GDF-5. This reduction in the number of primary dendrites is of a similar magnitude to that produced when control transfected neurons are cultured with 100ng/ml GDF-5. Whilst this data is counter intuitive, it may reflect that GDF-5 can signal through other type II BMP receptors, in a redundant manner, to regulate the number of primary dendrites. Although the primary role of type II BMP receptors is thought to be to phosphorylate and activate type I BMP receptors upon ligand binding, thereby initiating Smad-dependent signalling[273,274], some studies suggest that BMPR-II can signal autonomously. A link has previously been made between BMPR-II dependent signalling and the regulation of actin dynamics in non-neuronal cell lines[469]. In the absence of ligand binding, the cytoplasmic domain of BMPR-II associates with LIM Kinase 1 (LIMK1), thereby inactivating it. LIMK1 is a kinase that phosphorylates and inactivates cofilin, preventing cofilin from promoting actin depolymerisation. Upon BMP-4 stimulation, LIMK1 dissociates from the cytoplasmic tail of BMPR-II resulting in cofilin phosphorylation and an increase in actin stability[469]. Evidence from a motor neuron like cell line, NSC-34, suggests that BMPR-II dependent signalling may also play a role in regulating motor neuron differentiation. BMPR-II is upregulated and accumulates in the soma and growth cones of NSC-34 cells when they are stimulated to differentiate into neuronal type cells by culture in minimal media without serum[470]. Interestingly, the addition of BMP-2 to differentiating cultures increases the expression of BMPR-II whilst concomitantly inhibiting NSC-34 cell differentiation.

Having identified BMPR-Ib/BMPR-II as the receptor complex that can mediate GDF-5 promoted dendrite growth; the next step of the project was to determine the intracellular signalling pathways that are activated following the binding of GDF-5 to its receptors. It is well established that Smad transcription factors comprise an important signalling pathway downstream of activated

BMPR complexes[274,293]. Ligand/receptor binding induces serine phosphorylation of receptor-regulated Smads, allowing them to form complexes with Smad4 that translocate to the nucleus where they regulate the transcription of a wide variety of target genes by binding to the respective promoter elements of these genes[471]. The first indication that GDF-5 promotes dendrite growth from hippocampal neurons by a Smad-dependent signalling cascade came from the observation that the addition of GDF-5 to hippocampal cultures induces a rapid and sustained phosphorylation of Smad1, Smad5 and Smad8 (Fig.60). Moreover, the expression of DN Smad4 completely eliminates GDF-5-promoted dendrite growth and reduces the length of hippocampal neuron dendrites compared to control transfected neurons in the absence of GDF-5 (Fig.61). Since Smad4 is a common link in Smad-dependent signalling, this latter observation may indicate that Smad-dependent signalling mediates dendrite elongation from hippocampal neurons by other endogenously synthesized and secreted trophic factors or that autocrine/paracrine GDF-5 signalling promotes dendrite growth in the absence of exogenous recombinant GDF-5. Additional evidence that Smads mediate GDF-5 promoted dendrite growth comes from the observation that overexpression of the inhibitory Smads, Smad6 and Smad7, in cultured hippocampal neurons abolishes GDF-5 promoted dendrite growth (Fig.62). Finally, the addition of GDF-5 to hippocampal neurons transfected with a luciferase reporter construct containing a BMP response element increases luciferase activity and this affect can be blocked by co-expression of either Smad6 or Smad7 (Fig.63). Taken together, these results strongly suggest that Smad signalling plays a crucial role in mediating the striking effects of GDF-5 on pyramidal neuron dendrite growth in the developing hippocampus.

Whilst the link between Smad signalling and the regulation of neurite growth is not well established in the literature, some examples have emerged. In cultured sympathetic neurons, BMP-7 treatment leads to phosphorylation and nuclear translocation of Smad1 and expression of DN Smad1 inhibits BMP-7 induced dendritic growth[472]. Conversely, BMP-2 activates Smads1, 5 and 8 and inhibits neurite growth in cultured cerebellar neurons[473]. The role that Smad-independent signalling pathways play in mediating GDF-5

promoted dendrite growth from hippocampal neurons is certainly worth investigating in future studies. From previously published literature, one pathway that will be worth investigating is the activation of the JNKs; JNK1, JNK2, and JNK3. Following the addition of BMP-7 to cortical neuron cultures, JNKs have been shown to rapidly associate with the C-terminal of BMPR-II where they become activated and promote local microtubule stabilization and dendrite formation[474].

The Hes5 transcription factor gene is among the many genes that possess a Smad binding motif in its promoter[346], and together with its homologue Hes1, Hes5 has been linked to the regulation of dendrite growth by both Notch-delta signalling and NGF induced, p75 mediated, NF-κB signalling in cultured hippocampal neurons[110]. All four neurotrophins NGF, BDNF, NT3 and NT4, increase the levels of Hes1 and Hes5 mRNAs when added to 7DIVs hippocampal cultures. High levels of these transcription factors decrease dendrite initiation, reducing the number of primary dendrites, and allow NGF to stimulate dendrite elongation[110]. Similar results are observed in hippocampal pyramidal neurons cultured in the presence of GDF-5. GDF-5 enhances Hes1 and Hes5 mRNA expression in hippocampal neurons in a similar manner to neurotrophins (Fig.64). GDF-5 also enhances transcriptional activity from an intact Hes5 promoter, but not one that has a disrupted Smad binding motif, suggesting that Hes5 is a direct transcriptional target of GDF-5-activated Smad signalling in hippocampal neurons (Fig.65). The bHLH gene Hes6 is known to inhibit the ability of Hes1 to regulate transcription[475] and, in the chicken embryo, overexpression of cHES6-2 can represses the expression of cHes5[476]. In accordance with this, overexpression of Hes6 prevents GDF-5 from promoting dendrite elongation from hippocampal neurons (Fig.66). A requirement for an increase in the expression of functional Hes5 for GDF-5 promoted dendrite growth was demonstrated by two separate approaches: shRNA knockdown of Hes5 and the expression of a truncated, non-functional Hes5 protein (Fig.67 and Fig.68). In both cases, compromising the function of Hes5 completely eliminates the ability of GDF-5 to enhance dendrite elongation from cultured

hippocampal neurons. Finally, Hes5 overexpression in cultured hippocampal neurons promotes dendritic growth in the absence of GDF-5 and the addition of recombinant GDF-5 does not further enhance dendrite length. Together, this data demonstrate that Smad-dependent upregulation of Hes5 is an essential part of the signalling mechanism that GDF-5 uses to increase dendrite length.

The bHLH proteins, Hes1 and Hes5 are essential effectors for Notch signalling and regulate the maintenance of undifferentiated cells, such as neuronal stem cells. Hes1 and Hes5 repress the expression of genes that promote neuronal differentiation and *Hes1/5* deficient mice display premature neuronal differentiation[477]. However, the roles that these two transcription factors play in postmitotic neurons during development and in the adult are still largely unknown[478]. How Hes5 regulates the molecular machinery that modulates dendrite growth is not understood. In future work it will be important to determine the genes that are subject to Hes5-dependent transcriptional activation and repression and ascertain how they regulate the cytoskelatal changes that lead to dendrite elongation.

To validate the physiological relevance of GDF-5 promoted dendrite growth in cultures of embryonic hippocampal neurons, dendrites from P10 WT, Het and *Gdf-5*^{bp} mice were subject to Sholl analysis in Golgi stained preparations. The dendrites of P10 hippocampal pyramidal neurons in mice lacking GDF-5 are markedly stunted compared with those of WT mice. The intermediate, though highly significant, reduction in the size and complexity of pyramidal neuron dendrites in mice that are heterozygous for the *Gdf-5*^{bp} null mutation clearly demonstrates a gene dosage effect, implying that dendrite size and complexity are exquisitely sensitive to the levels of endogenous GDF-5 in the hippocampus. Quantitative analysis of the CA1 region from *Gdf-5*^{bp} mice indicates that both the apical and basal components of the dendritic arbors of pyramidal neurons are very significantly smaller and less branched than those of age-matched WT mice (Fig.69). Although both components of the dendritic arbors of these neurons are very significantly stunted in *Gdf-5*^{bp}, they are nonetheless morphologically discernible. This suggests that the early differentiation of the dendritic arbors of pyramidal neurons into apical

and basal components is unaffected in *Gdf-5*^{bp} mice, but that the subsequent growth and elaboration of both components is impaired. These analyses were carried out at P10, when the dendritic arbors of hippocampal pyramidal neurons are normally well developed *in vivo*, and are some 10 days after the peak of GDF-5 mRNA expression in the developing hippocampus. In future work, it will be informative to determine exactly when in development the abnormal pyramidal neuron phenotype first becomes apparent in *Gdf-5*^{bp} mice and whether further changes occur in these dendrites as the mice age, which might indicate an ongoing role for GDF-5 in dendrite maintenance and/or plasticity.

Since the *in vitro* data clearly shows that GDF-5 promoted dendrite growth can be mediated by a BMPR-Ib/BMPR-II receptor complex, it will be valuable to analyse dendrite morphology in *Bmpr-Ib*^{429} and *Bmpr-II*^{301} null-mutant mice in future work. Given that there is a degree of functional redundancy between type I and type II BMPR, and BMPR-Ib and BMPR-II are receptors for other members of the BMP family, it seems unlikely that the hippocampal phenotype of *Bmpr-Ib* and *Bmpr-II* deficient mice will be a copy of *Gdf-5*^{bp} mice. For example, the phenotype may be less severe if there is a compensatory upregulation of other type I or type II BMPR. Alternatively, the phenotype may be more severe in *Bmpr* deficient mice compared to *Gdf-5*^{bp} mice if the functions of other BMP family members that may regulate hippocampal neuron morphology are disrupted. It would also be informative to quantify to the levels of Hes5 transcripts and protein in the hippocampi of *Gdf-5*^{bp}, *Bmpr-Ib* and *Bmpr-II* mutant mice at different developmental time points and compare them to the levels in wild type mice. As a first step to gaining an insight into the functional consequences of shortened dendritic arbors in G*df-5*^{bp} mice, hippocampal slices prepared from P10 WT, Het and *Gdf-5*^{bp} mice should be subject to investigation by electrophysiological recording. If *Bmpr-Ib* and *Bmpr-II* deficient mice prove to have abnormal dendritic arbors, hippocampal slices should also be prepared from them and age matched WT mice for investigation by electrophysiology.

To better understand the functional consequences of the lack of GDF-5/BMP receptor signalling in the developing hippocampus, adult *Gdf-5*^{bp} mice need to be subjected to a battery of behavioral tests and their performance in these tests compared to adult wild type mice. Appropriate behavioural tests include T-maze continuous alternation task (T-CAT), context dependent fear conditioning (CDFC), and MWM[479]. Since homozygous *Gdf-5*^{bp} mice have shortened limbs and impaired movement compared to WT mice, they cannot be used for behavioural testing. However, heterozygous *Gdf-5*^{bp} mice are physically indistinguishable from WT mice and have significantly smaller dendrites than their WT counterparts at P10. Therefore, comparative behavioural testing between heterozygous *Gdf-5*^{bp} and WT mice may yield valuable data on the functional consequences of shortened hippocampal neuron dendrites. A more satisfactory approach to determining the functional consequences of a lack of functional GDF-5/BMP signalling during hippocampal development, would be to use a conditional loxP/Cre transgenic approach to ablate functional GDF-5/BMP receptor signalling specifically in the nervous system or, even better, specifically in the CA regions of the hippocampus. Such an approach would circumvent the problems with limb development and allow in depth behavioural testing of mice totally lacking GDF-5 expression in the developing hippocampus in comparison to WT mice. At present, mice containing floxed exons within either the *Gdf-5* or *Bmpr-Ib* gene have not been generated. However, it may be worth the time and financial investment to generate these mice. Moreover, the use of transgenic mice carrying a neuron specific creERT2 transgene that allows temporally controlled, tamoxifen inducible deletion of floxed exons[480] would allow an investigation of the roles of GDF-5/BMP receptor signalling specifically in the adult hippocampus, especially with regards to potential roles for GDF-5 in LTP in learning and memory.

Taken together, this work demonstrates a novel physiological role for GDF-5 in the developing mouse hippocampus. GDF-5 regulates the developmental elongation of hippocampal pyramidal neuronal dendrites. This finding needs to be further explored in subsequent studies, so that the functional consequences of a lack of GDF-5/BMP receptor signalling in the developing and adult hippocampus can be determined and other potential roles for GDF-5 in the developing and adult hippocampus can be identified.

Chapter 7

General Discussion, Conclusions and Future Work

7. General Discussion, Conclusions and Future Work

The overall aim of this study was to identify novel neurotrophic factors for developing mouse hippocampal neurons. In particular, to identify proteins that could promote the growth and elaboration of neuritic processes from hippocampal neurons and characterise the signalling pathways that these proteins use to promote growth. The two candidate proteins selected for investigation were the TNF superfamily member, APRIL and the TGF-β family member, GDF-5. To provide evidence that these proteins could potentially be neurotrophic factors for developing hippocampal neurons, first, the expression of APRIL, GDF-5 and their cognate receptors was analysed in dissociated hippocampal cultures established from E18 mouse embryos and sections of the hippocampus from embryonic and postnatal mice. Expression was analysed at both the mRNA and protein level using a wide range of techniques. Having established that both ligands and their receptors are expressed by developing hippocampal neurons, it was investigated whether APRIL and GDF-5 could modulate process outgrowth from cultured hippocampal neurons. Both proteins regulated the morphology of hippocampal neurons, with APRIL and GDF-5 promoting the growth of axons and dendrites, respectively. Next, the receptors and intracellular signalling pathways that mediate enhanced process outgrowth by both factors were characterised. Finally, the physiological relevance of APRIL and GDF-5 promoted process outgrowth in hippocampal cultures, was assessed using transgenic mouse models.

Reverse transcriptase real-time PCR, Western blotting, immunocytochemistry and immunohistochemistry were used to demonstrate that APRIL and its receptor, BCMA are expressed by developing hippocampal neurons. In contrast, the alternative APRIL receptor, TACI was barely detectable by real-time PCR and Western Blotting and not detectable by immunocytochemistry or immunohistochemistry. APRIL and BCMA are both present in the soma and axons of cultured hippocampal neurons and expressed at increasingly high levels in the stratum pyramidale of the CA region of the hippocampus as development proceeds from E18 to P10. Moreover, APRIL is secreted from cultured hippocampal neurons into the culture medium. Together, the expression data suggested that APRIL-BCMA autocrine/paracrine signalling might regulate some aspect of hippocampus development (Chapter 3).

The addition of recombinant APRIL to cultures of E18 hippocampal neurons was shown to significantly increase axon length, but have no effect on dendrite morphology. A combination of cell culture, together with the transfection of expression vectors encoding full length and truncated BCMA, pharmacological inhibition of signalling molecules and Western blotting, was used to characterise the signalling pathways that APRIL uses to promote axon growth. BCMA mediates the axon growth enhancing effects of APRIL and HSPGs are not required for effective APRIL signalling. The binding of APRIL to BCMA leads to the activation of ERK1/2 and PI3K/Akt signalling pathways and inhibition of either pathway prevents axon growth promoted by APRIL. Activation of GSK-3β, by supplementation of cultures with LPA, also prevents APRIL promoted axon growth and APRIL induces the phosphorylation of GSK-3β, and hence its inhibition (Chapter 4). The inhibition of GSK-3β activity has previously been shown to enhance axonal elongation[416,417,482]. It is currently not clear what the interaction between ERK1/2 and PI3K/Akt signalling is, nor is it clear whether activated Akt and/or ERK1/2 mediates the phosphorylation of GSK-3β. The signalling pathways that mediate APRIL promoted growth of hippocampal neuron axons are summarised in figure 74.

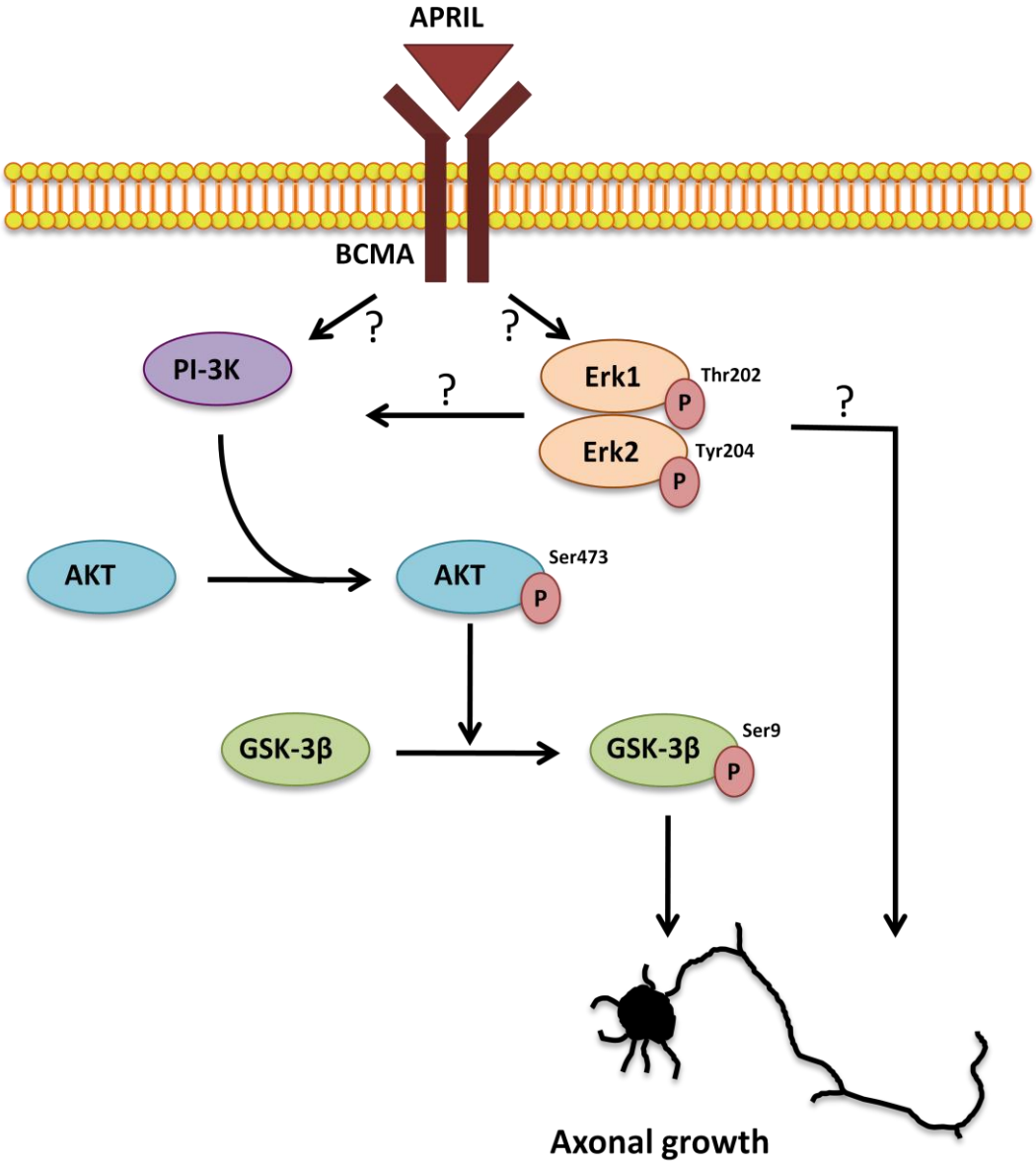

Figure 74: APRIL promotes hippocampal axonal growth by binding to BCMA and inducing the activation of ERK1/2 and PI3K/Akt signalling. The phosphorylation of GSK-3β is downstream of PI3K/Akt and/or ERK1/2 signalling. Question marks denote signalling steps that have yet to be characterised and/or validated.

Although a role for APRIL in the nervous system is described for the first time in this thesis, other members of the TNFSF have previously been investigated as possible extracellular cues for the survival and morphogenesis of neurons. For example, TWEAK, which is located in the same chromosome as APRIL allowing the formation of a splicing-derived fusion ligand, TWE-PRIL, has been studied in the nervous system, particularly in a neuropathological context[483-485]. TWEAK and its receptor, Fn14 are upregulated in rodent models of stroke and contribute to ischemic cell death[483,485]. Interestingly, TWEAK-Fn14 signalling appears to contribute to the protection from stroke damage that is afforded by a preconditioning injury[484]. Fn14 is induced in mouse DRG neurons following sciatic nerve damage[238]. Overexpression of Fn14 in PC12 cells promotes neurite outgrowth by a TWEAK independent mechanism that is dependent upon activation of the small GTPase, Rac1 suggesting that the upregulation of Fn14 by DRG neurons following sciatic nerve damage may contribute to nerve regeneration[238]. Preliminary experiments have shown that TWEAK and Fn14 mRNA are expressed in developing hippocampal neurons (data not shown). Recombinant TWEAK significantly increases the extent of axonal and dendritic outgrowth in E18 mouse hippocampal cultures (data not shown). Whilst these results need additional confirmation, they suggest a possible role for TWEAK-Fn14 signalling in modulating neurite development in the hippocampus. It will be interesting to further explore the role of TWEAK in the developing hippocampus and examine TWEAK-Fn14 mediated signal transduction.

The extension of an axon is a highly regulated process that comprises extracellular signals, gene expression in the nucleus, anterograde transport of proteins and their incorporation into the cytoskeleton[482]. Intracellular processes can limit axon extension in the absence of stimulation by extracellular factors; therefore, signalling initiated by extracellular factors facilitates long distance axon extension. Neurotrophins are the most extensively characterized group of extracellular factors that induce axon growth by binding to and activating their corresponding receptors[482]. The identification of APRIL as an extracellular signal that regulates axon elongation raises several important questions. One of these questions concerns the identity of the intracellular signalling processes

that result in axon growth and their similarity to the signalling pathways used by neurotrophins to regulate process outgrowth. The data in Chapter 4 have revealed that APRIL-BCMA signalling promotes the activation of ERK1/2 and PI3K in cultured hippocampal neurons. PI3K has previously been shown to play an important role in controlling axonal elongation and specification. PI3K regulates localized axonal growth at the growth cone by regulating GSK-3β activity and consequently microtubule polymerization[486]. GSK-3β has multiple substrates including proteins that bind to the plus ends of the microtubules stabilizing their growing ends such as: adenomatous polyposis coli (APC)[416], CLIP-associated proteins (CLASP)[487] and CRMP-2[417]. Other GSK-3β substrates include the microtubule associated proteins, MAP1B and tau[486,488]. Inactivation of GSK-3β prevents the phosphorylation of APC, thereby allowing it to bind to the microtubule plus ends and promote microtubule assembly[416]. Likewise, non-phosphorylated, active CRMP-2 interacts with tubulin heterodimers and promotes microtubule assembly[417]. Assessing the level of phosphorylation of GSK-3β substrates in hippocampal neurons that have been treated with APRIL, compared to non-treated neurons, would facilitate an understanding of the mechanisms by which APRIL regulates axon elongation.

Furthermore, as mentioned previously, during neuronal morphogenesis axonal growth cone is modulated by molecular interactions between microtubules and actin filaments[38]. Local inactivation of GSK-3β at the growth cone has been shown to promote growth cone extension. This might occur through increasing microtubule stability with the consequent accumulation of material within the growth cone. Moreover, inactivation of GSK-3β also leads to a reduction of both extension and retraction of filopodia in the growth cone[489]. Others studies have demonstrated that inactive phosphorylated GSK-3β colocalises with F-actin in neuronal cells and Sema3 activates GSK-3β leading to growth cone collapse[490]. Additionally, GSK-3β can influence filopodial dynamics in growth cones through some of its substrates. For instance, CLASP has been shown to bind to actin filaments in the growth cones[491] or to actin-binding proteins[492]. Also, it has been suggested that MAP1b phosphorylation modules filopodia dynamics. In fact, DRG neurons from a *Map1b* deficient mutant mouse show a reduction in axon elongation and an increase in growth cone area[493].

Although, cultures treated with APRIL at 7DIVs show no differences in the development and morphology of primary dendrites, it is still unclear whether APRIL could affect dendrite development at other developmental stages. The data have shown no immunostaining of APRIL or BCMA on hippocampal dendrites at 7DIVs. In fact, the staining profile of both proteins was localised in the soma and axons. Furthermore, early PI3K-Akt-GSK-3β signalling is often associated with early stages of axonal growth, which may partly explain the lack of effect of extracellular APRIL on early dendrite development.

Axon specification and the acquisition of polarity are closely linked with axon elongation and share some of the same signalling molecules and pathways. PI3K-dependent activation of the Rho GTPase, Rac1, which is enriched in the axons of developing hippocampal neurons[494], has been shown to inhibit the activity of RhoA, a negative regulator of actin polymerization, thereby inducing axon specification[495]. The mPar3-mPar6-aPKC complex also plays a role in regulating hippocampal neuron polarity. PI3K activity is necessary for the correct localisation and activation of the mPar3-mPar6-aPKC complex and the Rho GTPase, Cdc42 at the tip of future axons. Since Cdc42 increases the activity of the mPar3-mPar6-aPKC complex and PI3K increases the activity of Cdc42, PI3K activity ensures a positive feedback loop that acts to reorganize the cytoskeleton and modulate intracellular trafficking to allow the rapid axon extension[42,496]. It will certainly be interesting to determine in the future whether the mPar3-mPar6-aPKC complex, Cdc42 and Rac1 are targets of activated PI3K following the addition of APRIL to cultured hippocampal neurons.

In addition to further clarifying the signalling mechanisms that lead to APRIL promoted axon elongation in developing hippocampal neurons, it will be important to explore whether APRIL-BCMA signalling has a role in the adult hippocampus, either with regard to the aetiology of neuropathologies associated with the hippocampus, such as Alzheimer´s disease, or in modulating plasticity, learning and memory. There is a significant body of evidence suggesting that aberrant GSK-3β signalling may contribute to the development of Alzheimer´s disease. Tau is a neuronal microtubule-associated protein that is important for

establishing neuronal polarity and plays a role in regulating axonal transport[497]. Whilst Tau can be phosphorylated by a number of different kinases, it is a major target of GSK-3β. GSK-3β phosphorylates sites in Tau that are important for microtubule binding, thereby preventing Tau from interacting with microtubules with the result that microtubule stability and dynamics are altered. In the brain of patients with Alzheimer´s disease, Tau protein becomes abnormally hyper-phosphorylated changing from 2-5 phosphate groups per molecule to up to 10[498]. The resulting enhanced Tau detachment from microtubules is likely to favour Tau aggregation into paired helical filaments and neurofibrillary tangles and lead to microtubule disruption, pathological phenomena frequently observed in Alzheimer´s disease[499]. Transgenic mice overexpressing *Gsk-3β* display Tau hyperphosphorylation, disrupted microtubules and increased cell death within their hippocampi[500]. Moreover, lithium chloride induced inhibition of GSK-3β in transgenic mice expressing a mutant form of *Tau* (that leads to the production of neurofibrillary tangles, axonal degeneration and behavioural deficits) significantly reduces the levels of Tau phosphorylation and reduces axonal degeneration[501]. One of the hallmarks of Alzheimer´s disease is the accumulation of Aβ peptides. Curiously, GSK-3α, but not GSK-3β, is required for processing the APP leading to an increased production of Aβ[502]. In hippocampal neuron cultures, Aβ peptides induce inactivation of PI3K. Reduced PI3K activity results in increased GSK-3β activity, enhanced Tau phosphorylation and neuronal death[503]. Although aberrant GSK-3β activity is unlikely to be the sole underlying cause of Alzheimer´s disease, it may potentiate the development of Alzheimer´s disease by augmenting Aβ production and Tau hyper-phosphorylation. Since APRIL-BCMA signalling appears to reduce GSK-3β activity within hippocampal neurons, it may have a neuroprotective effect on these neurons as they age and could delay the onset of Alzheimer´s disease pathology and symptoms. In accordance with this, *April* and/or *Bcma* null mutant mice may be more likely to display Aβ accumulation and Tau hyperphosphorylation as they age and this is something that should be investigated. In addition, it will be interesting to determine whether crossing *April* and/or *Bcma* null mice with some of the many Alzheimer´s disease mouse models that express mutant APP and tau isoforms[504] accelerates the development of Alzheimer´s disease pathology and behavioural deficits.

In Chapter 5, the expression of GDF-5 and its receptors, BMPR-Ib and BMPR-II, were characterised in the developing hippocampus by reverse transcriptase real-time PCR, Western blotting, immunocytochemistry and immunohistochemistry. Whilst GDF-5 is mainly detected in the nucleus and cytoplasm of pyramidal neurons, its receptors are predominantly expressed in the cytoplasm and dendrites of these neurons. The expression pattern of both ligand and receptors suggested a possible role for GDF-5 in regulating some aspect of hippocampal neuron development. In addition, the expression of GDF-5, BMPR-Ib and BMPR-II within individual hippocampal neurons raised the possibility that GDF-5 may act in an autocrine and/or paracrine way to exert potential trophic effects. Further work will be needed to clarify whether GDF-5 is constitutively synthesised and secreted by pyramidal neurons or whether its synthesis and/or release are regulated.

In Chapter 6, potential roles for GDF-5 in the developing hippocampus were explored by culturing E18 hippocampal neurons in the presence or absence of GDF-5 and measuring axonal and dendritic lengths. This revealed that GDF-5 substantially increases dendrite, but not axon, elongation from cultured hippocampal neurons. Further investigation identified BMPR-Ib and BMPR-II as receptors that mediate the growth promoting effect of GDF-5 on dendrites and revealed that the signalling mechanism downstream of BMPR involves activation of Smads 1/5/8 and upregulation of the Hes5 transcription factor. *In vivo*, the apical and basal dendritic arbors of pyramidal neurons throughout the hippocampus are markedly stunted in homozygous and heterozygous *Gdf-5*^{bp} mutants at P10, in comparison to WT mice, indicating that dendrite size and complexity are exquisitely sensitive to the level of GDF-5 in the developing hippocampus. The signalling pathway that mediates GDF-5 promoted dendrite growth is summarised in figure 75.

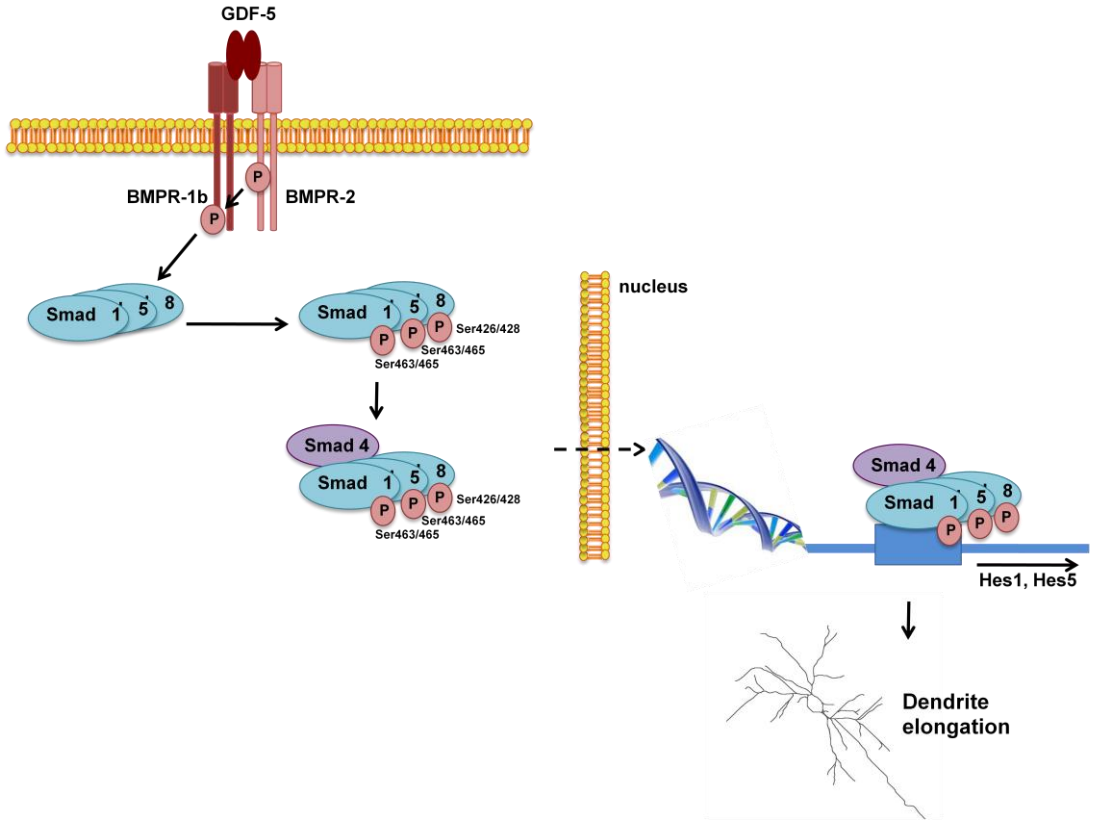

Figure 75: GDF-5 promotes hippocampal dendrite elongation by binding to a receptor complex consisting of BMPR-Ib and BMPR-II. Ligand binding leads to activation and nuclear translocation of Smads 1/5/8 and induction of Hes1/Hes5 transcription factors expression.

Although the results do not reveal any effect of GDF-5 on axonal growth at 3DIVs, a possible role for GDF-5 in regulating axon growth could be further investigated. The expression of BMPR-Ib mRNA increases with development (Fig.46) and at 7DIVs it is possible to distinguish expression of both BMPR-Ib and BMPR-II proteins (Fig.47). Hence, although technically more challenging, axonal extension should be analysed at later stages.

Whilst the data in this thesis has identified that GDF-5 is a novel, key regulator of the growth and elaboration of pyramidal dendrites in the developing hippocampus, further investigation is needed to determine the functional consequences of reduced GDF-5/BMP receptor signalling for hippocampal function in adult mice (discussed in Chapter 6). Furthermore, the potential roles that compromised GDF-5/BMP receptor signalling may play in both age related cognitive decline and the aetiology of Alzheimer´s disease need to be explored.

Perturbed TGF-β/TGF-βR signalling has previously been implicated in the development of Alzheimer´s disease. For example, expression of the TGF-β receptor, TGF-β RII is reduced early in the course of Alzheimer´s disease in human patients and expression levels are inversely correlated with the number of amyloid plaques and neurofibrillary tangles in patients' brains[505]. Moreover, transgenic mice expressing signalling deficient TGF-β RII show increased Aβ deposition and significant dendritic loss compared to their wild type counterparts[505]. In cultures of embryonic mouse hippocampal neurons, oligomeric Aβ decreases the length and increases the number of primary dendrites, reduces GABAergic connectivity and inhibits neuronal survival[175]. The addition of soluble TGF-β1 to cultures ameliorates the detrimental effects of Aβ by a signalling mechanism that involves activation of NF-κB and the upregulation of Hes1 expression[175]. Since GDF-5 is a member of the TGF-β superfamily and, like TGF-β1, GDF-5 promotes dendrite elongation and reduces the number of primary dendrites in hippocampal cultures, GDF-5 may also promote neuronal survival in cultures of hippocampal neurons exposed to oligomeric Aβ.

Adult neurogenesis in the DG can be positively or negatively modulated by members of the TGF-β superfamily[506,507]. In Alzheimer´s disease brains, adult neurogenesis in the DG becomes deregulated. For example, BMP-6 mRNA and protein levels are increased compared with controls in the hippocampi of human patients with Alzheimer´s disease and in mouse models. Increased levels of BMP-6 result in compromised neurogenesis in both Alzheimer´s disease patients and transgenic mice[506]. In contrast, Noggin can block the action of endogenous BMP-4 leading to an increase of the number of proliferating cells in the DG in an Alzheimer´s disease mouse model[507]. In Chapter 5, GDF-5, BMPR-Ib and BMPR-II were detected by immunohistochemistry in the outer layer of the DG of P10 mice, suggesting a possible role for GDF-5/BMP receptor signalling in the modulation of adult neurogenesis in the hippocampus. Although there are no obvious differences in the DG area between *Gdf-5*^{bp} and WT mice at P10, this does not rule out the possibility that some aspect of adult neurogenesis is regulated by GDF-5 and this should be explored in the future.

Some members of the TGF-β superfamily have also been implicated in modulating synapse formation. For example, the homologue of the vertebrate BMP type II receptor, wishful thinking (Wit) is expressed in *Drosophila* motor neurons. *Wit* mutant larvae have small synapses, alterations in the structure of active synaptic zones and a lower frequency of spontaneous vesicle release at neuromuscular junctions, thereby demonstrating that Wit plays a role in synaptic growth and the assembly of the *Drosophila* neuromuscular junction[508-510]. Recently, BMP signalling has been implicated in specifying synapses in the auditory system of rodents. In particular, conditional deletion of *Bmp* receptors leads to aberrations of synapse morphology and function and, impairment of nerve terminal growth[511]. Interestingly, astrocyte-derived TGF-β induces the formation of functional synapses in the cerebral cortex of humans and mice[512]. In addition, BMP-4 has been shown to increase the expression of the pre-synaptic membrane associated proteins, synaptotagmin I and neurexin I in sympathetic neurons[513]. Moreover, *Tgf-β2* null-mutant mice display impaired GABAergic and glutamatergic synaptic transmission[514], whilst soluble TGF-β2 modulates synaptic plasticity in cultures of embryonic hippocampal neurons through phosphorylation of cAMP response element-binding protein (CREB)[515]. Finally, activin is upregulated during hippocampal LTP and increases the number of pre-synaptic contacts made on dendritic spines by modulating spinal F-actin morphology and increasing the length of spinal necks[516,517].

With increasing evidence that TGF-β superfamily members play important roles in regulating synapse assembly and function, it will be informative to investigate whether GDF-5 regulates dendritic spine formation and/or changes in spine morphology or modulates any other aspects of functional synapse formation. A high magnification analyses of Golgi stained preparations from *Gdf-5^{bp}* and WT adult mice will hopefully clarify how important this protein is for the modulation of spine formation and spine shape. Further immunohistochemical studies should also be performed to determine the expression of pre-synaptic and post-synaptic proteins in the hippocampi of *Gdf-5^{bp}* mice compared to wild type mice. Ideally, immunohistochemistry data will be complemented by electrophysiological recording from hippocampal slices to determine whether the lack of functional GDF-5 interferes with the induction of

LTP and/or LTD.

In conclusion, the results described in this thesis contribute to the increasingly large body of knowledge on the mechanisms that modulate axonal and dendritic growth in the developing mouse hippocampus. Understanding the extracellular signals and intracellular signalling pathways that regulate the specification and length of hippocampal neuron axons and dendrites during development may provide clues about the mechanisms that lead to age related degeneration of hippocampal function and cognitive decline. Moreover, this knowledge may provide a potentially important insight into the aetiology of Alzheimer's disease in which the pyramidal neurons of the hippocampus become damaged and hippocampal circuitry and function is compromised.

References

1 Purves, D. *Neuroscience*. 3rd Revised edition edn, (Elsevier - Health Sciences Division, 2004).

2 Super, H., Soriano, E. & Uylings, H. B. The functions of the preplate in development and evolution of the neocortex and hippocampus. *Brain Res Brain Res Rev* 27, 40-64, (1998).

3 Danglot, L., Triller, A. & Marty, S. The development of hippocampal interneurons in rodents. *Hippocampus* 16, 1032-1060, (2006).

4 Bayer, S. A. Development of the hippocampal region in the rat. II. Morphogenesis during embryonic and early postnatal life. *J Comp Neurol* 190, 115-134, (1980).

5 Tole, S. & Grove, E. A. Detailed field pattern is intrinsic to the embryonic mouse hippocampus early in neurogenesis. *J Neurosci* 21, 1580-1589, (2001).

6 Grove, E. A. & Tole, S. Patterning events and specification signals in the developing hippocampus. *Cereb Cortex* 9, 551-561 (1999).

7 Turner, D. A., Buhl, E. H., Hailer, N. P. & Nitsch, R. Morphological features of the entorhinal-hippocampal connection. *Prog Neurobiol* 55, 537-562, (1998).

8 Altman, J. & Bayer, S. A. Mosaic organization of the hippocampal neuroepithelium and the multiple germinal sources of dentate granule cells. *J Comp Neurol* 301, 325-342, (1990).

9 Altman, J. & Bayer, S. A. Prolonged sojourn of developing pyramidal cells in the intermediate zone of the hippocampus and their settling in the stratum pyramidale. *J Comp Neurol* 301, 343-364, (1990).

10 Amaral, D. G. & Witter, M. P. The three-dimensional organization of the hippocampal formation: a review of anatomical data. *Neuroscience* 31, 571-591, (1989).

11 Andersen, P., Morris, R., Amaral, D., Bliss, T. & O'Keefe, J. *The Hippocampus Book*. 1st Edition edn, (Oxford University Press, USA, 2006).

12 Sokolowski, K. & Corbin, J. G. Wired for behaviors: from development to function of innate limbic system circuitry. *Front Mol Neurosci* 5, 55, (2012).

13 Neves, G., Cooke, S. F. & Bliss, T. V. Synaptic plasticity, memory and the hippocampus: a neural network approach to causality. *Nat Rev Neurosci* 9, 65-75, (2008).

14 Zhang, X. M. & Zhu, J. Kainic Acid-induced neurotoxicity: targeting glial responses and glia-derived cytokines. *Curr Neuropharmacol* 9, 388-398, (2011).

15 Altman, J., Brunner, R. L. & Bayer, S. A. The hippocampus and behavioral maturation. *Behav Biol* 8, 557-596 (1973).

16 Super, H. & Soriano, E. The organization of the embryonic and early postnatal murine hippocampus. II. Development of entorhinal, commissural, and septal connections studied with the lipophilic tracer DiI. *J Comp Neurol* 344, 101-120, (1994).

17 Deng, J. B., Yu, D. M., Wu, P. & Li, M. S. The tracing study of developing entorhino-hippocampal pathway. *Int J Dev Neurosci* 25, 251-258, (2007).

18 Anderson, S. A., Eisenstat, D. D., Shi, L. & Rubenstein, J. L. Interneuron migration from basal forebrain to neocortex: dependence on Dlx genes. *Science* 278, 474-476 (1997).

19 Pleasure, S. J. *et al.* Cell migration from the ganglionic eminences is required for the development of hippocampal GABAergic interneurons. *Neuron* 28, 727-740, (2000).

20 Qian, X. *et al.* Timing of CNS cell generation: a programmed sequence of neuron and glial cell production from isolated murine cortical stem cells. *Neuron* 28, 69-80, (2000).

21 Sauvageot, C. M. & Stiles, C. D. Molecular mechanisms controlling cortical gliogenesis. *Curr Opin Neurobiol* 12, 244-249, (2002).

22 Dotti, C. G., Sullivan, C. A. & Banker, G. A. The establishment of polarity by hippocampal neurons in culture. *J Neurosci* 8, 1454-1468 (1988).

23 Bradke, F. & Dotti, C. G. Establishment of neuronal polarity: lessons from cultured hippocampal neurons. *Curr Opin Neurobiol* 10, 574-581, (2000).

24 Fukata, Y., Kimura, T. & Kaibuchi, K. Axon specification in hippocampal neurons. *Neurosci Res* 43, 305-315, (2002).

25 Yoshimura, T., Arimura, N. & Kaibuchi, K. Signaling networks in neuronal polarization. *J Neurosci* 26, 10626-10630, (2006).

26 Deitch, J. S. & Banker, G. A. An electron microscopic analysis of hippocampal neurons developing in culture: early stages in the emergence of polarity. *J Neurosci* 13, 4301-4315 (1993).

27 Baas, P. W., Black, M. M. & Banker, G. A. Changes in microtubule polarity orientation during the development of hippocampal neurons in culture. *J Cell Biol* 109, 3085-3094 (1989).

28 Craig, A. M. & Banker, G. Neuronal polarity. *Annu Rev Neurosci* 17, 267-310, (1994).

29 Li, R. & Gundersen, G. G. Beyond polymer polarity: how the cytoskeleton builds a polarized cell. *Nat Rev Mol Cell Biol* 9, 860-873, (2008).

30 Lowery, L. A. & Van Vactor, D. The trip of the tip: understanding the growth cone machinery. *Nat Rev Mol Cell Biol* 10, 332-343, (2009).

31 Forscher, P. & Smith, S. J. Actions of cytochalasins on the organization of actin filaments and microtubules in a neuronal growth cone. *J Cell Biol* 107, 1505-1516 (1988).

32 Mallavarapu, A. & Mitchison, T. Regulated actin cytoskeleton assembly at filopodium tips controls their extension and retraction. *J Cell Biol* 146, 1097-1106 (1999).

33 Goldberg, D. J. & Burmeister, D. W. Stages in axon formation: observations of growth of Aplysia axons in culture using video-enhanced contrast-differential interference contrast microscopy. *J Cell Biol* 103, 1921-1931 (1986).

34 Medeiros, N. A., Burnette, D. T. & Forscher, P. Myosin II functions in actin-bundle turnover in neuronal growth cones. *Nat Cell Biol* 8, 215-226, (2006).

35 Yu, W. *et al.* Depletion of a microtubule-associated motor protein induces the loss of dendritic identity. *J Neurosci* 20, 5782-5791, (2000).

36 Farah, C. A. & Leclerc, N. HMWMAP2: new perspectives on a pathway to dendritic identity. *Cell Motil Cytoskeleton* 65, 515-527, (2008).

37 Szebenyi, G. *et al.* Activity-driven dendritic remodeling requires microtubule-associated protein 1A. *Curr Biol* 15, 1820-1826, (2005).

38 Conde, C. & Caceres, A. Microtubule assembly, organization and dynamics in axons and dendrites. *Nat Rev Neurosci* 10, 319-332, (2009).

39 Fukata, Y. *et al.* CRMP-2 binds to tubulin heterodimers to promote microtubule assembly. *Nat Cell Biol* 4, 583-591, (2002).

40 Luo, L. *et al.* Differential effects of the Rac GTPase on Purkinje cell axons and dendritic trunks and spines. *Nature* 379, 837-840, (1996).

41 Horton, A. C. & Ehlers, M. D. Neuronal polarity and trafficking. *Neuron* 40, 277-295, (2003).

42 Shi, S. H., Jan, L. Y. & Jan, Y. N. Hippocampal neuronal polarity specified by spatially localized mPar3/mPar6 and PI 3-kinase activity. *Cell* 112, 63-75, (2003).

43 Polleux, F., Morrow, T. & Ghosh, A. Semaphorin 3A is a chemoattractant for cortical apical dendrites. *Nature* 404, 567-573, (2000).

44 Bonhoeffer, T. & Yuste, R. Spine motility. Phenomenology, mechanisms, and function. *Neuron* 35, 1019-1027, (2002).

45 Calabrese, B., Wilson, M. S. & Halpain, S. Development and regulation of dendritic spine synapses. *Physiology (Bethesda)* 21, 38-47, (2006).

46 Halpain, S., Hipolito, A. & Saffer, L. Regulation of F-actin stability in dendritic spines by glutamate receptors and calcineurin. *J Neurosci* 18, 9835-9844 (1998).

47 Fischer, M., Kaech, S., Knutti, D. & Matus, A. Rapid actin-based plasticity in dendritic spines. *Neuron* 20, 847-854, (1998).

48 Tashiro, A. & Yuste, R. Regulation of dendritic spine motility and stability by Rac1 and Rho kinase: evidence for two forms of spine motility. *Mol Cell Neurosci* 26, 429-440, (2004).

49 Jan, Y. N. & Jan, L. Y. The control of dendrite development. *Neuron* 40, 229-242, (2003).

50 Scott, E. K. & Luo, L. How do dendrites take their shape? *Nat Neurosci* 4, 359-365, (2001).

51 Grueber, W. B. & Sagasti, A. Self-avoidance and tiling: Mechanisms of dendrite and axon spacing. *Cold Spring Harb Perspect Biol* 2, a001750, (2010).

52 Whitlock, J. R., Heynen, A. J., Shuler, M. G. & Bear, M. F. Learning induces long-term potentiation in the hippocampus. *Science* 313, 1093-1097, (2006).

53 Scoville, W. B. & Milner, B. Loss of recent memory after bilateral hippocampal lesions. *J Neurol Neurosurg Psychiatry* 20, 11-21 (1957).

54 Iaria, G., Chen, J. K., Guariglia, C., Ptito, A. & Petrides, M. Retrosplenial and hippocampal brain regions in human navigation: complementary functional contributions to the formation and use of cognitive maps. *Eur J Neurosci* 25, 890-899, (2007).

55 Wilson, M. A. & McNaughton, B. L. Dynamics of the hippocampal ensemble code for space. *Science* 261, 1055-1058 (1993).

56 Iaria, G., Petrides, M., Dagher, A., Pike, B. & Bohbot, V. D. Cognitive strategies dependent on the hippocampus and caudate nucleus in human navigation: variability and change with practice. *J Neurosci* 23, 5945-5952, (2003).

57 Eichenbaum, H. Hippocampus: cognitive processes and neural representations that underlie declarative memory. *Neuron* 44, 109-120, (2004).

58 Lu, Y., Christian, K. & Lu, B. BDNF: a key regulator for protein synthesis-dependent LTP and long-term memory? *Neurobiol Learn Mem* 89, 312-323, (2008).

59 Pang, P. T. & Lu, B. Regulation of late-phase LTP and long-term memory in normal and aging hippocampus: role of secreted proteins tPA and BDNF. *Ageing Res Rev* 3, 407-430, (2004).

60 Diarra, A., Geetha, T., Potter, P. & Babu, J. R. Signaling of the neurotrophin receptor p75 in relation to Alzheimer's disease. *Biochem Biophys Res Commun* 390, 352-356, (2009).

61 Moolman, D. L., Vitolo, O. V., Vonsattel, J. P. & Shelanski, M. L. Dendrite and dendritic spine alterations in Alzheimer models. *J Neurocytol* 33, 377-387, (2004).

62 Auffret, A. *et al.* Age-dependent impairment of spine morphology and synaptic plasticity in hippocampal CA1 neurons of a presenilin 1 transgenic mouse model of Alzheimer's disease. *J Neurosci* 29, 10144-10152, (2009).

63 Tang, F. R. & Loke, W. K. Cyto-, axo- and dendro-architectonic changes of neurons in the limbic system in the mouse pilocarpine model of temporal lobe epilepsy. *Epilepsy Res* 89, 43-51, (2010).

64 Sperk, G., Drexel, M. & Pirker, S. Neuronal plasticity in animal models and the epileptic human hippocampus. *Epilepsia* 50 Suppl 12, 29-31, (2009).

65 Benes, F. M., Kwok, E. W., Vincent, S. L. & Todtenkopf, M. S. A reduction of nonpyramidal cells in sector CA2 of schizophrenics and manic depressives. *Biol Psychiatry* 44, 88-97, (1998).

66 Harrison, P. J. The hippocampus in schizophrenia: a review of the neuropathological evidence and its pathophysiological implications. *Psychopharmacology (Berl)* 174, 151-162, (2004).

67 Campbell, S. & Macqueen, G. The role of the hippocampus in the pathophysiology of major depression. *J Psychiatry Neurosci* 29, 417-426 (2004).

68 Ming, G. L. & Song, H. Adult neurogenesis in the mammalian brain: significant answers and significant questions. *Neuron* 70, 687-702, (2011).

69 Zhao, C., Teng, E. M., Summers, R. G., Jr., Ming, G. L. & Gage, F. H. Distinct morphological stages of dentate granule neuron maturation in the adult mouse hippocampus. *J Neurosci* 26, 3-11, (2006).

70 Bruel-Jungerman, E., Davis, S., Rampon, C. & Laroche, S. Long-term potentiation enhances neurogenesis in the adult dentate gyrus. *J Neurosci* 26, 5888-5893, (2006).

71 Deng, W., Aimone, J. B. & Gage, F. H. New neurons and new memories: how does adult hippocampal neurogenesis affect learning and memory? *Nat Rev Neurosci* 11, 339-350, (2010).

72 Bruel-Jungerman, E., Laroche, S. & Rampon, C. New neurons in the dentate gyrus are involved in the expression of enhanced long-term memory following environmental enrichment. *Eur J Neurosci* 21, 513-521, (2005).

73 Shors, T. J., Townsend, D. A., Zhao, M., Kozorovitskiy, Y. & Gould, E. Neurogenesis may relate to some but not all types of hippocampal-dependent learning. *Hippocampus* 12, 578-584, (2002).

74 Jessberger, S. *et al.* Epigenetic modulation of seizure-induced neurogenesis and cognitive decline. *J Neurosci* 27, 5967-5975, (2007).

75 Mu, Y. & Gage, F. H. Adult hippocampal neurogenesis and its role in Alzheimer's disease. *Mol Neurodegener* 6, 85, (2011).

76 Drew, M. R. & Hen, R. Adult hippocampal neurogenesis as target for the treatment of depression. *CNS Neurol Disord Drug Targets* 6, 205-218 (2007).

77 Levi-Montalcini, R. & Angeletti, P. U. Nerve growth factor. *Physiol Rev* 48, 534-569 (1968).

78 Purves, D., Snider, W. D. & Voyvodic, J. T. Trophic regulation of nerve cell morphology and innervation in the autonomic nervous system. *Nature* 336, 123-128, (1988).

79 Hamburger, V. & Yip, J. W. Reduction of experimentally induced neuronal death in spinal ganglia of the chick embryo by nerve growth factor. *J Neurosci* 4, 767-774 (1984).

80 Davies, A. M. The neurotrophic hypothesis: where does it stand? *Philos Trans R Soc Lond B Biol Sci* 351, 389-394, (1996).

81 Levi-Montalcini, R. & Angeletti, P. U. Essential role of the nerve growth factor in the survival and maintenance of dissociated sensory and sympathetic embryonic nerve cells in vitro. *Dev Biol* 6, 653-659 (1963).

82 Levi-Montalcini, R. The nerve growth factor: thirty-five years later. *Embo J* 6, 1145-1154 (1987).

83 Davies, A. M. Regulation of neuronal survival and death by extracellular signals during development. *Embo J* 22, 2537-2545, (2003).

84 Davies, A. M. Neurobiology. Tracking neurotrophin function. *Nature* 368, 193-194, (1994).

85 Smeyne, R. J. *et al.* Severe sensory and sympathetic neuropathies in mice carrying a disrupted Trk/NGF receptor gene. *Nature* 368, 246-249, (1994).

86 Huang, E. J. & Reichardt, L. F. Neurotrophins: roles in neuronal development and function. *Annu Rev Neurosci* 24, 677-736, (2001).

87 Teng, K. K. & Hempstead, B. L. Neurotrophins and their receptors: signaling trios in complex biological systems. *Cell Mol Life Sci* 61, 35-48, (2004).

88 Arevalo, J. C. & Wu, S. H. Neurotrophin signaling: many exciting surprises! *Cell Mol Life Sci* 63, 1523-1537, (2006).

89 Reichardt, L. F. Neurotrophin-regulated signalling pathways. *Philos Trans R Soc Lond B Biol Sci* 361, 1545-1564, (2006).

90 Chen, Y. *et al.* Multiple roles of the p75 neurotrophin receptor in the nervous system. *J Int Med Res* 37, 281-288 (2009).

91 Teng, K. K., Felice, S., Kim, T. & Hempstead, B. L. Understanding proneurotrophin actions: Recent advances and challenges. *Dev Neurobiol* 70, 350-359, (2010).

92 Chao, M. V. Neurotrophins and their receptors: a convergence point for many signalling pathways. *Nat Rev Neurosci* 4, 299-309, (2003).

93 Airaksinen, M. S. & Saarma, M. The GDNF family: signalling, biological functions and therapeutic value. *Nat Rev Neurosci* 3, 383-394, (2002).

94 Maina, F. & Klein, R. Hepatocyte growth factor, a versatile signal for developing neurons. *Nat Neurosci* 2, 213-217, (1999).

95 Forgie, A., Wyatt, S., Correll, P. H. & Davies, A. M. Macrophage stimulating protein is a target-derived neurotrophic factor for developing sensory and sympathetic neurons. *Development* 130, 995-1002 (2003).

96 Ledda, F., Paratcha, G., Sandoval-Guzman, T. & Ibanez, C. F. GDNF and GFRalpha1 promote formation of neuronal synapses by ligand-induced cell adhesion. *Nat Neurosci* 10, 293-300, (2007).

97 Shelton, D. L. & Reichardt, L. F. Studies on the expression of the beta nerve growth factor (NGF) gene in the central nervous system: level and regional distribution of NGF mRNA suggest that NGF functions as a trophic factor for several distinct populations of neurons. *Proc Natl Acad Sci U S A* 83, 2714-2718 (1986).

98 Sobreviela, T. *et al.* TrkA-immunoreactive profiles in the central nervous system: colocalization with neurons containing p75 nerve growth factor receptor, choline acetyltransferase, and serotonin. *J Comp Neurol* 350, 587-611, (1994).

99 Muller, M. *et al.* Loss of NGF-TrkA signaling from the CNS is not sufficient to induce cognitive impairments in young adult or intermediate-aged mice. *J Neurosci* 32, 14885-14898, (2012).

100 Sanchez-Ortiz, E. *et al.* TrkA gene ablation in basal forebrain results in dysfunction of the cholinergic circuitry. *J Neurosci* 32, 4065-4079, (2012).

101 Thoenen, H., Zafra, F., Hengerer, B. & Lindholm, D. The synthesis of nerve growth factor and brain-derived neurotrophic factor in hippocampal and cortical neurons is regulated by specific transmitter systems. *Ann N Y Acad Sci* 640, 86-90 (1991).

102 da Penha Berzaghi, M. *et al.* Cholinergic regulation of brain-derived neurotrophic factor (BDNF) and nerve growth factor (NGF) but not neurotrophin-3 (NT-3) mRNA levels in the developing rat hippocampus. *J Neurosci* 13, 3818-3826 (1993).

103 Chen, K. S. *et al.* Disruption of a single allele of the nerve growth factor gene results in atrophy of basal forebrain cholinergic neurons and memory deficits. *J Neurosci* 17, 7288-7296 (1997).

104 Conner, J. M. *et al.* NGF is essential for hippocampal plasticity and learning. *J Neurosci* 29, 10883-10889, (2009).

105 Maguire, C., Casey, M., Kelly, A., Mullany, P. M. & Lynch, M. A. Activation of tyrosine receptor kinase plays a role in expression of long-term potentiation in the rat dentate gyrus. *Hippocampus* 9, 519-526, (1999).

106 Wang, S. H. *et al.* NGF promotes long-term memory formation by activating poly(ADP-ribose)polymerase-1. *Neuropharmacology* 63, 1085-1092, (2012).

107 Merlio, J. P., Ernfors, P., Jaber, M. & Persson, H. Molecular cloning of rat trkC and distribution of cells expressing messenger RNAs for members of the trk family in the rat central nervous system. *Neuroscience* 51, 513-532, (1992).

108 Culmsee, C. *et al.* Nerve growth factor survival signaling in cultured hippocampal neurons is mediated through TrkA and requires the common neurotrophin receptor P75. *Neuroscience* 115, 1089-1108, (2002).

109 Arevalo, M. A. & Rodriguez-Tebar, A. Activation of casein kinase II and inhibition of phosphatase and tensin homologue deleted on chromosome 10 phosphatase by nerve growth factor/p75NTR inhibit glycogen synthase kinase-3beta and stimulate axonal growth. *Mol Biol Cell* 17, 3369-3377, (2006).

110 Salama-Cohen, P., Arevalo, M. A., Meier, J., Grantyn, R. & Rodriguez-Tebar, A. NGF controls dendrite development in hippocampal neurons by binding to p75NTR and modulating the cellular targets of Notch. *Mol Biol Cell* 16, 339-347, (2005).

111 Chacon, P. J., Arevalo, M. A. & Tebar, A. R. NGF-activated protein tyrosine phosphatase 1B mediates the phosphorylation and degradation of I-kappa-Balpha coupled to NF-kappa-B activation, thereby controlling dendrite morphology. *Mol Cell Neurosci* 43, 384-393, (2010).

112 Schecterson, L. C. & Bothwell, M. Novel roles for neurotrophins are suggested by BDNF and NT-3 mRNA expression in developing neurons. *Neuron* 9, 449-463, (1992).

113 Ernfors, P., Wetmore, C., Olson, L. & Persson, H. Identification of cells in rat brain and peripheral tissues expressing mRNA for members of the nerve growth factor family. *Neuron* 5, 511-526, (1990).

114 Ohsawa, F., Widmer, H. R., Knusel, B., Denton, T. L. & Hefti, F. Response of embryonic rat hippocampal neurons in culture to neurotrophin-3, brain-derived neurotrophic factor and basic fibroblast growth factor. *Neuroscience* 57, 67-77, (1993).

115 Ip, N. Y., Li, Y., Yancopoulos, G. D. & Lindsay, R. M. Cultured hippocampal neurons show responses to BDNF, NT-3, and NT-4, but not NGF. *J Neurosci* 13, 3394-3405 (1993).

116 Marsh, H. N. & Palfrey, H. C. Neurotrophin-3 and brain-derived neurotrophic factor activate multiple signal transduction events but are not survival factors for hippocampal pyramidal neurons. *J Neurochem* 67, 952-963 (1996).

117 Vicario-Abejon, C., Johe, K. K., Hazel, T. G., Collazo, D. & McKay, R. D. Functions of basic fibroblast growth factor and neurotrophins in the differentiation of hippocampal neurons. *Neuron* 15, 105-114, (1995).

118 Pieraut, S. *et al.* Spontaneous glutamate release controls NT-3-dependent development of hippocampal calbindin-D(28k) phenotype through activation of sodium channels ex vivo. *Eur J Neurosci* 25, 2629-2639, (2007).

119 Vicario-Abejon, C., Collin, C., McKay, R. D. & Segal, M. Neurotrophins induce formation of functional excitatory and inhibitory synapses between cultured hippocampal neurons. *J Neurosci* 18, 7256-7271, (1998).

120 Martinez, A. *et al.* TrkB and TrkC signaling are required for maturation and synaptogenesis of hippocampal connections. *J Neurosci* 18, 7336-7350, (1998).

121 He, Z. *et al.* TRPC5 channel is the mediator of neurotrophin-3 in regulating dendritic growth via CaMKIIalpha in rat hippocampal neurons. *J Neurosci* 32, 9383-9395, (2012).

122 Labelle, C. & Leclerc, N. Exogenous BDNF, NT-3 and NT-4 differentially regulate neurite outgrowth in cultured hippocampal neurons. *Brain Res Dev Brain Res* 123, 1-11, (2000).

123 Rauskolb, S. *et al.* Global deprivation of brain-derived neurotrophic factor in the CNS reveals an area-specific requirement for dendritic growth. *J Neurosci* 30, 1739-1749, (2010).

124 Lindholm, D., Carroll, P., Tzimagiogis, G. & Thoenen, H. Autocrine-paracrine regulation of hippocampal neuron survival by IGF-1 and the neurotrophins BDNF, NT-3 and NT-4. *Eur J Neurosci* 8, 1452-1460, (1996).

125 Ernfors, P., Lee, K. F. & Jaenisch, R. Mice lacking brain-derived neurotrophic factor develop with sensory deficits. *Nature* 368, 147-150, (1994).

126 Jones, K. R., Farinas, I., Backus, C. & Reichardt, L. F. Targeted disruption of the BDNF gene perturbs brain and sensory neuron development but not motor neuron development. *Cell* 76, 989-999, (1994).

127 Xu, B. *et al.* The role of brain-derived neurotrophic factor receptors in the mature hippocampus: modulation of long-term potentiation through a presynaptic mechanism involving TrkB. *J Neurosci* 20, 6888-6897, (2000).

128 McAllister, A. K., Lo, D. C. & Katz, L. C. Neurotrophins regulate dendritic growth in developing visual cortex. *Neuron* 15, 791-803, (1995).

129 Kwon, M., Fernandez, J. R., Zegarek, G. F., Lo, S. B. & Firestein, B. L. BDNF-promoted increases in proximal dendrites occur via CREB-dependent transcriptional regulation of cypin. *J Neurosci* 31, 9735-9745, (2011).

130 Alonso, M., Medina, J. H. & Pozzo-Miller, L. ERK1/2 activation is necessary for BDNF to increase dendritic spine density in hippocampal CA1 pyramidal neurons. *Learn Mem* 11, 172-178, (2004).

131 Aguado, F. *et al.* BDNF regulates spontaneous correlated activity at early developmental stages by increasing synaptogenesis and expression of the K+/Cl- co-transporter KCC2. *Development* 130, 1267-1280, (2003).

132 Tanaka, T., Saito, H. & Matsuki, N. Inhibition of GABA(A) synaptic responses by brain-derived neurotrophic factor (BDNF) in rat hippocampus. *Journal of Neuroscience* 17, 2959-2966 (1997).

133 Lessmann, V., Gottmann, K. & Heumann, R. Bdnf and Nt-4/5 Enhance Glutamatergic Synaptic Transmission in Cultured Hippocampal-Neurons. *Neuroreport* 6, 21-25, (1994).

134 Levine, E. S., Dreyfus, C. F., Black, I. B. & Plummer, M. R. Brain-Derived Neurotrophic Factor Rapidly Enhances Synaptic Transmission in Hippocampal-Neurons Via Postsynaptic Tyrosine Kinase Receptors. *Proc Natl Acad Sci U S A* 92, 8074-8077, (1995).

135 Li, Y. X., Zhang, Y. O., Lester, H. A., Schuman, E. M. & Davidson, N. Enhancement of neurotransmitter release induced by brain-derived neurotrophic factor in cultured hippocampal neurons. *Journal of Neuroscience* 18, 10231-10240, (1998).

136 Li, Y. X. *et al.* Expression of a dominant negative TrkB receptor, T1, reveals a requirement for presynaptic signaling in BDNF-induced synaptic potentiation in cultured hippocampal neurons. *Proc Natl Acad Sci U S A* 95, 10884-10889, (1998).

137 Luikart, B. W. *et al.* TrkB has a cell-autonomous role in the establishment of hippocampal schaffer collateral synapses. *Journal of Neuroscience* 25, 3774-3786, (2005).

138 Tyler, W. J. & Pozzo-Miller, L. Miniature synaptic transmission and BDNF modulate dendritic spine growth and form in rat CA1 neurones. *J Physiol* 553, 497-509, (2003).

139 Tyler, W. J. & Pozzo-Miller, L. D. BDNF enhances quantal neurotransmitter release and increases the number of docked vesicles at the active zones of hippocampal excitatory synapses. *Journal of Neuroscience* 21, 4249-4258, (2001).

140 Chapleau, C. A., Carlo, M. E., Larimore, J. L. & Pozzo-Miller, L. The actions of BDNF on dendritic spine density and morphology in organotypic slice cultures depend on the presence of serum in culture media. *J Neurosci Methods* 169, 182-190, (2008).

141 Danzer, S. C., Crooks, K. R. C., Lo, D. C. & McNamara, J. O. Increased expression of brain-derived neurotrophic factor induces formation of basal dendrites and axonal branching in dentate granule cells in hippocampal explant cultures. *Journal of Neuroscience* 22, 9754-9763, (2002).

142 Dieni, S. *et al.* BDNF and its pro-peptide are stored in presynaptic dense core vesicles in brain neurons. *Journal of Cell Biology* 196, 775-788, (2012).

143 Egan, M. F. *et al.* The BDNF val66met polymorphism affects activity-dependent secretion of BDNF and human memory and hippocampal function. *Cell* 112, 257-269, (2003).

144 Chen, W. G. *et al.* Derepression of BDNF transcription involves calcium-dependent phosphorylation of MeCP2. *Science* 302, 885-889, (2003).

145 Korte, M. *et al.* Hippocampal Long-Term Potentiation Is Impaired in Mice Lacking Brain-Derived Neurotrophic Factor. *Proc Natl Acad Sci U S A* 92, 8856-8860, (1995).

146 Patterson, S. L. *et al.* Some forms of cAMP-mediated long-lasting potentiation are associated with release of BDNF and nuclear translocation of phospho-MAP kinase. *Neuron* 32, 123-140, (2001).

147 Kang, H. J., Welcher, A. A., Shelton, D. & Schuman, E. M. Neurotrophins and time: Different roles for TrkB signaling in hippocampal long-term potentiation. *Neuron* 19, 653-664, (1997).

148 Minichiello, L. *et al.* Essential role for TrkB receptors in hippocampus-mediated learning. *Neuron* 24, 401-414, (1999).

149 Chen, G. Q., Kolbeck, R., Barde, Y. A., Bonhoeffer, T. & Kossel, A. Relative contribution of endogenous neurotrophins in hippocampal long-term potentiation. *Journal of Neuroscience* 19, 7983-7990 (1999).

150 Pang, P. T. *et al.* Cleavage of proBDNF by tPA/plasmin is essential for long-term hippocampal plasticity. *Science* 306, 487-491, (2004).

151 Woo, N. H. *et al.* Activation of p75NTR by proBDNF facilitates hippocampal long-term depression. *Nat Neurosci* 8, 1069-1077, (2005).

152 Barker, P. A. Whither proBDNF? *Nat Neurosci* 12, 105-106, (2009).

153 Zagrebelsky, M. *et al.* The p75 neurotrophin receptor negatively modulates dendrite complexity and spine density in hippocampal neurons. *J Neurosci* 25, 9989-9999, (2005).

154 Kesslak, J. P., So, V., Choi, J., Cotman, C. W. & Gomez-Pinilla, F. Learning upregulates brain-derived neurotrophic factor messenger ribonucleic acid: A mechanism to facilitate encoding and circuit maintenance? *Behav Neurosci* 112, 1012-1019, (1998).

155 Alonso, M. *et al.* BDNF-triggered events in the rat hippocampus are required for both short- and long-term memory formation. *Hippocampus* 12, 551-560, (2002).

156 Hall, J., Thomas, K. L. & Everitt, B. J. Rapid and selective induction of BDNF expression in the hippocampus during contextual learning. *Nat Neurosci* 3, 533-535, (2000).

157 Linnarsson, S., Bjorklund, A. & Ernfors, P. Learning deficit in BDNF mutant mice. *European Journal of Neuroscience* 9, 2581-2587, (1997).

158 Liu, I. Y. C., Lyons, W. E., Mamounas, L. A. & Thompson, R. F. Brain-derived neurotrophic factor plays a critical role in contextual fear conditioning. *Journal of Neuroscience* 24, 7958-7963, (2004).

159 Koponen, E. *et al.* Transgenic mice overexpressing the full-length neurotrophin receptor trkB exhibit increased activation of the trkB-PLC gamma pathway, reduced anxiety, and facilitated learning. *Molecular and Cellular Neuroscience* 26, 166-181, (2004).

160 Ma, Y. L., Wang, H. L., Wu, H. C., Wei, C. L. & Lee, E. H. Y. Brain-derived neurotrophic factor antisense oligonucleotide impairs memory retention and inhibits long-term potentiation in rats. *Neuroscience* 82, 957-967, (1998).

161 Mizuno, M., Yamada, K., Olariu, A., Nawa, H. & Nabeshima, T. Involvement of brain-derived neurotrophic factor in spatial memory formation and maintenance in a radial arm maze test in rats. *Journal of Neuroscience* 20, 7116-7121, (2000).

162 Hopkins, S. J. & Rothwell, N. J. Cytokines and the nervous system. I: Expression and recognition. *Trends Neurosci* 18, 83-88, (1995).

163 Munoz-Fernandez, M. A. & Fresno, M. The role of tumour necrosis factor, interleukin 6, interferon-gamma and inducible nitric oxide synthase in the development and pathology of the nervous system. *Prog Neurobiol* 56, 307-340, (1998).

164 Wallach, D. *et al.* Cell death induction by receptors of the TNF family: Towards a molecular understanding. *Febs Lett* 410, 96-106, (1997).

165 Yang, L., Lindholm, K., Konishi, Y., Li, R. & Shen, Y. Target depletion of distinct tumor necrosis factor receptor subtypes reveals hippocampal neuron death and survival through different signal transduction pathways. *J Neurosci* 22, 3025-3032, (2002).

166 Neumann, H. *et al.* Tumor necrosis factor inhibits neurite outgrowth and branching of hippocampal neurons by a rho-dependent mechanism. *J Neurosci* 22, 854-862, (2002).

167 Golan, H., Levav, T., Mendelsohn, A. & Huleihel, M. Involvement of tumor necrosis factor alpha in hippocampal development and function. *Cereb Cortex* 14, 97-105, (2004).

168 Liu, T. *et al.* Tumor necrosis factor-alpha expression in ischemic neurons. *Stroke* 25, 1481-1488, (1994).

169 Feuerstein, G. Z., Liu, T. & Barone, F. C. Cytokines, inflammation, and brain injury: role of tumor necrosis factor-alpha. *Cerebrovasc Brain Metab Rev* 6, 341-360, (1994).

170 Hofman, F. M., Hinton, D. R., Johnson, K. & Merrill, J. E. Tumor necrosis factor identified in multiple sclerosis brain. *J Exp Med* 170, 607-612, (1989).

171 Fillit, H. *et al.* Elevated circulating tumor necrosis factor levels in Alzheimer's disease. *Neurosci Lett* 129, 318-320, (1991).

172 Boka, G. *et al.* Immunocytochemical analysis of tumor necrosis factor and its receptors in Parkinson's disease. *Neurosci Lett* 172, 151-154, (1994).

173 Zhu, Y. *et al.* The expression of transforming growth factor-beta1 (TGF-beta1) in hippocampal neurons: a temporary upregulated protein level after transient forebrain ischemia in the rat. *Brain Res* 866, 286-298, (2000).

174 Zhu, Y., Ahlemeyer, B., Bauerbach, E. & Krieglstein, J. TGF-beta1 inhibits caspase-3 activation and neuronal apoptosis in rat hippocampal cultures. *Neurochem Int* 38, 227-235, (2001).

175 Chacon, P. J. & Rodriguez-Tebar, A. Increased expression of the homologue of enhancer-of-split 1 protects neurons from beta amyloid neurotoxicity and hints at an alternative role for transforming growth factor beta1 as a neuroprotector. *Alzheimers Res Ther* 4, 31, (2012).

176 Gutierrez, H. *et al.* Regulation of neurite growth by tumour necrosis superfamily member RANKL. *Open Biol* 3, (2013).

177 Gavalda, N., Gutierrez, H. & Davies, A. M. Developmental regulation of sensory neurite growth by the tumor necrosis factor superfamily member LIGHT. *J Neurosci* 29, 1599-1607, (2009).

178 O'Keeffe, G. W., Gutierrez, H., Pandolfi, P. P., Riccardi, C. & Davies, A. M. NGF-promoted axon growth and target innervation requires GITRL-GITR signaling. *Nat Neurosci* 11, 135-142, (2008).

179 Perron, J. C. & Dodd, J. Structural distinctions in BMPs underlie divergent signaling in spinal neurons. *Neural Dev* 7, (2012).

180 Le Dreau, G. *et al.* Canonical BMP7 activity is required for the generation of discrete neuronal populations in the dorsal spinal cord. *Development* 139, 259-268, (2012).

181 Mensching, L. *et al.* Local substitution of GDF-15 improves axonal and sensory recovery after peripheral nerve injury. *Cell Tissue Res* 350, 225-238, (2012).

182 Coley, W. B. II. Contribution to the Knowledge of Sarcoma. *Ann Surg* 14, 199-220, (1891).

183 Shear, M. J. Chemical Treatment of Tumors. V. Isolation of the Hemorrhage-Producing Fraction from Serratia marcescens (Bacillus prodigiosus) Culture Filtrate. *JNCI J Natl Cancer Inst*, 81-97, (1943).

184 O'Malley, W. E., Achinstein, B. & Shear, M. J. Action of Bacterial Polysaccharide on Tumors. II. Damage of Sarcoma 37 by Serum of Mice Treated With Serratia

Marcescens Polysaccharide, and Induced Tolerance. *JNCI J Natl Cancer Inst* 1169-1175, (1962).

185 Carswell, E. A. *et al.* An endotoxin-induced serum factor that causes necrosis of tumors. *Proc Natl Acad Sci U S A* 72, 3666-3670, (1975).

186 Old, L. J. Tumor necrosis factor (TNF). *Science* 230, 630-632, (1985).

187 Locksley, R. M., Killeen, N. & Lenardo, M. J. The TNF and TNF receptor superfamilies: integrating mammalian biology. *Cell* 104, 487-501, (2001).

188 Hehlgans, T. & Pfeffer, K. The intriguing biology of the tumour necrosis factor/tumour necrosis factor receptor superfamily: players, rules and the games. *Immunology* 115, 1-20, (2005).

189 Aggarwal, B. B., Gupta, S. C. & Kim, J. H. Historical perspectives on tumor necrosis factor and its superfamily: 25 years later, a golden journey. *Blood* 119, 651-665, (2012).

190 Aggarwal, B. B. Signalling pathways of the TNF superfamily: a double-edged sword. *Nat Rev Immunol* 3, 745-756, (2003).

191 Black, R. A. *et al.* A metalloproteinase disintegrin that releases tumour-necrosis factor-alpha from cells. *Nature* 385, 729-733, (1997).

192 Powell, W. C., Fingleton, B., Wilson, C. L., Boothby, M. & Matrisian, L. M. The metalloproteinase matrilysin proteolytically generates active soluble Fas ligand and potentiates epithelial cell apoptosis. *Current Biology* 9, 1441-1447, (1999).

193 Bodmer, J. L., Schneider, P. & Tschopp, J. The molecular architecture of the TNF superfamily. *Trends Biochem Sci* 27, 19-26, (2002).

194 Fesik, S. W. Insights into programmed cell death through structural biology. *Cell* 103, 273-282, (2000).

195 Chan, F. K. The pre-ligand binding assembly domain: a potential target of inhibition of tumour necrosis factor receptor function. *Ann Rheum Dis* 59 Suppl 1, i50-53 (2000).

196 Ware, C. F. The TNF superfamily. *Cytokine Growth Factor Rev* 14, 181-184, (2003).

197 Chan, F. K. Three is better than one: pre-ligand receptor assembly in the regulation of TNF receptor signaling. *Cytokine* 37, 101-107, (2007).

198 Chan, F. K. *et al.* A domain in TNF receptors that mediates ligand-independent receptor assembly and signaling. *Science* 288, 2351-2354, (2000).

199 Zhang, G. Tumor necrosis factor family ligand-receptor binding. *Curr Opin Struct Biol* 14, 154-160, (2004).

200 Kischkel, F. C. *et al.* Apo2L/TRAIL-dependent recruitment of endogenous FADD and caspase-8 to death receptors 4 and 5. *J Invest Dermatol* 115, 1171-1171, (2000).

201 Kischkel, F. C. *et al.* Cytotoxicity-Dependent Apo-1 (Fas/Cd95)-Associated Proteins Form a Death-Inducing Signaling Complex (Disc) with the Receptor. *Embo Journal* 14, 5579-5588, (1995).

202 Haridas, V. *et al.* VEGI, a new member of the TNF family activates nuclear factor-kappa B and c-Jun N-terminal kinase and modulates cell growth. *Oncogene* 18, 6496-6504, (1999).

203 Dempsey, P. W., Doyle, S. E., He, J. Q. & Cheng, G. H. The signaling adaptors and pathways activated by TNF superfamily. *Cytokine Growth Factor Rev* 14, 193-209, (2003).

204 Grech, A., Quinn, R., Srinivasan, D., Badoux, X. & Brink, R. Complete structural characterisation of the mammalian and Drosophila TRAF genes: implications for TRAF evolution and the role of RING finger splice variants. *Mol Immunol* 37, 721-734, (2000).

205 Kayagaki, N. *et al.* BAFF/BLyS receptor 3 binds the B cell survival factor BAFF ligand through a discrete surface loop and promotes processing of NF-kappaB2. *Immunity* 17, 515-524, (2002).

206 Zhai, Y. *et al.* LIGHT, a novel ligand for lymphotoxin beta receptor and TR2/HVEM induces apoptosis and suppresses in vivo tumor formation via gene transfer. *J Clin Invest* 102, 1142-1151, (1998).

207 Vanessen, D., Kikutani, H. & Gray, D. Cd40 Ligand-Transduced Co-Stimulation of T-Cells in the Development of Helper Function. *Nature* 378, 620-623, (1995).

208 Stuber, E., Neurath, M., Calderhead, D., Fell, H. F. & Strober, W. Cross-Linking of Ox40 Ligand, a Member of the Tnf/Ngf Cytokine Family, Induces Proliferation and Differentiation in Murine Splenic B-Cells. *Immunity* 2, 507-521, (1995).

209 Wiley, S. R., Goodwin, R. G. & Smith, C. A. Reverse signaling via CD30 ligand. *J Immunol* 157, 3635-3639, (1996).

210 Kim, H. J. *et al.* Reverse signaling through the costimulatory ligand CD137L in epithelial cells is essential for natural killer cell-mediated acute tissue inflammation. *Proc Natl Acad Sci U S A* 109, E13-22, (2012).

211 Watts, A. D. *et al.* A casein kinase I motif present in the cytoplasmic domain of members of the tumour necrosis factor ligand family is implicated in 'reverse signalling'. *Embo J* 18, 2119-2126, (1999).

212 Eissner, G. *et al.* Reverse signaling through transmembrane TNF confers resistance to lipopolysaccharide in human monocytes and macrophages. *J Immunol* 164, 6193-6198, (2000).

213 Waetzig, G. H. *et al.* Soluble tumor necrosis factor (TNF) receptor-1 induces apoptosis via reverse TNF signaling and autocrine transforming growth factor-beta 1. *Faseb Journal* 18, (2004).

214 Fu, Y. X. & Chaplin, D. D. Development and maturation of secondary lymphoid tissues. *Annu Rev Immunol* 17, 399-433, (1999).

215 Dougall, W. C. *et al.* RANK is essential for osteoclast and lymph node development. *Genes Dev* 13, 2412-2424, (1999).

216 Kong, Y. Y. *et al.* OPGL is a key regulator of osteoclastogenesis, lymphocyte development and lymph-node organogenesis. *Nature* 397, 315-323, (1999).

217 Grewal, I. S. & Flavell, R. A. A central role of CD40 ligand in the regulation of CD4(+) T-cell responses. *Immunol Today* 17, 410-414, (1996).

218 Stuber, E. & Strober, W. The T cell B cell interaction via OX40-OX40L is necessary for the T cell-dependent humoral immune response. *Journal of Experimental Medicine* 183, 979-989, (1996).

219 Nagata, S. & Golstein, P. The Fas death factor. *Science* 267, 1449-1456, (1995).

220 Song, K. *et al.* Tumor necrosis factor-related apoptosis-inducing ligand (TRAIL) is an inhibitor of autoimmune inflammation and cell cycle progression. *J Exp Med* 191, 1095-1104, (2000).

221 Ehlers, S. *et al.* The lymphotoxin beta receptor is critically involved in controlling infections with the intracellular pathogens Mycobacterium tuberculosis and Listeria monocytogenes. *J Immunol* 170, 5210-5218, (2003).

222 Bekker, L. G., Freeman, S., Murray, P. J., Ryffel, B. & Kaplan, G. TNF-alpha controls intracellular mycobacterial growth by both inducible nitric oxide synthase-dependent and inducible nitric oxide synthase-independent pathways. *J Immunol* 166, 6728-6734, (2001).

223 Prehn, J. L. *et al.* Potential role for TL1A, the new TNF-family member and potent costimulator of IFN-gamma, in mucosal inflammation. *Clin Immunol* 112, 66-77, (2004).

224 Wang, H. *et al.* TACI-ligand interactions are required for T cell activation and collagen-induced arthritis in mice. *Nat Immunol* 2, 632-637, (2001).

225 Saidenberg-Kermanac'h, N., Cohen-Solal, M., Bessis, N., De Vernejoul, M. C. & Boissier, M. C. Role for osteoprotegerin in rheumatoid inflammation. *Joint Bone Spine* 71, 9-13, (2004).

226 Balkwill, F. Tumour necrosis factor and cancer. *Nat Rev Cancer* 9, 361-371, (2009).

227 Moore, R. J. *et al.* Mice deficient in tumor necrosis factor-alpha are resistant to skin carcinogenesis. *Nat Med* 5, 828-831, (1999).

228 Arnott, C. H. *et al.* Expression of both TNF-alpha receptor subtypes is essential for optimal skin tumour development. *Oncogene* 23, 1902-1910, (2004).

229 Lee, D. F. *et al.* IKK beta suppression of TSC1 links inflammation and tumor angiogenesis via the mTOR pathway. *Cell* 130, 440-455, (2007).

230 Wiley, S. R. *et al.* Identification and characterization of a new member of the TNF family that induces apoptosis. *Immunity* 3, 673-682 (1995).

231 Vinay, D. S. & Kwon, B. S. The tumour necrosis factor/TNF receptor superfamily: therapeutic targets in autoimmune diseases. *Clin Exp Immunol* 164, 145-157, (2011).

232 Feldmann, M. Gene therapy for rheumatoid arthritis? *J Clin Invest* 107, 1353, (2001).

233 Chaudhari, U. *et al.* Efficacy and safety of infliximab monotherapy for plaque-type psoriasis: a randomised trial. *Lancet* 357, 1842-1847, (2001).

234 Cheema, G. S., Roschke, V., Hilbert, D. M. & Stohl, W. Elevated serum B lymphocyte stimulator levels in patients with systemic immune-based rheumatic diseases. *Arthritis Rheum* 44, 1313-1319, (2001).

235 Diwan, A., Tran, T., Misra, A. & Mann, D. L. Inflammatory mediators and the failing heart: a translational approach. *Curr Mol Med* 3, 161-182, (2003).

236 Bucay, N. *et al.* osteoprotegerin-deficient mice develop early onset osteoporosis and arterial calcification. *Genes Dev* 12, 1260-1268, (1998).

237 Barker, V., Middleton, G., Davey, F. & Davies, A. M. TNFalpha contributes to the death of NGF-dependent neurons during development. *Nat Neurosci* 4, 1194-1198, (2001).

238 Tanabe, K., Bonilla, I., Winkles, J. A. & Strittmatter, S. M. Fibroblast growth factor-inducible-14 is induced in axotomized neurons and promotes neurite outgrowth. *J Neurosci* 23, 9675-9686, (2003).

239 Desbarats, J. *et al.* Fas engagement induces neurite growth through ERK activation and p35 upregulation. *Nat Cell Biol* 5, 118-125, (2003).

240 Zuliani, C. *et al.* Control of neuronal branching by the death receptor CD95 (Fas/Apo-1). *Cell Death Differ* 13, 31-40, (2006).

241 Niu, Y. *et al.* Death receptor 5 and neuroproliferation. *Cell Mol Neurobiol* 32, 255-265, (2012).

242 Yepes, M. TWEAK and the central nervous system. *Mol Neurobiol* 35, 255-265, (2007).

243 Haile, W. B. *et al.* Tumor Necrosis Factor-Like Weak Inducer of Apoptosis and Fibroblast Growth Factor-Inducible 14 Mediate Cerebral Ischemia-Induced Poly(Adp-Ribose) Polymerase-1 Activation and Neuronal Death. *Neuroscience* 171, 1256-1264, (2010).

244 Echeverry, R., Wu, F., Haile, W. B., Wu, J. L. & Yepes, M. The cytokine tumor necrosis factor-like weak inducer of apoptosis and its receptor fibroblast growth factor-inducible 14 have a neuroprotective effect in the central nervous system. *J Neuroinflammation* 9, (2012).

245 Sporn, M. B. & Todaro, G. J. Autocrine secretion and malignant transformation of cells. *N Engl J Med* 303, 878-880, (1980).

246 Roberts, A. B. *et al.* Transforming growth factors: isolation of polypeptides from virally and chemically transformed cells by acid/ethanol extraction. *Proc Natl Acad Sci U S A* 77, 3494-3498, (1980).

247 Moses, H. L., Branum, E. L., Proper, J. A. & Robinson, R. A. Transforming growth factor production by chemically transformed cells. *Cancer Res* 41, 2842-2848, (1981).

248 Sporn, M. B. *et al.* Polypeptide transforming growth factors isolated from bovine sources and used for wound healing in vivo. *Science* 219, 1329-1331, (1983).

249 Tucker, R. F., Shipley, G. D., Moses, H. L. & Holley, R. W. Growth inhibitor from BSC-1 cells closely related to platelet type beta transforming growth factor. *Science* 226, 705-707, (1984).

250 Bottner, M., Krieglstein, K. & Unsicker, K. The transforming growth factor-betas: structure, signaling, and roles in nervous system development and functions. *J Neurochem* 75, 2227-2240, (2000).

251 Weiskirchen, R. *et al.* BMP-7 as antagonist of organ fibrosis. *Front Biosci* 14, 4992-5012, (2009).

252 Kingsley, D. M. The TGF-beta superfamily: new members, new receptors, and new genetic tests of function in different organisms. *Genes Dev* 8, 133-146, (1994).

253 Dubois, C. M., Laprise, M. H., Blanchette, F., Gentry, L. E. & Leduc, R. Processing of transforming growth factor beta 1 precursor by human furin convertase. *J Biol Chem* 270, 10618-10624, (1995).

254 Constam, D. B. & Robertson, E. J. Regulation of bone morphogenetic protein activity by pro domains and proprotein convertases. *J Cell Biol* 144, 139-149, (1999).

255 Massague, J. The transforming growth factor-beta family. *Annu Rev Cell Biol* 6, 597-641, (1990).

256 Ben-Haim, N. *et al.* The nodal precursor acting via activin receptors induces mesoderm by maintaining a source of its convertases and BMP4. *Dev Cell* 11, 313-323, (2006).

257 Annes, J. P., Munger, J. S. & Rifkin, D. B. Making sense of latent TGFbeta activation. *J Cell Sci* 116, 217-224, (2003).

258 Chang, H., Brown, C. W. & Matzuk, M. M. Genetic analysis of the mammalian transforming growth factor-beta superfamily. *Endocr Rev* 23, 787-823, (2002).

259 Ge, G., Hopkins, D. R., Ho, W. B. & Greenspan, D. S. GDF11 forms a bone morphogenetic protein 1-activated latent complex that can modulate nerve growth factor-induced differentiation of PC12 cells. *Mol Cell Biol* 25, 5846-5858, (2005).

260 McDonald, N. Q. & Hendrickson, W. A. A structural superfamily of growth factors containing a cystine knot motif. *Cell* 73, 421-424, (1993).

261 McPherron, A. C. & Lee, S. J. GDF-3 and GDF-9: two new members of the transforming growth factor-beta superfamily containing a novel pattern of cysteines. *J Biol Chem* 268, 3444-3449, (1993).

262 Yeo, C. & Whitman, M. Nodal signals to Smads through Cripto-dependent and Cripto-independent mechanisms. *Mol Cell* 7, 949-957, (2001).

263 Saarma, M. GDNF - a stranger in the TGF-beta superfamily? *Eur J Biochem* 267, 6968-6971, (2000).

264 Shi, Y. & Massague, J. Mechanisms of TGF-beta signaling from cell membrane to the nucleus. *Cell* 113, 685-700, (2003).

265 Schmierer, B. & Hill, C. S. TGFbeta-SMAD signal transduction: molecular specificity and functional flexibility. *Nat Rev Mol Cell Biol* 8, 970-982, (2007).

266 Allendorph, G. P., Vale, W. W. & Choe, S. Structure of the ternary signaling complex of a TGF-beta superfamily member. *Proc Natl Acad Sci U S A* 103, 7643-7648, (2006).

267 Wrana, J. L. *et al.* TGF beta signals through a heteromeric protein kinase receptor complex. *Cell* 71, 1003-1014, (1992).

268 Luo, K. & Lodish, H. F. Positive and negative regulation of type II TGF-beta receptor signal transduction by autophosphorylation on multiple serine residues. *Embo J* 16, 1970-1981, (1997).

269 Lawler, S. *et al.* The type II transforming growth factor-beta receptor autophosphorylates not only on serine and threonine but also on tyrosine residues. *J Biol Chem* 272, 14850-14859, (1997).

270 Wrana, J. L., Attisano, L., Wieser, R., Ventura, F. & Massague, J. Mechanism of activation of the TGF-beta receptor. *Nature* 370, 341-347, (1994).

271 Massague, J. TGF-beta signal transduction. *Annu Rev Biochem* 67, 753-791, (1998).

272 Derynck, R. Tgf-Beta-Receptor-Mediated Signaling. *Trends Biochem Sci* 19, 548-553, (1994).

273 Liu, F., Ventura, F., Doody, J. & Massague, J. Human type II receptor for bone morphogenic proteins (BMPs): extension of the two-kinase receptor model to the BMPs. *Mol Cell Biol* 15, 3479-3486, (1995).

274 Derynck, R. & Zhang, Y. E. Smad-dependent and Smad-independent pathways in TGF-beta family signalling. *Nature* 425, 577-584, (2003).

275 Lopez-Casillas, F., Wrana, J. L. & Massague, J. Betaglycan presents ligand to the TGF beta signaling receptor. *Cell* 73, 1435-1444, (1993).

276 Cheifetz, S. *et al.* Endoglin is a component of the transforming growth factor-beta receptor system in human endothelial cells. *J Biol Chem* 267, 19027-19030, (1992).

277 Barbara, N. P., Wrana, J. L. & Letarte, M. Endoglin is an accessory protein that interacts with the signaling receptor complex of multiple members of the transforming growth factor-beta superfamily. *J Biol Chem* 274, 584-594, (1999).

278 Sekelsky, J. J., Newfeld, S. J., Raftery, L. A., Chartoff, E. H. & Gelbart, W. M. Genetic-Characterization and Cloning of Mothers against Dpp, a Gene Required for Decapentaplegic Function in Drosophila-Melanogaster. *Genetics* 139, 1347-1358, (1995).

279 Savage, C. *et al.* Caenorhabditis elegans genes sma2, sma-3, and sma-4 define a conserved family of transforming growth factor beta pathway components. *Proc Natl Acad Sci U S A* 93, 790-794, (1996).

280 Lagna, G., Hata, A., Hemmati-Brivanlou, A. & Massague, J. Partnership between DPC4 and SMAD proteins in TGF-beta signalling pathways. *Nature* 383, 832-836, (1996).

281 Liu, F. *et al.* A human Mad protein acting as a BMP-regulated transcriptional activator. *Nature* 381, 620-623, (1996).

282 Hoodless, P. A. *et al.* MADR1, a MAD-related protein that functions in BMP2 signaling pathways. *Cell* 85, 489-500, (1996).

283 Nakao, A. *et al.* Identification of Smad7, a TGFbeta-inducible antagonist of TGF-beta signalling. *Nature* 389, 631-635, (1997).

284 Hata, A., Lagna, G., Massague, J. & Hemmati-Brivanlou, A. Smad6 inhibits BMP/Smad1 signaling by specifically competing with the Smad4 tumor suppressor. *Genes Dev* 12, 186-197, (1998).

285 Kavsak, P. *et al.* Smad7 binds to Smurf2 to form an E3 ubiquitin ligase that targets the TGF beta receptor for degradation. *Mol Cell* 6, 1365-1375, (2000).

286 Moustakas, A., Souchelnytskyi, S. & Heldin, C. H. Smad regulation in TGF-beta signal transduction. *J Cell Sci* 114, 4359-4369 (2001).

287 Kretzschmar, M., Doody, J., Timokhina, I. & Massague, J. A mechanism of repression of TGFbeta/ Smad signaling by oncogenic Ras. *Genes Dev* 13, 804-816 (1999).

288 Engel, M. E., McDonnell, M. A., Law, B. K. & Moses, H. L. Interdependent SMAD and JNK signaling in transforming growth factor-beta-mediated transcription. *J Biol Chem* 274, 37413-37420, (1999).

289 Wicks, S. J., Lui, S., Abdel-Wahab, N., Mason, R. M. & Chantry, A. Inactivation of smad-transforming growth factor beta signaling by Ca(2+)-calmodulin-dependent protein kinase II. *Mol Cell Biol* 20, 8103-8111, (2000).

290 Yakymovych, I., Ten Dijke, P., Heldin, C. H. & Souchelnytskyi, S. Regulation of Smad signaling by protein kinase C. *Faseb J* 15, 553-555, (2001).

291 Bray, S. J. Notch signalling: a simple pathway becomes complex. *Nat Rev Mol Cell Biol* 7, 678-689, (2006).

292 Dahlqvist, C. *et al.* Functional Notch signaling is required for BMP4-induced inhibition of myogenic differentiation. *Development* 130, 6089-6099, (2003).

293 Zamurovic, N., Cappellen, D., Rohner, D. & Susa, M. Coordinated activation of notch, Wnt, and transforming growth factor-beta signaling pathways in bone morphogenic protein 2-induced osteogenesis. Notch target gene Hey1 inhibits mineralization and Runx2 transcriptional activity. *J Biol Chem* 279, 37704-37715, (2004).

294 Labbe, E., Letamendia, A. & Attisano, L. Association of Smads with lymphoid enhancer binding factor 1/T cell-specific factor mediates cooperative signaling by the transforming growth factor-beta and wnt pathways. *Proc Natl Acad Sci U S A* 97, 8358-8363, (2000).

295 Yu, L., Hebert, M. C. & Zhang, Y. E. TGF-beta receptor-activated p38 MAP kinase mediates Smad-independent TGF-beta responses. *Embo J* 21, 3749-3759, (2002).

296 Yamaguchi, K. *et al.* XIAP, a cellular member of the inhibitor of apoptosis protein family, links the receptors to TAB1-TAK1 in the BMP signaling pathway. *Embo J* 18, 179-187, (1999).

297 Edlund, S., Landstrom, M., Heldin, C. H. & Aspenstrom, P. Transforming growth factor-beta-induced mobilization of actin cytoskeleton requires signaling by small GTPases Cdc42 and RhoA. *Mol Biol Cell* 13, 902-914, (2002).

298 Engel, M. E., Datta, P. K. & Moses, H. L. RhoB is stabilized by transforming growth factor beta and antagonizes transcriptional activation. *J Biol Chem* 273, 9921-9926, (1998).

299 Bakin, A. V., Tomlinson, A. K., Bhowmick, N. A., Moses, H. L. & Arteaga, C. L. Phosphatidylinositol 3-kinase function is required for transforming growth factor beta-mediated epithelial to mesenchymal transition and cell migration. *J Biol Chem* 275, 36803-36810, (2000).

300 Petritsch, C., Beug, H., Balmain, A. & Oft, M. TGF-beta inhibits p70 S6 kinase via protein phosphatase 2A to induce G(1) arrest. *Genes Dev* 14, 3093-3101, (2000).

301 Beppu, H. *et al.* BMP type II receptor is required for gastrulation and early development of mouse embryos. *Dev Biol* 221, 249-258, (2000).

302 Meno, C. *et al.* lefty-1 is required for left-right determination as a regulator of lefty-2 and nodal. *Cell* 94, 287-297, (1998).

303 Goumans, M. J. & Mummery, C. Functional analysis of the TGF beta receptor/Smad pathway through gene ablation in mice. *Int J Dev Biol* 44, 253-265, (2000).

304 Solloway, M. J. & Robertson, E. J. Early embryonic lethality in Bmp5;Bmp7 double mutant mice suggests functional redundancy within the 60A subgroup. *Development* 126, 1753-1768, (1999).

305 Kim, R. Y., Robertson, E. J. & Solloway, M. J. Bmp6 and Bmp7 are required for cushion formation and septation in the developing mouse heart. *Dev Biol* 235, 449-466, (2001).

306 Gaussin, V. *et al.* Endocardial cushion and myocardial defects after cardiac myocyte-specific conditional deletion of the bone morphogenetic protein receptor ALK3. *Proc Natl Acad Sci U S A* 99, 2878-2883, (2002).

307 Lane, K. B. *et al.* Heterozygous germline mutations in BMPR2, encoding a TGF-beta receptor, cause familial primary pulmonary hypertension. *Nat Genet* 26, 81-84, (2000).

308 Li, D. Y. *et al.* Defective angiogenesis in mice lacking endoglin. *Science* 284, 1534-1537, (1999).

309 Oh, S. P. *et al.* Activin receptor-like kinase 1 modulates transforming growth factor-beta 1 signaling in the regulation of angiogenesis. *Proc Natl Acad Sci U S A* 97, 2626-2631, (2000).

310 Abdalla, S. A. & Letarte, M. Hereditary haemorrhagic telangiectasia: current views on genetics and mechanisms of disease. *J Med Genet* 43, 97-110, (2006).

311 Tucker, A. S., Matthews, K. L. & Sharpe, P. T. Transformation of tooth type induced by inhibition of BMP signaling. *Science* 282, 1136-1138, (1998).

312 Furuta, Y. & Hogan, B. L. BMP4 is essential for lens induction in the mouse embryo. *Genes Dev* 12, 3764-3775, (1998).

313 Sanford, L. P. *et al.* TGFbeta2 knockout mice have multiple developmental defects that are non-overlapping with other TGFbeta knockout phenotypes. *Development* 124, 2659-2670, (1997).

314 McPherron, A. C., Lawler, A. M. & Lee, S. J. Regulation of anterior/posterior patterning of the axial skeleton by growth/differentiation factor 11. *Nat Genet* 22, 260-264, (1999).

315 Mustoe, T. A. *et al.* Accelerated healing of incisional wounds in rats induced by transforming growth factor-beta. *Science* 237, 1333-1336, (1987).

316 Gordon, K. J. & Blobe, G. C. Role of transforming growth factor-beta superfamily signaling pathways in human disease. *Biochim Biophys Acta* 1782, 197-228, (2008).

317 Lamb, T. M. *et al.* Neural induction by the secreted polypeptide noggin. *Science* 262, 713-718, (1993).

318 Zimmermann, B., Moegelin, A., de Souza, P. & Bier, J. Morphology of the development of the sagittal suture of mice. *Anat Embryol* 197, 155-165, (1998).

319 Reissmann, E. *et al.* Involvement of bone morphogenetic protein-4 and bone morphogenetic protein-7 in the differentiation of the adrenergic phenotype in developing sympathetic neurons. *Development* 122, 2079-2088, (1996).

320 Johns, L. D. *et al.* Transforming growth factor-beta 1 differentially regulates proliferation and MHC class-II antigen expression in forebrain and brainstem astrocyte primary cultures. *Brain Res* 585, 229-236, (1992).

321 McKinnon, R. D., Piras, G., Ida, J. A., Jr. & Dubois-Dalcq, M. A role for TGF-beta in oligodendrocyte differentiation. *J Cell Biol* 121, 1397-1407, (1993).

322 Chesnutt, C., Burrus, L. W., Brown, A. M. & Niswander, L. Coordinate regulation of neural tube patterning and proliferation by TGFbeta and WNT activity. *Dev Biol* 274, 334-347, (2004).

323 Panchision, D. M. *et al.* Sequential actions of BMP receptors control neural precursor cell production and fate. *Genes Dev* 15, 2094-2110, (2001).

324 Krieglstein, K. & Unsicker, K. Distinct modulatory actions of TGF-beta and LIF on neurotrophin-mediated survival of developing sensory neurons. *Neurochem Res* 21, 843-850 ,(1996).

325 Lin, L. F., Doherty, D. H., Lile, J. D., Bektesh, S. & Collins, F. GDNF: a glial cell line-derived neurotrophic factor for midbrain dopaminergic neurons. *Science* 260, 1130-1132, (1993).

326 Tomac, A. *et al.* Protection and repair of the nigrostriatal dopaminergic system by GDNF in vivo. *Nature* 373, 335-339, (1995).

327 Krieglstein, K. *et al.* Glial cell line-derived neurotrophic factor requires transforming growth factor-beta for exerting its full neurotrophic potential on peripheral and CNS neurons. *J Neurosci* 18, 9822-9834, (1998).

328 Butler, S. J. & Dodd, J. A role for BMP heterodimers in roof plate-mediated repulsion of commissural axons. *Neuron* 38, 389-401, (2003).

329 Ishihara, A., Saito, H. & Abe, K. Transforming growth factor-beta 1 and -beta 2 promote neurite sprouting and elongation of cultured rat hippocampal neurons. *Brain Res* 639, 21-25, (1994).

330 Lein, P., Johnson, M., Guo, X., Rueger, D. & Higgins, D. Osteogenic Protein-1 Induces Dendritic Growth in Rat Sympathetic Neurons. *Neuron* 15, 597-605, (1995).

331 Le Roux, P., Behar, S., Higgins, D. & Charette, M. OP-1 enhances dendritic growth from cerebral cortical neurons in vitro. *Exp Neurol* 160, 151-163, (1999).

332 Withers, G. S., Higgins, D., Charette, M. & Banker, G. Bone morphogenetic protein-7 enhances dendritic growth and receptivity to innervation in cultured hippocampal neurons. *European Journal of Neuroscience* 12, 106-116, (2000).

333 Lee-Hoeflich, S. T. *et al.* Activation of LIMK1 by binding to the BMP receptor, BMPRII, regulates BMP-dependent dendritogenesis. *Embo J* 23, 4792-4801, (2004).

334 Meng, Y. *et al.* Abnormal spine morphology and enhanced LTP in LIMK-1 knockout mice. *Neuron* 35, 121-133, (2002).

335 Katsuno, M. *et al.* Transforming growth factor-beta signaling in motor neuron diseases. *Curr Mol Med* 11, 48-56, (2011).

336 Vivien, D. & Ali, C. Transforming growth factor-beta signalling in brain disorders. *Cytokine Growth Factor Rev* 17, 121-128, (2006).

337 Caraci, F. *et al.* TGF-beta 1 protects against Abeta-neurotoxicity via the phosphatidylinositol-3-kinase pathway. *Neurobiol Dis* 30, 234-242, (2008).

338 Theiler, K. *The House Mouse - Atlas of Embryonic Development*. (Springer-Verlag, 1989).

339 Fath, T., Ke, Y. D., Gunning, P., Gotz, J. & Ittner, L. M. Primary support cultures of hippocampal and substantia nigra neurons. *Nat Protoc* 4, 78-85, (2009).

340 Gil, V. & del Rio, J. A. Analysis of axonal growth and cell migration in 3D hydrogel cultures of embryonic mouse CNS tissue. *Nat Protoc* 7, 268-280, (2012).

341 Ingold, K. *et al.* Identification of proteoglycans as the APRIL-specific binding partners. *Journal of Experimental Medicine* 201, 1375-1383, (2005).

342 Yang, M. *et al.* B cell maturation antigen, the receptor for a proliferation-inducing ligand and B cell-activating factor of the TNF family, induces antigen presentation in B cells. *J Immunol* 175, 2814-2824, (2005).

343 Ho, C. C. & Bernard, D. J. Bone Morphogenetic Protein 2 Signals via BMPR1A to Regulate Murine Follicle-Stimulating Hormone Beta Subunit Transcription. *Biol Reprod* 81, 133-141, (2009).

344 Jiang, Y. X. *et al.* Trapping of BMP receptors in distinct membrane domains inhibits their function in pulmonary arterial hypertension. *Am J Physiol-Lung C* 301, L218-L227, (2011).

345 Liu, I. M. *et al.* TGF beta-stimulated Smad1/5 phosphorylation requires the ALK5 L45 loop and mediates the pro-migratory TGF beta switch. *Embo Journal* 28, 88-98, (2009).

346 Takizawa, T., Ochiai, W., Nakashima, K. & Taga, T. Enhanced gene activation by Notch and BMP signaling cross-talk. *Nucleic Acids Res* 31, 5723-5731, (2003).

347 Cossins, J., Vernon, A. E., Zhang, Y., Philpott, A. & Jones, P. H. Hes6 regulates myogenic differentiation. *Brit J Cancer* 86, S83-S83, (2002).

348 Zhang, Y., Feng, X. H., Wu, R. Y. & Derynck, R. Receptor-associated Mad homologues synergize as effectors of the TGF-beta response. *Nature* 383, 168-172, (1996).

349 Hayashi, H. *et al.* The MAD-related protein Smad7 associates with the TGF beta receptor and functions as an antagonist of TGF beta signaling. *Cell* 89, 1165-1173, (1997).

350 Hojo, M. *et al.* Glial cell fate specification modulated by the bHLH gene Hes5 in mouse retina. *Development* 127, 2515-2522, (2000).

351 Gutierrez, H. & Davies, A. M. A fast and accurate procedure for deriving the Sholl profile in quantitative studies of neuronal morphology. *J Neurosci Methods* 163, 24-30, (2007).

352 Lopez-Fraga, M., Fernandez, R., Albar, J. P. & Hahne, M. Biologically active APRIL is secreted following intracellular processing in the Golgi apparatus by furin convertase. *EMBO Rep* 2, 945-951, (2001).

353 Hahne, M. *et al.* APRIL, a new ligand of the tumor necrosis factor family, stimulates tumor cell growth. *J Exp Med* 188, 1185-1190, (1998).

354 Yu, G. *et al.* APRIL and TALL-I and receptors BCMA and TACI: system for regulating humoral immunity. *Nat Immunol* 1, 252-256, (2000).

355 Litinskiy, M. B. *et al.* DCs induce CD40-independent immunoglobulin class switching through BLyS and APRIL. *Nat Immunol* 3, 822-829, (2002).

356 Moreaux, J. *et al.* The level of TACI gene expression in myeloma cells is associated with a signature of microenvironment dependence versus a plasmablastic signature. *Blood* 106, 1021-1030, (2005).

357 Rennert, P. *et al.* A soluble form of B cell maturation antigen, a receptor for the tumor necrosis factor family member APRIL, inhibits tumor cell growth. *J Exp Med* 192, 1677-1684, (2000).

358 Laabi, Y. *et al.* The BCMA gene, preferentially expressed during B lymphoid maturation, is bidirectionally transcribed. *Nucleic Acids Res* 22, 1147-1154, (1994).

359 Ng, L. G. *et al.* B cell-activating factor belonging to the TNF family (BAFF)-R is the principal BAFF receptor facilitating BAFF costimulation of circulating T and B cells. *J Immunol* 173, 807-817, (2004).

360 Moreaux, J. *et al.* BAFF and APRIL protect myeloma cells from apoptosis induced by interleukin 6 deprivation and dexamethasone. *Blood* 103, 3148-3157, (2004).

361 Schiemann, B. *et al.* An essential role for BAFF in the normal development of B cells through a BCMA-independent pathway. *Science* 293, 2111-2114, (2001).

362 O'Connor, B. P. *et al.* BCMA is essential for the survival of long-lived bone marrow plasma cells. *J Exp Med* 199, 91-98, (2004).

363 von Bulow, G. U., van Deursen, J. M. & Bram, R. J. Regulation of the T-independent humoral response by TACI. *Immunity* 14, 573-582, (2001).

364 Yan, M. *et al.* Activation and accumulation of B cells in TACI-deficient mice. *Nat Immunol* 2, 638-643, (2001).

365 Marsters, S. A. *et al.* Interaction of the TNF homologues BLyS and APRIL with the TNF receptor homologues BCMA and TACI. *Curr Biol* 10, 785-788, (2000).

366 Stein, J. V. *et al.* APRIL modulates B and T cell immunity. *J Clin Invest* 109, 1587-1598, (2002).

367 Varfolomeev, E. *et al.* APRIL-deficient mice have normal immune system development. *Mol Cell Biol* 24, 997-1006, (2004).

368 Castigli, E. *et al.* Impaired IgA class switching in APRIL-deficient mice. *Proc Natl Acad Sci U S A* 101, 3903-3908, (2004).

369 Koyama, T. *et al.* Raised serum APRIL levels in patients with systemic lupus erythematosus. *Ann Rheum Dis* 64, 1065-1067, (2005).

370 Koyama, T. *et al.* A novel polymorphism of the human APRIL gene is associated with systemic lupus erythematosus. *Rheumatology (Oxford)* 42, 980-985, (2003).

371 Huard, B., Tran, N. L., Benkhoucha, M., Manzin-Lorenzi, C. & Santiago-Raber, M. L. Selective APRIL blockade delays systemic lupus erythematosus in mouse. *PLoS One* 7, (2012).

372 Tan, S. M. *et al.* Local production of B lymphocyte stimulator protein and APRIL in arthritic joints of patients with inflammatory arthritis. *Arthritis Rheum* 48, 982-992, (2003).

373 Thangarajh, M. *et al.* Increased levels of APRIL (a proliferation-inducing ligand) mRNA in multiple sclerosis. *J Neuroimmunol* 167, 210-214, (2005).

374 Deshayes, F. *et al.* Abnormal production of the TNF-homologue APRIL increases the proliferation of human malignant glioblastoma cell lines via a specific receptor. *Oncogene* 23, 3005-3012, (2004).

375 Mhawech-Fauceglia, P. *et al.* The source of APRIL up-regulation in human solid tumor lesions. *J Leukoc Biol* 80, 697-704, (2006).

376 Tecchio, C. *et al.* A proliferation-inducing ligand (APRIL) serum levels predict time to first treatment in patients affected by B-cell chronic lymphocytic leukemia. *Eur J Haematol* 87, 228-234, (2011).

377 Bojarska-Junak, A. *et al.* BAFF and APRIL expression in B-cell chronic lymphocytic leukemia: correlation with biological and clinical features. *Leuk Res* 33, 1319-1327, (2009).

378 Kern, C. *et al.* Involvement of BAFF and APRIL in the resistance to apoptosis of B-CLL through an autocrine pathway. *Blood* 103, 679-688, (2004).

379 He, B. *et al.* Lymphoma B cells evade apoptosis through the TNF family members BAFF/BLyS and APRIL. *J Immunol* 172, 3268-3279, (2004).

380 Thangarajh, M., Masterman, T., Hillert, J., Moerk, S. & Jonsson, R. A proliferation-inducing ligand (APRIL) is expressed by astrocytes and is increased in multiple sclerosis. *Scand J Immunol* 65, 92-98, (2007).

381 Guan, Z. B., Shui, Y. & Zhang, S. Q. Two related ligands of the TNF family, BAFF and APRIL, in rabbit: molecular cloning, 3D modeling, and tissue distribution. *Cytokine* 39, 192-200, (2007).

382 Wallweber, H. J., Compaan, D. M., Starovasnik, M. A. & Hymowitz, S. G. The crystal structure of a proliferation-inducing ligand, APRIL. *J Mol Biol* 343, 283-290, (2004).

383 Kolfschoten, G. M., Pradet-Balade, B., Hahne, M. & Medema, J. P. TWE-PRIL; a fusion protein of TWEAK and APRIL. *Biochem Pharmacol* 66, 1427-1432, (2003).

384 Daridon, C., Youinou, P. & Pers, J. O. BAFF, APRIL, TWE-PRIL: who's who? *Autoimmun Rev* 7, 267-271, (2008).

385 Roschke, V. *et al.* BLyS and APRIL form biologically active heterotrimers that are expressed in patients with systemic immune-based rheumatic diseases. *J Immunol* 169, 4314-4321, (2002).

386 Patel, D. R. *et al.* Engineering an APRIL-specific B-cell maturation antigen (BCMA). *Protein Science* 13, 95-95, (2004).

387 Baker, K. P. BLyS - an essential survival factor for B cells: basic biology, links to pathology and therapeutic target. *Autoimmun Rev* 3, 368-375, (2004).

388 Hymowitz, S. G. *et al.* Structures of APRIL-receptor complexes: like BCMA, TACI employs only a single cysteine-rich domain for high affinity ligand binding. *J Biol Chem* 280, 7218-7227, (2005).

389 Hendriks, J. *et al.* Heparan sulfate proteoglycan binding promotes APRIL-induced tumor cell proliferation. *Cell Death Differ* 12, 637-648, (2005).

390 Hatzoglou, A. *et al.* TNF receptor family member BCMA (B cell maturation) associates with TNF receptor-associated factor (TRAF) 1, TRAF2, and TRAF3 and activates NF-kappa B, elk-1, c-Jun N-terminal kinase, and p38 mitogen-activated protein kinase. *J Immunol* 165, 1322-1330, (2000).

391 Xia, X. Z. *et al.* TACI is a TRAF-interacting receptor for TALL-1, a tumor necrosis factor family member involved in B cell regulation. *J Exp Med* 192, 137-143, (2000).

392 von Bulow, G. U. & Bram, R. J. NF-AT activation induced by a CAML-interacting member of the tumor necrosis factor receptor superfamily. *Science* 278, 138-141, (1997).

393 Touyz, R. M. *et al.* Inhibition of mitogen-activated protein/extracellular signal-regulated kinase improves endothelial function and attenuates Ang II-induced

contractility of mesenteric resistance arteries from spontaneously hypertensive rats. *J Hypertens* 20, 1127-1134, (2002).

394 Vlahos, C. J., Matter, W. F. & Brown, R. F. A Specific Inhibitor of Phosphatidylinositol 3-Kinase. *J Cell Biochem*, 274-274, (1994).

395 Garrido, J. J., Simon, D., Varea, O. & Wandosell, F. GSK3 alpha and GSK3 beta are necessary for axon formation. *Febs Lett* 581, 1579-1586, (2007).

396 Sayas, C. L., Ariaens, A., Ponsioen, B. & Moolenaar, W. H. GSK-3 is activated by the tyrosine kinase Pyk2 during LPA(1)-mediated neurite retraction. *Mol Biol Cell* 17, 1834-1844, (2006).

397 Kisiswa, L. *et al.* TNF alpha reverse signaling promotes sympathetic axon growth and target innervation. *Nat Neurosci* 16, 865-U264, (2013).

398 Chiu, A. *et al.* Hodgkin lymphoma cells express TACI and BCMA receptors and generate survival and proliferation signals in response to BAFF and APRIL. *Blood* 109, 729-739, (2007).

399 Bonci, D., Hahne, M., Felli, N., Peschle, C. & De Maria, R. Potential role of APRIL as autocrine growth factor for megakaryocytopoiesis. *Blood* 104, 3169-3172, (2004).

400 Perrimon, N. & Bernfield, M. Specificities of heparan sulphate proteoglycans in developmental processes. *Nature* 404, 725-728, (2000).

401 Sarrazin, S., Lamanna, W. C. & Esko, J. D. Heparan Sulfate Proteoglycans. *Cold Spring Harb Perspect Biol* 3, (2011).

402 Colombres, M. *et al.* Heparin activates Wnt signaling for neuronal morphogenesis. *J Cell Physiol* 216, 805-815, (2008).

403 Bespalov, M. M. *et al.* Heparan sulfate proteoglycan syndecan-3 is a novel receptor for GDNF, neurturin, and artemin. *Journal of Cell Biology* 192, 153-169, (2011).

404 Kimberley, F. C. *et al.* The proteoglycan (heparan sulfate proteoglycan) binding domain of APRIL serves as a platform for ligand multimerization and cross-linking. *Faseb Journal* 23, 1584-1595, (2009).

405 Atwal, J. K., Massie, B., Miller, F. D. & Kaplan, D. R. The TrkB-Shc site signals neuronal survival and local axon growth via MEK and PI3-kinase. *Neuron* 27, 265-277, (2000).

406 Forcet, C. *et al.* Netrin-1-mediated axon outgrowth requires deleted in colorectal cancer-dependent MAPK activation. *Nature* 417, 443-447, (2002).

407 Pasterkamp, R. J., Peschon, J. J., Spriggs, M. K. & Kolodkin, A. L. Semaphorin 7A promotes axon outgrowth through integrins and MAPKs. *Nature* 424, 398-405, (2003).

408 McKelvey, L. *et al.* The intracellular portion of GITR enhances NGF-promoted neurite growth through an inverse modulation of Erk and NF-kappaB signalling. *Biol Open* 1, 1016-1023, (2012).

409 Ray, L. B. & Sturgill, T. W. Rapid Stimulation by Insulin of a Serine Threonine Kinase in 3t3-L1 Adipocytes That Phosphorylates Microtubule-Associated Protein-2 Invitro. *Proc Natl Acad Sci U S A* 84, 1502-1506, (1987).

410 Atwal, J. K., Singh, K. K., Tessier-Lavigne, M., Miller, F. D. & Kaplan, D. R. Semaphorin 3F antagonizes neurotrophin-induced phosphatidylinositol 3-kinase and mitogen-activated protein kinase kinase signaling: A mechanism for growth cone collapse. *Journal of Neuroscience* 23, 7602-7609, (2003).

411 Campbell, D. S. & Holt, C. E. Apoptotic pathway and MAPKs differentially regulate chemotropic responses of retinal growth cones. *Neuron* 37, 939-952, (2003).

412 MacInnis, B. L. & Campenot, R. B. Regulation of Wallerian degeneration and nerve growth factor withdrawal-induced pruning of axons of sympathetic neurons by the proteasome and the MEK/Erk pathway. *Molecular and Cellular Neuroscience* 28, 430-439, (2005).

413 Zonca, M. *et al.* APRIL and BAFF Proteins Increase Proliferation of Human Adipose-Derived Stem Cells Through Activation of Erk1/2 MAP Kinase. *Tissue Eng Pt A* 18, 853-860, (2012).

414 Gupta, M. *et al.* A proliferation-inducing ligand mediates follicular lymphoma B-cell proliferation and cyclin D1 expression through phosphatidylinositol 3-kinase-regulated mammalian target of rapamycin activation. *Blood* 113, 5206-5216, (2009).

415 Cosker, K. E. & Eickholt, B. J. Phosphoinositide 3-kinase signalling events controlling axonal morphogenesis. *Biochem Soc T* 35, 207-210, (2007).

416 Zhou, F. Q., Zhou, J., Dedhar, S., Wu, Y. H. & Snider, W. D. NGF-induced axon growth is mediated by localized inactivation of GSK-30 and functions of the microtubule plus end binding protein APC. *Neuron* 42, 897-912, (2004).

417 Yoshimura, T. *et al.* Ras regulates neuronal polarity via the PI3-kinase/Akt/GSK-3 beta/CRMP-2 pathway. *Biochem Biophys Res Commun* 340, 62-68, (2006).

418 Namikawa, K. *et al.* Akt/protein kinase B prevents injury-induced motoneuron death and accelerates axonal regeneration. *Journal of Neuroscience* 20, 2875-2886, (2000).

419 Kim, W. Y. *et al.* Essential roles for GSK-3s and GSK-3-primed substrates in neurotrophin-induced and hippocampal axon growth. *Neuron* 52, 981-996, (2006).

420 Zhou, F. Q. & Snider, W. D. Intracellular control of developmental and regenerative axon growth. *Philos T R Soc B* 361, 1575-1592, (2006).

421 Segal, R. A. Selectivity inneurotrophin signaling: Theme and variations. *Annu Rev Neurosci* 26, 299-330, (2003).

422 Hildt, E. & Oess, S. Identification of Grb2 as a novel binding partner of tumor necrosis factor (TNF) receptor I. *Journal of Experimental Medicine* 189, 1707-1714, (1999).

423 Goold, R. G. & Gordon-Weeks, P. R. The MAP kinase pathway is upstream of the activation of GSK3 beta that enables it to phosphorylate MAP1B and contributes to

the stimulation of axon growth. *Molecular and Cellular Neuroscience* 28, 524-534, (2005).

424 Stambolic, V. & Woodgett, J. R. Mitogen Inactivation of Glycogen-Synthase Kinase-3-Beta in Intact-Cells Via Serine-9 Phosphorylation. *Biochem J* 303, 701-704, (1994).

425 Storm, E. E. *et al.* Limb alterations in brachypodism mice due to mutations in a new member of the TGF beta-superfamily. *Nature* 368, 639-643, (1994).

426 Polinkovsky, A. *et al.* Mutations in CDMP1 cause autosomal dominant brachydactyly type C. *Nat Genet* 17, 18-19, (1997).

427 Thomas, J. T. *et al.* A human chondrodysplasia due to a mutation in a TGF-beta superfamily member. *Nat Genet* 12, 315-317, (1996).

428 Thomas, J. T. *et al.* Disruption of human limb morphogenesis by a dominant negative mutation in CDMP1. *Nat Genet* 17, 58-64, (1997).

429 Yi, S. E., Daluiski, A., Pederson, R., Rosen, V. & Lyons, K. M. The type I BMP receptor BMPRIB is required for chondrogenesis in the mouse limb. *Development* 127, 621-630, (2000).

430 Storm, E. E. & Kingsley, D. M. Joint patterning defects caused by single and double mutations in members of the bone morphogenetic protein (BMP) family. *Development* 122, 3969-3979, (1996).

431 Storm, E. E. & Kingsley, D. M. GDF5 coordinates bone and joint formation during digit development. *Dev Biol* 209, 11-27, (1999).

432 Francis-West, P. H. *et al.* Mechanisms of GDF-5 action during skeletal development. *Development* 126, 1305-1315, (1999).

433 Erlacher, L. *et al.* Cartilage-derived morphogenetic proteins and osteogenic protein-1 differentially regulate osteogenesis. *J Bone Miner Res* 13, 383-392, (1998).

434 Wolfman, N. M. *et al.* Ectopic induction of tendon and ligament in rats by growth and differentiation factors 5, 6, and 7, members of the TGF-beta gene family. *J Clin Invest* 100, 321-330, (1997).

435 Morotome, Y., Goseki-Sone, M., Ishikawa, I. & Oida, S. Gene expression of growth and differentiation factors-5, -6, and -7 in developing bovine tooth at the root forming stage. *Biochem Biophys Res Commun* 244, 85-90, (1998).

436 Yoon, B. S. *et al.* Bmpr1a and Bmpr1b have overlapping functions and are essential for chondrogenesis in vivo. *Proc Natl Acad Sci U S A* 102, 5062-5067, (2005).

437 Sammar, M. *et al.* Modulation of GDF5/BRI-b signalling through interaction with the tyrosine kinase receptor Ror2. *Genes Cells* 9, 1227-1238, (2004).

438 Delot, E. C., Bahamonde, M. E., Zhao, M. & Lyons, K. M. BMP signaling is required for septation of the outflow tract of the mammalian heart. *Development* 130, 209-220, (2003).

439 Deng, Z. *et al.* Familial primary pulmonary hypertension (gene PPH1) is caused by mutations in the bone morphogenetic protein receptor-II gene. *Am J Hum Genet* 67, 737-744, (2000).

440 Yamashita, H. *et al.* Growth/differentiation factor-5 induces angiogenesis in vivo. *Exp Cell Res* 235, 218-226, (1997).

441 Farkas, L. M., Scheuermann, S., Pohl, J., Unsicker, K. & Krieglstein, K. Characterization of growth/differentiation factor 5 (GDF-5) as a neurotrophic factor for cultured neurons from chicken dorsal root ganglia. *Neurosci Lett* 236, 120-122, (1997).

442 Niere, M., Braun, B., Gass, R., Sturany, S. & Volkmer, H. Combination of engineered neural cell adhesion molecules and GDF-5 for improved neurite extension in nerve guide concepts. *Biomaterials* 27, 3432-3440, (2006).

443 O'Keeffe, G. W., Hanke, M., Pohl, J. & Sullivan, A. M. Expression of growth differentiation factor-5 in the developing and adult rat brain. *Brain Res Dev Brain Res* 151, 199-202, (2004).

444 Wood, T. K., McDermott, K. W. & Sullivan, A. M. Differential effects of growth/differentiation factor 5 and glial cell line-derived neurotrophic factor on dopaminergic neurons and astroglia in cultures of embryonic rat midbrain. *J Neurosci Res* 80, 759-766, (2005).

445 Hurley, F. M., Costello, D. J. & Sullivan, A. M. Neuroprotective effects of delayed administration of growth/differentiation factor-5 in the partial lesion model of Parkinson's disease. *Exp Neurol* 185, 281-289, (2004).

446 Sullivan, A. M., Pohl, J. & Blunt, S. B. Growth/differentiation factor 5 and glial cell line-derived neurotrophic factor enhance survival and function of dopaminergic grafts in a rat model of Parkinson's disease. *Eur J Neurosci* 10, 3681-3688, (1998).

447 Costello, D. J., O'Keeffe, G. W., Hurley, F. M. & Sullivan, A. M. Transplantation of novel human GDF5-expressing CHO cells is neuroprotective in models of Parkinson's disease. *J Cell Mol Med* 16, 2451-2460, (2012).

448 Dewulf, N. *et al.* Distinct spatial and temporal expression patterns of two type I receptors for bone morphogenetic proteins during mouse embryogenesis. *Endocrinology* 136, 2652-2663, (1995).

449 Miyagi, M. *et al.* Bone morphogenetic protein receptor expressions in the adult rat brain. *Neuroscience* 176, 93-109, (2011).

450 Soderstrom, S., Bengtsson, H. & Ebendal, T. Expression of serine/threonine kinase receptors including the bone morphogenetic factor type II receptor in the developing and adult rat brain. *Cell Tissue Res* 286, 269-279, (1996).

451 Cejalvo, T. *et al.* Bone morphogenetic protein-2/4 signalling pathway components are expressed in the human thymus and inhibit early T-cell development. *Immunology* 121, 94-104, (2007).

452 Bernhardt, R. & Matus, A. Light and Electron-Microscopic Studies of the Distribution of Microtubule-Associated Protein-2 in Rat-Brain - a Difference between Dendritic and Axonal Cytoskeletons. *Journal of Comparative Neurology* 226, 203-221, (1984).

453 Felin, J. E. *et al.* Nuclear variants of bone morphogenetic proteins. *BMC Cell Biol* 11, 20, (2010).

454 Schreuder, H., Liesum, A., Pohl, J., Kruse, M. & Koyama, M. Crystal structure of recombinant human growth and differentiation factor 5: evidence for interaction of the type I and type II receptor-binding sites. *Biochem Biophys Res Commun* 329, 1076-1086, (2005).

455 Nishitoh, H. *et al.* Identification of type I and type II serine/threonine kinase receptors for growth/differentiation factor-5. *J Biol Chem* 271, 21345-21352, (1996).

456 Baur, S. T., Mai, J. J. & Dymecki, S. M. Combinatorial signaling through BMP receptor IB and GDF5: shaping of the distal mouse limb and the genetics of distal limb diversity. *Development* 127, 605-619, (2000).

457 Nickel, J., Kotzsch, A., Sebald, W. & Mueller, T. D. A single residue of GDF-5 defines binding specificity to BMP receptor IB. *J Mol Biol* 349, 933-947, (2005).

458 Chen, X. *et al.* Upregulation of ID protein by growth and differentiation factor 5 (GDF5) through a smad-dependent and MAPK-independent pathway in HUVSMC. *J Mol Cell Cardiol* 41, 26-33, (2006).

459 Zhong, Z. M. *et al.* Growth/differentiation factor-5 induces osteogenic differentiation of human ligamentum flavum cells through activation of ERK1/2 and p38 MAPK. *Cell Physiol Biochem* 26, 179-186, (2010).

460 Gratton, M. O. *et al.* Hes6 promotes cortical neurogenesis and inhibits Hes1 transcription repression activity by multiple mechanisms. *Mol Cell Biol* 23, 6922-6935, (2003).

461 Fior, R. & Henrique, D. A novel hes5/hes6 circuitry of negative regulation controls Notch activity during neurogenesis. *Dev Biol* 281, 318-333, (2005).

462 Garcia-Finana, M., Cruz-Orive, L. M., Mackay, C. E., Pakkenberg, B. & Roberts, N. Comparison of MR imaging against physical sectioning to estimate the volume of human cerebral compartments. *Neuroimage* 18, 505-516, (2003).

463 Cho, Y. D. *et al.* Wnt3a stimulates Mepe, matrix extracellular phosphoglycoprotein, expression directly by the activation of the canonical Wnt signaling pathway and indirectly through the stimulation of autocrine Bmp-2 expression. *J Cell Physiol* 227, 2287-2296, (2012).

464 Theriault, B. L. & Nachtigal, M. W. Human ovarian cancer cell morphology, motility, and proliferation are differentially influenced by autocrine TGFbeta superfamily signalling. *Cancer Lett* 313, 108-121, (2011).

465 Perron, J. C. & Dodd, J. Inductive specification and axonal orientation of spinal neurons mediated by divergent bone morphogenetic protein signaling pathways. *Neural Dev* 6, 36, (2011).

466 Parikh, P. *et al.* Regeneration of axons in injured spinal cord by activation of bone morphogenetic protein/Smad1 signaling pathway in adult neurons. *Proc Natl Acad Sci U S A* 108, E99-107, (2011).

467 Caronia, G., Wilcoxon, J., Feldman, P. & Grove, E. A. Bone morphogenetic protein signaling in the developing telencephalon controls formation of the hippocampal dentate gyrus and modifies fear-related behavior. *J Neurosci* 30, 6291-6301, (2010).

468 Yamauchi, K., Phan, K. D. & Butler, S. J. BMP type I receptor complexes have distinct activities mediating cell fate and axon guidance decisions. *Development* 135, 1119-1128, (2008).

469 Foletta, V. C. *et al.* Direct signaling by the BMP type II receptor via the cytoskeletal regulator LIMK1. *J Cell Biol* 162, 1089-1098, (2003).

470 Benavente, F., Pinto, C., Parada, M., Henriquez, J. P. & Osses, N. Bone morphogenetic protein 2 inhibits neurite outgrowth of motor neuron-like NSC-34 cells and up-regulates its type II receptor. *J Neurochem* 122, 594-604, (2012).

471 Ross, S. & Hill, C. S. How the Smads regulate transcription. *Int J Biochem Cell Biol* 40, 383-408, (2008).

472 Guo, X. *et al.* Dendritic growth induced by BMP-7 requires Smad1 and proteasome activity. *J Neurobiol* 48, 120-130, (2001).

473 Matsuura, I. *et al.* BMP inhibits neurite growth by a mechanism dependent on LIM-kinase. *Biochem Biophys Res Commun* 360, 868-873, (2007).

474 Podkowa, M. *et al.* Microtubule stabilization by bone morphogenetic protein receptor-mediated scaffolding of c-Jun N-terminal kinase promotes dendrite formation. *Mol Cell Biol* 30, 2241-2250, (2010).

475 Bae, S., Bessho, Y., Hojo, M. & Kageyama, R. The bHLH gene Hes6, an inhibitor of Hes1, promotes neuronal differentiation. *Development* 127, 2933-2943, (2000).

476 Vilas-Boas, F. & Henrique, D. HES6-1 and HES6-2 function through different mechanisms during neuronal differentiation. *PLoS One* 5, (2010).

477 Hatakeyama, J. *et al.* Hes genes regulate size, shape and histogenesis of the nervous system by control of the timing of neural stem cell differentiation. *Development* 131, 5539-5550, (2004).

478 Holmberg, J. *et al.* SoxB1 transcription factors and Notch signaling use distinct mechanisms to regulate proneural gene function and neural progenitor differentiation. *Development* 135, 1843-1851, (2008).

479 Gerlai, R. Behavioral tests of hippocampal function: simple paradigms complex problems. *Behav Brain Res* 125, 269-277, (2001).

480 Deisseroth, K. *et al.* Next-generation optical technologies for illuminating genetically targeted brain circuits. *Journal of Neuroscience* 26, 10380-10386, (2006).

481 Kuhn, H. G. & Cooper-Kuhn, C. M. Bromodeoxyuridine and the detection of neurogenesis. *Curr Pharm Biotechnol* 8, 127-131, (2007).

482 Zhou, F. Q. & Snider, W. D. Intracellular control of developmental and regenerative axon growth. *Philos Trans R Soc Lond B Biol Sci* 361, 1575-1592, (2006).

483 Potrovita, I. *et al.* Tumor necrosis factor-like weak inducer of apoptosis-induced neurodegeneration. *J Neurosci* 24, 8237-8244, (2004).

484 Echeverry, R., Wu, F., Haile, W. B., Wu, J. & Yepes, M. The cytokine tumor necrosis factor-like weak inducer of apoptosis and its receptor fibroblast growth factor-inducible 14 have a neuroprotective effect in the central nervous system. *J Neuroinflammation* 9, 45, (2012).

485 Zhang, X. *et al.* TWEAK-Fn14 pathway inhibition protects the integrity of the neurovascular unit during cerebral ischemia. *J Cereb Blood Flow Metab* 27, 534-544, (2007).

486 Meske, V., Albert, F. & Ohm, T. G. Coupling of mammalian target of rapamycin with phosphoinositide 3-kinase signaling pathway regulates protein phosphatase 2A- and glycogen synthase kinase-3 -dependent phosphorylation of Tau. *J Biol Chem* 283, 100-109, (2008).

487 Akhmanova, A. *et al.* Clasps are CLIP-115 and -170 associating proteins involved in the regional regulation of microtubule dynamics in motile fibroblasts. *Cell* 104, 923-935, (2001).

488 Goold, R. G. & Gordon-Weeks, P. R. The MAP kinase pathway is upstream of the activation of GSK3beta that enables it to phosphorylate MAP1B and contributes to the stimulation of axon growth. *Mol Cell Neurosci* 28, 524-534, (2005).

489 Owen, R. & Gordon-Weeks, P. R. Inhibition of glycogen synthase kinase 3beta in sensory neurons in culture alters filopodia dynamics and microtubule distribution in growth cones. *Mol Cell Neurosci* 23, 626-637, (2003).

490 Eickholt, B. J., Walsh, F. S. & Doherty, P. An inactive pool of GSK-3 at the leading edge of growth cones is implicated in Semaphorin 3A signaling. *J Cell Biol* 157, 211-217, (2002).

491 Tsvetkov, A. S., Samsonov, A., Akhmanova, A., Galjart, N. & Popov, S. V. Microtubule-binding proteins CLASP1 and CLASP2 interact with actin filaments. *Cell Motil Cytoskeleton* 64, 519-530, (2007).

492 Watanabe, T. *et al.* Phosphorylation of CLASP2 by GSK-3beta regulates its interaction with IQGAP1, EB1 and microtubules. *J Cell Sci* 122, 2969-2979, (2009).

493 Gonzalez-Billault, C., Owen, R., Gordon-Weeks, P. R. & Avila, J. Microtubule-associated protein 1B is involved in the initial stages of axonogenesis in peripheral nervous system cultured neurons. *Brain Res* 943, 56-67, (2002).

494 Santos Da Silva, J., Schubert, V. & Dotti, C. G. RhoA, Rac1, and cdc42 intracellular distribution shift during hippocampal neuron development. *Mol Cell Neurosci* 27, 1-7, (2004).

495 Da Silva, J. S., Hasegawa, T., Miyagi, T., Dotti, C. G. & Abad-Rodriguez, J. Asymmetric membrane ganglioside sialidase activity specifies axonal fate. *Nat Neurosci* 8, 606-615, (2005).

496 Schwamborn, J. C. & Puschel, A. W. The sequential activity of the GTPases Rap1B and Cdc42 determines neuronal polarity. *Nat Neurosci* 7, 923-929, (2004).

497 Ebneth, A. *et al.* Overexpression of tau protein inhibits kinesin-dependent trafficking of vesicles, mitochondria, and endoplasmic reticulum: implications for Alzheimer's disease. *J Cell Biol* 143, 777-794, (1998).

498 Hernandez, F., Gomez de Barreda, E., Fuster-Matanzo, A., Lucas, J. J. & Avila, J. GSK3: a possible link between beta amyloid peptide and tau protein. *Exp Neurol* 223, 322-325, (2010).

499 Perez, M., Valpuesta, J. M., Medina, M., Montejo de Garcini, E. & Avila, J. Polymerization of tau into filaments in the presence of heparin: the minimal sequence required for tau-tau interaction. *J Neurochem* 67, 1183-1190, (1996).

500 Lucas, J. J. *et al.* Decreased nuclear beta-catenin, tau hyperphosphorylation and neurodegeneration in GSK-3 beta conditional transgenic mice. *Embo Journal* 20, 27-39, (2001).

501 Noble, W. *et al.* Inhibition of glycogen synthase kinase-3 by lithium correlates with reduced tauopathy and degeneration in vivo. *Proc Natl Acad Sci U S A* 102, 6990-6995, (2005).

502 Phiel, C. J., Wilson, C. A., Lee, V. M. & Klein, P. S. GSK-3alpha regulates production of Alzheimer's disease amyloid-beta peptides. *Nature* 423, 435-439, (2003).

503 Takashima, A. *et al.* Exposure of rat hippocampal neurons to amyloid beta peptide (25-35) induces the inactivation of phosphatidyl inositol-3 kinase and the activation of tau protein kinase I/glycogen synthase kinase-3 beta. *Neurosci Lett* 203, 33-36, (1996).

504 LaFerla, F. M. & Green, K. N. Animal Models of Alzheimer Disease. *Csh Perspect Med* 2, (2012).

505 Tesseur, I. *et al.* Deficiency in neuronal TGF-beta signaling promotes neurodegeneration and Alzheimer's pathology. *J Clin Invest* 116, 3060-3069, (2006).

506 Crews, L. *et al.* Increased BMP6 levels in the brains of Alzheimer's disease patients and APP transgenic mice are accompanied by impaired neurogenesis. *J Neurosci* 30, 12252-12262, (2010).

507 Tang, J. *et al.* Noggin and BMP4 co-modulate adult hippocampal neurogenesis in the APP(swe)/PS1(DeltaE9) transgenic mouse model of Alzheimer's disease. *Biochem Biophys Res Commun* 385, 341-345, (2009).

508 Marques, G. *et al.* The Drosophila BMP type II receptor Wishful Thinking regulates neuromuscular synapse morphology and function. *Neuron* 33, 529-543, (2002).

509 Aberle, H. *et al.* wishful thinking encodes a BMP type II receptor that regulates synaptic growth in Drosophila. *Neuron* 33, 545-558, (2002).

510 Salinas, P. C. Synaptogenesis: Wnt and TGF-beta take centre stage. *Curr Biol* 13, R60-62, (2003).

511 Xiao, L. *et al.* BMP signaling specifies the development of a large and fast CNS synapse. *Nat Neurosci*, (2013).

512 Diniz, L. P. *et al.* Astrocyte-induced synaptogenesis is mediated by transforming growth factor beta signaling through modulation of D-serine levels in cerebral cortex neurons. *J Biol Chem* 287, 41432-41445, (2012).

513 Patzke, H., Reissmann, E., Stanke, M., Bixby, J. L. & Ernsberger, U. BMP growth factors and Phox2 transcription factors can induce synaptotagmin I and neurexin I during sympathetic neuron development. *Mech Dev* 108, 149-159, (2001).

514 Heupel, K. *et al.* Loss of transforming growth factor-beta 2 leads to impairment of central synapse function. *Neural Dev* 3, 25, (2008).

515 Fukushima, T., Liu, R. Y. & Byrne, J. H. Transforming growth factor-beta2 modulates synaptic efficacy and plasticity and induces phosphorylation of CREB in hippocampal neurons. *Hippocampus* 17, 5-9, (2007).

516 Shoji-Kasai, Y. *et al.* Activin increases the number of synaptic contacts and the length of dendritic spine necks by modulating spinal actin dynamics. *J Cell Sci* 120, 3830-3837, (2007).

517 Salinas, P. C. Signaling at the vertebrate synapse: new roles for embryonic morphogens? *J Neurobiol* 64, 435-445, (2005).

Appendices

Appendix I

Publications

Osório C., Chacón PJ., White M., Kisiswa L, Wyatt S., Rodríguez-Tébar A. and Davies AM. Selective regulation of axonal growth from developing hippocampal neurons by tumour necrosis factor superfamily member APRIL. Molecular and Cellular Neuroscience (MCN-13-139 manuscript under review).

Osório C., Chacón PJ., Kisiswa L, White M., Wyatt S., Rodríguez-Tébar A. and Davies AM. Growth differentiation factor-5 is a major regulator of dendrite growth during development. Development. 2013 Dec;140(23):4751-4762

Kisiswa L, Osório C., Erice C, Vizard T, Wyatt S, Davies AM. TNF-α reverse signaling promotes sympathetic axon growth and target innervation. Nat Neurosci. 2013 Jul;16(7):865-73.

Oral presentations

"miRNAs in sympathetic neuron development", MolPark – Santorini, Greece, November 1st, 2011

Poster presentations

Osório C., et al "Role of GDF-5 in regulating dendritic morphology in developing hippocampal neurons" Gordon Research conference: Neurotrophic Factors. Salve Regina University, June 1-7, 2013, Newport, RI, USA

Osório C., et al "Role of APRIL in regulating axon growth from developing hippocampal neurons" Neuroscience 2012, Society for Neuroscience's 42nd annual meeting. New Orleans, October 13-17, 2012. New Orleans, LA, USA.

Osório C., "Role of microRNAs in sympathetic axon growth", September 8-9, 2011. Munich, Germany.

Osório C. “Role of microRNAs in sympathetic axon growth” 2nd year Poster Session, School of Biosciences, Cardiff University, March, 2011. Cardiff, Wales, UK.

Osório C., “Role of the tumour necrosis factor superfamily in regulating dendritic growth and morphology in the developing central nervous system” 1st year Poster Session, School of Biosciences, Cardiff University, February 10th, 2010. Cardiff, Wales, UK.

Appendix II

Transgenic mice genotyping

Alk-6 mice genotyping

Primers:

Alk6-I: 5'- TGG TGA GTG GTT ACA ACA AGA TCA GCA -3'

Alk6-E: 5'- CTC GGC CCA AGA TCC TAC GTT G -3'

Neo-Al2: 5'- GAA AGA ACC AGC TGG GGC TCG AG -3'

Estimated band size: WT=350bp

KO=300bp

PCR reaction (Paq5000 Hotstart DNA Polymerase, Agilent Technologies):

Buffer 10x	2.5µl
dNTPs	0.25µl
Alk6-I	1µl
Alk6-E	0.5µl
Neo-Al2	0.5µl
Herculase	0.25µl
Nuclease free water	18µl

Reaction mix: 2µl of DNA + 23µl of PCR mix

PCR Program:

Step 1: 95°C 2min

Step 2: 95°C 30secs

Step 3: 63°C 30secs

Step 4: 72°C 50secs

Step 5: 72°C 3min

Cycle 2 to 4: 40x

Solutions for cell culture

Poly-L-lysine (0.5mg/ml)

50mg of poly-L-lysine was dissolved in 100ml of autoclaved milli-Q water, in a plastic beaker. The final solution was filtered using a 0.2μm filter. The solution was then stored at -20°C in 10ml aliquots.

Trypsin (10mg/ml)

10mg of trypsin was dissolved in 1ml of HBSS 1x without Ca^{2+} and Mg^{2+}. The final solution was filtered using a 0.2μm filter. This solution was freshly made on the dissection day.

Trypsin inhibitor (10mg/ml)

10mg of trypsin inhibitor was dissolved in 1ml of HBSS 1x without Ca^{2+} and Mg^{2+}. The final solution was filtered using a 0.2μm filter. This solution was freshly made on the dissection day.

DNase I (1mg/ml)

100mg of DNase I was dissolved in 100ml of autoclaved milli-Q water. The final solution was filtered using a 0.2μm filter. The solution was then stored at -20°C in 100μl aliquots.

Transfection vectors

pCDH-CMV-MCS-EF1-copGFP

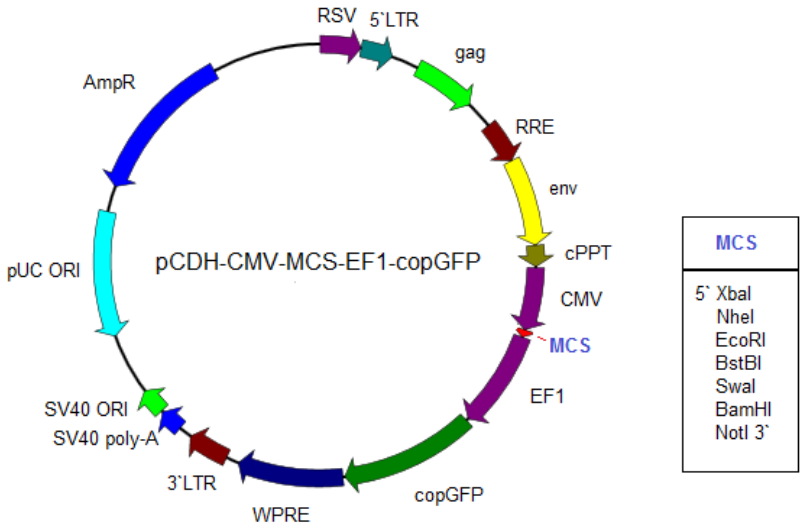

RSV: Hybrid RSV promoter-R; required for viral packaging and transcription

5'LTR: U5 long terminal repeat; required for viral packaging and transcription

Gag: Packaging signal

RRE: Rev response element binds gag and it is involved in packaging of viral transcripts

Env: Packaging signal

cPPT: Central polypurine tract (includes DNA Flap region) involved in nuclear translocation and integration of transduced viral genome

CMV: Constitutive Human cytomegalovirus (CMV) promoter for transcription of cloned cDNA insert

EF1: Constitutive Elongation factor 1α promoter for transcription of reporter

copGFP: Copepod green fluorescent protein (similar to regular EGFP, but with brighter color) as a reporter for the transfected/transduced cells

WPRE: Woodchuck hepatitis virus posttranscriptional regulatory element—enhances the stability of the viral transcripts

3'LTR: Required for viral reverse transcription; self-inactivating 3' LTR with deletion in U3 region prevents formation of replication-competent viral particles after integration into genomic DNA

SV40polyA: Transcription termination and polyadenylation

SV40 ORI: Allows for episomal replication of plasmid in eukaryotic cells

pUC ORI: Allows for high-copy replication in *E. coli*

AmpR: Ampicillin resistant gene for selection of the plasmid in *E. coli*

Solutions for Immunohistochemistry

4% PFA (paraformaldehyde) (100ml)

80ml of PBS was heated up to 60°C in a ventilated hood. Then 4mg of PFA powder were added to the heated PBS solution. The pH was raised by adding 1N NaOH dropwise until the solution was clear. Once the PFA was dissolved, the solution was cooled, aliquoted and frozen at -20°C.

Solutions for western blot

RIPA lysis buffer (**R**adio **I**mmuno **P**recipitation **A**ssay buffer)

150 mM sodium chloride

1.0% Triton X-100

0.5% sodium deoxycholate

0.1% SDS (sodium dodecyl sulphate)

50 mM Tris, pH 8.0

Store at -20°C in 1ml aliquots.

5x Laemmli sample buffer

0.05% bromophenol blue

300 mM Tris–HCl 2M pH 6.8

50% glycerol

10% SDS

25% β-mercaptoethanol

Store at -20°C in 1ml aliquots.

10% running gel (5 ml)

2.01 ml distilled water

1.25 ml Tris–HCl 1.5M pH 8.8

50 μl SDS 10%

1.67 ml 30% acrylamide/bis solution 29:1

25 μl ammonium persulfate 10%

5 μl TEMED

5% stacking gel (3 ml)

1.7 ml distilled water

750 μl Tris–HCl 0.5M pH 6.8

30 μl SDS 10%

500 μl acrylamide/bis solution 29:1

15 μl ammonium persulfate 10%

5 μl TEMED

1x Running buffer

25 mM Tris

192 mM Glycine

0.1% SDS

Dissolve in water.

1x Transfer buffer

48 mM Tris

39 mM Glycine

5% methanol

Dissolve in water.

Ponceau S staining solution

0.1% (w/v) Ponceau S

5% (v/v) acetic acid

Dissolve in water.